University of Alberta

The Origin and Evolution of North American Kimberlites

by

Shannon E. Zurevinski

A thesis submitted to the Faculty of Graduate Studies and Research
in partial fulfillment of the requirements for the degree of

Doctor of Philosophy

Dept. of Earth and Atmospheric Sciences

Fall 2009
Edmonton, Alberta

Examining Committee

Dr. Larry Heaman, Department of Earth and Atmospheric Sciences

Dr. Robert Luth, Department of Earth and Atmospheric Sciences

Dr. Robert Creaser, Department of Earth and Atmospheric Sciences

Dr. Thomas Stachel, Department of Earth and Atmospheric Sciences

Dr. Vadim Kravchinsky, Department of Physics

Dr. Herb Helmstaedt, Department of Geological Sciences and Geological Engineering, Queen's University

Abstract

Recent discoveries of kimberlites in North America have revealed that different processes are involved in the generation of kimberlite magma. A multi-disciplinary approach combining mineralogical, petrological, geochemical, and geochronological methods is used to classify the kimberlites, investigate possible sources of magma and evaluate current tectonic models proposed for the generation of kimberlite magma. The two main study areas are 1) the diamond-poor Churchill kimberlite field (Nunavut); and 2) the highly diamondiferous Lac de Gras kimberlite field (NWT). The Attawapiskat kimberlite field, the Kirkland Lake kimberlite field and the Timiskaming kimberlite field (Ontario) are also included in this study.

The 55-56 Ma Diavik kimberlite cluster (NWT) have been classified as resedimented volcaniclastic > olivine-bearing volcaniclastic > mud-bearing volcaniclastic > macrocrystic oxide-bearing hypabyssal kimberlite > calcite oxide hypabyssal kimberlite > tuffisitic kimberlite breccia. Geochemical features of Diavik kimberlites include: 1) LREE enrichment, 2) large intra-field range in REE content, and 3) highly diamondiferous kimberlites at Diavik with primitive geochemical signatures.

The Churchill kimberlites are classified as sparsely macrocrystic, oxide-rich calcite evolved hypabyssal kimberlite and macrocrystic oxide-rich monticellite phlogopite hypabyssal kimberlite. Electron microprobe analyses of olivine, phlogopite, spinel and perovskite support this petrographical classification. Twenty-seven precise U-Pb perovskite and Rb-Sr phlogopite emplacement ages indicate that magmatism spans ~45 million years (225-170 Ma).

The crystallization ages and the Sr and Nd isotopic compositions of groundmass perovskite from a well-established, SE-trending Triassic-Jurassic corridor of kimberlite magmatism in Eastern North America (ENA) were determined to investigate the origin of this magmatism. The Sr isotopic results indicate that the Churchill (0.7032-0.7036) and Attawapiskat kimberlites (0.7049-0.7042) have unique isotopic compositions, while Kirkland Lake/Timiskaming perovskite have a larger range of $^{87}Sr/^{86}Sr$ ratios. This implies the derivation of kimberlite magma from two distinct sources in the mantle, a depleted MORB mantle source and a kimberlite magma with a Bulk Silicate Earth signature. The pattern of increasing

$^{87}Sr/^{86}Sr_{initial}$ with younging of kimberlite magmatism along the ~2000 km corridor of continuous Triassic/Jurassic magmatism could be explained from either a single or multiple hotspot track(s), responsible for the addition of heat required to generate small volume mantle melting of a kimberlite source.

Acknowledgements

We would like to thank Diavik Diamond Mines Inc. (Rio Tinto) for access to many samples and financial support. We also greatly appreciate the generosity of Shear Minerals Ltd., for the donation of samples. Special thanks to G. Hatchard and J. Schultz, S. Matveev, J. Donnelly, A. Simonetti and H. McLean for their patience and assistance. The Radiogenic Isotope Facility at the University of Alberta is supported, in part, by an NSERC Major Resources Support Grant.

Table of Contents

List of Tables

List of Figures

List of Abbreviations

A154AA	Kimberlite A154 (Diavik) Age Array
amu	Atomic Mass Unit
BSE	Bulk Silicate Earth
C.I.	Contamination Indices
CHUR	Chondrite Uniform Reservoir
DDMI	Diavik Diamond Mines Inc.
DMM	Depleted MORB Mantle
EMPA	Electron Microprobe Analyses
ENA	Eastern North American
Fo	Forsterite
Ga	Billion years
ha	Hectare
HK	Hypabyssal kimberlite
HREE	Heavy Rare Earth Elements
ICP-OES	Inductively Coupled Plasma- Optical Emission Spectroscopy
ICP-MS	Inductively Coupled Plasma- Mass Spectrometry
ID-TIMS	Isotope Dilutions- Thermal Ionization Mass Spectrometry
Lat/Long	Latitude/Longitude
LA-MC-ICP-MS	Laser Alblation- Multi- collector- Inductively Coupled Plasma- Mass Spectrometer
LREE	Light Rare Earth Elements
Ma	Million years
MC-ICP-MS	Multi-collector- Inductively Coupled Plasma- Mass Spectrometry
Mg number	Magnesium Number ($MgO/MgO + FeO_{Total}$) *100
MK	Magmatic kimberlite
mol. %	Molecular percent
MORB	Mid Ocean Ridge Basalt

MSWD	Mean Standard Weighted Deviates
MUM	Magnesian ulvöspinel- ulvöspinel- Magnetites
N	Normality
NWT	Northwest Territories
OIB	Ocean Island Basalt
oVK	olivine Volcaniclastic kimberlite
PAA	Panda Age Array
pg	picogram
ppb	parts per billion
ppm	parts per million
REE	Rare Earth Element
RVK	Resedimented Volcaniclastic kimberlite
SE	Standard Error
SCLM	Subcontinental Lithospheric Mantle
TiMAC	Titano- magnesian aluminochromite
TKB	Tuffisitic kimberlite Breccia
VK	Volcaniclastic kimberlite
vol. %	volume percent
WDS	Wavelength dispersive spectroscopy
wt. %	weight percent
XRD	X-ray diffractrometry

Chapter 1

Introduction

Kimberlite has long been considered a potassic rock (Foley et al. 1987). The current formal definition of kimberlite is as follows: a clan of volatile-rich (dominantly CO_2) potassic ultrabasic rocks that may occur as small volcanic pipes, dykes and sills (Skinner and Clement 1979; Clement et al. 1984). Kjarsgaard et al. (2008) re-investigated this definition, and based on the most primitive geochemistry of worldwide kimberlite occurrences, concluded that archetypal kimberlite is not formed from CO_2-rich, alkaline, potassic melt. Incorporating kimberlites from North America, which had not been previously investigated at the time of the original classification, Kjarsgaard et al. (2008) concluded that kimberlites are not an alkaline rock (defined by (Na+K)/Al <1), therefore could not be further classified as "sodic" or "potassic", and that potassium contents are similar to those in mid-ocean ridge basalts (MORBs) and ocean island basalts (OIBs). Furthermore, whole rock H_2O and CO_2 data from kimberlites which were considered to be volatile-rich shows that in fact kimberlites are only water-rich, concluding that kimberlites are high H_2O/CO_2, MgO-rich, Al- and K-poor, silica undersaturated magmas (Kjarsgaard et al. 2008). The scientific community has had an arduous task of producing a unified classification scheme for kimberlites, perhaps made more difficult by the occurrence of kimberlites in North America that do not conform with classifications previously based largely on South African kimberlites.

Kimberlites occur in all of the main Archean cratons worldwide, and are generated from the earth's mantle. They sample the mantle at deeper levels (>150 kms) than any other volcanic rock, and transport diamonds and mantle samples to the earth's surface. Kimberlites are thus a unique source of deep mantle samples, and therefore are beneficial not only for their diamond content, but also for investigating deep mantle processes. A large number of kimberlites have been discovered worldwide, however there are still many questions that relate to the origin of kimberlite and the occurrence of diamond deposits. Although kimberlites are generally emplaced into ancient Archean cratonic rocks, their style of emplacement, textures, facies type and style of alteration are quite different.

Following the 1991 discovery of diamonds in Canada's north, there has been an explosion of activity searching for diamondiferous kimberlites. With the discovery of kimberlites in North America, it is revealed that very different processes are involved in the generation and emplacement of kimberlite magma, and that information constrained from South African kimberlite magmatism does not readily apply to North American kimberlites. For example, South African kimberlites are often modeled as large carrot-shaped vertical intrusions, consisting of root zone facies, a diatreme facies and sometimes crater facies (Mitchell 1986 and references therein). North American kimberlites tend to be much smaller, irregular shaped intrusions sometimes consisting of only a single rock type (Kjarsgaard et al. 2008). Many different tectonic models have been hypothesized to be responsible for the generation of primary kimberlite magma, and many models have been invoked to explain the evolution and final emplacement mechanisms of kimberlites. Each of these models has some merit in the explanation of deep mantle processes involved in kimberlite magmatism, but unfortunately these models have many discrepancies. The source of the small volume ultrabasic potassic magmas, the mantle depth for kimberlite magma formation, and the triggering mechanisms of mantle melting processes have yet to be agreed upon by the scientific community. This study uses a multi-disciplinary approach to investigate the origin and final emplacement of a number of kimberlite fields in North America. It involves two main study areas: the highly diamondiferous Lac de Gras kimberlite field (NWT); and the diamond-poor Churchill kimberlite field (Nunavut), both kimberlite fields have been emplaced within stable Archean cratons. Other kimberlites fields, such as the Attawapiskat (Northern Ontario), Kirkland Lake (Ontario/Quebec), and Timiskaming (Ontario) kimberlite fields are also investigated in the study. The kimberlite fields chosen for the study cover a large portion of Canada, intrude several different Archean cratons (Slave, Churchill and Superior), and represent a large range of emplacement ages from Triassic to Eocene. A combination of mineralogical, petrological, geochemical, and geochronological studies are used in order to; 1) classify the kimberlite fields, 2) investigate the sources of the kimberlite magma, and 3) evaluate tectonic models proposed for the generation of the kimberlite magma.

North American Kimberlites

Most kimberlites in North America occur as discrete fields and clusters in stable Archean cratons. The major kimberlite fields of North America include: Victoria Island (Nunavut), Somerset Island (Nunavut), Lac de Gras (N.W.T.), Torngat (Labrador), Otish Mountains (Quebec), Buffalo Head Hills (Alberta), Fort à la Corne (Saskatchewan), Attawapiskat (Ontario), Timiskaming (Ontario and Quebec), Wawa (Ontario), Finger Lakes (New York), State Line (Colorado and Wyoming). Heaman et al. (2003) identified four broad kimberlite emplacement patterns for North American kimberlites, based on a compilation of more than 100 emplacement ages: 1) a northeast Neoproterozoic/Cambrian Labrador Sea Province (Labrador, Quebec), 2) an eastern Jurassic province (Ontario, Quebec, New York and Pennsylvania) (Heaman and Kjarsgaard 2000 and references therein), 3) a Cretaceous central corridor (Nunavut, Saskatchewan, central USA) (Kjarsgaard 1996; Leckie et al. 1997; Heaman et al. 2003), and 4) a western mixed Type 3 kimberlite province (Cambrian-Eocene) (Alberta, Nunavut, N.W.T., Colorado/Wyoming). Heaman et al. (2003) further subdivided the kimberlites of the Slave Province based on emplacement ages. Four kimberlite age domains were revealed: I-a southwestern Siluro-Ordovician domain (~450 Ma), II-a SE Cambrian domain (~540 Ma), III- a central Tertiary/Cretaceous domain (48-74 Ma) and IV-a northern mixed domain consisting of Jurassic and Permian kimberlite fields.

Two kimberlite fields in Northern Canada were chosen for a detailed study, the diamondiferous Diavik kimberlites of the Slave Province, N.W.T., and the currently non-economic Churchill Province kimberlites, Nunavut. The highly diamondiferous Diavik kimberlites occur within the granite-greenstone belt of the central Slave craton, in the Lac de Gras region. The Slave craton forms part of the Archean Shield (4.2 to 3.0 Ga) (Iizuka et al. 2006). The Slave craton is dominated by 2.73 to 2.58 Ga supracrustal assemblages and plutonic suites (Bowring et al. 1999; Davis et al. 1999). Previous emplacement ages for the economic Diavik kimberlites are Eocene, while the non-economic kimberlites have older emplacement ages, mainly Cretaceous (Creaser et al. 2004). It is currently unknown as to why the kimberlites belonging to the Eocene episodes of emplacement have a higher diamond potential. In Chapter

2, the mineralogy and petrology of the Diavik kimberlites are investigated and documented for the first time. Major and trace element geochemistry on fresh hypabyssal kimberlite has been completed on the Diavik kimberlite samples, providing valuable insight into the nature of the primary kimberlite magma.

The Churchill kimberlite field is one of Canada's newly discovered kimberlite fields, situated within the cratonic rocks of the Churchill Province. Geophysical evidence suggests that a cluster of more than 100 pipes is present on the Churchill Diamond Property, located immediately West of Hudson Bay, and encompassing in excess of 2.5 million acres in the Kivalliq region of Nunavut. The Churchill Diamond Property is immediately underlain by rocks of the metamorphosed Archean Rankin Inlet Group, and surrounded by Archean metaplutonic rocks. Exploration in the Churchill Province thus far has yielded non-economic kimberlite intrusions. In Chapter 3, twenty seven new highly precise emplacement ages have been determined for the Churchill kimberlites in this study. The mineralogy and petrology of the kimberlites has been extensively studied, they are formally classified in this study as bonafide kimberlites. The Churchill kimberlites are interpreted to be the current most northerly emplacement of kimberlite magma along the NW-SE trending corridor of Jurassic/Triassic kimberlite magmatism in central and eastern North America. This corridor was previously shown to include the Kirkland Lake, Timiskaming and Attawapiskat fields with a progressive SE younging of kimberlite magmatism from ~180 Ma (James Bay lowlands) to ~135 Ma, in the Timiskaming field (Heaman and Kjarsgaard 2000). In Chapter 4, selected kimberlites belonging to this corridor have been chosen for Sr-Nd isotopic perovskite analysis, in order to better constrain the mantle source region of primary kimberlite magma. This allows for a re-investigation into the tectonic models proposed for the eastern North American kimberlites.

Significance of Research

A large contribution has been made to the geochronological database of North American kimberlite emplacement ages, allowing for tectonic models to be re-evaluated. The timing of kimberlite emplacement allows an evaluation of whether there is any temporal correlation between the timing of kimberlite emplacement and major tectonic processes that

may have triggered kimberlite magmatism (e.g. subduction, mantle plume activity, rifting). Mineralogical classifications provide an important link to geochemical observations. We must be careful assessing geochemical data from kimberlites as they are hybrid rocks with possible magma contamination resulting from numerous small-scale processes involving generation of the magma, ascent through the sub-continental lithospheric mantle (SCLM), and final emplacement in the crust. Textures and alteration patterns provide clues to final emplacement mechanisms in the crust. In the past, tracer isotope studies have mainly been completed on whole rock samples of "fresh" hypabyssal kimberlite and previous studies of southern African kimberlites have indicated at least two broad mantle sources; distinguished as Group I and II kimberlites (Smith 1983).

Perovskite is a primary magmatic groundmass mineral that crystallizes directly from kimberlite magma, and therefore is an excellent mineral to obtain primary mantle signatures (Heaman 1989; Chakmouradian and Mitchell 2000). Tracer isotope studies using kimberlitic perovskite can reveal information crucial to understanding the source and depth of generation of kimberlite magma. Multiple disciplines of research are used in conjunction to address the unanswered question: What is the nature of the source of kimberlite magma? The answer to this question is crucial to the study of the origin and evolution of kimberlites in North America.

References

Bowring, S.A., and Williams, I.S. 1999. Priscoan (4.00-4.03 Ga) orthogneisses from northwestern Canada. Contributions to Mineralogy and Petrology, 134:3-16.

Chakhmouradian, A.R. and Mitchell, R.H. 2000. Occurrence, alteration patterns and compositional variation of perovskite in kimberlites. Canadian Mineralogist, 38:907-948.

Clement, C.R., Skinner, E.M.W., and Scott Smith, B.H. 1984. Kimberlites redefined. Journal of Geology, 32:223-228.

Creaser, R. A., Grűtter, H., Carlson, J. & Crawford, B. 2004. Macrocrystal phlogopite Rb-Sr dates for the Ekati property kimberlites, Slave Province, Canada: evidence for multiple intrusive episodes in the Paleocene and Eocene. Lithos, 76: 399-414.

Davis, W.J., and Bleeker, W. 1999. Timing of plutonism, deformation and metamorphism in the Yellowknife domain, Slave province, Canada. Canadian Journal of Earth Sciences, 36:1169-1187.

Foley, S., Venturelli, G., Green, D.H., Toscani, L. 1987. The ultrapotassic rocks: Characteristics, classification and constraints for petrogenic models. Earth Science Reviews, 24:81-134.

Heaman, L.M. & Kjarsgaard, B.A. 2000. Timing of Eastern North American kimberlite magmatism: continental extension of the Great Meteor Hotspot Track? Earth and Planetary Science Letters, 178: 253-268.

Heaman, L.M., Kjarsgaard, B.A. & Creaser, R.A. 2003. The timing of kimberlite magmatism in North America: implications for global kimberlite genesis and diamond exploration. Lithos, 71: 153-184.

Iizuka, T., Horie, K., Komiya, T., Maruyama, S., Hirata, T., Hidaka, H., and Windley, B.F. 2006. 4.2 Ga zircon xenocrysts in an Acasta gneiss from Northwestern Canada: Evidence for early continental crust. Geology, 34: 245-248.

Kjarsgaard, B.A. 1996. Slave province kimberlites, NWT. In: LeCheminant, A.N., Richardson, D.G., DiLabio, R.N.W., Richardson, K.A. (Eds.), Searching for diamonds in Canada. Geological Survey of Canada Open File, vol. 3228, pp. 55-60.

Kjarsgaard, B.A., Pearson, D.G., Tappe, S., Nowell, G.M., and D.P. Powell. 2008. Kimberlites: High H_2O/CO_2, MgO-rich, Al- and K-poor, Silica Undersaturated Magmas. 9th International Kimberlite Conference Extended Abstract No. 9IKC-A-00187. Frankfurt, Germany.

Leckie, D.A., Kjarsgaard, B.A., Bloch, J., McIntyre, D., McNeil, D., Stasiuk, L.S., Heaman. L.M. 1997. Emplacement and re-working of Cretaceous, Diamond-bearing, crater facies kimberlites of central Saskachewan, Canada. Geological Society of America Bulletin, 109: 1000-1020.

Mitchell, R.H. 1986. Kimberlites: Mineralogy, Geochemistry and Petrology. Plenum Publ. Corp., New York.

Skinner, E.M.W., and Clement, C.R. 1979. Mineralogical classification of Southern African Kimberlites. *In* Boyd, F.R. & Meyer, H.O.A. eds., Kimberlites, Diatremes and Diamonds: Their Geology, Petrology and Geochemistry, pp. 129-139. American Geophysical Union, Washington, D.C.

Smith, C.B. 1983. Pb, Sr and Nd isotopic evidence for sources of African Cretaceous Kimberlite. Nature, 304:51-54.

Chapter 2

The geochemistry of Diavik kimberlites, Lac de Gras, Slave Province, Northwest Territories, Canada*

*some of the contents of this chapter will be submitted for publication to the Canadian Journal of Earth Sciences. Zurevinski, S.E., Heaman, L.M., Creaser, R.A., and Eichenberg, D. 2009.

Introduction

The Diavik diamond mine is located on a 20 km^2 island in Lac de Gras, approximately 300 kilometers NE of Yellowknife, Northwest Territories, Canada. Diavik Diamond Mines Inc. (DDMI) operates the mine, which opened in 1996 when DDMI assumed project responsibility from the Rio Tinto subsidiary Kennecott Canada Exploration Inc. Production began in early 2003, and diamonds are currently mined/or completed from three kimberlites, A154N, A154S and A418 (Figure 2-1). Diavik reserves in these three kimberlites are estimated at 90.2 million carats of rough diamonds. After beginning development in 2006, underground mining in A154S is set to commence in 2009. Sixty-eight kimberlites are currently recognized on the Diavik property and five of these have been dated, yielding emplacement ages between 54.7 and 56.0 Ma (Graham et al. 1999; Creaser et al. 2004).

The main objectives of this study are to establish the petrographic and geochemical nature of the Diavik kimberlites, provide constraints on the origin of the kimberlites and evaluate whether there are diagnostic geochemical features that distinguish the diamond-bearing economic from non-economic kimberlite in this cluster. Over 125 kimberlite samples were collected for this study from drill core and the A154N and A154S pits, representing a total of 38 kimberlites on the property. A petrographic study of most samples was conducted to classify the samples and to search for the least altered and least contaminated material for geochemical study. During this petrographic evaluation, a search for suitable samples for age dating was also conducted.

Methodology and analytical techniques

The petrographic and geochemical results presented here are based on the investigation of approximately 95 thin sections prepared from drill core specimens and some kimberlite pit samples. Where possible, competent samples exhibiting minor alteration were

chosen. Detailed petrographic analyses were used to classify each of the kimberlite occurrences on the basis of mineralogy and textural information. The terminology used to describe kimberlite textures and classification follows the scheme recommended by Field and Scott Smith (1998). In order to understand better the mineralogical and geochemical differences between kimberlites of the Diavik property, a distinction between "economic" and "non-economic" kimberlites has been used. For the purpose of this study, "economic" kimberlite implies the highly diamondiferous A154N, A154S, and A418 (the three kimberlite bodies that are currently being mined). "Non-economic" kimberlite refers to the remaining kimberlites on the Diavik property. This is an important distinction that allows for a better comparison of the kimberlites, investigation of their geochemical signatures, and possibly interpretation of the parent kimberlite magmas, as well as any final emplacement controls or features responsible for generating a highly diamondiferous kimberlite.

Polished thin sections of selected samples were prepared for analysis on the electron microprobe. EMPA (Electron Microprobe Analyses) was performed using a JEOL JXA-8200 Superprobe at the University of Calgary. Mineral compositions of selected samples were measured using wavelength-dispersion spectrometry (WDS). Analyses were acquired for 20-90 seconds with an accelerating voltage of 20 kV, and a 20 nA beam current. Accuracy of major elements is better than 1%. The following well-characterized natural and synthetic standards were employed for analysis: albite (Na), apatite (P), metallic Ni, pyrope (Mg, Al, Si), diopside (Ca), ilmenite (Mn), kaersutite (K, Fe, Ti), and chromite (Cr).

For Rb-Sr age dating, relatively unaltered macrocrystal phlogopite was extracted from kimberlite drill core, using a tungsten carbide tipped tool, without crushing or pulverizing the entire sample. Phlogopite macrocrysts selected for Rb-Sr analysis were examined using a binocular microscope and preliminary cleaning was conducted using fine tipped tweezers to eliminate altered material, chlorite rims, and any adhering kimberlitic matrix. The analytical procedures for Rb-Sr phlogopite dating and sequential leaching techniques are given by Creaser et al. (2004). Rb and Sr were loaded onto separate Re filaments using a tantalum gel loading technique and their isotopic compositions were determined using a Sector54 Thermal

Ionization Mass Spectrometer. All analyses are normalized to the recommended $^{87}Sr/^{86}Sr$ value of 0.71025 reported for the SRM987 Sr isotopic standard. The measured value of SRM987 over the period of analysis during this study ranged from 0.71016 to 0.71019. Blanket errors of ± 1.5% and 0.005% (2 sigma) were assigned to the $^{87}Rb/^{86}Sr$ and $^{87}Sr/^{86}Sr$ ratios, respectively and ages were calculated using Isoplot version 3.0 (Ludwig 2003). All isochron and model ages were calculated using a decay constant of $\lambda^{87}Rb = 1.42 \times 10^{-11}$ yr^{-1} (Steiger and Jager 1977). Phlogopite Rb-Sr model ages are calculated using an assumed initial $^{87}Sr/^{86}Sr$ ratio of 0.705. Selected powders that were chosen for whole rock Sr and Nd isotope analyses. Methods for analysis of whole-rock powders for Sm-Nd and Rb-Sr isotopes follow those described by Unterschutz et al. (2002), Creaser et al. (2004), and Schmidberger et al. (2007).

Selected samples for geochemistry were crushed to ~2cm and visible country rock xenoliths were removed. The remaining material was pulverized to a fine powder using a tungsten carbide shatterbox. These sample powders were analysed by ACTLABS using their Litho4Research program. For major elements, the samples powders were fused using a $LiBO_2$ flux, the glass bead was dissolved in HNO_3, and the major element contents were determined by inductively coupled plasma optical emission spectroscopy (ICP-OES). For trace elements, the sample powders were dissolved and resulting solutions were analysed by inductively coupled plasma mass spectrometry (ICP-MS).

Regional Geology

The Diavik kimberlite cluster is located within the Archean Slave Province, a composite 2.72-2.62 Ga granite-greenstone terrane comprised of volcano-sedimentary successions overlying older (>2.8 Ga) sialic basement, and intruded by 2.7-2.6 Ga syn- to post-volcanic and tectonic granitoids (Armstrong and Kjarsgaard, 2003; Davis et al. 2003). There are multiple periods of kimberlite emplacement in the Slave craton with discrete episodes of magmatism during the Neoproterozoic, Cambrian, Siluro-Ordivician, Permian, Jurassic, Cretaceous, and Eocene, representing more than 600 Ma of kimberlite magmatism (Heaman et al. 2003). There are a large number of kimberlite fields and clusters within the Lac de Gras area and emplacement spans most of the Phanerozoic, similar to the highly diamondiferous Type 3

kimberlite provinces of South Africa and Yakutia (Kjarsgaard and Heaman 1995). Based on temporal patterns of kimberlite emplacement, the Slave craton has been previously divided into four kimberlite age domains (Figure 2-2): I – a southwestern domain characterized by Siluro-Ordovician kimberlite magmatism, II – a southeastern domain characterized by Cambrian kimberlite magmatism, III – a central domain dominated by Cretaceous and Eocene kimberlite magmatism, including the Diavik kimberlites, and IV – a northern mixed domain consisting of Jurassic, Permian and Neoproterozoic kimberlite magmatism (Heaman et al. 2004).

In the central Slave Domain III, the kimberlite occurrences are focused within a 100 km x 150 km area in the Lac de Gras region (Heaman et al. 2004). This encompasses both the Ekati and Diavik properties. The Diavik kimberlites are emplaced into three main Archean rock units, greywacke-mudstone, metaturbidites, tonalite-quartz diorite (hosting the A21 kimberlite), and two mica-granites (hosting the A154S, A154N, and A418 kimberlites). Surface expression of the pipes varies between 1.1 and 1.6 hectares (e.g. A154N- 1.1032 ha; A154S- 1.5595 ha; and A418- 1.3331 ha). The economic kimberlites extend to depths of greater than 400 meters below the surface (Armstrong and Kjarsgaard, 2003).

Based on a compilation of Rb-Sr phlogopite ages obtained for 27 kimberlites in the Lac de Gras field, Creaser et al. (2004) identified four distinct episodes of Eocene kimberlite magmatism: the Mark Array (47.8 ± 0.3 Ma), the Panda Array (53.2 ± 0.3 Ma), the A154 Array (55.3 ± 0.3 Ma) and the Cobra Array (59.0 ± 0.7 Ma). Creaser et al. (2004) concluded that the kimberlite pipes within the Lac de Gras region with the highest diamond grades appear to be restricted to two distinct periods of magmatism, 51-53 Ma and 55-56 Ma. Lockhart et al. (2004) reported U-Pb perovskite emplacement ages for some Lac de Gras kimberlites occurring on the Ekati property from 74.7-63.9 Ma (n=5).

Kimberlite Petrography

A suite of 95 thin sections of kimberlite were examined and classified on the basis of lithology and texture (Appendix I). Classification of the kimberlites was based on the terminology of Scott Smith and Skinner (1984). Identification of all primary minerals present in the kimberlites was difficult due to the alteration and high abundance of lithic material. Table

2-1 is a summary of the petrographic classification of the Diavik kimberlites. The kimberlites have been classified as follows: resedimented volcaniclastic (RVK) > volcaniclastic (VK) > olivine-bearing volcaniclastic (oVK) > mud-bearing volcaniclastic (mudVK) > macrocrystic oxide-bearing hypabyssal kimberlite (HK) > sparsely macrocrystic calcite oxide hypabyssal kimberlite (HK) > tuffisitic kimberlite breccia (TKB).

VK and RVK are the most common kimberlite types observed in this sample suite, most are commonly clast supported. Both cored and uncored juvenile lapilli were noted. Hypabyssal kimberlite from Diavik commonly exhibits calcite and serpentine segregationary textures, and are most commonly is sparsely macrocrystic, less commonly macrocrystic. Kimberlite from T146 exhibited a preferred flow orientation in the matrix of the kimberlite. TK and TKB rarely occur at Diavik, are lithic-rich and often contain small pelletal lapilli.

Some pipes show changing facies with depth. For example, kimberlite A1039 is classified as TK and TKB at lower depths (67-72 meters) and as HK at greater depths (75-85 meters). Kimberlite A154S contains autoliths of HK surrounded by a mud-rich VK (Figure 2-3). Further review of facies with depth are needed in order to properly constrain the changing facies of each individual kimberlite intrusion.

Mineral Chemistry

Olivine

Anhedral macrocrystal olivine is abundant in the Diavik kimberlites, identified on the basis of grain size (~1.5 mm or larger). The olivine macrocrysts show strain-related features and are often fragmental. Megacrystal olivine (>1cm) was not present in this particular suite of samples. Phenocrystal and microphenocrystal olivine was abundant (up to 60 modal %) and commonly serpentinized, or completely pseudomorphed by serpentine. Microprobe analysis of olivine from four Diavik kimberlites (T33, A44, A5 and A154S) shows significant overlap between the macrocrystal and phenocrystal populations. Core analysis of Diavik olivine reveal low CaO (0.08 wt. %), MnO (0.12 wt. %), Cr_2O_3 (0.04 wt. %), Al_2O_3 (0.01 wt. %) and TiO_2 (0.02 wt. %). NiO content averages 0.34 wt. %.

There is complete overlap of forsterite content (Fo) for macrocrystal and phenocrystal olivines from kimberlite T33 (Fo 90-91). Kimberlite A44 olivine macrocrysts have a slightly higher Fo content (91-93), compared to the phenocrystal population (90-91). Kimberlite A5 macrocrysts and phenocrysts have overlapping Fo content (90-93), with an abundant microphenocrystal/fragmental population with a lower Fo content (89-91). The low Fo content of the microphenocrystal olivine from A5 (89-91), combined with a low NiO content (0-0.1 wt. %), classify the microphenocrystal olivine as kimberlitic, supported by petrographic results indicating a hypabyssal kimberlite (HK). Samples analysed from kimberlite A154S show complete overlap of macrocrystal and phenocrystal olivine content (Fo 89-92). Figure 2-4 shows a Fo (mol. %) vs. NiO (wt. %) for the Diavik kimberlitic olivines. All olivine compositions plot in the kimberlite field (from Mitchell, 1986) and exhibit large variations in NiO content. High NiO olivines can be interpreted as originated from the SCLM or early-crystallizing olivines from the kimberlite melt.

Spinel

Spinel occurs as euhedral to subhedral grains ranging in abundance from 1 to 7 modal percent. Larger crystals commonly exhibit corrosion on their rims. Groundmass spinel typically occurs as necklace textures surrounding altered olivine macrocrysts and fragments. Based on 124 spinel analyses from six Diavik kimberlites (A154N, A154S, T33, T31, A4 and A5), spinel compositions follow the "magmatic trend 1" or "magnesian ulvöspinel trend" (after Haggerty, 1976) (Figure 2-5). Overall, the compositional trend across the spinel prism shown in Figure 2-5 represents Fe- and Ti-enrichment, crystallizing TiMACs (Titianium-Magnesium-AluminoChromites), to MUMs (Magnesian ulvöspinel-Ulvöspinel-Magnetites). Samples from T33, A154S, A5 and A4 plot along the trend, while A154N and T31 plot only at the beginning of the trend (Cr-enriched). Fe/(Fe+Mg) ratios for Diavik spinel range from 0.33-0.74 and average 0.54.

Ilmenite

Anhedral ilmenite macrocrysts are present in Diavik kimberlites, ranging from trace to 10 modal percent. Ilmenite occurs as discrete grains, up to 10mm in diameter. Microprobe

analyses from four kimberlites A154N, A154S, A21 and A418 (n=784) have compositions typical for kimberlitic ilmenite; 46-59 wt. % TiO_2, 9-14 wt. % MgO, and 19-39 wt. % FeO.

Geochemistry

Major Element Geochemistry

Following completion of petrography and classification, selected samples were carefully chosen for whole-rock geochemistry (Appendix I). Only the freshest samples were chosen, and any visible crustal fragments were removed. Contamination indices (C.I. = SiO_2 + Al_2O_3 + Na_2O / MgO + K_2O; Clement 1982) have been calculated in order to assess the degree of country rock entrainment and alteration. The contamination index of the Diavik kimberlite samples varies between 0.92 and 2.70. Relatively fresh samples are considered to have a contamination index of less than 1.2 (Clement 1982). Of the 48 samples analysed, 32 samples have C.I.'s <1.2. The samples with C.I.'s >1.2 are not useful when dealing with primary magma compositions, however the samples are still suitable for evaluating the cause of intrafield geochemical variations. The bulk composition of samples from Diavik with a C.I. <1.2 are consistent with the range of kimberlites worldwide (Mitchell 1986).

The Na_2O/K_2O range from 0.02 to 0.24. These low ratios illustrate the potassic nature of the Diavik kimberlites. The wt. % $(Na_2O+K_2O)/Al_2O_3$ ratios range from 0.15 to 1.29, indicating the miascitic affinities of the kimberlites. The Mg numbers [Mg# = $(MgO/(MgO+FeO_{Total})*100$] range from 73 to 87. Figure 2-6 is a plot of Mg# vs. TiO_2 comparing the Diavik economic kimberlites to the non-economic kimberlites. Economic kimberlites have higher Mg numbers, potentially due to higher macrocrystal and phenocrystal olivine contents. Figure 2-6 also indicates the low TiO_2 nature of the Diavik kimberlites, compared to the fields for South African Group I and II kimberlites (Clement 1982; Smith et al. 1985). In general, the compositions of economic Diavik kimberlites (A154N, A154S, and A418) have the highest Mg# and a, A154N sample plots close to the composition of the Leslie kimberlite in the nearby Ekati cluster (Berg and Carlson, 1998) and an estimate for primitive kimberlite magma, as determined from the Jericho kimberlite, NWT (Price et al. 2000). The

non-economic Diavik kimberlites plot along a trend towards decreasing Mg#, possibly reflecting a more evolved signature (Figure 2-6).

Trace Element Geochemistry

The trace elements hosted mainly by spinel and olivine exhibit large ranges and do not appear to differ between economic and non-economic kimberlite. Higher V (33-194 ppm; mean 102), Cr (510-5470 ppm; mean 1159), and Ni (360-1580 ppm; mean 835) are characteristic of the Diavik kimberlites. The incompatible elements (Ba, Sr, Zr, Hf, Nb, Ta, U, and Th) are not removed until the final stage of crystallization of the groundmass kimberlite, therefore the whole rock analyses of the HK samples are a good estimate of the primary magmatic abundances of these elements.

Hosted by primarily phlogopite and calcite, Ba concentrations range from 347-8896 ppm, and have a mean of 2039 ppm. Hosted by apatite and carbonates (and possibly perovskite), Sr ranges from 223-2599 ppm, and has a mean 1006 ppm concentration. The Ba/Sr ratios for Diavik kimberlites ranges from 1-3, all above unity. Elements hosted mainly by ilmenite, perovskite, and apatite exhibit large ranges and appear to differ between economic and non-economic kimberlite. Zr and Hf are primarily hosted by kimberlitic minerals such as perovskite, ilmenite and garnet (Hf). Perovskite and ilmenite rarely occur in the Diavik kimberlites, therefore the range of abundances of these elements is considerably lower than most kimberlites (Group I kimberlites- Zr mean 184 ppm; Hf mean 5.6 ppm (Mitchell 1986)). Zr has a range of 21-120 ppm (mean 69), and Hf has a range of 0.6-3.1 ppm (mean 1.8). Kimberlite samples from economic pipes have generally lower Zr and Hf abundances (Zr: 21-63 ppm, Hf <2 ppm). There is no correlation between the Zr and Hf contents in the Diavik kimberlites, a feature also observed in other kimberlites (Mitchell 1986). Zr/Hf ratios from Diavik kimberlites range from 35-46. Mitchell (1986) reports Zr/Hf ratios of South African kimberlites from 35-50. Therefore, even though the abundances of Zr and Hf vary, the Zr/Hf ratios are consistent worldwide independent of the age of magmatism and variety of kimberlite (Fesq et al. 1975). Diavik kimberlites have consistent Zr/Hf ratios, but lower than average Zr

and Hf contents, which may reflect a different degree of partial melting, from the same kimberlitic source.

Mainly hosted by perovskite and ilmenite, Nb and Ta ranges from Diavik kimberlites are very similar to worldwide kimberlite ranges (Mitchell 1986). Nb ranges from 57-450 ppm, with a mean of 148. Ta ranges from 3-19 ppm (mean 8.3). Economic samples are much lower, with Nb ranging from 58-110 ppm (exception of one sample, Nb = 202 ppm), and Ta ranging from 3-8 ppm. With the lack of perovskite present in most Diavik kimberlites, Nb and Ta are most likely hosted by macrocrystal ilmenite. Nb and Ta show a good correlation, and behave as incompatible elements in the kimberlitic melts at Diavik. Diavik kimberlite Nb/Ta ratios are ~17, which compares well with other kimberlites worldwide (e.g. Kimberley kimberlites vary between 11-16; Mitchell 1986).

Diavik has low and restricted ranges in U and Th content. U ranges from 1-10 ppm (mean 3.6). Th ranges from 5-45 ppm (mean 17.7). U and Th are mainly hosted by perovskite and apatite in kimberlites (Mitchell 1986). Therefore, the low Th and U contents in Diavik kimberlites likely reflect the general absence of these minerals. Th and U correlate well, behaving as incompatible elements, and the low ranges show that the Diavik kimberlites must be derived from a low Th/U source.

Rare Earth Element Geochemistry

The chondrite-normalized rare earth element patterns shown in Figure 3-7 show the LREE-enriched pattern typical of kimberlites worldwide. La abundances range up to 1450x chondrite, while Lu is 1.5x chondritic values. All kimberlites from the study were included in Figure 2-7, as crustal contamination will have little influence on the rare earth elements. Although all of the samples show a subparallel pattern, there is a very large intrafield range in REE contents. The non-economic kimberlites from Diavik are clearly more enriched in REEs, as expected if they do reflect a more evolved character. The economic kimberlites have a subparallel pattern to the non-economic kimberlites, however have La abundances ranging from 400x chondrite, and chondritic Lu abundances (Figure 2-7).

La/Yb ratios for Diavik kimberlites range from 60 to 436 (mean 195). This is a significant range that shows that the non-economic Diavik kimberlites show an extreme LREE enrichment (i.e. La/Yb > 350), whereas the majority indicate values typical of Group 1 and Group 2 kimberlites (La/Yb <300; Mitchell 1986; Armstrong and Kjarsgaard, 2003). Diavik kimberlites exhibiting this LREE enrichment include A4, A5, T237, T33 and A154S.

When normalized to primitive mantle abundances, the Diavik kimberlites are all roughly sub-parallel and show trace element enrichment relative to primitive mantle(Figure 2-8). Only samples with a low contamination index (i.e. <1.2) are shown in Figure 2-8. The maximum trace element enrichment recorded by both the non-economic and economic samples occurs in the region between Cs to Nb (Figure 2-8). The Diavik kimberlites have slight positive Ba, Pb and P anomalies (Figure 2-8). This is interpreted as reflecting slight degrees of crustal contamination. These Diavik kimberlites also display negative K and Zr anomalies and slight negative U and Rb anomalies. Overall, the economic samples show the least enrichment, while the non-economic show the highest enrichment and are thus considered more evolved. With the exception of sample A21, there are no large differences in the primitive mantle normalized patterns between the non-economic and economic kimberlites at Diavik.

Whole rock isotope geochemistry

Eight samples from six kimberlite pipes were selected for whole rock Sm-Nd and Rb-Sr isotopes and the results are presented in Table 2-2 and illustrated in Figure 2-9. Initial $^{87}Sr/^{86}Sr$ (T = 56 Ma) compositions range from 0.70468 to 0.70604. Three samples from the A11 pipe sampling slightly different kimberlite depths have relatively uniform isotopic compositions indicating that the whole rock data may be good proxies for the primary magma compositions. Two economic samples were included in the study, and interestingly have the two highest initial $^{87}Sr/^{86}Sr$ compositions of 0.70615 (A154S) and 0.70604 (A418). Initial $^{143}Nd/^{144}Nd$ (56 Ma) compositions range from 0.51228 to 0.51249 (ε_{Nd} = -1.5 to -5.6). The kimberlites plot between the South African Group I and South African Group II fields, near or within the field for transitional kimberlites (Figure 2-9). These findings are in agreement with

the isotopic results reported previously for a number of Slave Province kimberlites by Dowall et al. (1998).

Rb-Sr Phlogopite Geochronology

From the available sample material, unaltered good quality macrocrystal phlogopite was present in only the A154S and A841 (named Piranha on Ekati side) kimberlite samples investigated in this study, and yields Rb-Sr Model Ages of 55.8±0.6 Ma and 56.7±0.6 Ma, respectively, interpreted to reflect a good estimate for the emplacement age of these pipes (Table 2-3). These Model Ages were calculated using an assumed initial $^{87}Sr/^{86}Sr$ isotopic composition of 0.705. The high $^{87}Rb/^{86}Sr$ ratios (Table 2-3) of both samples makes the calculation insensitive to the choice of initial ratio. For example, if an initial ratio of 0.7025 is chosen, the two ages become 56.2 and 57.0 Ma, respectively. A 1% total analytical uncertainty on the Model Age (2σ) is quoted. Further attempts at determining emplacement ages for several other Diavik kimberlites in this study were unsuccessful because of the absence of perovskite and extreme alteration and replacement of macrocrystal phlogopite.

Discussion

Classification

The Diavik kimberlites are classified as resedimented volcaniclastic > volcaniclastic > olivine-bearing volcaniclastic > mud-bearing volcaniclastic > macrocrystic oxide-bearing hypabyssal kimberlite > sparsely macrocrystic calcite oxide hypabyssal kimberlite > tuffisitic kimberlite breccia. Many of the samples in this study were too altered to properly classify, as the primary minerals were indistinguishable. Diavik kimberlites exhibit many of the mineralogical features as Group 1 kimberlites (Mitchell 1986). Geochemical bulk samples (with C.I. <1.2) are in the range of Group I kimberlites worldwide (Mitchell 1986).

Late Paleocene kimberlite emplacement

Although the Rb-Sr phlogopite ages obtained here agree within analytical uncertainty of previously reported Rb-Sr ages for these pipes (Table 2-4: Moser and Amelin, 1996; Graham et al. 1999), during mining activity at Diavik it has been revealed that there are multiple kimberlite intrusions within a single pipe so more detailed geochronology is required to

establish the duration of this magmatism. In the case of the A154S sample investigated here, the macrocrystal phlogopite was extracted from extremely fresh magmatic kimberlite that was exposed at the 352m level and there is no resolvable age difference among the three Rb-Sr phlogopite ages determined for this pipe so far (Table 2-4).

Previous geochronology studies on Diavik kimberlites and nearby kimberlites on the southern part of the Ekati property have yielded a narrow range of emplacement ages between 54.7-55.8 Ma (Moser and Amelin, 1996; Graham et al, 1999; Creaser et al, 2004). Table 2-4 is a compilation of previous emplacement ages for Diavik kimberlites, as well as the emplacement ages determined in this study. The Late Paleocene emplacement ages obtained in this study are in excellent agreement with previous ages reported from the Diavik property. Figure 2-10 shows that the A154S and A841 samples analysed in this study plot on the A154 Isochron and Age Array "A154AA" from Creaser et al. (2004), whereas the A841 sample plots slightly above the isochron. With the current data, it is possible that the A841 phlogopite emplacement age is slightly older than the A154 Age Array. This isochron was first constructed by Graham et al. (1999), using Rb-Sr analyses from 15 phlogopite samples, and having an isochron age of 55.5 ± 0.7 Ma (2σ). Samples from three kimberlites occurring on the Ekati property (Cardinal, Piranha, and Bison) were found to have indistinguishable ages from the A154N and A154S kimberlites, and were plotted on the isochron of Graham et al. (1999). Creaser et al. (2004) define this reference isochron as the "A154 Age Array" for Late Paleocene kimberlite magmatism at Lac de Gras. Creaser et al. (2004) found that there was evidence for multiple intrusive episodes during the Paleocene and Eocene kimberlite activity in the Lac de Gras area, and that the kimberlites with the highest diamond potential are currently restricted to the 51-53 and the 55-56 Ma periods of kimberlite magmatism. The A154S sample from this study falls into the 55-56 Ma period of magmatism. The A841 sample is slightly older and supports previous conclusions that the older kimberlites are typically not economic (Creaser et al. 2004). Both are well-established ages for the A154S and A841 kimberlites, and complement previously reported emplacement ages (Graham et al. 1999; Moser and Amelin 1996; and Creaser et al. 2004).

When comparing the emplacement ages of the Diavik and Ekati kimberlites, one feature that is different is the range in ages of emplacement. Creaser et al. (2004) and Lockhart et al. (2004) report emplacement ages at Ekati that vary between 45-75 Ma. Furthermore, five apparent age groupings were noted: 48 Ma, 52-53 Ma, 55 Ma, 58.5 Ma, and 64-75 Ma. Creaser et al. (2004) noted the importance of ~53 Ma kimberlite magmatism at Ekati (the Panda Age Array "PAA"), where the highest diamond potential at Ekati is currently restricted to between 51-53 Ma. The Ekati cluster also contains kimberlites with emplacement ages equivalent to the "Diavik A154 Age Array"; located in the region across the SE margin, along the boundary between the Diavik and Ekati properties. The spatially closest kimberlite to the Diavik pipes is the Piranha kimberlite, which intrudes the boundary of both properties (known as A841 on the Diavik property). The Cardinal, Bison and Lynx kimberlites are in close proximity, and are indistinguishable in age (Creaser et al. 2004). Currently, Diavik kimberlites only fall into one age array of Creaser et al. (2004), the A154 Age Array (Figure 2-10). There are many kimberlites of unknown age on the Diavik property so it is still a possibility that there are kimberlites with multiple emplacement ages on the property, however further geochronology is required to evaluate this. The lack of perovskite and phlogopite suitable for age dating makes this a very difficult task with respect to the Diavik kimberlites.

Intrafield variability and comparison

When comparing the mineralogy of the economic and non-economic kimberlites, no large discrepancies exist. The economic kimberlites have a slightly greater macrocrystic population. Economic kimberlites have higher Mg numbers, most likely as a result of increased macrocrystal and phenocrystal olivine content. A similar form and degree of alteration exists across the Diavik property.

Differences do exist when comparing the geochemistry of the two groups. Compositions of economic Diavik kimberlite have close geochemical affinities to estimates for primitive kimberlite (Figure 2-6). The non-economic kimberlites resemble ultrabasic rock types. The economic kimberlites have lower Zr, Hf, Nb and Ta than average Group I kimberlites. The non-economic kimberlites show a greater enrichment in REEs, but both groups

show subparallel patterns of REEs with a specific enrichment in LREE contents (Figure 2-7). Overall, both groups exhibit a smaller than usual K anomaly, and neither group exhibits an Eu anomaly. There is a wide range of variability in the REE content of the two groups, and some of this variability is most likely due to a dilution effect controlled by the abundance of olivine. There are no large differences in the primitive mantle normalized patterns between the two groups (Figure 2-8). The economic kimberlites appear to have a more primitive geochemical signature, whereas the non-economic kimberlites have a more evolved geochemical signature.

The "transitional kimberlite" signature (Figure 2-9) has also been noted by Dowall et al. (2003), where an isotopic study of Hf-Nd-Sr characteristics of Slave Province kimberlites revealed that a "transitional" epsilon Nd signature of 0 to -5 units was exhibited by the Lac de Gras kimberlite samples. The slightly different Sr and Nd isotopic compositions between economic and non-economic kimberlites at Diavik observed in this study has not been noted in previous studies, and may reflect important differences in the primary source rock compositions, or different levels of contamination through the SCLM. The Sr-Nd isotopic values obtained for the Diavik kimberlites can be used to evaluate primary magma compositions. The samples chosen for whole rock isotopes were selected on the basis of the results from the whole rock analyses. In addition, multiple samples from the A11 kimberlite (representing varying depths) were chosen for analyses, and the Sr and Nd isotopic results were relatively uniform. Economic Diavik kimberlites seem to have a more radiogenic isotopic signature, possibly reflecting the enriched nature of their mantle source. Schmidberger et al. (2001) revealed evidence for lithospheric stratification beneath Arctic Canada through Sr-Nd-Pb isotopic systematics of xenoliths hosted by the Nikos kimberlite (Somerset Island, NWT). The isotopic study involved both low temperature (<1100ºC) and high temperature (>1100ºC) peridotite xenoliths and findings revealed that the high temperature xenoliths carried a more radiogenic Sr signature and Nd values which were similar or slightly depleted relative to CHUR. Schmidberger et al. (2001) interpreted this to imply that the mantle root beneath the northern Canadian craton is characterized by a depth stratification in isotopic composition, where the deeper lithosphere exhibited more radiogenic Sr compositions. If the Sr-Nd isotopic

values obtained from the Diavik kimberlites are an accepted proxy for primary magma composition, this would imply a lithospheric source for the kimberlites (and a deeper lithospheric source for the economic kimberlites occurring on the property).

The Ekati property is directly north of the Diavik property and is host to over 150 kimberlites (as of 2004), including five economic pipes. The close proximity of the properties allows for an investigation into their similarities and differences. The two properties are included in Domain III (Heaman et al. 2004), where kimberlites from both properties have similar emplacement ages. Ekati kimberlites are also small, pipe-like bodies, ranging from < 3 to 20 ha, and extend to depths of 400 to 600 m (Nowicki et al. 2004). In depth petrography indicates that Ekati kimberlites also consist mainly of variably bedded VK, and are dominated by olivine, kimberlite ash and exotic sediments such as mud and wood (Nowicki et al. 2004). Similar to Diavik pipes, there is a wide range of kimberlite types at Ekati, including mud-rich VK, mud-rich resedimented VK, olivine VK, TK and HK (Nowicki et al. 2004). TK is rare at Ekati, a feature also seen in the Diavik kimberlites.

Nowicki et al. (2004) report bulk rock geochemistry for the Ekati kimberlites, and there are many similarities to the Diavik kimberlites. Ekati kimberlites also have high MgO contents, and there are also lower Zr and Hf than normal Group I kimberlites, and a strong LREE enrichment noted for the Ekati kimberlites. When comparing the mineralogy, emplacement ages and bulk rock geochemistry of the spatially close Ekati and Diavik kimberlites, there is clear evidence that the kimberlites are related, implying that the source of the parent kimberlite magmas is similar.

Menzies et al. (2004) classified the mantle xenoliths from Ekati, focusing on the peridotitic xenoliths while noting that eclogitic xenoliths are also present in abundance. The two dominant peridotitic mantle xenoliths classified from over 300 samples were garnet-bearing harzburgite and, much more abundant, garnet-bearing lherzolite. There were also rare occurrences of chromite-bearing peridotite, and wehrlite. Using geothermobarometry, Griffin et al. (1999) divided the peridotites into two compositional zones in the central Slave lithospheric mantle. The first, a shallow layer which straddles the diamond-garnet boundary and

is dominated by garnet harzburgite, and a second, deeper layer of garnet lherzolite. This information is critical in evaluating the source and role of kimberlite magmatism in the Lac de Gras kimberlites. It is clear on the Diavik property that there is a large spectrum of magma compositions; however most of the differences may be described by the process of magmatic differentiation, and more precisely, the role of olivine fractionation and accumulation in the magmas. The highly enriched LREEs are most likely present due to mantle metasomatism, which would have occurred either before or at the same time as the kimberlitic melt formation. As mentioned above, the high Ni, Cr, and Mg numbers of the Diavik kimberlites gives some evidence of being derived from, or contaminated with, a depleted harzburgite source. This new information from the bulk rock chemistry of Diavik kimberlites is useful is assessing the source of the primary kimberlitic magmas.

Comprehensive bulk-rock geochemical studies of Group I and Group II South African kimberlites are presented by le Roex et al. (2003), Harris et al. (2004), and Becker and le Roex (2006).

le Roex et al. (2003) reports bulk rock geochemical results from the five major kimberlite pipes in the Kimberley area of South Africa; De Beers, DuToitspan, Buffontein, Wesselton and Kimberley. Many similarities with the Diavik bulk-rock geochemical results are noted. Mg numbers for the Kimberley cluster range from 67-89 (Diavik Mg-number range: 73-87) (le Roex et al. 2003). Very similar to Diavik kimberlites, the macrocrystic varieties have the highest SiO_2 and MgO. Ni concentrations range from 350-1500, overlapping Diavik concentrations. There are positive correlations with Th and U shown from both areas. The chondrite-normalized REE patterns completely overlap, with both exhibiting the pronounced LREE-enrichment. le Roex et al. (2003) reports La concentrations 300-1400x chondrite, and Lu 3-10x chondrite, which is almost identical to the enrichment of the Diavik kimberlites. Negative anomalies are reported for Ti, Sr, K and Rb, while the Diavik kimberlites only show negative anomalies for K, Zr, U and Rb. Importantly, le Roex et al. (2003) identifies the macrocrystic kimberlite samples and olivine phenocryst-rich aphanitic kimberlites as having the least absolute enrichment, and the more-evolved varieties showing the strongest absolute

enrichment, a trend also identified at the Diavik cluster with the non-economic kimberlites exhibiting a strong absolute enrichment. The $^{143}Nd/^{144}Nd_{(initial)}$ ratios for Group I South African kimberlites (on and off craton) range from 0.51249 to 0.51271, whereas $^{87}Sr/^{86}Sr_{(initial)}$ range from 0.70328 to 0.70537 (Becker and le Roex., 2006); characteristic of the "Group I" kimberlites Smith (1983), whereas Diavik Sr and Nd isotopic results display a more transitional signature. Evaluating potential sources of the Group I South African kimberlites, le Roex et al. (2003) utilized semi-quantitative modeling of partial melting processes and determined that the geochemical signatures of the kimberlites could be explained by silicate melt equilibration at low degrees of melting of garnet lherzolite. le Roex (2003) presents a model where a fluid or melt from a deeper sub-lithospheric source region precipitates phlogopite en route to metasomatize the overlying SCLM, and imprinting a K and Rb- depleted signature on a source region which was previously depleted in HREE relative to primitive mantle. This metasomatized region would then undergo small degree partial melting and produce a kimberlite with a trace element signature of the Group I South African Kimberley cluster. This model would imply a deep lithospheric source of kimberlite from South Africa. le Roex advocates a two-stage process in the formation of a Group I kimberlite primary magma, whereby fluids derived from an upwelling mantle plume initially metasomatize the overlying SCLM (which would introduce the geochemical signature of a deeper source into the depleted SCLM). Subsequent melting of this area would then give rise to the kimberlite melt which would carry the OIB-like incompatible trace element ratios that are seen in the Kimberley kimberlite cluster (le Roex et al., 2003).

The trace element geochemical results as well as the Sr-Nd isotopic evidence from the Diavik kimberlites can be used in speculating a magma source for Lac de Gras kimberlites. The isotopic evidence advocates a lithospheric source for the kimberlites, with more radiogenic Sr signatures for the economic kimberlites.

Conclusions

The following can be concluded from the integration of petrography, mineral chemistry, bulk rock geochemistry and geochronology of the Diavik kimberlites:

1- The kimberlite mineralogy is typical of Group I kimberlites.

2- It is useful to compare the intrafield bulk rock geochemistry of minimally contaminated kimberlites. Geochemical bulk samples (with C.I. <1.2) are in the range of Group I kimberlites worldwide.

3- The highly diamondiferous kimberlites at Diavik display a more primitive kimberlite signature, while the remaining kimberlites show varying degrees of evolution.

4- The REE pattern of Diavik kimberlites compares well to other world localities of kimberlites, with a pronounced LREE enrichment.

5- Some of the ranges of REEs at Diavik can be explained by the process of magmatic differentiation of macrocrystal and phenocrystal olivine.

6- Isotopic comparisons of Diavik kimberlites with South African Group I and II kimberlites reveal more of a “transitional” signature.

7- Economic Diavik kimberlites have a slightly more radiogenic isotopic signature, possibly reflecting a source characteristic of the kimberlite magma.

References

Amelin, Y., 1996. Report on U-Th-Pb and Rb-Sr dating of Alberta kimberlites. Kennecott Internal Report, pp. 1-26.

Armstrong, J., Kjarsgaard, B.A., 2003. Geological setting of kimberlites in the Archean Slave Province. 8th International Kimberlite Conference, Slave Province and Northern Alberta Field Trip Guidebook, B.A. Kjarsgaard, (ed); pp. 31-38.

Armstrong, J., Wilson, M., Barnett, R.L., Nowicki, T., Kjarsgaard, B.A., 2004. Mineralogy of primary carbonate-bearing hypabyssal kimberlite, Lac de Gras, Slave Province, Northwest Territories, Canada. Lithos, 76:415-433.

Becker, M., le Roex, A., 2006. Geochemistry of South African On- and Off- craton, Group I and Group II kimberlites: Petrogenesis and Source Region Evolution. Journal of Petrology, 47: 673-703.

Berg, G.W., Carlson, J.A., 1998. The Leslie Kimberlite Pipe of the Lac de Gras, Northwest Territories, Canada: evidence for the near surface hypabyssal emplacement. In: Proceedings of the 7th International Kimberlite Conference, Cape Town, South Africa, 1998, Extended Abstracts. Red Roof Design, pp. 81-83.

Clement, C.R., 1982. A comparative geological study of some major kimberlite pipes in the Northern Cape and Orange Free State. PhD Thesis (2 vols.). University of Cape Town, South Africa.

Creaser, R. A., Grűtter, H., Carlson, J., Crawford, B., 2004. Macrocrystal phlogopite Rb-Sr dates for the Ekati property kimberlites, Slave Province, Canada: evidence for multiple intrusive episodes in the Paleocene and Eocene. Lithos, 76:399-414.

Davis, W.J., Jones, A.G., Bleeker, W., Grütter, H., 2003. Lithosphere development in the Slave craton: a linked crustal and mantle perspective. Lithos, 71:575-589.

Dowall, D.P., Pearson, D.G., Nowell, G.M., Kjarsgaard, B.A., Armstrong, J., Horstwood, M.S.A., 2003. Comparitive geochemistry of kimberlites from the Lac de Gras Field, NWT- and integrated isotopic and elemental study. 8th International Kimberlite Conference Long Abstract.

Eccles, D.R., Heaman, L.M., Luth, R. W., Creaser, R.A., 2004. Petrogenesis of the Late Cretaceous northern Alberta kimberlite province. Lithos, 76:435-459.

Fesq, H.W., Kable, E.J.D., Gurney, J.J., 1975. Aspects of the geochemistry of kimberlites from the Premier Mine and other South African occurrences, with particular reference to the rare earth elements. Physical Chemistry of Earth, 9:686-707.

Field, M., Scott-Smith, B.H., 1998. Textural and genetic classification schemes for kimberlites: a new perspective. Extended abstracts of the VIIth International Kimberlite Conference. Cape Town, South Africa pp. 214-216.

Fraser, K.J., Hawkesworth, C.J., 1992. The petrogenesis of group 2 ultrapotassic kimberlite from the Finsch mine, South Africa. Lithos, 28:327-345.

Graham, I., Burgess, J. L., Bryan, D., Ravenscroft, P.J., Thomas, E., Doyle, B.J., Hopkins, R., K.A. Armstrong., 1999. Exploration history and geology of the Diavik kimberlites, Lac de Gras, Northwest Territories, Canada. Seventh International Kimberlite Conference: Red Roof Design vol.1, pp. 262-279.

Haggerty, S., 1976. Opaque mineral oxides in terrestrial igneous rocks. In: Rumble, D., ed, *Oxide Minerals Short Course Notes*, Mineralogical Society of America, 3:101-300.

Harris, M., le Roex, A.P., and Class, C. 2004. Geochemistry of the Uintjiesberg kimberlite, South Africa: petrogenesis of an off-craton group I kimberlite. Lithos, 74:149-165.

Heaman, L.M., Kjarsgaard, B.A., Creaser, R.A., 2003. The timing of kimberlite magmatism in North America: implications for global kimberlite genesis and diamond exploration. Lithos, 71:153-184.

Heaman, L.M., Kjarsgaard, B.A., Creaser, R.A., 2004. The temporal evolution of North American kimberlites. Lithos, 76:377-397.

Kjarsgaard, B.A., Heaman, L.M., 1995. Distinct emplacement periods of Phanerozoic kimberlites in North America, and implications for the Slave Province. In: Exploration Overview 1995, E.I. Igboji (comp); NWT Geology Division, Department of Indian and Northern Affairs, Yellowknife p. 3-22.

le Roex, A., Bell, D., Davis, P., 2003. Petrogenesis of Kimberley Group I Hypabyssal Kimberlites: Evidence from Bulk Rock Geochemistry. 2003. Journal of Petrology, 44:2261-2286.

Lockhart, G.D., Grütter, H.S., and Carlson, J.A. 2003. Temporal and geomagnetic relationships of Ekati economic kimberlite. Extended abstracts of the 8th International Kimberlite Conference.

Ludwig, K.R., 2003. Isoplot/Ex version 3.0; a geochronological toolkit for Microsoft Excel; Berkeley Geochronology Center Special Publication No. 1a; Berkeley, California.

Menzies, A., Westerlund, K., Grütter, H., Gurney, J., Carlson, J., Fung, A., Nowicki, T., 2004. Peridotitic mantle xenoliths from kimberlites on the Ekati Diamond Mine property, N.W.T., Canada: major element compositions and implications for the lithosphere beneath the central Slave craton. Lithos, 77**:** 395-412.

Mitchell, R.H., Clarke, D.B., 1976. Oxide and sulfide mineralogy of the Peuyuk kimberlite, Somerset Island, N.W.T., Canada. Contributions to Mineralogy and Petrology, 56:157-172.

Mitchell, R.H., 1986. Kimberlites. Plenum Press, New York.

Moser, D., Amelin, Y., 1996. Report on Rb-Sr dating of Alberta kimberlites. Kennecott Internal Report pp. 1-7.

Mitchell, R.H., 1995. Kimberlites, orangeites, and related rocks. Plenum Press, New York.

Mitchell, R.H., Clarke, D.B., 1976. Oxide and sulphide mineralogy of the Peuyuk kimberlite, Somerset Island, N.W.T., Canada. Contributions to Mineralogy and Petrology, 56:157-172.

Nowell, G.M., Pearson, D.G., Kempton, P.D., Noble, S.R., Smith, C.B., 1999. Origins of kimberlites: a hafnium perspective. In: Gurney, J.J., Gurney, J.L., Pascoe, M.D., Richardson, S.H. (eds). Proceedings of the VIIth International Kimberlite Conference. Cape Town: Red Roof Design, pp. 616-624.

Nowicki, T., Crawford, B., Dyck, D., Carlson, J., McElroy, R., Oshust, P., Helmstaedt, H., 2004. The geology of kimberlite pipes of the Ekati property, Northwest Territories, Canada. Lithos, 76:1-27.

Price, S.E., Russell, J.K., Kopylova, M.G., 2000. Primitive magma from the Jericho Pipe, N.W.T., Canada: constraints on primary kimberlite melt chemistry. Journal of Petrology, 41: 789-808.

Smith, C.B., 1983. Pb, Sr and Nd isotopic evidence for sources of southern African Cretaceous kimberlites. Nature, 304:51-54.

Schmidberger, S.S., Simonetti, A., and Francis, D. 2001. Sr-Nd-Pb isotope systematics of mantle xenoliths from Somerset Island kimberlites: Evidence for lithospheric stratification beneath Arctic Canada. Geochimica et Cosmochimica Acta, 65:4243-4355.

Schmidberger, S.S., Heaman, L.M., Simonetti, A., Creaser, R.A., Whiteford, S. 2007. Lu-Hf, in-situ Sr and Pb isotope and trace element systematics for mantle eclogites from the Diavik diamond mine: Evidence for Paleoproterozoic subduction beneath the Slave craton, Canada. Earth and Planetary Science Letters, 254:55-58.

Smith, C.B., Gurney, J.J., Skinner, E.M.W., Clement, C.R., N. Ebrahim., 1985. Geochemical character of South African kimberlites: a new approach based on isotopic constraints. Transactions Geological Society South Africa, 88:267-281.

Steiger, R.H., Jager, E., 1977. Subcommission on Geochronology: convention on the use of decay constants in geo- and cosmo-chronology. Earth and Planetary Science Letters, 36:359-362.

Sun, S., McDonough, W.F., 1989. Chemical and isotope systematics of oceanic basalts: implications for mantle compositions and processes. In: Saunders, A.D. and Norry, M.J. (eds) Magmatism in the Ocean Basins. Geological Society of London, Special Publications 42, 313-345.

Tainton, K.M., 1992. The petrogenesis of Group-2 kimberlites and lamproites from the Northern Cape Province, South Africa. Ph.D. thesis, Cambridge.

Unterschutz, J.L.E., Creaser, R.A., Erdmer, P., Thompson, R.I., Daughtry, K.L. 2002. North American margin origin of Quesnel terrane strata in the southern Canadian Cordillera: Inferences from geochemical and Nd isotopic characteristics of Triassic metasedimentary rocks. Geological Society of America Bulletin, 114:462-475.

Table 2-1. Petrographic classification of Diavik kimberlites

Kimberlite	Description	Classification
A2	very altered	crustal-rich TK
A4	calcite & serpentine segregationary textures, macrocrystic or sparsely macrocrystic.	spinel-rich HK
A5	macrocrystal, high lithic abundance, high alteration	calcite oxide HK
All	no primary mineralogy, juvenile lapilli (cored and uncored)	VK & RVK
A44	sparsely macrocrystic	olivine HK
A154N	juvenile lapilli (cored and uncored), variable alteration	VK, RVK, olivine VK, mud VK
A180	high alteration, pelletal lapilli	olivine VK (85m), TKB (226m)
A418	clast-supported	VK
A840	juvenile lapilli	VK
A841	globular segregationary textures, juvenile lapilli, high alteration	VK & RVK
A1039	pelletal lapilli at 67m	TK, TKB and spinel HK
A1245	heavy alteration, juvenile lapilli	VK & RVK
A1620	abundant altered phlogopite	VK & RVK
A1621	cored juvenile lapilli	mud-rich RVK
ABZ	heavy alteration	mud rich VK & RVK
ANIK	abundant olivine macrocrysts	olivine-rich VK
DD	clay alteration	olivine-rich VK
A154S	two facies, VK at 37m, HK at greater depths, autolithic	mud-rich VK, olivine-rich HK
T19	sparsely macrocrystic	oxide-rich HK
T31	heavy alteration, matrix-supported	serpentine oxide HK
T32	clast-supported with clay matrix	olivine-rich VK & RVK
T33	sparsely macrocrystic, primary calcite, necklace oxides	oxide-rich HK
T146	flow orientation, macrocrystal	phlogopite oxide HK
T237	heavy alteration, segregationary textures	oxide olivine HK
T7E	heavy alteration, clay rich, juvenile lapilli present	olivine-rich VK
C53	heavy alteration, highly fragmental	VK
DVK	heavy alteration, microlitic textures in groundmass	serpentine-rich TK
C42	clay replacement, globular segregationary textures	TKB
A21	heavy alteration, juvenile lapilli present, flow banding	olivine-rich VK
C27	necklace and cumulate textures, juvenile lapilli	olivine-rich VK

TK = tuffisitic kimberlite; TKB = tuffisitic kimberlitic breccia; VK = volcaniclastic kimberlite; RVK = resedimented volcaniclastic kimberlite; HK = hypabyssal kimberlite

Table 2-2. Measured Sr and Nd isotope ratios and calculated parent/daughter ratios for uncontaminated Diavik kimberlites

Sample/ Depth	Rb	Sr	$^{87}Rb/^{86}Sr$	$^{87}Sr/^{86}Sr_{(m)}$	±2SE	$^{87}Sr/^{86}Sr_{(i)}$	Sm	Nd	$^{147}Sm/^{144}Nd$	$^{143}Nd/^{144}Nd_{(m)}$	±2SE	$^{143}Nd/^{144}Nd_{(i)}$
A4 139m	160.1	1500	0.3088	0.70493	0.00003	0.70468	7.0	71.0	0.0598	0.512350	0.000004	0.51233
A154S 351m	100.9	1078	0.2708	0.70636	0.00002	0.70615	5.4	47.8	0.0677	0.512442	0.000006	0.51242
A841 130m	45.8	303	0.4384	0.70610	0.00002	0.70575	3.4	30.3	0.0673	0.512459	0.000008	0.51243
T237 30m	604.7	3845	0.4550	0.70541	0.00003	0.70505	10.4	106.0	0.0593	0.512512	0.000006	0.51249
A11 116m	38.0	361	0.3045	0.70589	0.00002	0.70565	4.0	36.9	0.0647	0.512384	0.000007	0.51236
A11 119m	35.8	406	0.2550	0.70569	0.00002	0.70548	3.9	37.0	0.0639	0.512393	0.000005	0.51237
A11 114m	33.5	339	0.2861	0.70587	0.00003	0.70564	3.4	32.0	0.0652	0.512301	0.000008	0.51228
A418 377m	29.4	312	0.2733	0.70626	0.00002	0.70604	2.5	22.5	0.0673	0.512447	0.000005	0.51242

Element concentrations of kimberlite samples are from ICP-MS (Sm and Nd) and TIMS (Rb and Sr). All initial isotope ratios were calculated using an emplacement age of 56 Ma.
$\lambda^{87}Rb = 1.42 \times 10^{-11}\ a^{-1}$ and measured $^{87}Sr/^{86}Sr$ isotope ratios are normalized to $^{86}Sr/^{88}Sr = 0.1194$.
$\lambda^{147}Sm = 6.54 \times 10^{-12}\ a^{-1}$ and measured $^{143}Nd/^{144}Nd$ isotope ratios are normalized to $^{146}Nd/^{144}Nd = 0.7219$.

Table 2-3. Rb-Sr phlogopite isotope data from the Diavik kimberlites

Pipe	Depth (m)	Lithology	Rb (ppm)	Sr (ppm)	$^{87}Rb/^{86}Sr$	$^{87}Sr/^{86}Sr$	±2SE	Model Age (Ma)
A154S	352m	MK	623.0	4.496	413.4	1.03277	0.00004	55.8
A841	130m	MK	817.1	4.409	559.4	1.15562	0.00004	56.7

Both samples were individual macrocrysts.
MK= magmatic kimberlite

Table 2-4. Summary of emplacement ages of Diavik kimberlites

Kimberlite	Age	±	Method	Reference
A21	55.7	2.1	Rb-Sr phlogopite isochron	Graham et al. (1999), Moser and Amelin (1996)
A418	55.2	0.3	Rb-Sr phlogopite isochron	Graham et al. (1999), Amelin (1996)
A154S	55.5	0.5	Rb-Sr phlogopite WA (3)	Graham et al. (1999), Moser and Amelin (1996)
A154S-mix	54.8	0.3	Rb-Sr phlogopite isochron	Graham et al. (1999)
A154N	56.0	0.7	Rb-Sr phlogopite isochron	Graham et al. (1999), Moser and Amelin (1996)
A154S	55.8	0.6	Rb-Sr phlogopite Model Age	This study
A841	56.7	0.6	Rb-Sr phlogopite Model Age	This study
A841 (Piranha)	55.8	1.6	Rb-Sr phlogopite isochron	Creaser et al. (2004)

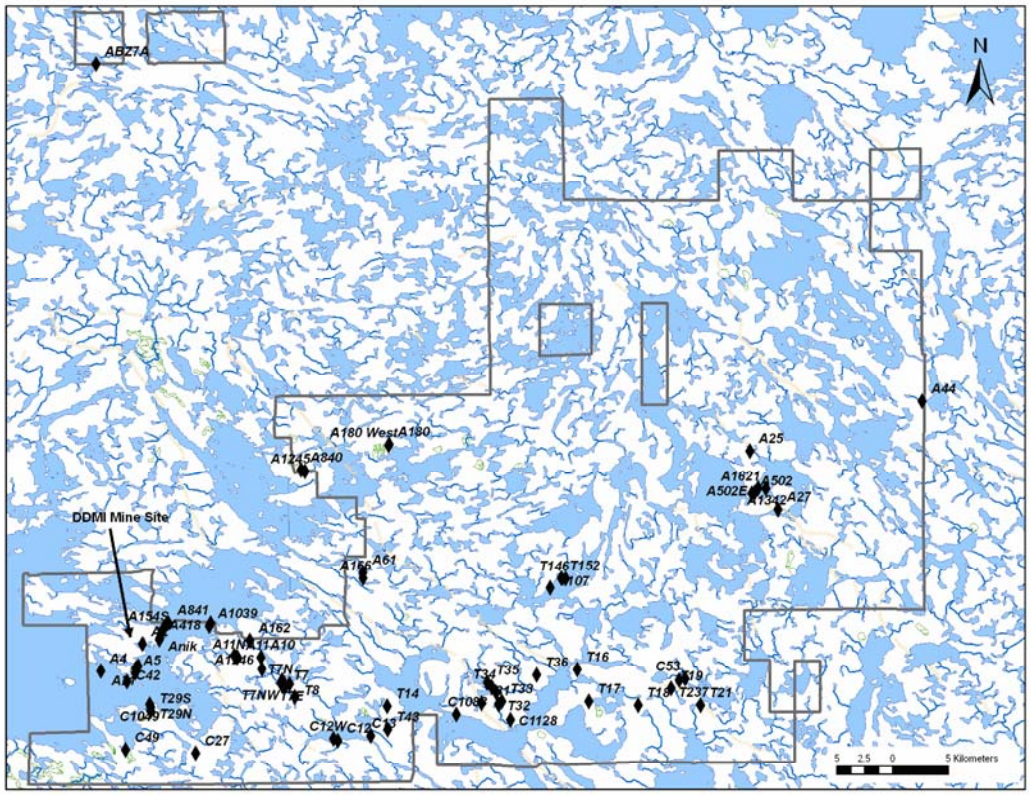

Figure 2-1. Map of the Diavik property, Lac de Gras, NWT (Rio Tinto).

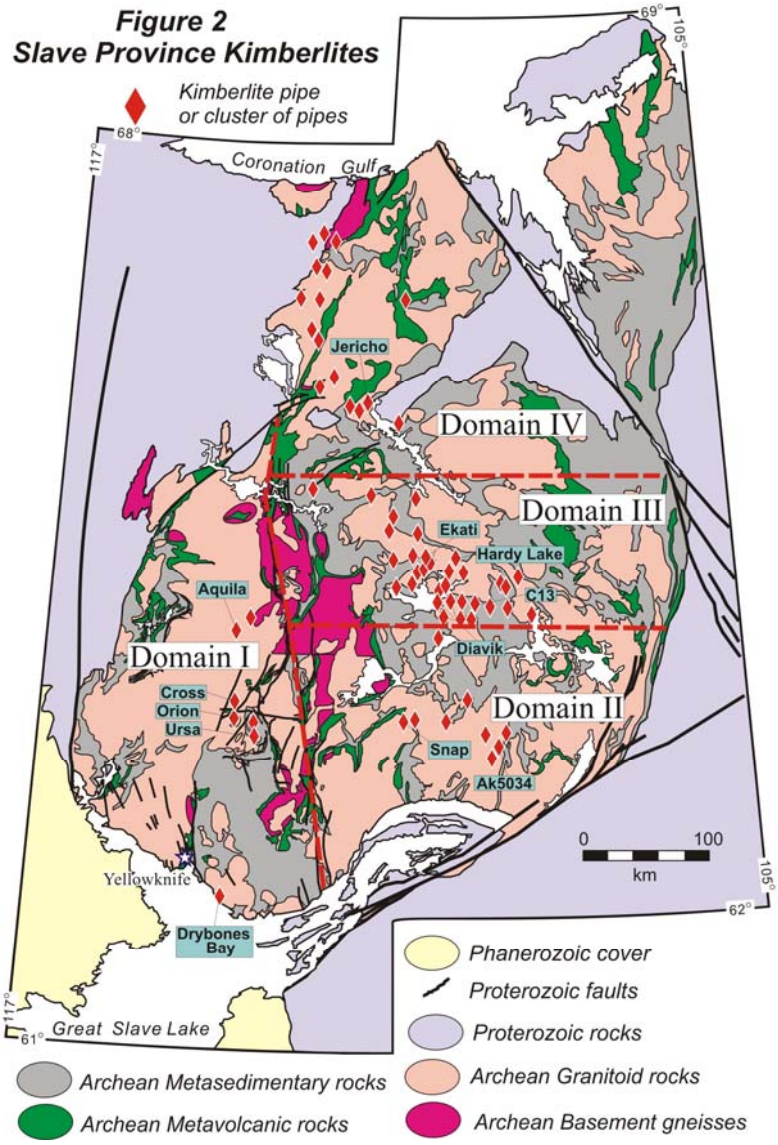

Figure 2-2. Geology map of the Slave craton in Northwestern Canada showing the distribution of kimberlites and subdivisions based on kimberlite emplacement age patterns (after Heaman et al. 2003).

Figure 2-3. Sample of drill core from A154S. Autolithic HK surrounded by a mud-rich VK.

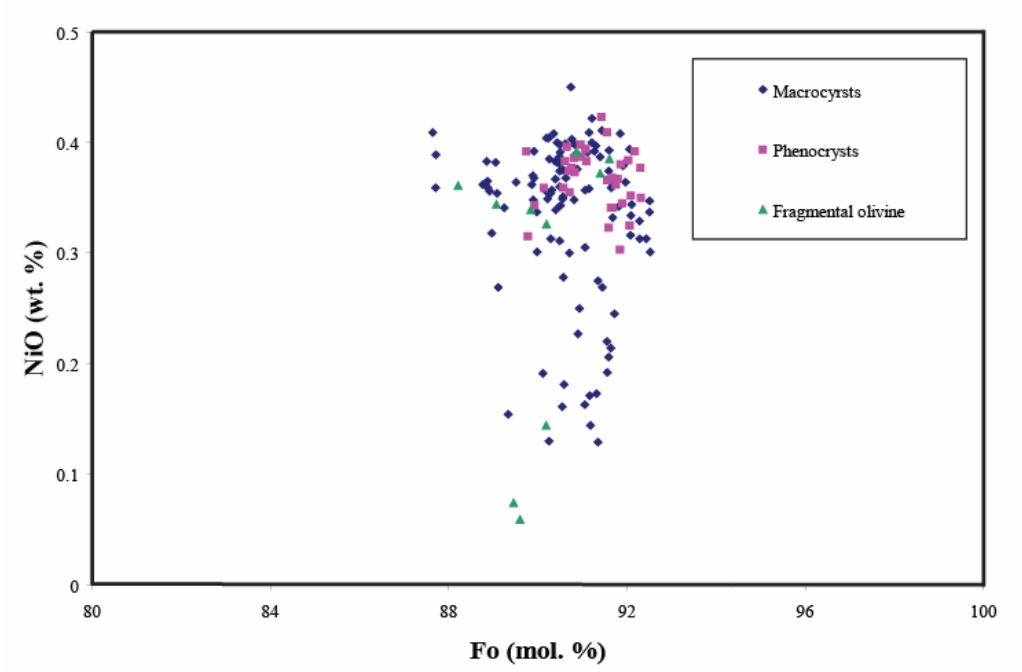

Figure 2-4. Fo (mol. %) vs. NiO (wt. %) for the Diavik kimberlites.

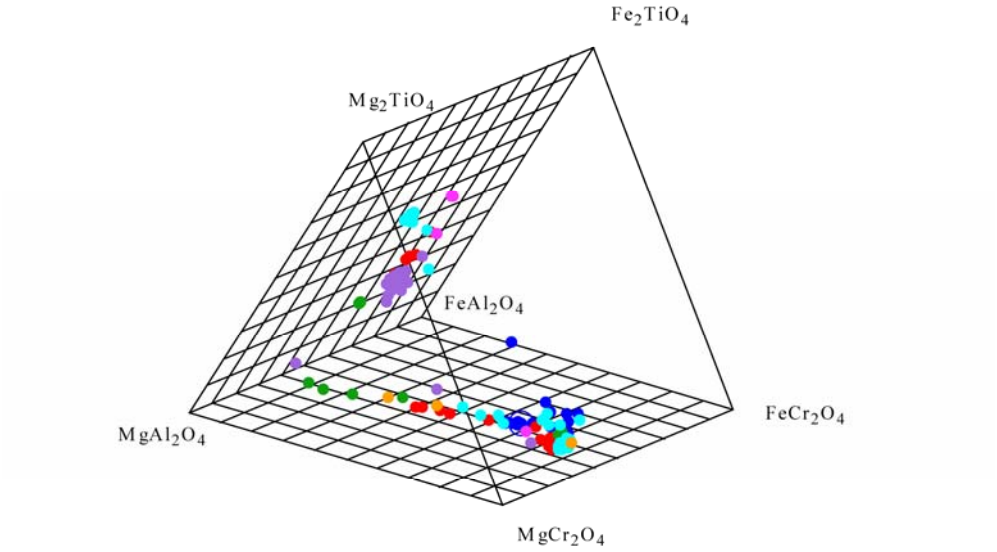

Figure 2-5. A reduced spinel prism with compositions of Diavik spinels representing the magnesian ulvöspinel trend (after Haggerty 1976). Varying colours represent different kimberlite intrusions from the Diavik kimberlites.

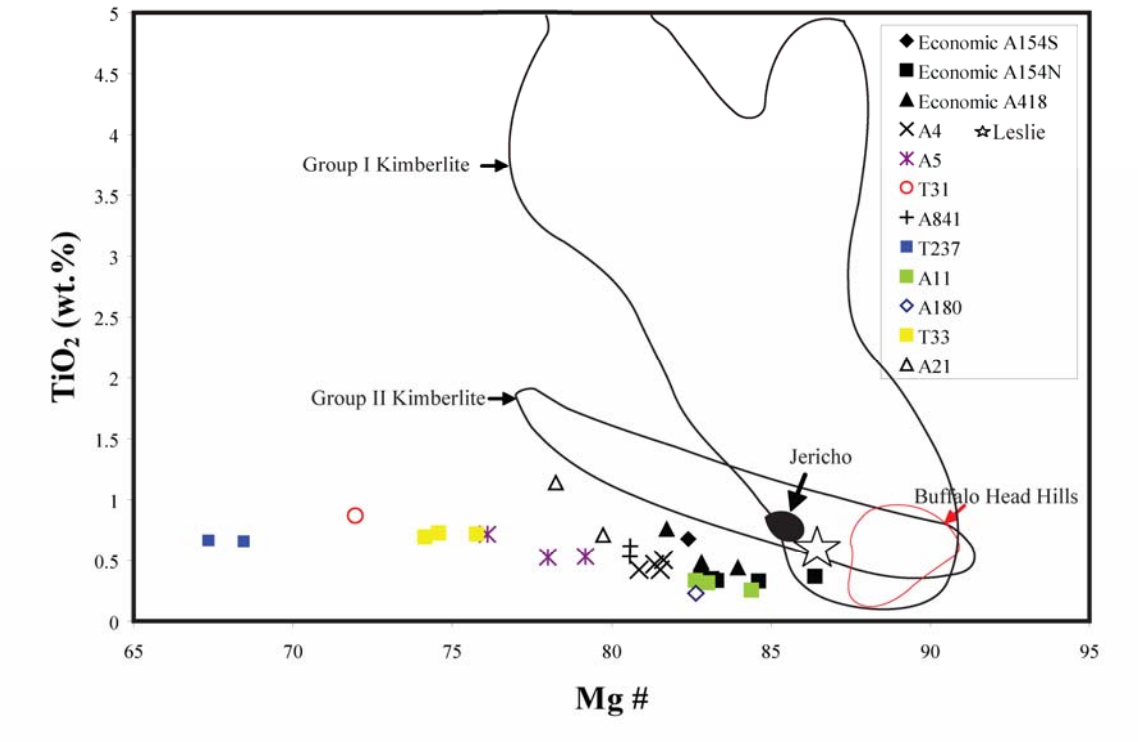

Figure 2-6. Plot of Mg # vs. TiO_2 for whole rock compositions of Diavik kimberlites. Fields for South African Group I and II kimberlites are from Clement (1982) and Smith et al. (1985). Primitive kimberlite compositions are from the Jericho kimberlite (Price et al. 2000); Leslie kimberlite (Berg and Carlson 1998); Buffalo Head Hills kimberlites (Eccles et al. 2004).

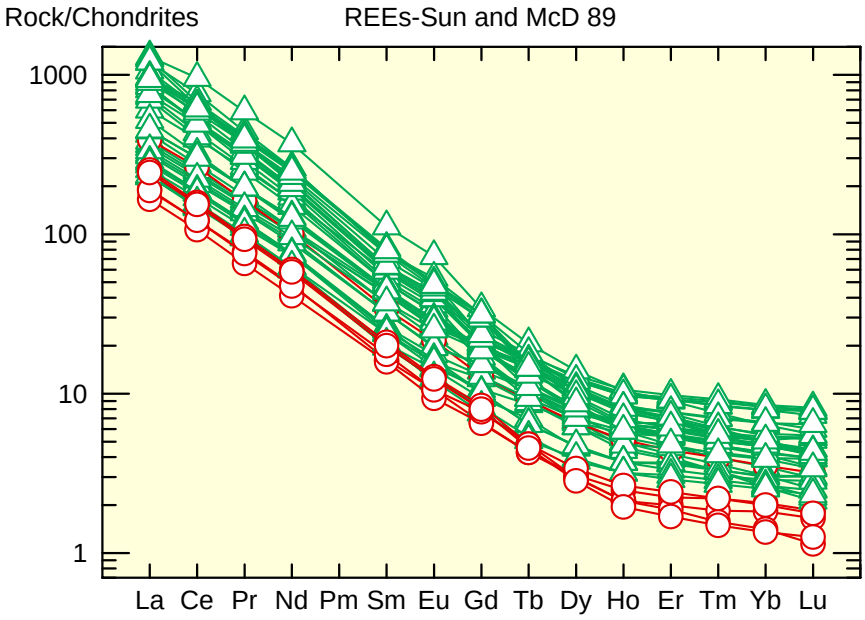

Figure 2-7. Chondrite normalized trace element pattern in Diavik kimberlites. Diavik economic samples are shown as circles, non-economic samples are shown as triangles. Normalizing values are from Sun & McDonough (1989).

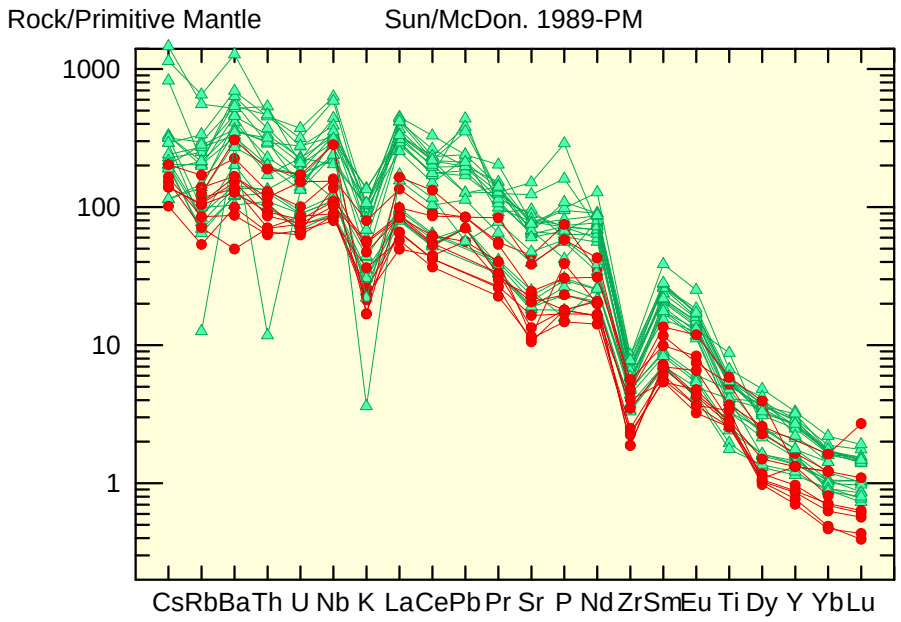

Figure 2-8. Primitive mantle normalized trace element pattern in Diavik kimberlites (only kimberlites with C.I. <1.2 are shown). Diavik economic samples are shown as solid circles, non-economic samples are shown as shaded triangles. Normalizing values are from Sun & McDonough (1989).

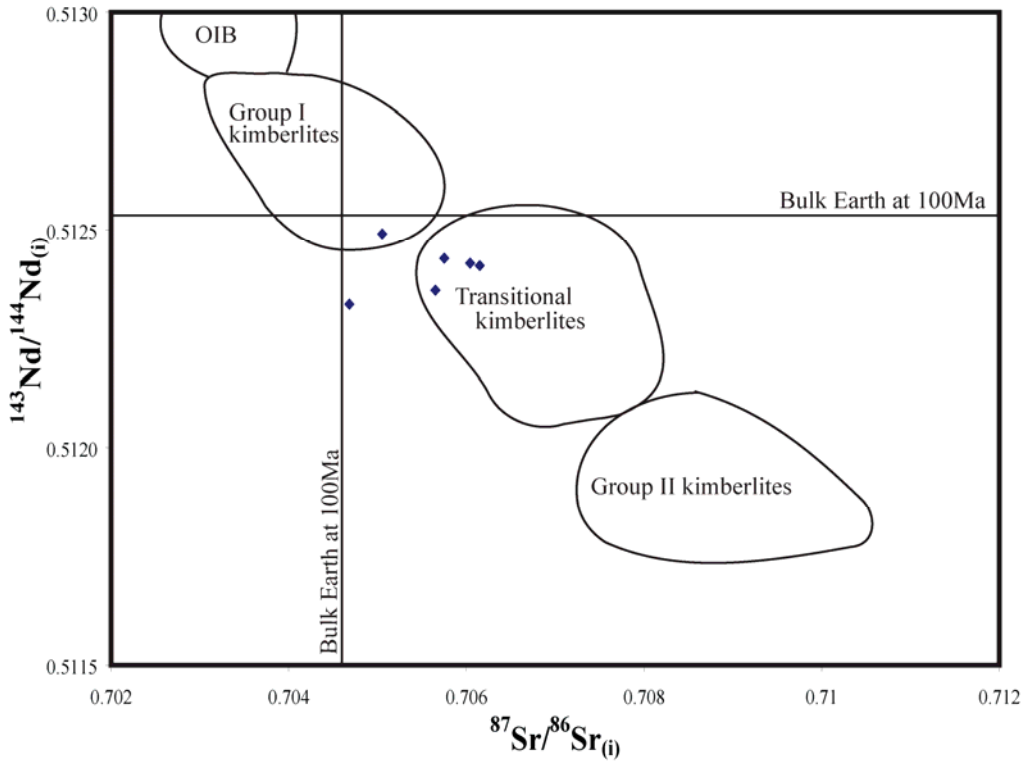

Figure 2-9. Initial $^{143}Nd/^{144}Nd$ and $^{87}Sr/^{86}Sr$ isotopic compositions for Diavik kimberlite samples. Solid diamonds represent non-economic kimberlite samples, while open diamonds represent economic samples from A154S and A418. South African Group I, II and Transitional kimberlitic fields are from Becker and Le Roex (2006) and references herein; Smith (1983); Fraser and Hawkesworth (1992); Tainton (1992); Clark (1994); Nowell et al. (1999).

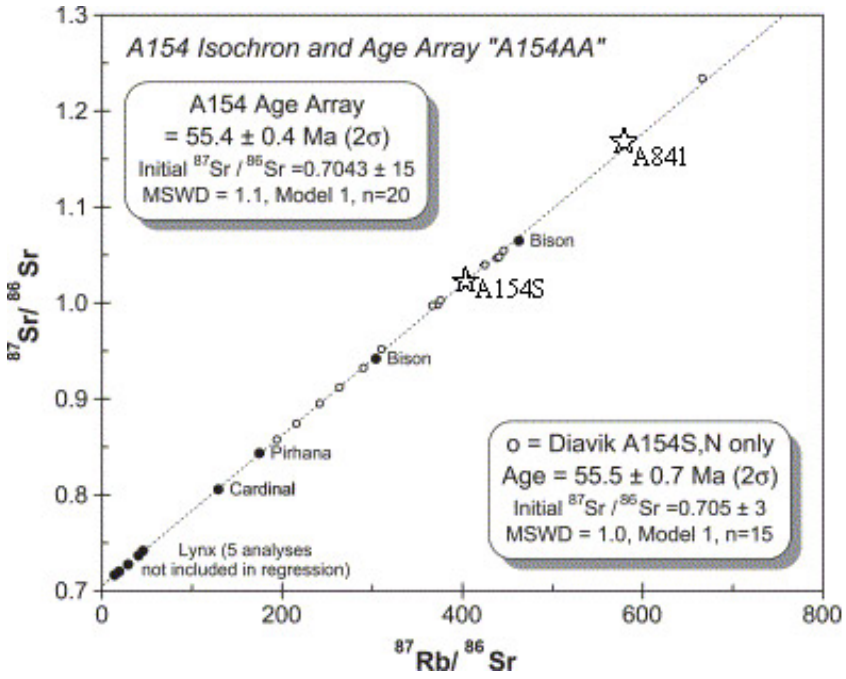

Figure 2-10. Rb-Sr isochron diagram showing phlogopite analyses for kimberlites on the Diavik property and analyses for four kimberlites from the nearby southern Ekati property (Bison, Cardinal, Piranha and Lynx). The two phlogopite analyses for Diavik kimberlites from this study are shown with a star symbol. Open circles are fractions used to derive the A154 isochron (dotted line). All the analyses combined are referred to as the A154 Age Array ("A154AA"). Sources: Graham et al. (1999), Creaser et al. (2004) and references herein.

Chapter 3

The Churchill Kimberlite Field, NU, Canada: Petrography, Mineral Chemistry, and Geochronology*

Zurevinski, S.E., Heaman, L.M., Creaser, R. A., Strand, P.

(*the contents of this chapter are published in the Canadian Journal of Earth Sciences v.45, 1039-1059. doi:10.1139/E08-052)

Introduction

After the initial discovery of diamond-bearing kimberlites in 1991 in the Slave province, exploration programs have discovered numerous kimberlite occurrences across the continent; many occur within discrete fields or clusters. As of 2002, over 600 kimberlites had been identified in North America (Kjarsgaard and Levinson 2002). Some of the larger kimberlite fields include: Attawapiskat (Ontario); Buffalo Head Hills (Alberta); Finger Lakes (New York); Fort à la Corne (Saskatchewan); Kirkland Lake (Ontario and Quebec); Lac de Gras (Northwest Territories); Somerset Island (Nunavut); State Line (Colorado and Wyoming); and Timiskaming (Ontario and Quebec). Some of the more recent discoveries include: Northern Slave Province (Nunavut); Otish Mountains (Quebec); Victoria Island (Nunavut), and Churchill (Nunavut).

Emplacement ages have been determined for many North American kimberlites (Heaman et al. 2004) and this magmatism spans a period of >1 billion years ranging from Mesoproterozoic kimberlites in the Lake Superior and James Bay lowlands (Ontario) areas to Eocene kimberlites in the Lac de Gras area, Northwest Territories. (Heaman et al. 2004). Heaman et al. (2004) subdivided North American kimberlite occurrences into five age domains: 1) Mesoproterozoic kimberlite province (Central Ontario); 2) Neoproterozoic/Cambrian Labrador Sea province (Northern Quebec and Labrador); 3) Eastern Jurassic province; 4) central Cretaceous corridor; and 5) Western mixed domain (Eocene to Neoproterozoic). Using the observed spatial and temporal patterns of kimberlite emplacement, Heaman et al. (2004) proposed at least three different origins for North American kimberlites; 1) intracontinental rifting, 2) changes in plate stress during subduction and 3) mantle plume hotspot tracks. For example, the Mesoproterozoic kimberlite province in central Ontario coincides with the timing of 1.1 Ga intracontinental rifting in the Lake Superior region (Midcontinent Rift); the 605-550

Ma Labrador Sea–West Greenland province kimberlites and related rocks (Heaman et al. 2004; Heaman 2005; Tappe et al. 2006) were emplaced after the opening of the Iapetus Ocean at ~615 Ma (Kamo et al. 1989); the 103-94 Ma central Cretaceous corridor was interpreted to reflect changes in plate geometry during the subduction of the Kula-Farallon plate (Heaman et al. 2004); and the eastern Jurassic/Triassic province age progression to be an example of kimberlite magmatism that may have been triggered by passage of one or more mantle plumes beneath eastern North America associated with the opening of the North Atlantic ocean (Heaman and Kjarsgaard 2000).

The NW-SE trending corridor of Jurassic/Triassic kimberlite magmatism in eastern North America includes the Kirkland Lake, Timiskaming and Attawapiskat fields with a progressive SE younging of kimberlite magmatism from ~180 Ma (James Bay lowlands) to ~135 Ma for some kimberlites in the Timiskaming field (e.g. the 134 Ma Glinkers kimberlite). In addition, an older 214-196 Ma set of kimberlite dykes was reported from the Rankin Inlet area (Miller et al. 1998; Heaman and Kjarsgaard 2000) and their location further extends this corridor ~800 km NW. Both the location and age of this kimberlite magmatism matches well the predicted location for the continental extension of the Great Meteor mantle plume hotspot track. A prediction of this hypothesis is that the hotspot track may continue even farther northwest and the age of kimberlite magmatism would continue to be progressively older in this direction. However, very little is known about the age and origin of Churchill kimberlite field. In this study, we present the first detailed investigation of the Churchill kimberlites; including mineralogy, petrology, mineral chemistry, and geochronology. Precise U-Pb perovskite and Rb-Sr phlogopite ages are reported for 27 Churchill kimberlite occurrences, which constitutes a significant contribution to the existing geochronological database for North American kimberlites. By integrating salient aspects of the petrography, geochemistry and geochronology of Churchill kimberlites, we speculate on the origin and mantle sources for these kimberlite magmas.

General Geology

The Churchill kimberlite field is located in the Churchill Province cratonic rocks, immediately west of Hudson Bay between the communities of Rankin Inlet and Chesterfield Inlet, Nunavut (Figure 3-1). The Churchill Province is divided into the Rae and Hearne structural provinces, which consist dominantly of Archean rocks (Hoffman 1990). However the region differs from cratons *sensu stricto* in their variable but widespread Paleoproterozoic reactivation (Percival 1996). The Churchill Kimberlite field is immediately underlain by rocks of the metamorphosed Archean Rankin Inlet Group. The Rankin Inlet Group is composed of metamorphosed and deformed sequences of mafic and felsic volcanics, sediments, iron formation, gabbros, and granite intrusions (Tella 1994). There is a W-NW trending series of faults that offset the Archean rocks and are associated with significant gold mineralization (Carpenter et al. 2005). Until recently, gold and base metals have been the main focus of exploration on the Churchill kimberlite property. The Churchill Province has a complex Quaternary history. Glacial till and sediments were deposited over much of Northern Canada (18,000 and 6500 years ago) in association with the Laurentide Ice Sheet (Dyke and Prest 1987). Areas proximal to the Hudson Bay coast were inundated with marine waters (Sankeralli 2004). This resulted in the reworking of primary glacial sediments (tills, glaciofluvial deposits), followed by the deposition of marine sediments. The result is a thick (10-30 m) cover of overburden across the Churchill province (Balzer 2004). This has been extremely beneficial for till sampling methods and the identification of indicator mineral corridors throughout the area.

The discovery of the Churchill kimberlite field (Churchill Diamond Property) was announced in 2003 by Shear Minerals Ltd., along with partners Stornoway Diamond Corp and BHP Billiton. Today the project encompasses an area in excess of 2.0 million acres. In addition to the early discovery of kimberlite float and outcrops, indicator mineral results defined several promising corridors for further kimberlite discovery on the property. At present, 79 kimberlites have been confirmed by drilling and more than 100 intrusions have been identified on the property through geophysical surveys (Figure 3-1). Churchill kimberlites have a variety of magnetic expressions (i.e. magnetic lows and magnetic highs), while the morphology of the

kimberlite intrusions ranges from narrow dykes, to irregular expressions, to larger (250m x 400m) "pipe-like" bodies. Currently there are two types of kimberlite on the Churchill property. Type A are low economic interest kimberlites drilled prior to 2006; and Type B are high interest intrusions, discovered between 2006 and 2007. The two types of kimberlite differ in their geophysical signature, petrography, mineral chemistry and diamond content (Strand et al. 2008). This study deals with the Churchill Type A kimberlites.

Previous Studies

Immediately south of the Churchill kimberlite field lies the Meliadine property where the discovery of ~11 kimberlite bodies was announced in 2003 (Miller et al. 1998). During drilling at the Meliadine gold deposit (~24 kilometres north of Rankin Inlet on the northwest coast of Hudson Bay), a few narrow kimberlite dykes were intersected, initiating the staking rush in the area. Miller et al. (1998) described subvertical tabular dykes consisting mainly of hypabyssal kimberlite. Petrographic results of the 1998 study were interpreted to indicate that there are two generations of both olivine and phlogopite, primary and secondary serpentine, primary calcite, and accessory minerals such as perovskite, spinel, Mg-ilmenite, apatite, pyrite, chalcopyrite, galena and uraninite. Xenolithic material was interpreted to be derived from local metasediment and metavolcanic host rocks. The kimberlite dykes were classified as an evolved calcite-rich hypabyssal kimberlite (Miller et al. 1998).

Emplacement ages were previously reported for two kimberlite dykes in the Rankin Inlet region; a Rb-Sr phlogopite age of 214.0 ± 1.0 Ma (2σ errors) was reported from one dyke (Davis and Miller 2001) and a U-Pb perovskite age of 196.2 ± 2.8 Ma was reported from a second dyke on the Meliadine property (Heaman and Kjarsgaard, 2000). These early age results indicated that the Late Triassic-Early Jurassic kimberlite event spanned at least 15 Ma. Miller et al. (1998) related the emplacement of the Rankin Inlet kimberlite dykes to Late Triassic to Early Jurassic regional reactivation in the Western Churchill Province. In contrast, Heaman and Kjarsgaard (2000) interpreted the Late Triassic-Early Jurassic ages at Rankin Inlet as part of a progression in kimberlite ages along a southwest trending zone from Rankin Inlet (214-192

Ma) through the Attawapiskat field in the James Bay lowlands (180 Ma) to the Kirkland Lake (165-152 Ma) and Timiskaming (154-134 Ma) kimberlite fields.

Analytical Methods

Samples

The petrographic and geochemical results presented here are based on the investigation of approximately 150 thin sections prepared from over 100 drill core specimens, some kimberlite outcrop samples plus a few kimberlite float samples.

Electron Microprobe

Polished thin sections of selected samples were prepared for analysis on the electron microprobe. EPMA was performed using a JEOL JXA-8900 Superprobe at the University of Alberta. Mineral compositions of selected samples were measured using wavelength-dispersion spectrometry (WDS). Analyses were acquired for 20-90 seconds with an accelerating voltage of 20 kV, and a 20 nA beam current. The following well-characterized natural and synthetic standards were employed for analysis: albite (Na), apatite (P), metallic V and Ni, pyrope (Mg, Al, Si), diopside (Ca), ilmenite (Mn), kaersuitite (K, Fe, Ti), and chromite (Cr). Accuracy of major elements is better than 1%.

Isotopic Methods

U-Pb Perovskite

The samples investigated consisted of small pieces of 2" drill core and were pulverized using a jaw crusher and shatter box. Perovskite was isolated using standard density (Methylene Iodide) and magnetic (Frantz Isodynamic Separator) mineral separation techniques. Perovskite fractions consisting of up to 400 grains were hand picked using a binocular microscope. The analytical procedures for purifying uranium and lead by anion exchange chromatography and determining their isotopic compositions using a VG354 thermal ionization mass spectrometer are outlined by Heaman and Kjarsgaard (2000). In most cases the amount of perovskite available was sufficient for only one analysis, therefore the $^{206}Pb/^{238}U$ age is taken as the best estimate for the timing of perovskite crystallization as this age is least sensitive to the common lead correction. Atomic ratios are corrected for mass spectrometer fractionation (Pb-

0.088%/amu; U- 0.155%/amu), blank (5 pg Pb; 1 pg U), and spike. In addition, the $^{206}Pb/^{238}U$ ratios were corrected for the presence of initial common Pb using the two stage average crustal Pb model of Stacey and Kramers (1975). Large uncertainties for the assumed initial Pb composition have been assigned (1% on the $^{206}Pb/^{204}Pb$ ratio), such that the error associated with single $^{206}Pb/^{238}U$ perovskite ages reported in Table 3-6 reflect the propagation of these uncertainties. For samples where two or more perovskite analyses were obtained, ages are calculated using a weighted mean $^{206}Pb/^{238}U$ age. The errors reported in Table 3-6 are quoted at two sigma and the uncertainties associated with age determinations are quoted at two sigma ($\lambda^{238}U$- 1.55125×10^{-10} year^{-1}; $\lambda^{235}U$- 9.8485×10^{-10} year^{-1}; Jaffey et al. 1971).

Sr Isotopic Studies (Perovskite)

The Sr isotopic composition of perovskite was determined on the same fractions prepared for U-Pb geochronology. The washes containing Sr from the uranium and lead purification were loaded onto standard cation exchange columns, with an initial separation of the rare earth elements (plus Sr), then further purification and isolation of Sr (Holmden et al. 1996). The purified Sr was loaded onto a single Re filament employing a tantalum gel loading method (Creaser et al. 2004) and the Sr isotopic compositions were determined using a Sector54 thermal ionization mass spectrometer in static multi-collector mode. Accuracy of the Sr isotopic composition was monitored using the NIST SRM 987 Sr isotopic standard, and all isotopic ratios are reported relative to a value of 0.71025.

Rb-Sr Phlogopite

Unaltered macrocrystal phlogopite was extracted from small pieces of 2" kimberlite drill core. The macrocrystal phlogopite was extricated by hand picking from the drill core using a tungsten carbide tipped tool, without crushing or pulverizing the entire sample. Phlogopite macrocrysts selected for Rb-Sr analysis were examined using a binocular microscope and preliminary cleaning was conducted using fine tipped tweezers to eliminate altered material, chlorite rims, and any adhering kimberlitic matrix. The analytical procedures for Rb-Sr phlogopite dating and sequential leaching techniques are given by Creaser et al. (2004). Isotopic analysis of both elements was performed using a Sector54 Thermal Ionization Mass

Spectrometer, a single Re filament, and the tantalum gel loading method. All analyses are presented corrected relative to a value of 0.71025 for a SRM987 Sr isotopic standard. The measured value of SRM987 over the period of analysis ranged from 0.71016 to 0.71019. Blanket errors of ± 1.5% and 0.005% (2 sigma) were assigned to the $^{87}Rb/^{86}Sr$ and $^{87}Sr/^{86}Sr$ ratios, respectively and ages were calculated using Isoplot version 3.0 (Ludwig 2003). All isochron and model ages were calculated using a decay constant of $\lambda^{87}Rb = 1.42 \times 10^{-11}$ yr^{-1} (Steiger and Jager 1977). Phlogopite Rb-Sr model ages are calculated using an assumed initial $^{87}Sr/^{86}Sr$ ratio of 0.7035. This value is considered representative of the initial Sr isotopic composition of Churchill kimberlites, based upon both the initial $^{87}Sr/^{86}Sr$ values derived from Churchill phlogopite Rb-Sr isochrons, as well as Churchill kimberlite perovskite results.

Results

Assessment of drill core samples

Exploration drilling intersected kimberlite at average depths of 10 to 20m. Unaltered Churchill kimberlite is very competent, ranging in colour from a grey to dark green to black. There is a large variation in the amount of alteration present. Olivine, ilmenite and phlogopite are the most common macrocrysts visible in drill core. The kimberlite hosts crustal xenoliths including granite, granodiorite and some carbonates, which are commonly angular clasts randomly distributed in the kimberlite, exhibiting thin reaction rims. A few of the carbonate xenoliths exhibit chlorite alteration rims. Some kimberlites are extremely altered, entirely masking the primary mineralogy. Kimberlite autoliths occur in some specimens, and were examined in detail in thin section. Both uniform and segregationary textures are present, and with most autoliths are matrix-supported. One kimberlite sample contained an aphanitic hypabyssal kimberlite autolith exhibiting a preferred flow orientation. The majority of kimberlite is sparsely macrocrystic to macrocrystic. Two phlogopite megacrysts were identified, one was found to be a crustal component, while the other was of kimberlitic origin. One occurrence of an ilmenite megacryst (6 cm diameter) has been documented. Megacrystal olivine has been identified in three kimberlite samples (CD-01 (2), KD235). Mantle xenoliths

are rare in the Churchill kimberlites studied here, being identified in only a few of the intrusions.

Petrography and mineral chemistry

The macrocrystal (0.5-10 mm) population is dominated by olivine, phlogopite, with lesser ilmenite. Groundmass mineralogy mainly consists of olivine, phlogopite, ilmenite, monticellite, perovskite, spinel, primary and secondary calcite, primary and secondary serpentine, apatite, chlorite, and rare accessory minerals such as djerfisherite $[K_6(Cu,Fe,Ni)_{24}S_{26}Cl]$, zircon and pyrite.

Table 3-1 summarizes the petrography of the Churchill kimberlites. The kimberlites are formally classified as sparsely macrocrystal oxide-rich carbonate hypabyssal kimberlite, with varying amounts of phlogopite, serpentine, monticellite, and carbonate. Samples which were too altered to be classified are reported as inconclusive.

Olivine

Olivine occurs in three parageneses in Churchill kimberlite: macrocrystal, phenocrystal (including microphenocrystal), as well as three rare occurrences of rounded megacrystal olivine. In kimberlite CD-01, one megacrystal olivine was found to have a small orthopyroxene inclusion. Churchill olivine megacrysts have Mg/(Mg+Fe)=0.83-0.84, and low NiO(0.07 to 0.16 wt % oxide) and Cr_2O_3 below detection limits. This Fe-enriched olivine is not typical of kimberlitic olivine and is interpreted as xenocrystic.

Anhedral macrocrystal olivine is the dominant macrocryst occurring in the Churchill kimberlites and its abundance is quite variable (ranging from 5-45 modal %). It is variably altered to serpentine and lesser calcite. Devoid of zoning, the macrocrysts commonly have dark optically distinct alteration rims. Due to this extensive alteration, many rims of the macrocrystal olivine could not be analyzed. Macrocrystal olivines have a small variation in Fo content from Fo90 to Fo92, low Cr_2O_3 (<0.08 wt. %), and NiO (0.11-0.40 wt %).

Phenocrystal (including microphenocrystal) euhedral to subhedral olivine are < 0.4 mm in length, more commonly <0.2 mm, and are variably altered at their margins and/or serpentinized along fractures, many are entirely pseudomorphed by serpentine and calcite. The

abundance of olivine in the groundmass of Churchill kimberlites varies, ranging from trace amounts up to 30% of the modal groundmass. Cr_2O_3 contents vary from 0.01 to 0.12 wt.%, while NiO ranges from 0.30-0.40 wt %. Ranging from Fo90- Fo91, compositions of both phenocrystal and microphenocrystal olivine overlap with the compositions of macrocrystal olivines. Overlapping compositions are common in kimberlitic olivines, providing some evidence that macrocrystal olivine crystallized directly from the kimberlite magma.

Phlogopite

The Churchill kimberlites contain megacrystal, macrocrystal, and microphenocrystal groundmass phlogopite. Rare anhedral megacrystal phlogopite (up to 4 cm in length) was identified in the drill core. Their presence in altered crustal xenolith-rich drill core, and their extensive alteration/complete replacement, suggest that their origin is from crustal contamination.

The majority of phlogopite macrocrysts are 5mm to 1.5 cm in length (Figure 3-2). The macrocrysts exhibit a range of alteration, including rounded macrocrysts with chlorite alteration along the cleavage planes, to pseudomorphs of chlorite/clay after phlogopite. The abundance of macrocrystal phlogopite averages around 1 modal %, with a few rare samples containing up to 10 modal %. Most macrocrystal phlogopite is slightly rounded to well-rounded, commonly kink-banded, and in some cases exhibiting epitaxial overgrowths (Figure 3-2a). An intriguing feature commonly seen in Churchill kimberlites is rounded macrocrystal phlogopite surrounded by a necklace of spinel and perovskite (Figure 3-2b). Mitchell (1986) attributes this spinel texture to be formed during a resorption processes. The macrocrystal phlogopite exhibits normal pleochroism and is typically relatively fresh. Representative compositions of the macrocrystal phlogopite are shown in Table 3-2. The Mg/(Mg+Fe) ratio for the macrocrystal phlogopite ranges from 0.86-0.88, with no tetrahedral site deficiency present.

Microphenocrystal phlogopite is less abundant, and in some cases non-existent. Comprising a small portion of the groundmass, the phlogopite is commonly lath shaped exhibiting distortion features such as kink banding. With the exception of a few samples, all of the microphenocrystal phlogopite at Churchill are randomly oriented within the groundmass of

the kimberlite. Some of the larger microphenocrystal phlogopite displays replacement with calcite/chlorite along cleavage planes. Representative compositions of the microphenocrystal phlogopites are shown in Table 3-3. There are intergrain variations between the core and the rim of some phlogopite grains. Columns 8 and 9 (Table 3-3) show a core to rim variation characteristic of groundmass phlogopite, with a core of typical magnesian phlogopite and a tetraferriphlogopite rim. The Mg/(Mg+Fe) ratio for the groundmass phlogopite is 0.814 - 0.958, and there is a tetrahedral site deficiency ranging from 0 (no deficiency) to 14% deficient. Smith et al. (1978) designate more magnesian [Mg/(Mg+Fe) = 0.82-0.93] and Ti-poor groundmass phlogopite as Type-II micas. The groundmass phlogopites are generally TiO_2-poor, common for kimberlitic type-II groundmass phlogopite.

The majority of mica in Churchill kimberlites is macrocrystal phlogopite. According to Mitchell (1986), in many serpentine/calcite kimberlites macrocrystal phlogopite forms the bulk of the mica population, and therefore groundmass micas may be just a minor late stage phase. Mitchell (1986) suggests there is a hiatus in the crystallization sequence of phlogopite. A similar relationship has been reported at the Elwin Bay kimberlite, Somerset Island (Mitchell, 1986). The macrocrystal phlogopite differs from the groundmass phlogopite in the examined samples as they contain 1-3% TiO_2, 4-7% FeO, and 0-2% Cr_2O_3. Figure 3-3 is an Al_2O_3 versus TiO_2 bivariate plot which demonstrates compositional trends of micas in kimberlites and related rocks (such as minettes, lampröites and orangeites). It demonstrates that most Churchill phlogopite (both the macrocrystal and groundmass) plot in the primary phlogopite field, and subsequently follows the kimberlitic phlogopite evolutionary trend (after Mitchell 1986, 1995).

Spinel

Spinel in Churchill kimberlites is generally small (<0.1 mm) and occurs mainly as a primary groundmass mineral (can comprise up to 20 modal % of the groundmass). The abundance of spinel varies throughout the kimberlite, as it may occur as accumulations in the groundmass. This is a common feature in kimberlites and is attributed to flow differentiation processes (Mitchell 1986). Spinel grains are euhedral to subhedral and commonly display oscillatory zoning. There is a clear spatial relationship of spinel-group minerals occurring

alongside perovskite. Commonly the two minerals surround a larger phenocryst or macrocryst, such as olivine or phlogopite in a necklace texture (Figure 3-2b). Atoll spinels are also common, occurring with a chromite core, a Ti, Mg, and Al-enriched rim, followed by evidence of corrosion and resorption resulting in a calcite lagoon, and rimmed by magnetite (Figure 3-4).

Representative compositions of spinel-group minerals are presented in Table 3-4. Spinel compositions follow the "magmatic trend 1" or "magnesian ulvöspinel trend" (after Mitchell and Clarke 1976) (Figure 3-5). Mitchell (1986) regards the "magmatic trend 1" as being confined to serpentine, calcite, monticellite, and diopside kimberlites. Overall the compositional trend across the spinel prism shown in Figure 3-5 represents a Fe- and Ti-enrichment, crystallizing TiMACs (Titianium-Magnesium-Aluminium Chromites), to MUMs (Magnesian ulvöspinel-Ulvöspinel-Magnetites) to Magnetite. Magnesian ulvöspinel is now known as qandilite (IMA1980-046) after Al-Hermezi (1985)). There is a discontinuum in the crystallization sequence of spinels, shown in Figure 3-5, where there are two distinct compositional groups of spinels representing the initial and the final portions of the spinel crystallization sequence. This has also been reported in kimberlitic spinel compositions from the Elwin Bay and Peuyuk kimberlites, Somerset Island (Mitchell and Clarke 1976).

Perovskite

Two morphologically distinct varieties of perovskite occur as a minor groundmass phase. Smaller (20-40 μm), cubo-octahedral orange-brown perovskite is typically more abundant and occurs in association with spinel-group minerals, which appear to be locally concentrated by magmatic processes. Smaller perovskite and chromite form necklace textures around earlier olivine macrocrysts and phlogopite phenocrysts (Figure 3-2b). In a few cases, perovskite occurs as the rim of an ilmenite grain. Larger (40-60 μm) euhedral pseudo-cubic perovskite is less abundant and commonly has dark brown cores and light brown rims and less commonly oscillatory-zoning. Both populations of perovskite can occur with prominent reaction rims (~1-10 μm). This style of alteration has been documented and discussed by Chakhmouradian and Mitchell (2000). They attribute the reaction rims to the final stages of kimberlite emplacement/evolution, where perovskite is unstable in a CO_2-rich, weakly acidic

environment, and commonly undergoes cation leaching and replacement by other Ti-bearing minerals. Formation of TiO_2 at the expense of $CaTiO_3$ involves leaching of Ca from the mineral structure, with the subsequent deposition of calcite (Nesbitt et al. 1981). The calcite is then deposited close to the perovskite, and the TiO_2 rim is left with a "spongy" appearance (Chakhmouradian and Mitchell 2000). The representative compositions of Churchill perovskite are given in Table 3-5. The data show that perovskite from the Churchill kimberlite province is close to the ideal composition $CaTiO_3$. Although there is the common occurrence of simple zoning and lesser oscillatory zoning in perovskites, there is a negligible compositional variation between the zones. There is a slight decrease from the core to the rim in Na_2O, Nb_2O_5, Ta_2O_5, ThO_2, and Ce_2O_3, with a slight increase in TiO_2. There is no compositional variation with FeO, Al_2O_3, CaO and SrO from the core to the rim. This pattern is common in kimberlitic perovskites, where there is a decrease in LREEs, Nb, Na, and Th towards the rim of the grains (Chakhmouradian and Mitchell 2000). The abundance of Churchill perovskite make it a useful dating tool for the determination of emplacement ages of the kimberlites.

Monticellite

Monticellite occurs as an accessory groundmass phase, ranging in abundance from trace up to 15 modal %. It commonly occurs as euhedral to subhedral, small (50 -100 μm) unaltered grains and occasionally is replaced by calcite. Monticellite is zonation-free and entirely devoid of inclusions. Churchill kimberlite monticellite is relatively pure $CaMgSiO_4$, a common feature of kimberlitic monticellite. It has a very small compositional range exhibiting solid solution toward kirschsteinite (4-7 mol. % $CaFeSiO_4$) and forsterite (0-7 mol. % Mg_2SiO_4). Figure 3-6 is a bivariate plot of Ca/(Ca+Mg) vs. Fe/(Fe+Mg), which outlines some features of Churchill monticellite, such as low Fe/(Fe+Mg) ratios, and a moderate range of Ca/(Ca+Mg) ratios (0.47-0.52). This is comparable to monticellite from both the Leslie hypabyssal kimberlite (Lac de Gras kimberlite province; Armstrong et al. 2004), and the Elwin Bay hypabyssal kimberlite (Somerset Island; Mitchell 1986), where both are primary carbonate-bearing kimberlites (Figure 3-6).

Calcite

Calcite is abundant in many of the Churchill kimberlites. Primary prismatic small (~15-25 μm) calcite rhombs are identified in the groundmass of the kimberlite. Calcite occurs as segregationary textures with serpentine and lesser chlorite. One occurrence of primary tabular laths exhibiting flow alignment was identified in thin section, similar to primary calcite occurring at the Jos and Nikos kimberlites, Somerset Island (Mitchell and Meyer 1980). Secondary calcite occurs as pseudomorphic replacements after monticellite, and as precipitates from a late stage secondary fluid (from crustal processes) in some of the more altered kimberlite. XRD and staining has not been completed on the Churchill calcite. However, qualitative microprobe analyses confirmed the presence of calcite, ruling out the presence of dolomite. Lastly, secondary calcite veins have been identified within heavily altered hypabyssal kimberlite, interpreted to be the result of hydrothermal processes.

Apatite

Apatite occurs as a late crystallizing groundmass phase, ranging in abundances from trace to 10 modal %. It mainly occurs as radiating sprays (regarded as a quenching texture), and less commonly occurs as prismatic crystals (~15 μm). In rare cases, the apatite is corroded and altered in the groundmass and in some rare cases replaced by calcite. Qualitative and quantitative analyses were difficult due to the small size, habit and extensive alteration, however it was determined that apatite in the examined samples is REE-poor, below the detection limits of the microprobe.

Serpentine

Serpentine is an abundant groundmass mineral, present both as groundmass phases and as pseudomorphic replacements after olivine. Fine-grained groundmass serpentine commonly forms segregationary textures. Multiple generations of pseudomorphic secondary serpentine are present, with each generation being optically distinct. Both macrocrystal and phenocrystal (and microphenocrystal) olivine is replaced by serpentine in some samples.

Djerfisherite and Pyrite

Occurring as a rare accessory mineral, djerfisherite [$K_6(Cu,Fe,Ni)_{24}S_{26}Cl$] has been identified via microprobe from some hypabyssal kimberlite at Churchill. It appears to have formed from a late-stage fluid, as it forms irregular clusters in the groundmass. Djerfisherite also occurs in the groundmass of the Elwin Bay kimberlite, Somerset Island (Clarke et al. 1994). Pyrite also occurs as a rare accessory mineral, commonly occurring as small (~10 μm) euhedral cubes in the groundmass.

Geochronology

U-Pb Perovskite

Small core samples (less than 1 kg) from the diamond drill exploration program were used to determine 12 precise U-Pb perovskite emplacement ages for Churchill kimberlites. The analyses represent multi-grain fractions (up to 400 single grains) as the grain size of perovskite is quite small (25-60 μm). In the majority of samples, multiple perovskite fractions were analysed. For six of these, two morphologically distinct varieties of perovskite were identified; Type 1- small octahedral (<40 μm); and Type 2- large pseudo-cubic (>40 μm) (See photomicrographs, Appendix II). The populations were analysed separately to test for age variation. Table 3-6 presents the U-Pb perovskite results for these 12 Churchill samples (errors associated with ages are reported at 2σ in text).

In sample 05KD244, two varieties of perovskite are present; Type 1- dark brown, anhedral habit and less abundant Type 2- larger dark brown to black, euhedral to subhedral "cubes". The $^{206}Pb/^{238}U$ model ages are 171.0 ± 5.4 Ma, and 187.5 ± 1.2 Ma respectively. Due to the abundance of Type 1 perovskite, the $^{206}Pb/^{238}U$ model age for the Type 1 population (171.0 ± 5.4 Ma) is considered to be the more reliable estimate for the 05KD244 emplacement age. The interpretation of the older perovskite population will be addressed in the discussion.

Kimberlite 05FWR005-A contains small (20 μm) dark brown euhedral cubic perovskite, separated from two separate float samples. The perovskite fractions from different samples were analyzed (05FWR005A-1 and 05FWR005A-2, Table 3-6) and yielded $^{206}Pb/^{238}U$ model ages of 216.2 ± 4.0 Ma and 225.3 ± 0.6 Ma, respectively. This result indicates that the

two samples located in close contact with each other may not have been from the same kimberlite, and therefore both ages will be taken as separate from each other.

Kimberlite 05KD573 was separated into two fractions, according to the size of the perovskite. The moderately abundant Type 1 perovskite (05KD573-S) consisted of euhedral crystals. The less abundant Type 2 perovskite (05KD573-L) consisted of subhedral cubic crystals. The $^{206}Pb/^{238}U$ model ages for both fractions (Type 1: 185.5 ± 1.8 Ma; Type 2: 185.2 ± 1.4 Ma) are identical within analytical uncertainty, and the weighted average $^{206}Pb/^{238}U$ age of 185.3 ± 1.1 Ma is interpreted as the best estimate for the emplacement age of kimberlite 05KD573.

Abundant perovskite was recovered from kimberlite 05KD636. A fraction consisting of small (~25 μm) brown, subhedral to anhedral crystals was analysed, and the $^{206}Pb/^{238}U$ model age of 188.1 ± 5.0 Ma is interpreted as the best estimate for the emplacement age of this kimberlite. A single fraction of perovskite was separated from kimberlite 05KD637. The abundant subhedral perovskite (~25 μm) is light to dark brown, and the $^{206}Pb/^{238}U$ model age is 170.4 ± 1.2 Ma.

Kimberlite 04KD568 contains two morphological types of perovskite. One fraction of rare Type 1 perovskite consisted of brown-orange, euhedral to subhedral crystals. Two fractions of Type 2 perovskite were analysed, both of which consisted of euhedral to subhedral grains. The $^{206}Pb/^{238}U$ model age for the Type 1 perovskite is 222.3 ± 1.8 Ma, while the model ages for the Type 2 perovskite are 227.6 ± 2.8 Ma, and 225.0 ± 3.6 Ma. The Type 2 model ages are identical within analytical uncertainty and the weighted average $^{206}Pb/^{238}U$ age is 226.6 ± 2.2 Ma.

Kimberlite 04KD230 also contains two morphological types of perovskite. Three Type 1 perovskite fractions (04KD230-1; 04KD230-2; 04KD230-3) and two Type 2 fractions (04KD230-4; 04KD230-5) were analyzed. The Type 1 perovskite crystals have a euhedral pseudo-cubic habit while the Type 2 fractions are of cubo-octahedral habit. The Type 1 fractions have $^{206}Pb/^{238}U$ model ages of 183.6 ± 1.6 Ma, 211.5 ± 3.8 Ma, and 216.7 ± 2.4 Ma. The discrepancy of the Type 1 fractions may indicate some mixing of perovskite populations

during the selection and picking stage of the U-Pb procedure. The Type 2 fractions have older $^{206}Pb/^{238}U$ model ages of 222.4 ± 4.0 Ma, and 223.8 ± 2.0 Ma (weighted average 223.5 ± 1.8 Ma).

A single perovskite fraction was separated from kimberlite 05KD217. The rare perovskite in this sample is brown, euhedral to subhedral, and relatively small (~30 μm). The $^{206}Pb/^{238}U$ model age of 175.4 ± 3.8 Ma is interpreted as the best estimate for the emplacement age of this kimberlite. Two perovskite morphologies (with similar modal abundances) were identified in kimberlite 04KD217. Type 1 perovskite is light brown and euhedral to subhedral. Type 2 perovskite is subhedral. The $^{206}Pb/^{238}U$ model ages for the Type 1 and Type 2 perovskite are indistinguishable, 192.4 ± 2.2 Ma and 188.6 ± 3.6 Ma, respectively. Therefore, the weighted average $^{206}Pb/^{238}U$ age of 191.4 ± 1.9 Ma is interpreted as the best estimate for the emplacement age of kimberlite 04KD217. Interpretation of the rare younger 05KD217 sample will be discussed below.

Two small fractions of perovskite from CD 009 were analyzed. The more abundant population (Type 1) consists of anhedral grains. The $^{206}Pb/^{238}U$ model ages are almost within error of each other (169.2 ± 3.3 Ma, 176.1 ± 3.2 Ma). The slight discrepancy of the Type 1 fractions may indicate some mixing of perovskite populations during the selection of suitable perovskite grains. One rare fraction of Type 2 larger (>50 μm) "cubic" grains (CD 009-3) has a moderate U concentration (117 ppm) and Th/U (19.5). The $^{206}Pb/^{238}U$ model age for the Type 2 perovskite is 196.5 ± 1.4 Ma. The rare Type 2 perovskite has an older age and will be addressed in the discussion.

Kimberlite CD 024 contains abundant, small (~25 μm), euhedral to subhedral brown orange perovskite. The $^{206}Pb/^{238}U$ model ages obtained for these two fractions are indistinguishable within analytical uncertainty; 189.7 ± 3.6 Ma and 192.4 ± 4.8 Ma, respectively. Therefore, the weighted average $^{206}Pb/^{238}U$ age of 190.7 ± 2.9 Ma is interpreted as the best estimate for the emplacement age of kimberlite CD 024.

A single fraction of perovskite was separated from kimberlite CD 001. Relatively abundant, CD 001 perovskite is small (~20-30 μm) and exhibits a euhedral to subhedral "cubic" habit. The $^{206}Pb/^{238}U$ model age is 198.4 ± 3.0 Ma.

Rb-Sr Phlogopite

Light brown, brown and reddish brown macrocrystal phlogopite was extracted from drill core specimens, and emplacement ages were determined for an additional 16 Churchill kimberlite intrusions. Macrocrystal phlogopite present in sufficient quantity was subdivided into multiple fractions in an attempt to determine an isochron age. For single phlogopite analyses where there was insufficient material for multiple analyses, a Model Age was calculated assuming an initial $^{87}Sr/^{86}Sr$ isotopic ratio of 0.7035. Rb-Sr isotope data for Churchill phlogopite are presented in Table 3-7.

Churchill phlogopite macrocrysts have high Rb, and moderate Sr abundances, which is typical of kimberlitic phlogopite. Individual phlogopite macrocrysts were used for the analyses where possible. One exception is sample (CD06-5) where material from two smaller macrocrystic grains was combined.

Five macrocrystal fragments of brown to red-brown phlogopite were analyzed from sample CD01; the Rb-Sr data and Model Ages are reported in Table 3-7 and are plotted in Figure 3-7(a). The phlogopite fractions have a range in $^{87}Rb/^{86}Sr$ (85-203) and define a Model 1 isochron age of 199.1 ± 5.1 Ma (MSWD = 0.45). The emplacement age for kimberlite CD01 was determined using both the U-Pb and Rb-Sr methods, and the results are analgous (e.g. U-Pb perovskite age is 198.4 ± 3.0 Ma (2σ)).

Four macrocrystal fragments of dark brown phlogopite were analyzed from sample CD02. The Rb-Sr results and Model Age calculations are reported for each in Table 3-7 and displayed on an isochron diagram in Figure 3-7(b). One macrocryst (CD02-1) has a high Sr content (75.2 ppm), possibly due to the presence of higher Sr mineral inclusions, or an impurity like carbonate that was not fully removed during HCl cleaning. The four macrocrysts have a range in $^{87}Rb/^{86}Sr$ (24-207) and together define a Model 1 isochron age of 181.4 ± 1.9 Ma (MSWD = 0.90) (Figure 3-7(b)).

Four macrocrystal fragments of red-brown phlogopite were analyzed from sample CD06, along with one fraction of smaller macrocrystal fragments. The Rb-Sr results are reported in Table 3-7 and displayed in Figure 3-7(c). The Model 1 isochron age of 199.3 ± 2.3 Ma (Figure 3-7(c)) is interpreted to be the best estimate age of the CD-06 kimberlite. This emplacement age is identical to the age calculated from kimberlite intrusion CD01.

Four macrocrystal fragments of grey-brown phlogopite were analyzed from sample CD13, and the model age for each is reported in Table 3-7. The Model 1 isochron age of 185.0 ± 2.7 Ma (MSWD = 0.16) (Figure 3-7(d)) is interpreted as the emplacement age for this kimberlite.

Model Ages have been calculated for 13 samples from which there was insufficient phlogopite for multiple analyses. The results are listed in Table 3-7, and range from ~173–226 Ma (middle-Triassic to middle-Jurassic). For the Model Age calculation, an assumed initial $^{87}Sr/^{86}Sr$ ratio of 0.7035 was used. The uncertainties on the Model Ages are estimated to be ~ ±3 Ma, based on their Rb/Sr ratios and likely variation in initial Sr isotopic composition. Many of these individual Model Ages have been plotted on an isochron diagram in Figure 3-8, and two reference isochrons are shown for CD02 and CD06. Sample KD209 was separated into two fractions, KD209-S (small) and KD209-L (large), due to different sizes and colours of phlogopite macrocrysts. KD209-S yielded a model age of ~226 Ma, while KD209-L yielded a single model age of ~218 Ma. KD209-L and KD5168 yield similar single model ages of ~218-219 Ma, and KD501 (2 analyses) and KD5821 yielded similar model ages of ~196 and ~197 Ma, respectively.

Overall, Rb-Sr macrocrystal phlogopite emplacement ages for Churchill kimberlites fall within the range of ~226-173 Ma (middle-Triassic to middle-Jurassic). This agrees well with the data from the U-Pb perovskite ages, and taken together demonstrates that these kimberlites were emplaced over an extended period of time, the product of ~50 million years of intrusive volcanic activity.

Sr isotopic analysis (perovskite)

Six perovskite fractions were chosen from 4 kimberlite intrusions emplaced within the Churchill kimberlite field to establish the primary Sr isotopic composition of these magmas. Where possible, perovskite populations from single kimberlite intrusions were divided into two size fractions and analysed separately. No correction for Rb decay was necessary due to the low Rb/Sr ratios for perovskite (Heaman 1989). Table 3-8 reports the measured $^{87}Sr/^{86}Sr$ ratios. These results indicate that Churchill kimberlites have initial $^{87}Sr/^{86}Sr$ ratios ranging from 0.7032-0.7036, and generally fall within the range previously reported for kimberlitic perovskite. The ratios are consistent with previous whole rock initial $^{87}Sr/^{86}Sr$ ratios from South African Group I kimberlites (0.7033-0.7049) (Smith 1983).

Interestingly, two populations of perovskite from kimberlite 04KD230, identified as small and large perovskite (with variable >20 Ma U-Pb ages), have identical $^{87}Sr/^{86}Sr$ ratios of 0.7036. On the other hand, two populations of perovskite from kimberlite CD 009, also separated into small and large perovskite that show a similar range in U-Pb age of >20 Ma, have slightly different $^{87}Sr/^{86}Sr$ ratios of 0.7035 and 0.7032, respectively.

Discussion

Classification of the Churchill kimberlites

The petrographic characteristics examined here indicate that hypabyssal kimberlite dominates Churchill rocks. This type of kimberlite is characteristic of the root zone, and intrusive dykes and sills of kimberlite intrusions. There is no evidence for the preservation of crater or diatreme facies kimberlite at Churchill. This is a reflection of either current erosional levels or magmatic processes. The internal geology of the kimberlite occurrences is poorly understood, and may be resolved in the later stages of exploration when bulk samples are available for study. The Churchill kimberlites are sparsely macrocrystic (evolved) to macrocrystic, and have experienced various degrees of both deuteric and secondary alteration. Following the mineralogical classification of Mitchell (1986), the Churchill intrusions are kimberlites *sensu stricto*, with the presence of Mg-ilmenite, two generations of olivine with different morphologies and restricted Fo content of > Fo 85, two generations of phlogopite

mica, abundant Nb-, REE-poor perovskite, primary serpentine in the groundmass, and importantly, a typical kimberlitic compositional trend in spinel compositions (magmatic trend #1). Evolved members of the kimberlite clan of rocks have also been identified, occurring as highly altered macrocryst-poor intrusions. Mantle xenoliths have been identified within some Churchill kimberlites but are in very low abundance. The xenolith population is dominated by locally derived supracrustal (sediments) material, incorporated during the final emplacement.

Extreme variation in the mineralogy of Churchill kimberlites was documented in this study. A mineralogical classification of the Churchill kimberlites, in order of abundance is as follows: a sparsely macrocrystic oxide-rich calcite evolved hypabyssal kimberlite > macrocrystic oxide-rich monticellite phlogopite hypabyssal kimberlite > an evolved serpentine hypabyssal kimberlite. Churchill kimberlites can be further classified as archetypal Group 1 kimberlites under the mineralogical classification scheme of Mitchell (1986). Evolved members of the kimberlite clan rocks commonly occur as calcite, serpentine, phlogopite, +/- apatite, +/- perovskite-bearing kimberlites (Mitchell 1986). In addition, the relatively unradiogenic Sr isotopic composition of perovskite indicate a Group 1 affinity.

Crystallization History of the Churchill kimberlites

Macrocrystal olivine was the first mineral to crystallize, shortly followed by macrocrystal Ti-enriched phlogopite, with the assumption that both have a kimberlitic origin. Both olivine and phlogopite were later subjected to corrosion, rounding and varying degrees of serpentinization as the groundmass crystallized. Ilmenite, perovskite and spinel-group minerals co-crystallized, commonly forming necklace textures around macrocrystal olivine and phlogopite. There is a strong spatial association between spinel group minerals and perovskite within the Churchill kimberlites. Chakhmouradian and Mitchell (2000) report that the crystallization of MUM spinels and groundmass perovskite is nearly simultaneous. Furthermore, the crystallization of perovskite ceases prior to the resorption of MUM spinels and the development of an atoll rim (Chakhmouradian and Mitchell 2000). Atoll textures are known to have multiple origins, and are known to form after MUM-type spinels and ferroan spinel (Mitchell 1986). Groundmass Ti-poor phlogopites and monticellite are next to crystallize

to form the groundmass. Monticellite crystallizes after spinel and perovskite, prior to serpentine and carbonate (Mitchell 1986). Primary calcite and serpentine form segregations around earlier crystallized macrocrysts and groundmass. Lastly, apatite and some rare sulphides form, crystallizing from late-stage fluids. Subsequent alteration (both deuteric and secondary) occurs. Olivine, monticellite and phlogopite are most susceptible to alteration, sometimes completely pseudomorphed by serpentine, chlorite and secondary calcite.

Emplacement of the Churchill Kimberlites

Emplacement ages for 27 Churchill kimberlites using both the Rb-Sr phlogopite and U-Pb perovskite techniques are summarized in Table 3-9. One kimberlite (CD01) was dated by both techniques (199.1±5.1 and 198.4±3.0 Ma, respectively) with excellent agreement. Considering the ages together, kimberlite magmatism in the Churchill field spans a period of ~55 Myr (225-170 Ma), with the majority of the Churchill kimberlites emplaced between 204 and 181 Ma (n=19). Some U-Pb perovskite age complexity was identified in three samples (05KD244, 04KD230, and CD009) in which individual fraction Model Ages are not in agreement within analytical uncertainty and in some instances span nearly 20 Ma. In two of these examples, the dominant perovskite population consisting of small euhedral cubes yielded younger ages whereas a smaller population of larger resorbed perovskite crystals yield older ages. One possible interpretation for this observed pattern is that the minor population of larger crystals represent an inherited perovskite component. Although inherited perovskite is relatively rare, the Elliott County kimberlite may be another example of a kimberlite with possible inherited perovskite (Heaman et al. 2004). The most reasonable way to preserve perovskite inheritance is if there is entrainment of older kimberlitic material in younger intrusions, a scenario that is more likely where there are multiple “pulses” of kimberlite magmatism over an extended period of time, such is the case for the Churchill kimberlite field.

The emplacement ages of the Churchill kimberlites reported in this paper add significantly to the geochronological database for Eastern North American kimberlite magmatism. Heaman and Kjarsgaard (2000) previously reported that Rankin Inlet kimberlite emplacement event spanning 18 Ma (214-196 Ma, n=2). This extends the duration of kimberlite

magmatism at the Churchill kimberlite field to ~55 Ma. Figure 3-9 presents the cumulative distribution of the Churchill kimberlite emplacement ages (both U-Pb and Rb-Sr). Although it shows continuous emplacement throughout the Middle Triassic to Middle Jurassic, three "pulses" of kimberlite magmatism are evident, the first smaller pulse occurring at ~225-219 Ma, the second from ~204-181 Ma, and the third from 175-170 Ma. In terms of mineralogy and mineral chemistry, there is no significant difference between the "older" and "younger" kimberlites on the property.

Sr isotopic composition of the Churchill Kimberlites

Strontium isotopes from kimberlitic rocks can reveal important information about the sub-continental lithospheric mantle (SCLM) source region (e.g. Smith 1983, Heaman 1989). The problem of characterizing the nature of the possible source SCLM is that the extent to which the magmas from the SCLM have interacted and subsequently been contaminated by continental crust is unknown. Kimberlites have relatively high trace element contents; generally high enough that any Sr (or Nd) derived from continental crust would have a minimal effect on the isotopic composition of the primary kimberlite magma (Smith 1983). However, leaching experiments on whole rock kimberlites from North America have previously identified that a crustal component can be present (e.g. Alibert and Albarède 1988). Using the isotopic compositions of an unaltered, primary mineral phase in a kimberlite is a substitute for obtaining the primary isotopic composition of a kimberlitic magma. For this reason, groundmass perovskite Sr isotopic compositions can represent reliable estimates for the original isotopic signatures of the magmas (Heaman 1989). An excellent recent example of this is the large range (0.7010-0.7066) in whole rock initial Sr isotopic compositions from 1.1 Ga Wajrakarur kimberlites in India compared to the corresponding narrow range of unradiogenic Sr isotopic compositions in perovskite (0.7023-0.7025; Paton et al. 2007). Similarly, the Narayanpet kimberlites in India have variable whole rock initial Sr isotopic compositions (0.7026-0.7088) compared to co-existing perovskite (0.7031-0.7033; Paton et al. 2007). Previous $^{87}Sr/^{86}Sr$ ratios for pure perovskite fractions isolated from North American kimberlites fall within the range 0.7034-0.7049 (Heaman 1989). Although the Sr isotopic composition of perovskite from

Churchill kimberlites reported here (0.7032-0.7036) overlaps this range, they are slightly less radiogenic than the ~90 Ma Ham kimberlite, Somerset Island (0.7040) and the ~160 Ma Kirkland Lake kimberlite, Quebec (0.7041). These low Sr isotopic compositions overlap the Group 1 southern Africa whole rock kimberlite field (0.7033-0.7055) of Smith (1983) and reflect derivation from a near chondritic mantle source.

Temporal evolution of eastern North American kimberlite magmatism: Churchill kimberlite field

There are two main models that have been proposed for the origin of kimberlite genesis; (1) a link to subduction of oceanic lithosphere (e.g. Sharp 1974; Helmstaedt and Schulze 1979; Helmstaedt and Gurney 1997; McCandless 1999), and (2) mantle plume hotspot tracks (e.g. Crough et al. 1980; Crough 1981; England and Houseman 1984; le Roex 1986, Haggerty 1994; Gibson et al. 1995; Heaman and Kjarsgaard 2000; Schissel and Smail 2001; Heaman et al. 2003; Heaman et al. 2004).

The subduction hypothesis refers to the decarbonation/dehydration of subducted oceanic crust and the partial melting of overlying mantle (McCandless 1999). In the case of North American kimberlite magmatism, McCandless (1999) proposes that from 175-125 Ma, the Farallon plate was subducted E-SE, extending the slab ~2700 km into the earth. This deep seated subduction produced entrapped fluids which released from the slab promoting small degree partial melting. The kimberlites produced would have a younging direction toward the trench, and the temporal-spatial patterns of North American kimberlites would reflect changes in the convergence velocity of the subducted Farallon plate. Heaman et al. (2003) find major difficulties with the subduction hypothesis relating to Cenozoic/Mesozoic North American kimberlites. The first difficulty deals with the timing and location of the Jurassic kimberlites, in particular, the Churchill and Attawapiskat kimberlites. The kimberlites are located >2000 kms from the Farallon subduction, and at 200 Ma, the Farallon plate is only starting to impact Western North American tectonics. The second difficulty deals with the geochemical signature of kimberlites, where fluids released from a subducting slab would be insufficent in

incompatible or high field strength elements to represent the precursor metasomatic agent that reflects a kimberlitic melt.

The other prevalent model proposed for kimberlite genesis relates to mantle plume hotspot tracks. It has been shown that many Mesozoic kimberlites in North America are located within five degrees of a predicted hotspot track (Crough et al. 1980; Crough 1981). Kimberlites in South Africa, Brazil and Eastern North America are located as clusters and fields along continental extensions of aseismic ridges and seamount chains that have been produced from magmatism associated with the trace of a current hotspot track (Crough 1981). The main argument against a hotspot model for kimberlite genesis is that large amounts of magma are produced by oceanic mantle plumes, unlike the small volume kimberlite magmas identified in the geological records (McCandless 1999). However, continental plume-related magmatism (basaltic or kimberlitic) may have solidified in the subcontinental mantle lithosphere, making it difficult to assess volumetric amounts (Heaman et al. 2003).

An important finding of this study is that kimberlite magmatism in the Churchill kimberlite field spans a relatively long period of ~45 Ma (225-170 Ma; n=27) compared to other well-studied kimberlite fields in North America. For example, the duration of kimberlite magmatism in the Kirkland Lake cluster spans ~13 Ma (165-152 Ma, n=12), the Timiskaming kimberlite cluster spans ~21 Ma (155-134 Ma, n=8), and the Attawapiskat cluster spans ~24 Ma (180-156 Ma, n=7) (Heaman and Kjarsgaard 2000; Heaman et al. 2004). It is important to note that results of the Heaman and Kjarsgaard (2000) study show the Attawapiskat cluster has younger or older kimberlites (i.e. the emplacement ages are either 155 or 180 Ma, with little in between). An important finding from this study is the progressive SE-younging of Triassic to Cretaceous kimberlitic magmatism along a NW-SE corridor extending for greater than 2000 km along strike, extending from the Rankin Inlet area through to the Attawapiskat, Kirkland Lake and Timiskaming fields. If this age progression is real, then one prediction of this hypothesis is that even older kimberlites should exist to the NW in the Churchill kimberlite field. The identification in this study of the oldest known kimberlites (225 Ma) in the Churchill kimberlite field supports a proposed hotspot track model. Heaman and Kjarsgaard (2000) interpreted this

as the continental expression of magmatism linked to a single mantle plume hotspot track, a pattern that is geographically coincident with independent estimates for the timing and location of the continental extension of the Great Meteor hotspot track. This large-scale, southeastward younging of kimberlite magmatism suggests that small volume mantle melting occurred along this portion of the Great Meteor hotspot track, identifying a possible subcontinental mantle process which may be linked to kimberlite melt formation. Heaman and Kjarsgaard (2000) considered the idea that eastern North American kimberlite magmatism could be linked to multiple hotspot tracks, however with the data obtained at the time of the study a single hotspot track model was preferred. Crough (1980) and Morgan (1983) discuss the Verde and the Great Meteor plume tracks as roughly parallel and closely spaced, passing through at approximately 40 Ma apart. While the results of this study support this single hotspot track model, there is also an indication that the kimberlite magmatism could be related to both the Mesozoic hotspot tracks: the Jurassic Verde hotspot track and the Cretaceous Great Meteor hotspot track. The ~220 Ma Churchill kimberlites could be related to the Great Meteor plume, while the 180-200 Ma kimberlites may be related to the Verde plume. This is supported by the apparent separation of the Attawapiskat emplacement ages (155, 180Ma) (Heaman and Kjarsgaard 2000).

Conclusions

An in-depth mineralogical and geochemical evaluation of the intrusive rocks on the Churchill property has confirmed the presence of bonafide kimberlites and related rocks. The Churchill kimberlites are classified as mainly sparsely macrocrystic, oxide-rich calcite evolved hypabyssal kimberlite and macrocrystic oxide-rich monticellite phlogopite hypabyssal kimberlite. These kimberlites exhibit varying degrees of both deuteric and secondary alteration and contain abundant lithic fragments. Based on the available drill core samples, Churchill kimberlites are mantle-xenolith poor. They are designated archetypal Group I kimberlites under the classification of Mitchell (1986), and the relatively unradiogenic Sr isotopic compositions (0.7032-0.7036) of groundmass perovskite support this contention. In total 27 new Rb-Sr phlogopite and U-Pb perovskite ages have been determined for the Churchill kimberlite

province, indicating an ~45 Ma span of kimberlite emplacement history (~225-170 Ma). In conclusion, radiometric ages compiled for the Churchill kimberlites record a complex kimberlite emplacement event spanning ~55 Myr, interpreted as occurring around 3 main pulses of magmatic emplacement, the first at ~225-219 Ma, the second at ~204-181 and the final at ~175-170 Ma. The Churchill kimberlites occur along a NW-SE trending corridor of Jurassic/Triassic magmatism and represent the oldest currently recognized kimberlite magmatism that could be linked to either a continental extension of the single Great Meteor mantle plume hotspot track, or multiple (Great Meteor and Verde plumes) mantle plume hotspot tracks initiated during the opening of the North Atlantic Ocean.

References

Al-Hermezi, H.M. 1985. Qandilite, a new spinel end-member, Mg_2TiO_4, from the Qala Dizeh region, N.E. Iraq. Mineralogical Magazine, 49:739-744.

Alibert, C. and Albarède, F. 1988. Relationships between mineralogical, chemical and isotopic properties of some North American kimberlites. Journal of Geophysical Research, 93:7643-7671.

Armstrong, J., Wilson, M., Barnett, R.L., Nowiki, T. and Kjarsgaard, B.A. 2004. Mineralogy of primary carbonate-bearing hypabyssal kimberlite, Lac de Gras, Slave Province, Northwest Territories, Canada. Lithos, 76:415-433.

Balzer, S. 2004. Surficial geology of the Churchill West Diamond project, unpublished, Apex Geosciences Ltd.

Carpenter, R.L., Duke, N.A., Sandeman, H.A., and Stern, R. 2005. Relative and absolute timing of gold mineralization along the Meliadine Trend, Nunavut, Canada: Evidence for Paleoproterozoic gold hosted in an Archean greenstone belt. Economic Geology, 100:567-576.

Chakhmouradian, A.R. and Mitchell, R.H. 2000. Occurrence, alteration patterns and compositional variation of perovskite in kimberlites. The Canadian Mineralogist, 38:975-994.

Clarke, D. B., Mitchell, R.H., Chapman, A. and MacKay, R. 1994. Occurrence and origin of Djerfisherite from the Elwin Bay Kimberlite, Somerset Island, Northwest Territories. The Canadian Mineralogist, 32:815-823.

Creaser, R. A., Grűtter, H., Carlson, J. and Crawford, B. 2004. Macrocrystal phlogopite Rb-Sr dates for the Ekati property kimberlites, Slave Province, Canada: evidence for multiple intrusive episodes in the Paleocene and Eocene. Lithos, 76:399-414.

Crough, S.T. 1981. Mesozoic hotpspot epeirogeny in Eastern North America. Geology, 9:2-6.

Crough, S.T., Morgan, W.J., and Hargraves, R.B. 1980. Kimberlites: their relation to mantle hotspots. Earth and Planetary Science Letters 50:260-274.

Davis, W.J. and Miller, A.R. 2001. A late Triassic Rb-Sr phlogopite isochron age for a kimberlite dyke from the Rankin Inlet area, Nunavut; Radiogenic Age and Isotope Studies: Report 14; Geological Survey of Canada, Current Research, 2001-F3, 7p.

Dyke, A. and Prest, V.K. 1987. The Late Wisconsinan and, Holocene history of the Laurentide Ice Sheet. Géographie physique et Quaternaire, 41:237-263.

England, P. and Houseman, G. 1984. On the geodynamic setting of kimberlite genesis. Earth and Planetary Science Letters, 67:109-122.

Gibson, S.A., Thompson, R.N., Leonardos, O.H., Dickin, A.P., and Mitchell, J.G. 1995. The late Cretaceous impact of the Trindade mantle plume: evidence from large-volume, mafic, potassic magmatism in SE Brazil. Journal of Petrology, 36:189-229.

Haggerty, S. 1976. Opaque mineral oxides in terrestrial igneous rocks. *In* Oxide Minerals Short Course Notes. *Edited by* D. Rumble. Mineralogical Society of America, 3:101-300.

Haggerty. S. 1994. Superkimberlites: a geodynamic window to the Earth's core. Earth and Planetary Science Letters, 122:57-69.

Heaman, L.M. 1989. The nature of the subcontinental mantle from Sr-Nd-Pb isotopic studies on kimberlitic perovskite. Earth and Planetary Science Letters, 92:323-334.

Heaman, L.M. 2005. Patterns of kimberlite emplacement – the importance of robust geochronology. Danmarks og Grønlands Undersøgelse Rapport, 2005/68: 25.

Heaman, L.M. and Kjarsgaard, B.A. 2000. Timing of Eastern North American kimberlite magmatism: continental extension of the Great Meteor Hotspot Track? Earth and Planetary Science Letters, 178:253-268.

Heaman, L.M., Kjarsgaard, B.A. and Creaser, R.A. 2003. The timing of kimberlite magmatism in North America: implications for global kimberlite genesis and diamond exploration. Lithos, 71**:**153-184.

Heaman, L.M., Kjarsgaard, B.A and Creaser R.A. 2004. The temporal evolution of North American kimberlites. Lithos, 76:377-397.

Helmstaedt, H. and Schulze, D.J. 1979. Type A-Type C eclogitic transition in xenoliths from the Moses Rock diatreme-further evidence for the presence of metamorphosed ophiolites beneath the Colorado Plateau. Second International Kimberlite Conference, vol 2, pp.357-365.

Helmstaedt, H. and Gurney, J.J. 1997. Geodynamic controls of kimberlites- What are the roles of hotspots and plate tectonics? Russian Geology and Geophysics, 38:492-508.

Hoffman, P.F. 1990. Subdivision of the Churchill Province and extent of the Trans-Hudson Orogen. *In* The Early Proterozoic Trans-Hudson Orogen of North America. *Edited by* J.F Lewry and M.R. Stauffer. Geological Association of Canada, Special paper 37, pp, 15-39.

Holmden, C.E., Creaser, R.A., Muehlenbachs, K., Bergstrom, S.A. and Leslie S.A. 1996. Isotopic and elemental systematics of Sr and Nd in 454 Ma biogenic apatites: implications for paleoseawater studies. Earth and Planetary Science Letters, 142:425-437.

Jaffey, A.H., Flynn, K.F., Glendenin, L.E., Bentley, W.C. and Essling, A.M. 1971. Precise measurement of half-lives and specific activities of ^{235}U and ^{238}U. Physics Review, C4:1989-1906.

Kamo, S.L., Gower, C.F. and Krough, T.E. 1989. Birthdate for the Iapetus Ocean? A precise U-Pb zircon and baddeleyite age for the Long Range dikes, southeast Labrador. Geology**,** 17**:** 602-605.

Kjarsgaard, B.A. and Levinson, A.A. 2002. Diamonds in Canada. Gems and Gemology, 38: 208-239.

Le Roex, A.P. 1986. Geochemical correlation between southern African kimberlites and South Atlantic hotspots. Nature, 324:243-245.

Ludwig, K.R. 2003. Isoplot/Ex version 3.0; a geochronological toolkit for Microsoft Excel; Berkeley Geochronology Center Special Publication No. 1a; Berkeley, California.

McCandless, T.E. 1999. Kimberlites: mantle expressions of deep-seated subduction. *In* Proceedings of the Seventh International Kimberlite Conference*. Edited by* J.J. Gurney, J.L. Gurney, M.D. Pacsoe and S.H. Richardson. Vol. 2, pp. 545-549.

Miller, A.R., Seller, M.H., Armitage, A.I., Davis, W.J. and Barnett, R.L. 1998. Triassic kimberlite magmatism, western Churchill Structural Province, Canada. Seventh International Kimberlite Conference, Extended Abstracts, Cape Town, South Africa, pp. 591-593.

Mitchell, R.H. 1986. Kimberlites. Plenum Press, New York.

Mitchell, R.H. 1995. Kimberlites, orangeites, and related rocks. Plenum Press, New York.

Mitchell, R.H. and Clarke, D.B. 1976. Oxide and sulphide mineralogy of the Peuyuk kimberlite, Somerset Island, N.W.T., Canada. Contributions to Mineralogy and Petrology**,** 56: 157-172.

Mitchell, R.H. and Meyer, H.O.A. 1980. Mineralogy of micaceous kimberlite from the Jos Dyke, Somerset Island, Northwest Territories. The Canadian Mineralogist, 18:241-250.

Morgan, W.J. 1983. Hotspot tracks and the early rifting of the Atlantic. Tectonophysics**,** 94: 123-139.

Nesbitt, H.W., Bancroft, M.G., Fyfe, W.S., Karkhanis, S.N., Nishijima, A. and Shin, S. 1981. Thermodynamic stability and kinetics of perovskite dissolution. Nature, 289:358-362.

Paton, C., Hergt, J.M., Phillips, D., Woodhead, J.D. and Shee, S.R. 2007. New insights into the genesis of Indian kimberlites from the Dharwar craton via in situ Sr isotope analysis of groundmass perovskite. Geology, 35**:**1011-1014.

Percival, J.A. 1996. Archean cratons, *In* Searching for Diamonds in Canada. *Edited by* A.N. LeCheminant, D.G. Richardson, R.N.W. DiLabio, and K.A. Richardson. Geological Survey of Canada, Open File 3228, p. 11-15.

Sankeralli, L.M. 2004. Churchill Diamond Project Glacial Geomorphology. Unpublished report, Shear Minerals Ltd.

Schissel, D., Smail, R. 2001. Deep mantle plumes and ore-deposits. *In* Mantle Plumes: Their Identification Through Time. *Edited by* Ernst, R.E. and K.L. Buchan. Geological Society of America Special Publication, vol. 352, p. 291-322.

Sharp, W.E. 1974. A plate tectonic origin for diamond-bearing kimberlite. Earth and Planetary Science Letters, 21:351-354.

Stacey, J.S. and Kramers, J.D. 1975. Approximation of terrestrial Pb isotope evolution by a two stage model. Earth and Planetary Science Letters, 26:207-221.

Steiger, R.H. and Jager, E. 1977. Subcommission on Geochronology: convention on the use of decay constants in geo- and cosmo-chronology. Earth and Planetary Science Letters**,** 36:359-362.

Strand, P., Banas, A., Burgess, J., Baumgartner, M. 2008. Two distinct kimberlite types at the Churchill Diamond Project. Extended abstracts of the 9th International Kimberlite Conference, 3p.

Smith, C.B. 1983. Pb, Sr, and Nd isotopic evidence for sources of African Cretaceous kimberlite. Nature, 304**:**51-54.

Smith, J.V., Brennesholtz, R. and Dawson, J.B. 1978. Chemistry of micas from kimberlites and xenoliths, I. Micaceous kimberlites. Geochemica et Cosmochimica Acta, 42:959-971.

Tappe, S., Foley, S.F., Jenner, G.A., Heaman, L.H., Kjarsgaard, B.A., Romer, R.L., Stracke, A., Joyce, N. and Hoefs, J. 2006. Genesis of ultramafic lamprophyres and carbonatites at Aillik Bay, Labrador: a consequence of incipient lithospheric thinning beneath the North Atlantic Craton. Journal of Petrology**,** 47:1261-1315.

Tella, S. 1994. Geology, Rankin Inlet (55 K/16), Falstaff Island (55 J/13), and Quarzite Island (55 J/11), District of Keewatin, Northwest Territories; Geological Survey of Canada, Open File 2968, scale 1:50 000.

Table 3-1. Summary of petrographic analyses of the Churchill kimberlites

Sample [Lat/Long]	*Texture*	*Alteration*	*Additional Information*	*Classification*
CWDH-3001 [63.34/-91.83]	sparsely macrocrystic	moderate	segregationary textures	carbonate hypabyssal kimberlite
CWDH-3003 [63.33/-91.77]	sparsely macrocrystic	low	carbonate forms tabular prisms, coarse matrix	oxide carbonate hypabyssal kimberlite
04KD597 [63.15/-91.72]	sparsely macrocrystic	extensive & low	abundant phlogopite, variable alteration with depth	phlogopite serpentine hypabyssal kimberlite
04KD568 [63.16/-91.66]	aphanitic	extensive	preferred flow orientation	serpentine-rich carbonate hypabyssal kimberlite
04KD428 [63.04/-91.33]	sparsely macrocrystic	extensive	n/a	inconclusive
04KD217 [63.14/-90.99]	sparsely macrocrystic	low	disaggregated macrocrystic olivines	carbonate hypabyssal kimberlite
04KD230 [63.13/-91.01]	sparsely macrocrystic	extensive	primary/secondary carbonate	inconclusive
04KD235 [63.12/-91.02]	sparsely macrocrystic	low	megacrystal olivine, abundant perovskite	oxide-rich carbonate hypabyssal kimberlite
CD001 [62.94/-91.34]	macrocrystic	moderate	olivine macrocrysts, pseudomorphs after olivine phenocrysts	oxide-rich serpentine carbonate hypabyssal kimberlite
CD002 [62.99/-91.35]	macrocrystic	low	ilmenite megacrysts, 2 generations of perovskite, primary matrix carbonate	oxide-rich monticellite phlogopite hypabyssal kimberlite
CD003 [62.99/-91.35]	sparsely macrocrystic	extensive	corroded atoll-spinels, flow banded phlogopites	phlogopite-rich hypabyssal kimberlite
CD004 [62.99/-91.29]	sparsely macrocrystic	moderate	matrix: spinels in a mesostasis of serpentine and carbonate	oxide-rich carbonate hypabyssal kimberlite
CD006 [62.94/-91.34]	sparsely macrocrystic	extensive	epitaxial overgrowths on phlogopite	inconclusive
CD007 [62.91/-91.30]	macrocrystic	low	coarse primary matrix carbonate	carbonatitic affinity
CD009 [62.94/-91.35]	aphanitic	moderate	segregationary textures, monticellite	oxide hypabyssal kimberlite
CD010 [63.02/-91.13]	macrocrystic	extensive	corroded atoll spinels	evolved serpentine hypabyssal kimberlite
CD013 [63.03/-90.74]	sparsely macrocrystic	moderate	pelletal lapilli	tuffisitic kimberlite with magmaclasts & uniform textured oxide hypabyssal kimberlite
CD015 [63.08/-90.84]	macrocrystic	extensive	primary and secondary carbonate	serpentine hypabyssal kimberlite
CD020 [63.06/-90.90]	sparsely macrocrystic	low	autolithic, atoll spinels	oxide hypabyssal kimberlite
CD021 [63.06/-90.85]	macrocrystic	extensive	primary and secondary calcite	carbonate hypabyssal kimberlite
CD024 [63.19/-90.88]	sparsely macrocrystic	low	fresh anhedral macrocrysts	oxide-rich carbonate hypabyssal kimberlite
CD025 [63.19/-90.88]	macrocrystic	moderate	atoll spinels, necklace textures, segregationary textures	oxide-rich carbonate hypabyssal kimberlite
CD026 [63.22/-90.80]	macrocrystic	moderate	segregationary and uniform textures	oxide hypabyssal kimberlite
CD029 [63.17/-91.88]	macrocrystic	low	abundant crustal material	carbonate-rich hypabyssal kimberlite

Table 3-2. Representative compositions of macrocrystal phlogopite from the Churchill kimberlites

	1	2	3	4	5	6	7	8	9
SiO_2	39.85	39.60	42.03	42.04	42.23	42.19	40.46	40.48	40.59
TiO_2	3.30	3.82	1.13	1.15	1.11	1.15	3.16	3.12	3.13
Al_2O_3	13.52	12.97	12.05	12.00	12.10	12.13	13.16	13.06	13.03
Cr_2O_3	1.50	0.97	0.04	0.04	0.06	0.04	0.15	0.14	0.14
FeO	5.16	5.03	5.80	5.99	6.02	6.12	6.23	6.34	6.31
MnO	0.02	0.03	0.03	0.03	0.04	0.02	0.04	0.04	0.03
MgO	21.59	20.74	23.44	23.65	23.27	23.32	21.91	21.86	21.96
CaO	0.01	1.60	0.00	0.02	0.00	0.02	0.02	0.01	0.01
Na_2O	0.29	0.34	0.30	0.23	0.26	0.25	0.29	0.33	0.31
K_2O	9.74	9.38	10.08	9.97	10.22	10.09	10.07	9.98	10.00
NiO	0.11	0.10	0.04	0.04	0.05	0.03	0.05	0.05	0.05
Total	95.09	94.58	94.94	95.16	95.36	95.36	95.54	95.41	95.56
Structural formulas based on 22 oxygens									
Si	5.713	5.721	6.017	6.006	6.027	6.019	5.788	5.799	5.804
Al	2.284	2.208	2.033	2.021	2.035	2.039	2.219	2.205	2.196
Ti	0.356	0.415	0.121	0.124	0.119	0.123	0.340	0.336	0.337
Cr	0.170	0.111	0.004	0.004	0.006	0.004	0.017	0.016	0.016
Fe	0.619	0.608	0.694	0.716	0.719	0.730	0.745	0.760	0.755
Mn	0.003	0.004	0.004	0.003	0.005	0.003	0.004	0.004	0.004
Mg	4.614	4.467	5.002	5.037	4.951	4.959	4.673	4.669	4.681
Ca	0.002	0.248	0.000	0.004	0.000	0.002	0.003	0.002	0.002
Na	0.079	0.096	0.082	0.062	0.071	0.070	0.080	0.090	0.085
K	1.781	1.729	1.841	1.817	1.861	1.836	1.838	1.824	1.824
Ni	0.012	0.011	0.005	0.005	0.005	0.003	0.005	0.006	0.006
Total	15.63	15.62	15.80	15.80	15.80	15.79	15.71	15.711	15.710

Analyses 1-5 CD02, 6-9 CD20

Table 3-3. Representative compositions of microphenocrystal phlogopite from the Churchill kimberlites

	1	2	3	4	5	6	7	8	9	10
SiO_2	41.97	42.97	40.23	41.07	40.42	41.41	40.06	40.78	38.04	39.15
TiO_2	0.02	0.05	0.07	0.37	0.79	0.00	0.42	0.01	0.96	0.72
Al_2O_3	8.78	9.79	14.34	6.82	11.63	5.26	8.44	4.19	14.17	15.96
Cr_2O_3	0.00	0.04	0.06	0.02	0.03	0.01	0.00	0.01	0.00	0.02
FeO^{tot}	4.29	3.53	2.08	7.71	4.52	9.60	7.89	11.26	4.99	3.70
MnO	0.08	0.04	0.03	0.08	0.05	0.05	0.06	0.05	0.07	0.06
MgO	29.99	29.02	26.84	31.40	25.92	28.48	27.36	27.73	24.53	25.39
CaO	0.16	0.23	0.22	0.01	0.00	0.01	0.03	0.02	0.00	0.13
Na_2O	0.12	0.14	0.38	0.12	0.09	0.10	0.11	0.03	0.03	0.06
K_2O	8.23	9.81	8.98	7.90	10.20	9.86	9.84	10.51	10.06	10.04
NiO	0.03	0.02	0.02	0.00	0.00	0.00	0.00	0.00	0.00	0.00
Total	93.67	95.64	93.25	95.50	93.65	94.78	94.21	94.59	92.85	95.23
Structural formulae based on 22 oxygens										
Si	6.018	6.049	5.743	5.895	5.863	6.112	5.894	6.122	5.586	5.549
Al	1.484	1.624	2.413	1.154	1.988	0.915	1.464	0.741	2.452	2.666
Ti	0.002	0.005	0.008	0.040	0.086	0.000	0.047	0.001	0.106	0.077
Cr	0.000	0.005	0.007	0.003	0.003	0.001	0.000	0.001	0.000	0.002
Fe	0.514	0.416	0.248	0.926	0.548	1.185	0.971	1.414	0.613	0.439
Mn	0.010	0.005	0.004	0.009	0.007	0.006	0.008	0.007	0.009	0.007
Mg	6.411	6.090	5.712	6.719	5.605	6.267	6.001	6.206	5.370	5.365
Ca	0.025	0.035	0.033	0.002	0.000	0.002	0.004	0.002	0.000	0.020
Na	0.033	0.039	0.104	0.034	0.024	0.028	0.030	0.009	0.008	0.015
K	1.506	1.762	1.635	1.447	1.887	1.857	1.847	2.013	1.885	1.815
Ni	0.003	0.003	0.002	0.000	0.000	0.000	0.000	0.000	0.000	0.000
Total	16.006	16.033	15.909	16.229	16.011	16.373	16.266	16.516	16.029	15.955

Analyses 1-4 CD01, 5 CD06, 6-8 CD02, 9-10 CD024

Table 3-4. Representative compositions of spinel-group minerals from the Churchill kimberlites

	1	2	3	4	5	6	7	8	9	10
TiO_2	4.18	4.20	9.93	6.44	9.20	4.67	5.77	18.37	20.68	19.33
Al_2O_3	12.17	11.96	7.47	11.30	10.49	11.55	11.32	5.38	4.93	7.21
Cr_2O_3	43.69	43.85	25.01	34.85	24.31	43.48	40.92	0.00	2.41	0.28
FeO	26.35	26.52	41.10	31.12	38.15	27.83	28.60	57.42	54.86	52.71
MnO	0.12	0.13	1.03	0.42	0.48	0.14	0.30	0.83	0.80	0.86
MgO	11.98	12.06	13.31	14.03	14.42	11.16	12.14	15.53	14.56	17.21
	98.49	98.72	97.85	98.16	97.05	98.83	99.05	97.53	98.24	97.60
Recalculated analyses										
Fe_2O_3	8.22	8.49	23.06	15.47	21.69	7.99	9.60	36.71	29.94	32.86
FeO	18.95	18.88	20.35	17.2	18.63	20.64	19.97	24.39	27.92	23.14
	99.33	99.58	100.32	99.98	99.52	99.64	100.10	101.55	101.71	100.96
Structural Formulae based on 4 oxygens										
Ti	0.102	0.103	0.245	0.156	0.224	0.115	0.141	0.449	0.507	0.465
Al	0.467	0.459	0.289	0.428	0.400	0.446	0.433	0.206	0.189	0.272
Cr	1.126	1.128	0.650	0.886	0.623	1.127	1.050	0.000	0.062	0.007
Fe^{3+}	0.202	0.208	0.570	0.374	0.529	0.197	0.234	0.897	0.734	0.791
Fe^{2+}	0.517	0.514	0.559	0.462	0.505	0.566	0.542	0.662	0.761	0.619
Mn	0.003	0.004	0.029	0.012	0.013	0.004	0.008	0.023	0.022	0.023
Mg	0.582	0.585	0.625	0.672	0.696	0.545	0.588	0.752	0.707	0.821
	3.000	3.000	3.000	3.000	3.000	3.000	3.000	3.000	3.000	3.000

Analyses 1-7: TiMACs (Titanium magnesian aluminous chromites)
Analyses 8-12: MUMs (Magnesian ulvospinel-ulvospinel magnetites)

Table 3-5. Representative compositions of perovskite from the Churchill kimberlites.

	1	2	3	4	5	6	7	8
Na_2O	0.39	0.35	0.45	0.40	0.42	0.37	0.28	0.32
CaO	37.53	38.76	37.16	36.89	37.08	37.21	38.23	38.37
SrO	0.19	0.18	0.12	0.12	0.13	0.16	0.17	0.18
La_2O_3	n.d.	n.d.	n.d.	n.d.	n.d.	n.d.	n.d.	n.d.
Ce_2O_3	1.92	1.37	2.05	2.07	1.89	1.85	1.43	1.42
Pr_2O_3	0.22	0.20	0.30	0.33	0.33	0.32	0.16	0.10
Nd_2O_3	n.d.	n.d.	n.d.	0.02	n.d.	n.d.	n.d.	n.d.
ThO_2	0.18	n.d.	0.50	0.54	0.34	0.12	n.d.	0.04
TiO_2	56.68	57.53	56.19	56.07	56.69	56.85	58.02	57.40
SiO_2	0.03	0.03	0.09	0.07	0.03	0.06	0.05	0.06
MgO	0.10	0.09	0.11	0.09	0.10	0.09	0.10	0.08
Al_2O_3	0.25	0.21	0.32	0.31	0.27	0.31	0.22	0.25
FeO^{tot}	1.22	1.12	1.38	1.48	1.36	1.46	1.30	1.31
Nb_2O_5	0.85	0.69	0.80	0.90	0.80	0.72	0.55	0.62
Ta_2O_5	0.12	0.04	0.19	0.20	0.13	0.04	0.04	0.06
	99.67	100.56	99.65	99.49	99.58	99.56	100.5	100.2
Structural formulae based on 3 atoms of oxygen								
Na	0.018	0.015	0.020	0.018	0.019	0.017	0.012	0.014
Ca	0.928	0.946	0.923	0.918	0.919	0.920	0.932	0.940
Sr	0.003	0.002	0.002	0.002	0.002	0.002	0.002	0.002
La	–	–	–	–	–	–	–	–
Ce	0.016	0.011	0.017	0.018	0.016	0.016	0.012	0.012
Pr	0.002	0.002	0.002	0.003	0.003	0.003	0.001	0.001
Nd	–	–	–	–	–	–	–	–
Th	0.001	–	0.003	0.003	0.002	0.001	–	–
Σ*A*	0.968	0.976	0.967	0.962	0.961	0.959	0.959	0.969
Ti	0.984	0.986	0.980	0.980	0.986	0.987	0.993	0.987
Al	0.007	0.006	0.009	0.008	0.007	0.008	0.006	0.007
Fe	0.023	0.021	0.027	0.029	0.026	0.028	0.025	0.025
Nb	0.009	0.007	0.008	0.009	0.008	0.008	0.006	0.006
Ta	0.001	–	0.001	0.001	0.001	–	–	–
Mg	0.003	0.003	0.004	0.003	0.003	0.003	0.003	0.003
Si	0.001	0.001	0.002	0.002	0.001	0.001	0.001	0.001
Σ*B*	1.028	1.024	1.031	1.032	1.032	1.035	1.034	1.029

Analyses 1-3 CD01, 3-5 CD024, 6-8 CD029

Table 3-6. U-Pb Perovskite Results for Churchill Kimberlites

	# of grains	Weight (µg)	U (ppm)	Th (ppm)	Pb (ppm)	Th/U	TCPb (pg)	$^{206}Pb/^{204}Pb$	$^{238}U/^{204}Pb$	$^{206}Pb/^{238}U$	Model Age $^{206}Pb/^{238}U$
05KD244-S 80.4m	75	90	267	5086	55	19.1	706	75.19±2.49	2111.96±73.37	0.02688±0.0004	171.0±5.4
05KD244-L 80.4m	350	126	104	6261	22	60.1	364	85.45±0.32	2272.64±9.60	0.02951±0.0001	187.5±1.2
05FWR005-A-1	350	65	266	267	12	1.0	142	287.50±2.98	7891.76±114.8	0.0341±0.0003	216.2±4.0
05FWR005-A-2	400	52	401	632	21	1.6	174	286.78±1.01	7547.83±29.06	0.0356±0.0001	225.3±0.6
05KD217 44.3m	275	41	204	2471	35	12.1	341	60.36±0.50	1521.12±17.85	0.0275±0.0003	175.4±3.8
05KD573-S 37.5m	450	76	121	23348	25	192.4	267	81.88±0.48	2175.26±13.85	0.0292±0.0001	185.5±1.8
05KD573-L 37.5m	130	71	73	1477	17	20.2	148	82.91±0.53	2213.97±15.30	0.0291±0.0001	185.2±1.4
05KD636 101m	300	63	83	1368	18	16.5	204	66.07±0.38	1610.46±22.48	0.02960±0.0004	188.1±5.0
05KD637 142.7m	170	14	184	679	17	3.7	57	95.86±0.90	2892.58±31.44	0.0268±0.0001	170.4±1.2
04KD568-A-(S)	175	39	90	1019	14	11.3	68	131.46±2.06	3222.22±56.55	0.0351±0.0001	222.3±1.8
04KD568-1-(L)	60	25	132	750	23	5.7	58	145.25±4.87	3529.45±122.0	0.0359±0.0002	227.6±2.8
04KD568-2-(L)	90	30	111	1294	19	11.6	62	137.08±4.03	3342.35±103.0	0.0355±0.0003	225.0±3.6
04KD230-1-(S)	275	39	255	1760	24	6.9	91	256.30±2.02	6959.37±67.10	0.0342±0.0002	216.7±2.4
04KD230-2-(S)	250	36	500	2613	44	5.2	174	240.25±2.41	6652.17±94.38	0.0333±0.0003	211.5±3.8
04KD230-3-(S)	380	60	347	1651	27	4.8	211	197.47±0.98	6199.92±40.03	0.0289±0.0001	183.6±1.6
04KD230-4-(L)	120	36	375	2419	40	6.5	134	247.60±2.94	6527.15±103.2	0.0351±0.0003	222.4±4.0
04KD230-5-(L)	140	52	289	2093	30	7.3	149	243.35±1.48	6367.75±47.28	0.0353±0.0002	223.8±2.0
04KD217(S)	150	12	129	2662	29	20.6	36	103.26±2.73	2801.64±87.75	0.0303±0.0002	192.4±2.2
04KD217(L)	300	23	147	3780	43	25.7	115	74.46±0.83	1888.53±26.77	0.0297±0.0003	188.6±3.6
CD 009-1-(S)	510	85	65	794	10	12.3	179	70.72±0.47	1966.89±25.50	0.0266±0.0003	169.2±3.3
CD 009-2-(S)	270	37	91	4405	15	48.4	127	64.69±0.46	1670.66±14.85	0.0277±0.0003	176.1±3.2
CD 009-3-(L)	80	90	117	2276	14	19.5	322	81.77±0.34	2044.15±9.70	0.0310±0.0001	196.5±1.4
CD 024-1 26.0m	400	59	73	1408	16	19.4	107	96.30±1.19	2608.36±16.42	0.0299±0.0003	189.7±3.6
CD 024-2 26.0m	250	33	132	2222	40	16.8	500	34.92±0.08	545.25±3.69	0.0303±0.0004	192.4±4.8
CD 001 61.02m	150	13	110	1488	16	13.5	62	65.75±0.81	1516.36±25.62	0.0313±0.0002	198.4±3.0

Perovskite $^{238}U/^{204}Pb$ and $^{206}U/^{204}Pb$ ratios were corrected for fractionation, blank and spike.
Th concentrations estimated from amount of ^{208}Pb and $^{206}Pb/^{238}U$ age.
Age uncertainties reported at 2 sigma.
TCPb: Total Common Pb
Atomic ratios corrected for mass spectrometer fractionation (Pb- 0.088%/amu; U- 0.155%/amu), blank (5 pg Pb; 1 pg U), spike, and initial common Pb (Stacey and Kramers 1975).

Table 3-7. Rb-Sr Phlogopite results for Churchill kimberlites

Sample	Type	Depth (m)	Lithology	Age Array	Rb (ppm)	Sr (ppm)	$^{87}Rb/^{86}Sr$	$^{87}Sr/^{86}Sr$	$^{87}Sr/^{86}Sr\pm$ 2SE	Ma
CD01-a	I	81.96	H	yes	780.7	18.78	124.3	1.05056	0.00002	196.3
CD01-b	I	81.96	H	yes	606.0	21.00	85.44	0.94336	0.00003	197.4
CD01-c	I	81.96	H	yes	630.4	15.96	117.9	1.03402	0.00002	197.1
CD01-d	I	91.50	H	yes	445.4	6.760	203.0	1.27668	0.00005	198.6
CD01-e	I	73.50	H	yes	605.0	14.23	127.3	1.06294	0.00002	198.5
CD02-1	I	32.00	H	yes	624.1	75.19	24.16	0.76600	0.00002	181.9
CD02-2	I	32.00	H	yes	677.5	9.960	206.9	1.23979	0.00003	182.3
CD02-3	I	32.00	H	yes	640.7	14.00	137.0	1.05784	0.00003	182.0
CD02-4	I	32.00	H	yes	603.0	15.60	115.0	0.99771	0.00002	179.9
CD06-1	I	36.00	H	yes	706.5	26.22	79.67	0.93051	0.00005	200.4
CD06-2	I	49.00	H	yes	486.9	11.26	129.5	1.07148	0.00002	199.8
CD06-3	I	65.00	H	yes	463.1	23.70	57.42	0.36616	0.00002	199.2
CD06-4	I	65.00	H	yes	506.5	68.53	21.51	0.76498	0.00002	201.0
CD06-5	C	65.00	H	yes	573.9	24.65	68.24	0.89821	0.00002	199.5
CD13-1	I	18.00	H	yes	481.1	6.920	211.8	1.26023	0.00007	184.9
CD13-2	I	18.00	H	yes	527.8	17.05	91.66	0.94419	0.00002	184.7
CD13-3	I	18.00	H	yes	552.7	5.620	306.4	1.50647	0.00003	184.3
CD13-4	I	18.00	H	yes	447.2	21.19	62.01	0.86671	0.00002	183.5
CD03	I	n/a	H	no	599.0	7.440	247.6	1.35060	0.00003	183.8
CD07	I	n/a	H	no	555.2	22.40	73.19	0.91570	0.00002	203.9
CD12A	I	n/a	H	no	444.7	10.17	130.4	1.03189	0.00003	177.1
CD12B	I	n/a	H	no	470.0	8.240	169.8	1.12274	0.00002	173.7
CD17	I	n/a	H	no	488.3	9.150	161.4	1.16685	0.00002	201.9
CD21	I	n/a	H	no	613.9	22.83	79.45	0.92403	0.00002	195.2
KD597	I	n/a	H	no	604.2	24.21	73.55	0.89584	0.00003	182.5
KD501-1	I	n/a	H	no	492.3	17.88	81.40	0.92967	0.00002	195.4
KD501-2	I	38.65	H	no	599.6	2.300	943.6	3.33290	0.00011	195.9
KD209-S	I	n/a	H	no	660.3	2.040	1309	4.91640	0.00599	226.1
KD209-L	I	n/a	H	no	611.8	1.340	2149	7.36532	0.00121	217.9
KD5821	I	n/a	H	no	563.9	20.56	81.10	0.93056	0.00005	196.9
KD5168	I	n/a	H	no	581.0	22.71	75.70	0.93956	0.00003	219.3
KD5108	I	n/a	H	no	352.0	3.410	323.9	1.57177	0.00005	188.5
KD900	I	n/a	H	no	136.6	5.420	74.30	0.89659	0.00005	182.7

I= individual macrocryst, or part thereof C=composite of up to five individual small macrocrysts
H=hypabyssal kimberlite

Table 3-8. Sr isotope results (perovskite) for the Churchill kimberlites

Sample	Description	Weight (μg)	$^{87}Sr/^{86}Sr$ ratio
FWR-005	euhedral, dk brown	65.1	0.70328±0.0001
CD024-Sm	euhedral, lgt brown	58.6	0.70317±0.0002
CD009-Sm	euhedral, dk brown	84.7	0.70346±0.0002
CD009-Lg	anhedral, dk brown	73.3	0.70327±0.0001
04KD230-Sm	subhedral, dk brown	35.9	0.70355±0.0001
04KD230-Lg	subhedral, dk brown	36	0.70358±0.0001

Table 3-9. Rb-Sr Phlogopite and U-Pb Perovskite emplacement ages for Churchill Kimberlites

Kimberlite	Age ±	Method	Source	# Analyses	Additional Information
CD24	190.7 ± 2.9	U-Pb Prv	Weighted avg/model	2	Data from 2 separate fractions showing excellent agreement
KD217	191.4 ± 1.9	U-Pb Prv	Weighted avg/model	2	Less abundant 2nd generation of Prv identified (~175Ma)
CD09	172.8 ± 2.3	U-Pb Prv	Weighted avg/model	3	Less abundant 2nd generation of Prv identified (~197Ma)
KD568	226.6 ± 2.2	U-Pb Prv	Weighted avg/model	2	Less abundant 2nd generation of Prv identified (~222 Ma)
KD573	185.3 ± 1.1	U-Pb Prv	Weighted avg/model	2	n/a
KD230	223.5 ± 1.8	U-Pb Prv	Weighted avg/model	2	Less abundant 2nd generation of Prv identified (~183Ma)
FWR005-1	216.2 ± 4.0	U-Pb Prv	Model age	1	n/a
FWR005-2	225.3 ± 0.6	U-Pb Prv	Model age	1	n/a
CD01	198.4 ± 3.0	U-Pb Prv	Model age	1	Excellent agreement with CD01 Rb-Sr Phl
KD244	171.0 ± 5.4	U-Pb Prv	Model age	2	Less abundant 2nd generation of Prv identified (~188Ma)
KD636	188.1 ± 5.0	U-Pb Prv	Model age	1	n/a
KD637	170.4 ± 1.2	U-Pb Prv	Model age	1	n/a
CD13	185.0 ± 2.7	Rb-Sr Phl	Model 1 isochron	4	n/a
CD02	181.4 ± 1.9	Rb-Sr Phl	Model 1 isochron	4	n/a
CD06	199.3 ± 2.3	Rb-Sr Phl	Model 1 isochron	5	n/a
KD209	222	Rb-Sr Phl	Average Model Age	2	n/a
CD12	175.4	Rb-Sr Phl	Average Model Age	2	n/a
KD501	195.7	Rb-Sr Phl	Average Model Age	2	Phl megacrysts
KD597	182.5	Rb-Sr Phl	Model	1	n/a
KD900	182.7	Rb-Sr Phl	Model	1	n/a
KD5108	188.5	Rb-Sr Phl	Model	1	n/a
KD5168	219.3	Rb-Sr Phl	Model	1	n/a
KD5821	196.9	Rb-Sr Phl	Model	1	n/a
CD17	201.9	Rb-Sr Phl	Model	1	n/a
CD21	195.2	Rb-Sr Phl	Model	1	n/a
CD07	203.9	Rb-Sr Phl	Model	1	n/a
CD03	183.8	Rb-Sr Phl	Model	1	n/a

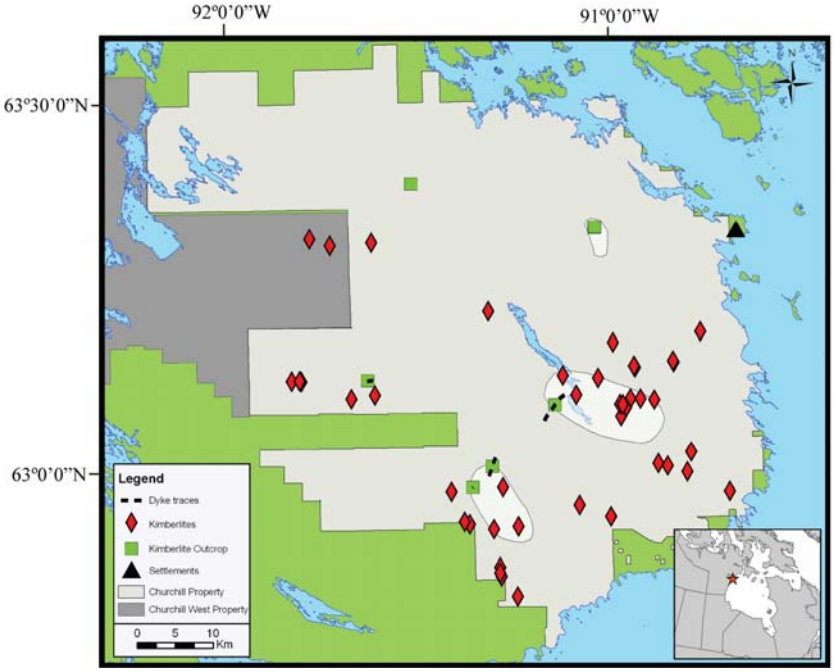

Figure 3-1. General geologic map of the Churchill kimberlite field, Nunavut.

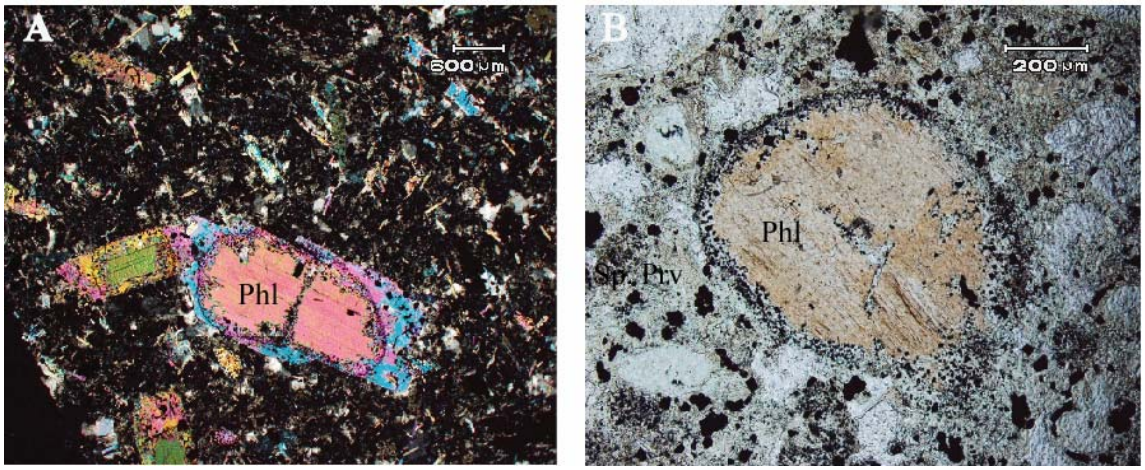

Figure 3-2. Photomicrographs of Churchill phlogopite (Phl). Left: Phlogopite laths exhibiting epitaxial overgrowths surrounded by a phlogopite-rich groundmass (cross-polarized light), Right: Altered, anhedral phlogopite surrounded by a necklace of spinel (Sp) and perovskite (Prv) (plain polarized light).

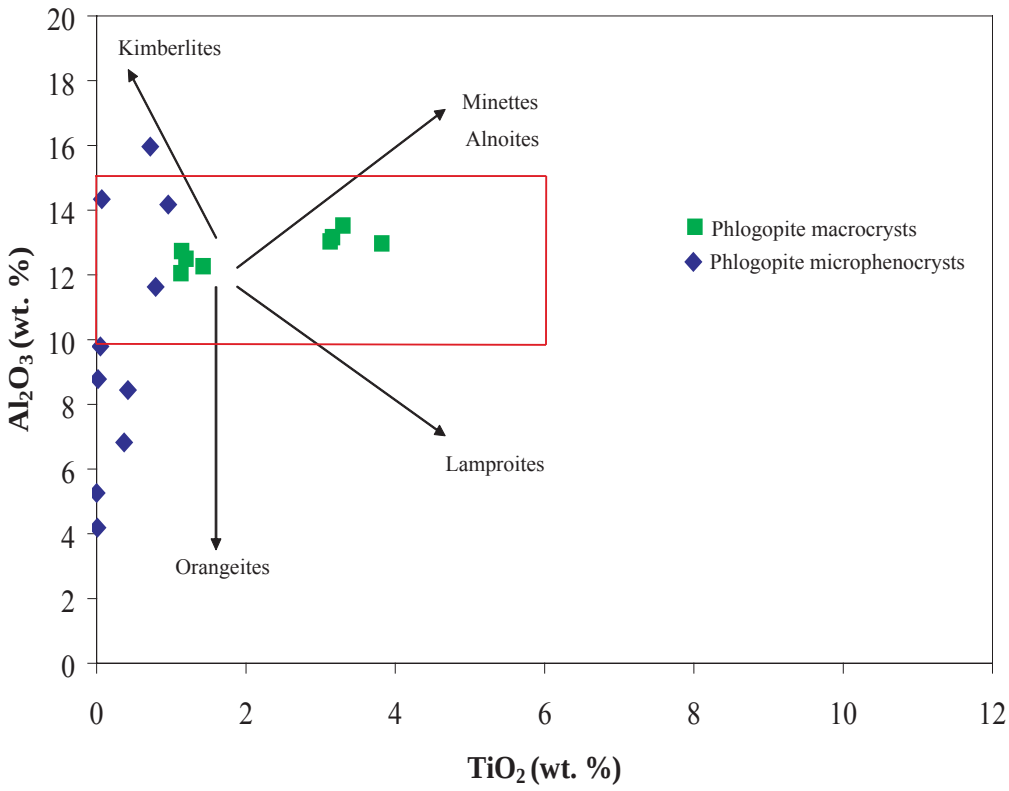

Figure 3-3. Bivariate plot of TiO_2 (wt. %) vs. Al_2O_3 (wt. %) for representative Churchill phlogopites (phenocrystal and microphenocrystal). Shown are evolutionary trends of phlogopites from kimberlites, minettes, lamproites, and orangeites (after Mitchell, 1986). Red box represents phlogopite compositions from Mitchell (1986) for Group I kimberlites.

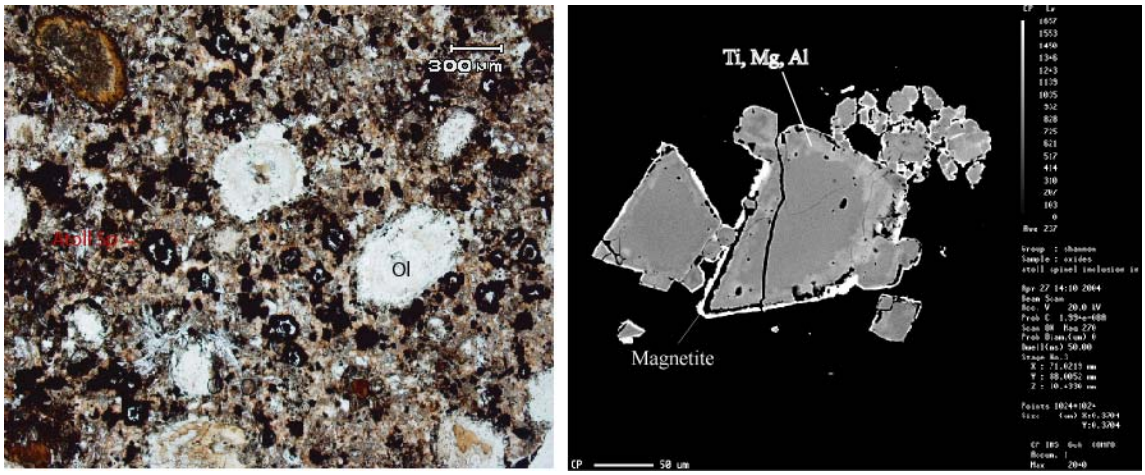

Figure 3-4. Photomicrograph (left) and back-scattered image (right) of Churchill spinel-group minerals. Left: Atoll spinels in the groundmass of an oxide-rich hypabyssal kimberlite (plain polarized light), Right: Back-scattered image of an atoll spinel with a Ti, Mg, and Al-enriched rim, surrounded by a calcite lagoon a bright rim of magnetite (Mag).

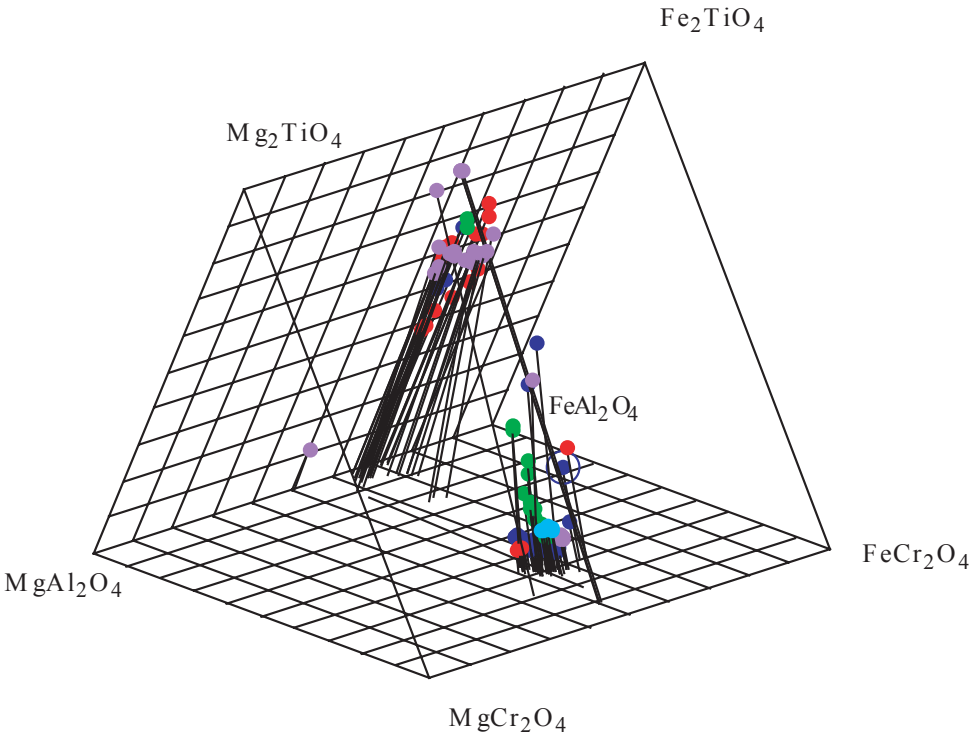

Figure 3-5. A reduced spinel prism with compositions of Churchill spinels shown representing the magnesian ulvöspinel trend (after Mitchell, 1976). Varying colours represent different kimberlite intrusions from the Churchill kimberlite field.

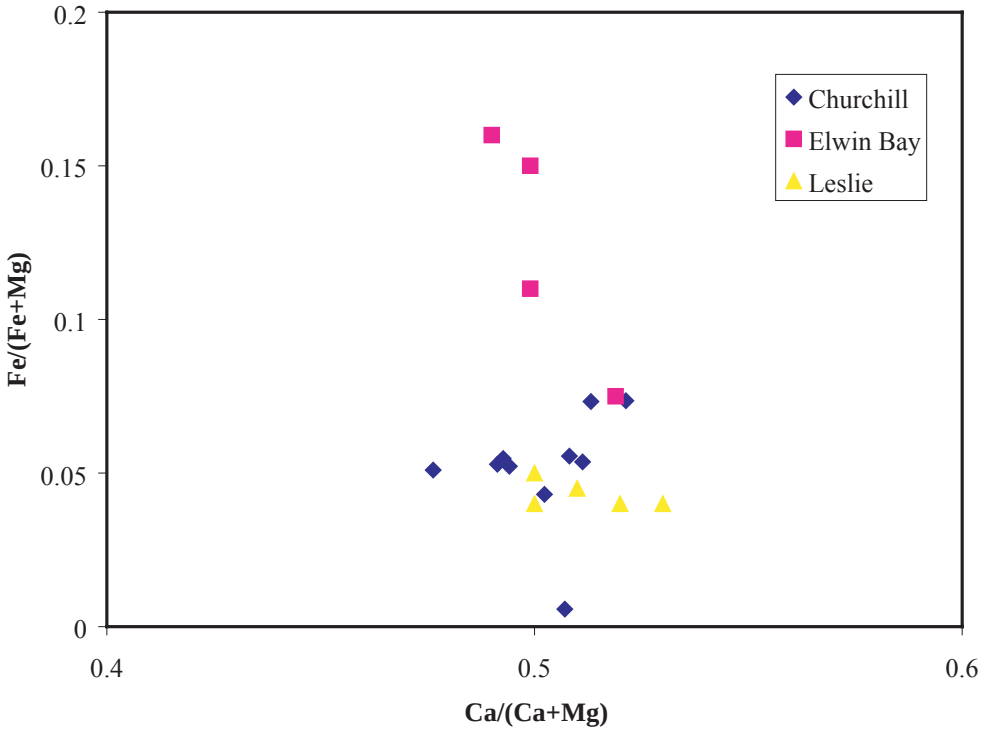

Figure 3-6. Bivariate plot of Ca/(Ca+Mg) vs. Fe/(Fe+Mg) for representative Churchill monticellite. Shown for comparison are compositions of monticellite from Elwin Bay (Somerset Island) kimberlites (Mitchell, 1986) and Leslie kimberlite (Lac de Gras, NWT) (Armstrong, 2004).

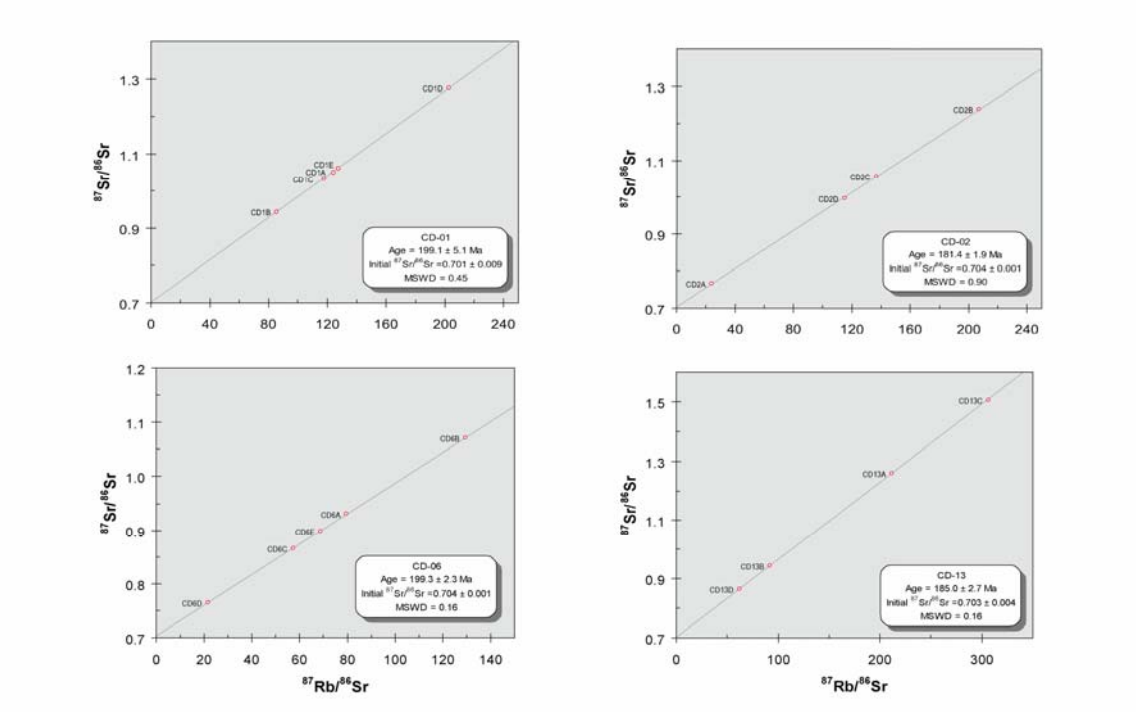

Figure 3-7. Rb-Sr isochron diagrams for the Churchill kimberlite property. (CD-01, CD-02, CD-06, CD-13).

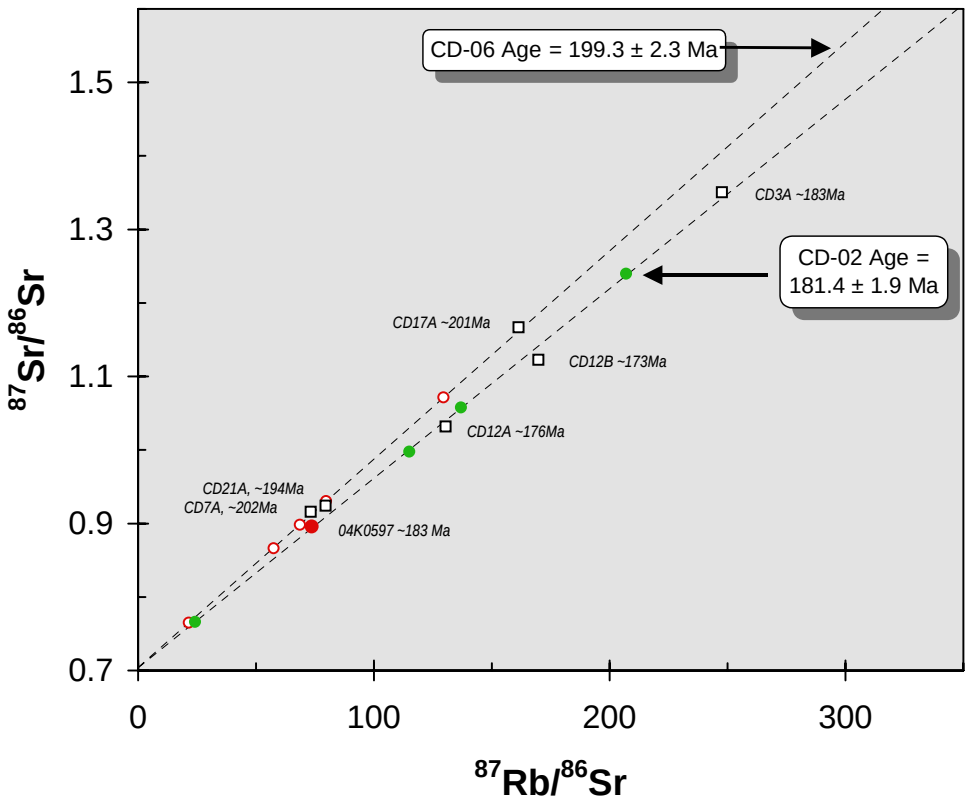

Figure 3-8. Rb-Sr isochron diagram for phlogopite from samples CD- 03, 07, 12, 17 & 21, and sample 04KD597, plotted using the CD-02 and CD-06 isochrons.

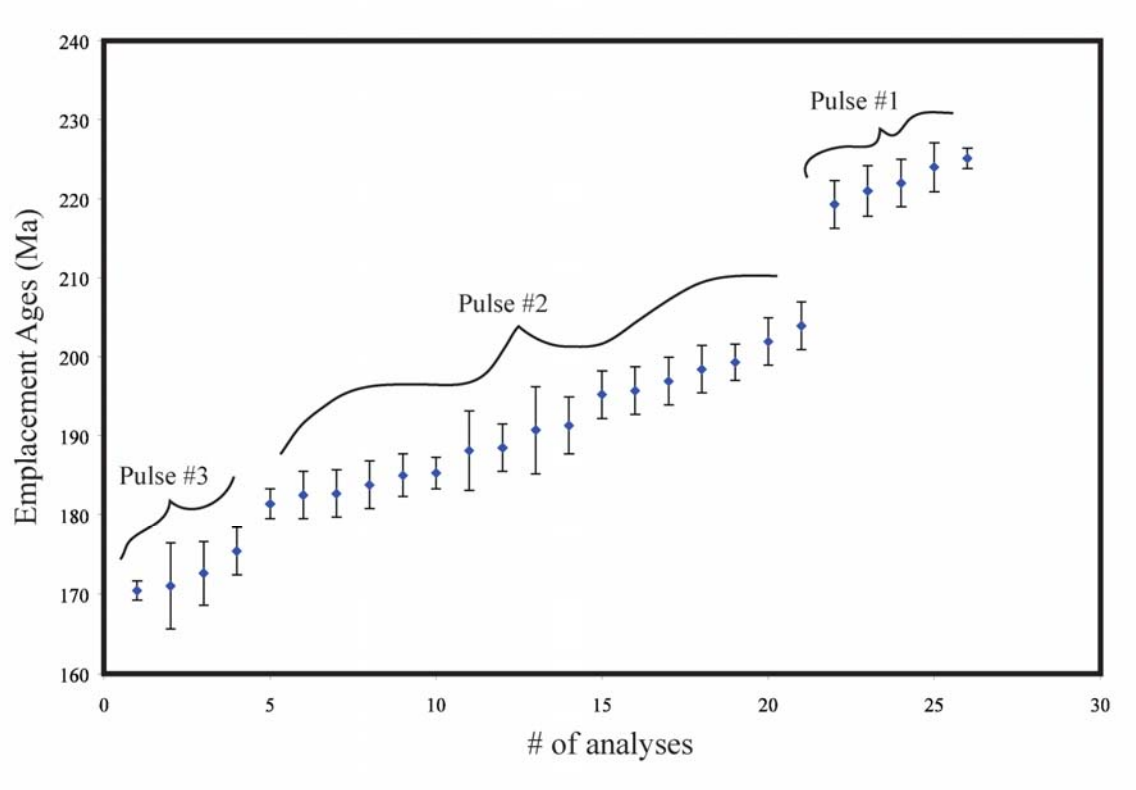

Figure 3-9. A distribution diagram of emplacement ages determined for the Churchill kimberlites, showing results from both U-Pb and Rb-Sr radiometric ages.

Chapter 4

The origin of Triassic/Jurassic kimberlite magmatism, Canada: Constraints from the Sr-Nd isotopic composition of groundmass perovskite*

*the contents of this chapter appear in a manuscript being prepared for EPSL

Introduction

Kimberlites are ultramafic rocks derived from small-volume mantle-derived magmas enriched in alkalis and volatiles (Mitchell 1986). There are numerous theories on: (1) the source components of kimberlite magma; and (2) the role that the sub-continental lithospheric mantle (SCLM) plays in the formation and/or contamination of kimberlite magmas during transport to the earth's surface. Kimberlites are complex rocks that contain a mixture of primary minerals that crystallize directly from the magma, xenocrystic material derived from contamination by mantle and crustal rocks during transport to the surface, and alteration mineral assemblages that form from interaction with fluids during and after emplacement. Deciphering the origin and primary isotopic composition of such complex rocks is very challenging. Many studies have pointed out the challenges of obtaining primary Sr isotopic compositions of whole rock kimberlites because of contamination and alteration, and concluded that whole rock kimberlite isotope geochemistry needs to be assessed with caution (e.g. Heaman 1989; Paton et al. 2007). It has been shown that primary unaltered minerals that have crystallized directly from kimberlite magma prior to entrainment of crustal material, such as perovskite, are the only materials that faithfully record the primary isotopic signature of the kimberlite magma, especially the Sr isotopic signature (e.g. Heaman, 1989; Paton et al., 2007). The primary isotopic signature of a kimberlite magma is of great importance in unraveling the nature of the mantle source of this magmatism (i.e. from the lithosphere or asthenosphere) and to evaluate the role of mantle and/or crustal contamination during emplacement.

Perovskite ($CaTiO_3$) is a common matrix mineral and has a well-established crystallization history, occurring in many kimberlites, and contains abundant U, Th, Sr and REE. As a result of these geochemical traits, perovskite is useful for obtaining U-Pb dates, interpreted to closely constrain the emplacement age of kimberlitic rocks, and more recently, Sr

and Nd isotopic compositions (Heaman 1989; Paton et al. 2007). Perovskite is resistant to alteration, recording primary isotopic compositions of the kimberlite magma from which it crystallized. In this study we investigate the U-Pb age, and Sr and Nd isotopic composition of groundmass perovskite from 16 kimberlites sampled along the well-established, SE-trending Triassic-Jurassic corridor of kimberlite magmatism in central and eastern North America. This corridor of kimberlite magmatism preserves ~90 m.y. of kimberlite magmatism in several clusters and fields, younging from NW to SE and includes; 1) the 225-170 Ma Churchill kimberlites west of Rankin Inlet, Nunavut, 2) the ~180-150 Ma Attawapiskat kimberlites in the James Bay Lowlands, Ontario and 3) the 165-135 Ma Kirkland Lake and Timiskaming kimberlite fields in central Ontario/Quebec (Figure 4-1) (Heaman and Kjarsgaard 2000). The known length of this corridor is approximately 2000 kms and has been interpreted by Heaman and Kjarsgaard (2000) to reflect the continental expression of magmatism linked to either a single or multiple mantle plume hotspot track(s), a pattern geographically coincident with independent estimates for the timing and location of the continental extension of both the Great Meteor and Verde hotspot tracks. Along this corridor, the kimberlite magmatism was emplaced into two Archean crustal blocks, the Churchill and Superior cratons, with distinctive crustal and lithospheric mantle histories. Therefore, this corridor of kimberlite magmatism provides an ideal setting to test the relative contributions of lithospheric versus asthenospheric mantle sources in their genesis. The isotopic compositions of lithosphere-derived kimberlite magmas should be high and variable (e.g. Group II kimberlites in southern Africa), whereas an origin in the asthenosphere would be expected to be much more homogeneous and independent of the craton transected. In this study, perovskite has been isolated from a number of kimberlites along this Triassic to Jurassic corridor to evaluate the origin of the magmatism.

Geologic Overview of the Triassic-Jurassic Kimberlites in Central and Eastern Canada

The Churchill kimberlites have been previously studied (Chapter 3, Zurevinski et al. 2008), and are classified as mainly evolved sparsely macrocrystic, oxide-rich calcite hypabyssal kimberlite and macrocrystic oxide-rich monticellite phlogopite hypabyssal kimberlite. The Churchill kimberlites intrude rocks of the metamorphosed Archean Rankin Inlet Group as well

as Archean metaplutonic rocks. Twenty seven precise U-Pb perovskite and Rb-Sr phlogopite emplacement ages for the Churchill kimberlites (representing 85% of the known kimberlites on the Churchill property) indicate that magmatism spans ~55 million years (225-170 Ma), with the majority of the kimberlites emplaced between 204 and 181 Ma (n=19) (Zurevinski et al. 2008). The identification of older kimberlites west of Rankin Inlet (Chapter 3), further NW along this Triassic-Jurassic corridor is consistent with the proposed hotspot track model of Heaman and Kjarsgaard (2000).

The Attawapiskat kimberlites, located in the James Bay Lowlands of Ontario (Figure 4-1), intrude a thick Phanerozoic carbonate sequence (Fowler et al. 2001). The Archean basement in the area is poorly understood because it is concealed beneath the Phanerozoic carbonates, which also mask the magnetic signatures of the kimberlites (Fowler et al. 2001). The kimberlite cluster at Attawapiskat includes 19 kimberlites, and 16 have been classified as diamondiferous, including the 15 ha economic Victor kimberlite (Fowler et al. 2001). Three archetypal "Group I" crater facies kimberlite samples from the Attawapiskat kimberlite field (MacFayden, Bravo and Charlie) have been previously dated (U-Pb perovskite) and are Jurassic, with ages in the 180-176 Ma range (Heaman and Kjarsgaard, 2000). The younger economic Victor kimberlite is predominantly pyroclastic kimberlite and is ca. 170 Ma (Webb et al. 2004). Rb-Sr dating on phlogopite for five of the Attawapiskat kimberlites is reported by Kong et al. (1999). Model ages determined range from 155-180 Ma (Kong et al. 1999).

Kirkland Lake and Timiskaming kimberlites are predominantly TK and HK, and are hosted within the Abitibi Greenstone belt of the Superior Province (Sage 1996). The kimberlites contain up to 25 modal percent mantle and crustal xenoliths, and are all diamondiferous, however, not considered economic (Sage 1996). The Diamond Lake kimberlite pipe (Kirkland Lake) consists mainly of kimberlite breccia and a 2-m-wide hypabyssal kimberlite (HK) dyke, intruding a north-trending Proterozoic diabase dyke (Sage 1996). The Buffonta kimberlite dyke (Kirkland Lake) intruded Archean mafic volcanic rocks along a shear-hosted quartz vein. The Peddie kimberlite intruded Precambrian diabase sills and Paleozoic carbonate rocks and consists of mainly HK (phlogopite macrocrystic monticellite

hypabyssal kimberlite) (Sage 1996). Kimberlites from Kirkland Lake have emplacement ages ranging from 165-152 Ma (n=12), and Timiskaming ranging from 142-134 Ma (n=8) (Heaman and Kjarsgaard 2000).

There is general agreement that the final controls of kimberlite emplacement for each of the kimberlite fields are related to older crustal structures (Heaman and Kjarsgaard 2000 and references therein). The Churchill Province kimberlites (Rankin Inlet) are associated with the Pyke fault; the Attawapiskat kimberlites are associated with the Winisk River structural zone; the emplacement of the Kirkland Lake kimberlites were controlled by the Porcupine-Destor and Cadillac fault systems; and the Timiskaming kimberlites were controlled by the Lake Timiskaming fault system (Sage 1996; Heaman and Kjarsgaard, 2000).

Previous isotopic studies of kimberlitic perovskite

Perovskite is a common accessory mineral that occurs in the groundmass of many kimberlites. It is stoichiometrically close to the end member $CaTiO_3$ (Chakmouradian and Mitchell 2000). It is typically present in concentrations below 10 vol. %, and is most commonly found occurring in magmatic kimberlite, either randomly or as necklace textures around earlier crystallizing olivines (Mitchell 1986). In diatreme and crater facies rocks perovskite occurs in the matrix of pelletal and juvenile lapilli, respectively (Chakmouradian and Mitchell 2000). The average size of groundmass perovskite is ~20-50 μm. There is general agreement that perovskite is resilient to alteration, and an early crystallizing phase in a kimberlite magma (e.g. Veksler and Teptelev, 1990; Chakmouradian and Mitchell 2000). It is ideal because it can be used to determine the emplacement age of the host kimberlite, as well as provide information about the origin of the magma from Sr and Nd isotopic compositions on the same mineral fraction.

Heaman (1989) investigated a suite of North American and South African kimberlitic perovskite, determining the U-Pb emplacement ages as well as their initial Sr-Nd-Pb isotopic compositions, and concluded that perovskite is extremely suitable for Sr isotopic tracer studies based on the following observations: 1) it was shown to be a major carrier of Sr (500-9000 ppm); 2) it has very low Rb/Sr ratios (<0.001) because of low Rb contents (0.05-1.63 ppm),

therefore the initial Sr compositions are insensitive to age corrections; and 3) it records a much more reliable initial Sr signature (i.e. initial Sr ratio is insensitive to age correction and to crustal contamination), interpreted to represent the initial Sr isotopic composition of the host kimberlite magma ($^{87}Sr/^{86}Sr_{initial}$= 0.70341-0.70485). Heaman (1989) reported Sm and Nd concentration data, as well as Nd isotopic data for perovskite and showed that the initial Nd isotopic compositions of perovskite were comparable to whole rock data for kimberlites; $^{147}Sm/^{144}Nd$ = 0.06-0.09, $^{143}Nd/^{144}Nd_{initial}$ = 0.51248-0.51286. Based on a small number of samples, Heaman (1989) interpreted the isotopic variations of Sr from different kimberlites to reflect either local isotopic heterogeneities in the mantle source region or the documentation of progressive modification of isotopically uniform kimberlite magma through the SCLM and continental crust. Heaman (1989) also showed that the initial Sr and Nd isotopic compositions displayed little variation even with a large range in emplacement ages.

Smith (1983) and Alibert and Albarède (1988) showed many examples of the usefulness of whole rock Sr and Nd isotopic studies on kimberlites. These classic Sr-isotope studies have been revisited and comparisons of Sm-Nd and Rb-Sr data of whole rock kimberlites and kimberlitic perovskite (e.g. Paton et al. 2007, Woodhead et al. 2008) have shown that perovskite is the preferred mineral for obtaining primary Sr isotopic signatures. Woodhead et al. (2008) has shown that in the case of Group I South African kimberlites, the Sr isotope data variations do not correlate with age and appear to reflect substantial differences in the magma source regions.

Methods

Kimberlite samples (mainly drill core) ranging from 0.1 to 1 kg were crushed to ~2 cm and then pulverized to a fine powder using a tungsten carbide shatterbox. Perovskite was separated using standard heavy liquid and magnetic separation techniques. Liberated perovskite grains ranged in size from 20-100 μm, and were handpicked with a binocular microscope at 100x magnification.

All grains with visible inclusions or imperfections were excluded. The fractions were washed in 4N HNO_3, given a 45 second bath in an ultrasonic cleaner, and then rinsed with

millipore water. Calibrated ^{150}Sm-^{149}Nd and ^{235}U-^{205}Pb tracer solutions were added prior to dissolution. Perovskite fractions were dissolved in teflon bombs in 48% HF and 7N HNO_3 (50/50), and were placed in an oven at ~230˚C. The analytical procedures for purifying uranium and lead by anion exchange chromatography and determining their isotopic compositions using a VG354 thermal ionization mass spectrometer are outlined by Heaman and Kjarsgaard (2000). In most cases the amount of perovskite available was sufficient for only one analysis; therefore the ^{206}Pb/^{238}U age is taken as the best estimate for the timing of perovskite crystallization as this age is least sensitive to the common lead correction. Atomic ratios are corrected for mass spectrometer fractionation (Pb- 0.088%/amu; U-0.155%/amu), blank (5 pg Pb; 1 pg U), and spike contribution. In addition, the ^{206}Pb/^{238}U ratios were corrected for the presence of initial common Pb using the two stage average crustal Pb model of Stacey and Kramers (1975). The errors reported in Table 4-1 and the uncertainties associated with age determinations are quoted at two sigma (λ^{238}U- 1.55125×10^{-10} year^{-1}; λ^{235}U- 9.8485×10^{-10} year^{-1}; Jaffey et al. 1971).

The Sr and Nd isotopic composition of perovskite was determined on the same fractions prepared for U-Pb geochronology. The washes containing Sr and Nd from the uranium and lead purification were loaded onto separate standard cation exchange columns, with an initial separation of the rare earth elements (including Sr), and then further purification and isolation of Sr and Nd (Holmden *et al.*, 1996). The purified Sr was loaded onto a single Re filament employing a tantalum gel loading method (Creaser et al., 2004) and the Sr isotopic compositions were determined using a Sector54 thermal ionization mass spectrometer in static multi-collector mode. Accuracy of the Sr isotopic composition was monitored using the NIST SRM 987 Sr isotopic standard (0.71022 ± 0.00002 average value obtained). To confirm the procedure for multiple isotopic analyses on a single perovskite fraction, two fractions of the in-house Ice River perovskite standard were analysed and the ^{87}Sr/^{86}Sr results obtained are 0.70288 ±0.00002 and 0.70276±0.00002. Nd and Sm were separated using Di (2-ethylhexyl phosphate) chromatography (HDEHP) (Creaser et al. 1997). The purified Nd was analysed via solution-mode using a Nu Plasma MC-ICP-MS in the Radiogenic Isotope Facility at the University of Alberta. Accuracy of the Nd isotopic composition was monitored using the La

Jolla Nd isotopic standard (0.511850 ± 17). Repeated analyses of a 200 ppb solution of the in-house alpha Nd standard (n=60) during this study yielded $^{143}Nd/^{144}Nd = 0.512270 \pm 20$.

Results

U-Pb Perovskite geochronology

Although U-Pb perovskite ages have been reported previously for the 16 kimberlite samples investigated in this study (Heaman and Kjarsgaard 2000; Zurevinski et al. 2008), most samples have been re-analyzed in order to confirm the age of perovskite crystallization for fractions investigated here, and ensure the correct formation age is used to calculate initial Nd isotopic compositions. Multi-grain fractions (up to 400 single grains) were analysed due to the small grain size of the perovskite (30-80 μm) and the results are presented in Table 4-1.

The study of perovskite from the Churchill kimberlites offers a unique perspective to this Sr and Nd isotope study, due to the presence of multiple age populations of perovskite occurring in a single kimberlite intrusion. As described in Chapter 3 and by Zurevinski et al. (2008), some Churchill kimberlites contain two distinct populations of perovskite (on the basis of size, colour and habit). U-Pb results indicated that in some cases, the different populations revealed similar emplacement ages and a weighted average of the $^{206}Pb/^{238}U$ dates is interpreted as the best estimate for the emplacement age of that particular pipe, while in other cases, distinct emplacement ages were obtained. In these cases, the older perovskite is interpreted as being derived from xenolithic kimberlite (kimberlite 'autoliths' are present in Churchill kimberlites). This interpretation is feasible based on the fact that the emplacement ages for Churchill kimberlites span nearly 55 m.y. from 225-170 Ma, making it a real possibility that younger kimberlite magmas could intrude older kimberlites. One example where this may be the case is kimberlite CD 009. In this kimberlite two perovskite fractions were selected (S and L), separated on the basis of size and colour, and they record distinct U-Pb ages of 176.1 Ma and 196.5 Ma, respectively (Chapter 3; Zurevinski et al. 2008). Samples were also selected to encompass the spectrum of kimberlite emplacement ages. For example, the 05FWR005-A-2 kimberlite is one of the oldest kimberlites on the property at 225.3 ± 0.6 Ma (Zurevinski et al.

2008) and kimberlite CD 024 yielded a single perovskite population with an age is 192.4±4.8 Ma (Chapter 3: Zurevinski et al. 2008).

A single perovskite fraction was analysed from each of the two Attawapiskat kimberlites, Bravo and Charlie. Both kimberlites contain abundant euhedral brownish black perovskite with moderate U concentrations (258 and 191 ppm, respectively) and moderate Th/U (14.4 and 20.8, respectively). The $^{206}Pb/^{238}U$ model age obtained for the Bravo perovskite fraction in this study is 178.9 ± 3.7 Ma, in excellent agreement with the two previously reported perovskite U-Pb ages for the Bravo kimberlite (179.4 ± 2.2, 175.7 ± 1.8 Ma; Heaman and Kjarsgaard 2000). The weighed mean of the three reported perovskite dates is 177.4 ± 1.3 Ma (MSWD=3.8) and recommended updated emplacement age for the Bravo kimberlite. The perovskite $^{206}Pb/^{238}U$ model age obtained in this study for a second fraction selected from the Charlie kimberlite is 168.4 ± 3.4 Ma. This age is younger than the previously reported perovskite U-Pb age of 179.9 ± 1.6 Ma (Heaman and Kjarsgaard 2000). The cause for this age difference is unknown, and the possibility that there could be multiple age populations of perovskite in this sample of Charlie kimberlite needs to be explored further. The age of 168.4 Ma obtained for Charlie perovskite in this study is used to calculate initial Sr and Nd isotopic compositions (see below).

Five perovskite fractions were analysed from the Kirkland Lake kimberlites (Buffonta, Buzz, Diamond Lake (x2), and Morissette Creek). Diamond Lake perovskite was separated into two fractions on the basis of size and colour; 1) a brown euhedral fraction of smaller (~30 μm) crystals and 2) a fraction consisting of larger (~60 μm) yellow euhedral cubes. The $^{206}Pb/^{238}U$ ages for both of the Diamond Lake perovskite fractions are within error (159.1 ± 3.8 and 161.4 ± 4.9 Ma, respectively). Therefore the weighted average $^{206}Pb/^{238}U$ age of 160.0 ±2.9 Ma (2σ error) is interpreted as the emplacement age of the Diamond Lake kimberlite. The previously reported age of 152.6 ± 2.2 Ma (Heaman and Kjarsgaard 2000) is younger than the ages determined in this study. A fraction of perovskite selected from the Buzz kimberlite in this study yields a $^{206}Pb/^{238}U$ model age of is 158.4 ± 3.7 Ma (2σ), which is in good agreement with the previously reported emplacement age of 153.5 ±1.3 Ma (Heaman and Kjarsgaard 2000).

The Buffonta kimberlite perovskite $^{206}Pb/^{238}U$ model age from this study is 155.7 ± 3.9 Ma (2σ), which is in agreement with the previously reported age of 153.4 ± 2.6 Ma (Heaman and Kjarsgaard 2000). The weighted mean $^{206}Pb/^{238}U$ age for these two fractions of 154.1 ±2.2 Ma is considered to be the current best estimate for the emplacement age of the Buffonta kimberlite. The Morissette Creek perovskite $^{206}Pb/^{238}U$ model age from this study is 161.6 ± 3.9 Ma (2σ). This age is almost within error of the previously reported age for Morissette Creek of 155.6 ± 2.0 Ma (Heaman and Kjarsgaard 2000). The U-Pb perovskite age results obtained in this study confirm that these Kirkland Lake kimberlites were emplaced between 162-156 Ma.

Three kimberlites from the Timiskaming cluster were analysed (Glinkers, Peddie and OPAP). The $^{206}Pb/^{238}U$ model age for the Glinkers kimberlite is 130.9 ± 3.1 Ma (2σ), which is in agreement with the previously reported ages of 133.9 ± 2.4 Ma and 133.9 ± 2.0 Ma (Heaman and Kjarsgaard 2000). The weighted average $^{206}Pb/^{238}U$ age for these three perovskite fractions is 133.3 ± 3.6 Ma and is considered the current best estimate for the emplacement age of the Glinkers kimberlite. The $^{206}Pb/^{238}U$ model age for perovskite from the Peddie kimberlite in this study is 156.1 ±3.3 Ma, which is in agreement with the previously reported age of 153.6 ± 2.4 Ma (Heaman and Kjarsgaard 2000). The weighted average $^{206}Pb/^{238}U$ age of 154.5 ±1.9 Ma is considered the current best estimate for the emplacement age of the Peddie kimberlite. Results indicate that there are multiple emplacement ages for this kimberlite field, with the emplacement ages ranging from 156 Ma to 131 Ma. This range has been noted previously has led to the interpretations as a "Type 3" kimberlite field (Heaman and Kjarsgaard 2000).

Perovskite Sr and Nd isotopic compositions

Table 4-2 presents the Sr and Nd isotopic compositions for perovskite isolated from the following kimberlite fields; Churchill (n=6), Attawapiskat (n=4), Kirkland Lake (n=6) and Timiskaming (n=4). Interestingly, the $^{87}Sr/^{86}Sr$ isotopic compositions obtained for samples with multiple perovskite populations (i.e. 04KD230 and CD-009 from the Churchill field and Diamond Lake from Kirkland Lake field) are identical within error, even though there are large variations in some of the crystallization ages (e.g. 197 and 176 Ma for the two perovskite fractions from CD-009; Table 4-1). There is only a slight variation in the $^{143}Nd/^{144}Nd_i$ for

samples that contain multiple age populations of perovskite (CD-009 and 04KD230). Two perovskite fractions were analysed for the Bravo kimberlite (Attawapiskat kimberlites), which were separated on the basis of size (both fractions were the same habit and colour). These two fractions have identical $^{87}Sr/^{86}Sr$ isotopic compositions (0.70419 and 0.70413, respectively), and highly positive εNd signatures (+13.7 and +9.3, respectively).

Overall, the most notable trend is the inverse correlation between initial $^{87}Sr/^{86}Sr$ and kimberlite emplacement age for most of the kimberlites. From NW to SE (i.e. oldest to youngest kimberlites) the range of initial $^{87}Sr/^{86}Sr$ ratios in perovskite is as follows: Churchill Province (0.70317-0.70359), Attawapiskat (0.70401-0.70419), Kirkland Lake (0.70417-0.70509), and Timiskaming (0.70346-0.70457). These data show: 1) clustering of initial $^{87}Sr/^{86}Sr$ ratios for the Churchill and Attawapiskat kimberlites, and 2) a general increase in $^{87}Sr/^{86}Sr$ ratio with younging direction of kimberlites, beginning with the oldest (Churchill) and ending with the Kirkland Lake/Timiskaming kimberlites. These relatively unradiogenic Sr isotopic compositions overlap the Group I South African whole rock kimberlite field of Smith (1983) and perovskite strontium isotopic compositions for select Cretaceous African (Woodhead et al. 2008: Group I kimberlitic perovskite $^{87}Sr/^{86}Sr$ = 0.7035-0.7050); and 1.1 Ga Indian kimberlites (Paton et al. 2007: Narayanpet Field: $^{87}Sr/^{86}Sr$ (average) =0.70321; Wajrakarar Field: $^{87}Sr/^{86}Sr$ (average) =0.70246).

The $^{147}Sm/^{144}Nd$ ratios obtained for perovskite from the kimberlites investigated in this study all fall within previously reported ratios for kimberlite perovskite (Heaman 1989): Churchill (0.0666 to 0.0870), Attawapiskat (0.0635-0.0734), and Kirkland Lake/Timiskaming (0.0600-0.0918). An interesting finding in this study is that the $^{143}Nd/^{144}Nd$ ratios for kimberlitic perovskite vary considerably with epsilon Nd values at the time of kimberlite emplacement (εNd_T) that span between -1.4 and +13.7 (Table 4-2). However, the majority of perovskite fractions have positive εNd_T values between +2.3 and +9.6 (Table 4-2): Churchill (εNd_T = -1.4 to 10.9); Attawapiskat (εNd_T = 5.8-13.7); Kirkland Lake (εNd_T = 4.8-7.8) and Timiskaming (εNd_T = 6.7-10.4). The Sr and Nd isotopic results for all available perovskite analyses from the Triassic-Jurassic central to eastern Canadian kimberlites and related rocks are

shown in Figure 4-2, including results from the Ham diatreme and Varty Lake ultramafic lamprophyre (Heaman 1989). The Nd isotopic compositions for all perovskite analyses in this study generally fall within the previously established field for ocean island basalts (OIBs) and Group I kimberlites, based on whole rock samples. With the exception of one perovskite sample from the Churchill kimberlites (CD 024), all of the εNd_T values are positive, implying derivation from a depleted mantle source. It would be useful to evaluate this further by comparing the bulk rock kimberlite chemistry of CD 024 with that of other Churchill kimberlites. The distinct clustering of perovskite Sr isotope compositions recorded in each of the kimberlite fields investigated is not observed in the Nd isotope data. In general, the perovskite εNd_T values are more variable and typically more positive in the Churchill and Attawapiskat kimberlites compared to the Kirkland Lake kimberlites (Table 4-2).

Discussion

There has been a renewed interest in using perovskite as a proxy for determining the primary isotopic composition of kimberlite magma. Maas et al. (2005) concluded that perovskite records a more straightforward and robust Sr isotopic record of a kimberlite melt, using perovskite separated from an autolith in the Devonian Udachnaya-East kimberlite pipe, Yakutia. The ultrafresh autolith whole-rock compositions yielded a range of $^{87}Sr/^{87}Sr_{initial}$= 0.7036-0.7049 whereas three perovskite analyses yielded similar low values of 0.70303, 0.70303 and 0.70308 (Maas et al. 2005). Maas et al. (2005) interpreted the initial Sr ratios from the perovskite to support the idea of Ringwood (1991), as evidence for recycled oceanic crust as a possible source of kimberlites. Paton et al. (2007) measured Sr isotopic compositions from groundmass perovskite via in-situ LA-MC-ICP-MS, providing insights into the primary isotopic signatures of ~1.1 Ga Indian kimberlites from the Dharwar Craton. This study also confirmed the robustness of perovskite compared to weathered kimberlite whole rock, highlighting the immunities of perovskite to late stage crustal contamination and alteration. The study compared kimberlitic perovskite from the Narayanpet Field and the Wajrakarar Field, concluding that each field had distinct $^{87}Sr/^{86}Sr_{initial}$ ratios (average $^{87}Sr/^{86}Sr$ of 0.70321 and 0.70246, respectively), significantly lower than the host kimberlite (0.701-0.709). Paton et al.

(2007) interpreted these slight differences in average perovskite Sr isotopic composition to reflect that each kimberlite field originated from isotopically distinct yet internally homogeneous mantle sources. Paton et al. (2007) further speculate on three potential mantle sources to explain these compositions: 1) subcontinental lithospheric mantle (SCLM); 2) the convecting upper mantle; and 3) ultra-deep mantle (at or below the transition zone). They note that while small degree partial melts of SCLM is the most common mantle source region proposed for the origin of kimberlite, the SCLM is heterogeneous in Sr isotopic composition, and a source here fails to explain the origin of majorite garnet inclusions in diamonds, typically inferred to be derived from depths greater than 400 km (Gurney, 1991). Paton et al. (2007) conclude that the 1.1 Ga Indian kimberlites may have formed by mantle melting at great depths via a "diapiric" model, allowing for the production of each kimberlite field from a single pool of homogenized melt.

The perovskite $^{87}Sr/^{86}Sr$ signatures from each of the kimberlite fields investigated in this study (Churchill, Attawapiskat, and Kirkland Lake/Timiskaming) exhibit a unique Sr isotopic signature, interpreted to reflect the nature of the mantle source rocks in which they have originated. Although a few studies have also shown clustering of the perovskite $^{87}Sr/^{86}Sr$ ratios within individual kimberlite fields (e.g. Paton et al. 2007, Woodhead et al. 2008), the results of this study clearly exhibit an increasing $^{87}Sr/^{86}Sr$ ratio with younging direction of kimberlites. This observed progressive increase in $^{87}Sr/^{86}Sr$ ratio cannot be due to radiogenic in-growth of ^{87}Sr because there is negligible Rb (<0.01 ppm) in perovskite (Heaman 1989; Paton et al. 2007). Groundmass perovskite is clearly capable of recording the original isotopic signatures of the kimberlite magma, allowing for a proper investigation into the source rock involved in producing kimberlite magma.

Figure 4-3 is a diagram of $^{87}Sr/^{86}Sr$ versus time, showing the Sr evolution of two reservoirs on earth: 1) Bulk Silicate Earth (BSE) and 2) Depleted MORB mantle (DMM) (Workman and Hart 2005). The initial $^{87}Sr/^{86}Sr$ signatures for kimberlitic perovskite determined in this study are also shown and the results from Churchill and Attawapiskat kimberlites are more clustered, while the Kirkland Lake and Timiskaming ratios are more variable. The

variability of the Kirkland Lake and Timiskaming perovskite Sr isotopic compositions will be addressed below. The most important feature to note in Figure 4-3 is that there is a strong correlation between the perovskite initial strontium isotopic composition and kimberlite emplacement age for the Churchill, Attawapiskat and Kirkland Lake samples, and is denoted as "The Triassic/Jurassic Kimberlite Sr Array" (Figure 4-3). The Churchill kimberlites are the oldest, have the least radiogenic Sr signatures (0.70317-0.70359), and plot between the BSE and DMM Sr evolution lines. The Attawapiskat kimberlites cluster on or near the BSE Sr evolution line, with a more radiogenic signature (0.70401-0.70419) than the Churchill kimberlites. The Kirkland Lake and Timiskaming kimberlite fields (assessed together due to their close geographical proximity) show more variation in Sr ratios (0.70417-0.70509), plotting on or above the BSE Sr evolutionary line. The exceptions are the occurrence of three less radiogenic Sr signatures (0.70364, 0.70338, 0.70337), recorded by perovskite from the younger Timiskaming kimberlites (Glinkers, OPAP, MacLean). One possible explanation for the offset of these three kimberlites is that they form (or belong) to another evolution trend line (i.e. are formed by some different mechanism). The Ham diatreme (Heaman 1989) is also shown to plot close to this trend. There are a few notable conclusions from this "Triassic/Jurassic Kimberlite Sr Array": 1) there is a clear Sr isotope composition versus age relationship within these kimberlites, 2) assuming the Sr ratios are representative of primary kimberlite magma Sr isotope compositions, the source rocks for each kimberlite field have clearly differing isotopic compositions, and 3) some of the kimberlites plot on or around the BSE Sr evolutionary line, with lesser involvement with a DMM source with time, demonstrating the potential of a distinctly different source region (Figure 4-3). Figure 4-4 is a diagram of $^{143}Nd/^{144}Nd$ versus time showing the Nd evolution of the two reservoirs on earth: 1) Bulk Silicate Earth (BSE) and 2) Depleted MORB mantle (DMM) (Workman and Hart 2005). In this diagram, there is less of a correlation (as shown in the Sr evolutionary diagram, Figure 4-3) of the kimberlitic perovskite with the BSE evolutionary line. The data plot on or around the depleted MORB mantle evolutionary line, and it is only the Kirkland Lake samples with show any trend toward the BSE field.

Three main models have been invoked to explain the origin of Eastern North American (ENA) kimberlite magmatism including rifting (Phipps 1988), subduction (Sharp 1974; McCandless 1999), and the passage of one or more mantle plumes (Crough 1981; Morgan 1983; and Sleep 1990; Heaman and Kjarsgaard 2000). Rifting associated with the opening of the North Atlantic Ocean at about 200 Ma has been proposed but does not readily explain all the Jurassic kimberlite magmatism in North America. There are Jurassic kimberlites and related rocks occurring on both margins of the Labrador Sea in Labrador (Tappe et al. 2006) and Greenland (Larsen 1992), therefore some Jurassic kimberlite magmatism in North America is related in time to the opening of the North Atlantic Ocean. However, the occurrence of the corridor of Triassic/Jurassic kimberlite magmatism is not explained by this rifting only model.

There have been two subduction hypotheses proposed for ENA kimberlite magmatism. West-dipping subduction-related magmatism linked to the development of the Appalachian Mountains (i.e. Paleozoic subduction) was proposed by Sharp (1974) but does not explain the much younger ENA Mesozoic kimberlite magmatism as subduction ceased more than 200 m.y. prior to the Jurassic kimberlite magmatism. A more recent model involves the subduction of the Farallon plate in the Pacific Ocean in an E-SE direction from 175-125 Ma (McCandless 1999). This "deep-seated" subduction, where the slab extends ~2700 km beneath North America (Grand et al. 1997), involves the process of progressive release of entrapped fluids from the downgoing slab and promoting small degree partial melts of the overlying mantle wedge to produce kimberlitic magma. The kimberlites are the result of partial melting, and as subduction continues fluids are released up the slab, therefore kimberlites would have a younging direction towards the trench (McCandless 1999). This subduction model would generate belts of magmatism that are roughly parallel to the margin where the subduction occurs. Heaman and Kjarsgaard (2000) maintain that the timing and location of the Rankin and Attawapiskat kimberlites does not fit this model due to the kimberlites occurring more than 2000 kms from the site of Farallon subduction at the time when the Farallon plate is just beginning to impact the tectonics of western North America at 200 Ma. In addition, the fluids

released from a subducting slab are insufficient in high field strength elements to represent the precursor metasomatic agent that reflects the geochemical signature of a kimberlitic melt.

The Sr and Nd isotopic data derived from the Churchill, Attawapiskat and Kirkland Lake/Timiskaming kimberlites support the model of kimberlite melt derivation by small degree melting caused by the passage of one or more mantle plumes. The mantle plume theory for the origin of ENA kimberlites has been proposed by several authors (Crough 1981; Morgan 1983; Sleep 1990; Heaman and Kjarsgaard 2000). The nature of continental magmatism is different from that of oceanic magmatism, based on the alkaline continental record where narrow linear belts of plutonism occur, and the tholeiitic oceanic record where linear chains of seamounts occur. The striking younging pattern of emplacement ages along the Great Meteor Hotspot track (Heaman and Kjarsgaard 2000), along with the increase in Sr isotope ratios (this study) is unquestionable. The Sr isotope data from this study also follows a progression along the proposed Great Meteor Hotspot track; Churchill (0.7032-0.7036, n=6), Attawapiskat (0.7040-0.7042, n= 4), and Kirkland Lake (0.7042-0.7051, n=6). The exceptions to this pattern are the results obtained for the three youngest kimberlites from the Timiskaming cluster (131 Ma Glinkers, 145 Ma OPAP, 142 Ma MacLean) with $^{87}Sr/^{86}Sr_i$ values of 0.7036, 0.7033 and 0.7034, respectively. The older 156.1 Ma Peddie kimberlite ($^{87}Sr/^{86}Sr_i$=0.7046) from the Timiskaming cluster does fit the Triassic/Jurassic kimberlite array (Table 4-2; Figure 4-3). There are a few viable explanations for the span of emplacement ages and differences in the perovskite initial $^{87}Sr/^{86}Sr$ ratios between the Kirkland Lake and majority of Timiskaming kimberlites: 1) the passage of two mantle plumes along the same corridor separated by about 30-40 m.y. (i.e. the Verde and Great Meteor Hotspot tracks) may both have played a role in generating the apparent prolonged kimberlite magmatism in these fields; 2) the source region may be isotopically heterogeneous, 3) changes in plate motions may have played a role in the emplacement patterns of these kimberlites (Heaman and Kjarsgaard 2000).

Figure 4-5 is a northwest to southeast cross-section of the Churchill and Superior cratons, which compiles information gleaned from the SCLM based on sampling by a number of kimberlite fields that crudely fall along this transect (Somerset Island southeast to the

Kirkland Lake/Timiskaming area). The position of the cratonic root (SCLM boundary) along this corridor has been interpreted from different sources. Schmidberger et al. (2001) recognized two lithospheric domains on the basis of $^{87}Sr/^{86}Sr$ of Archean garnet peridotites and garnet pyroxenite xenocrysts from the host Nikos kimberlite at Somerset Island, a shallow (0.704) and deep (0.706-0.708) zone. Using garnet chemistry, Griffin et al. (2004) estimated that the base of the depleted lithosphere beneath Somerset Island lies near 140 km. Since there are currently no mantle xenolith/xenocryst studies from the Churchill kimberlites, the base of the SCLM beneath the Churchill kimberlite field has been extrapolated using the information derived from the studies of Griffin et al. (2004) and Schmidberger et al. (2001) at Somerset Island, the margin of the Churchill craton. The SCLM lower boundary beneath the Trans-Hudson orogen, was estimated to be 180 kms by Griffin et al. (2004) using garnet chemistry on xenoliths from 7 kimberlites at the Fort a la Corne kimberlite field. Deep seismic tomography studies show the entire area as a high velocity root (~250 kms) that is continuous from the Hearne Domain across the Trans-Hudson Orogen and into the Superior craton (van der Lee 2001).

The new perovskite $^{87}Sr/^{86}Sr_{initial}$ ratios can be used to assess the hypothesis that the mantle plume responsible for the Great Meteor Hotspot track may have played an important role in generating Triassic-Jurassic kimberlite magmas along this corridor. The results show the distinct and uniform values representative of each kimberlite field, with the exception of the younger kimberlites of the Kirkland Lake and Timiskaming fields, which may be unrelated to the "ENA Triassic/Jurassic Kimberlite Array" (Figure 4-3). Figure 4-3 shows a clustering of $^{87}Sr/^{86}Sr$ values from each kimberlite field. The values show a stronger DMM signature at Churchill, and evolve towards BSE values at Attawapiskat. The highly positive εNd_T values from kimberlitic perovskite imply a depleted mantle source; furthermore, values of +10 may imply a relatively young depleted mantle source. While the Sr isotopic compositions for the Churchill kimberlites do not plot exactly on the DMM evolutionary line (Figure 4-3), the Nd compositions for the samples indicate DMM compositions (Figure 4-4). A possible interpretation of this is that the depleted mantle beneath the Churchill and Superior cratons is more enriched than the DMM shown. In some cases (Attawapiskat and Kirkland Lake), the

same perovskite fraction is recording a depleted mantle signature in Nd isotopes, and a BSE signature in Sr isotopes. One mechanism that could explain this would be that the Sr isotopes are reflecting varying degrees of contamination by lithosphere and the Nd isotopes are more immune to this. It is difficult to explain the clustering and trends shown in the Sr isotopic data if the Sr had been affected by varying degrees of lithospheric contamination, but nevertheless it remains a possibility. The isotopic variations between the Sr and Nd data are peculiar, and could reflect local heterogeneities in the mantle source regions.

A fundamental question is where in the mantle is it possible to generate kimberlite magmas that have the range of isotopic compositions observed in this study (i.e. a Group I kimberlite magma with a DMM signature and a Group I kimberlite magma with a BSE signature). In Figure 4-5, along with the NW-SE direction of the continental portion of the Great Meteor Plume track, potential regions of kimberlite melt formation generated from the heat transfer as a result of a plume have been assessed for each kimberlite field. The DMM Sr signatures of the perovskite allow the minimum depth of the Churchill kimberlite melt formation to be estimated at the base of the SCLM. The range of $^{87}Sr/^{86}Sr_{initial}$ for the Churchill kimberlites (0.7032-0.7036) is interpreted to represent a hybrid magma with a DMM influence. The Attawapiskat $^{87}Sr/^{86}Sr_{initial}$ ratios cluster (0.7040-0.7042) and represent a distinctly different source than that of the Churchill kimberlite magmas, which is interpreted to be a deeper source possibly in the transition zone. The Kirkland Lake and Timiskaming kimberlites are shown together due to their close geographical proximity and their $^{87}Sr/^{86}Sr_{initial}$ ratios range from 0.7034 to 0.7050. The emplacement ages of the kimberlites reveal this to be classified as a "type 3" kimberlite province (Heaman and Kjarsgaard 2000). If the kimberlites from the Kirkland Lake and Timiskaming area are grouped on the basis of emplacement ages instead of the kimberlite field that they belong to, the three younger kimberlites (Glinkers ~131 Ma; OPAP ~145 Ma; and MacLean ~142 Ma) have their own unique $^{87}Sr/^{86}Sr_{initial}$ ratios (0.7036, 0.7033 and 0.7034, respectively) (Table 4-2). This would give the older kimberlites (164-155 Ma) a $^{87}Sr/^{86}Sr_{initial}$ range of 0.7042-0.7051, and the younger kimberlites (145-131 Ma) a $^{87}Sr/^{86}Sr_{initial}$ range of 0.7033-0.7036. One possible interpretation for this difference in Sr

isotopic signature of old versus young kimberlites in the Kirkland Lake/Timiskaming field is that they have different mantle sources and were generated by two different mantle melting events. For example, the older kimberlites with an elevated Sr isotopic composition may have been derived from the asthenosphere and perhaps in the transition zone (Figure 4-3). The younger kimberlites may have melt formation located at the boundary of the transition zone or shallower, the variability in the Sr ratios and the ages make it difficult to estimate melt formation for these particular kimberlites, which may be altogether unrelated to the proposed Great Meteor Plume track kimberlites (Figure 4-3). A distinct possibility is that the younger kimberlites are related to the Verde plume, and there is need for further studies before it could be concluded that the mantle plume that caused the Verde hotspot track played a role in the generation of ENA kimberlite magmas.

Conclusion

The evolution of Eastern North American kimberlite magmatism

Perovskite is a robust mineral for obtaining the age of kimberlite emplacement and the primary Sr and Nd isotopic signature of a kimberlite magma. The initial $^{87}Sr/^{86}Sr$ ratios of primary kimberlite magma can be used as a proxy to constrain the nature of its mantle source region, as well as valuable information on the nature of the isotopic composition of the SCLM and asthenosphere. The results obtained in this study indicate that each Eastern North American kimberlite field (Churchill, Attawapiskat and Kirkland Lake/Timiskaming) has unique isotopic compositions indicating a distinct mantle source for each. The Churchill kimberlites have a depleted mantle source, while the Attawapiskat and Kirkland Lake/Timiskaming kimberlites have a more primitive, BSE-like source. The Sr and Nd results of this study indicate the possibility of multiple mantle sources for Group I kimberlites. The increase in perovskite $^{87}Sr/^{86}Sr_{initial}$ ratios along the ~2000-km-long corridor of near continuous Triassic/Jurassic kimberlite magmatism could be explained from either a single or multiple mantle plume hotspot track, responsible for the generation of kimberlite melts, as proposed by Heaman and Kjarsgaard (2000).

References

Alibert, C. & Albarède, F. 1988. Relationships between mineralogical, chemical and isotopic properties of some North American kimberlites. Journal of Geophysical Research, 93:7643-7671.

Becker, M. and Le Roex, A. 2006. Geochemistry of South African On- and Off-craton, Group I and Group II kimberlites: Petrogenesis and Source Region evolution. Journal of Petrology, 47: 673-703.

Chakhmouradian, A.R. and R.H. Mitchell. 2000. Occurrence, alteration patterns and compositional variation of perovskite in kimberlites. The Canadian Mineralogist, 38:975-994.

Creaser, R.A., Erdmer, P., Stevens, R.A., and Grant, S.L. 1997. Tectonic affinity of Nisutlin and Anvil assemblage strata from the Teslin tectonic zone, northern Canadian Cordillera: Constraints from neodymium isotope and geochemical evidence. Tectonics, 16:107-121.

Creaser, R. A., Grűtter, H., Carlson, J. & Crawford, B. 2004. Macrocrystal phlogopite Rb-Sr dates for the Ekati property kimberlites, Slave Province, Canada: evidence for multiple intrusive episodes in the Paleocene and Eocene. Lithos, 76:399-414.

Crough, S.T. 1981. Mesozoic hotpspot epeirogeny in Eastern North America. Geology, 9:2-6.

Duncan, R.A. 1984. Age progressive volcanism in the New England Seamounts and the opening of the central Atlantic Ocean. Journal of Geophysical Research, 89:9980-9990.

Fowler, J.A., Grutter, H.S., Kong, J.M., and Wood, B.D. 2001. Diamond exploration in Northern Ontario with reference to the Victor kimberlite, near Attawapiskat. Exploration and Mining Geology, 10:67-75.

Fraser, K.J. and Hawkesworth, C.J. 1992. The Petrogenesis of group 2 ultrapotassic kimberlite from the Finsch mine, South Africa. Lithos, 28:327-345.

Grand, S.P., Van der Hilst, R.D., Widiyantoro, S. 1997. Global seismic tomography: a snapshot of convection in the Earth: GSA today, 7:1-7.

Griffin, W.L., O'Reilly, S.Y., Doyle, B.J., Pearson, N.J., Coopersmith, H., Kivi, K., Malkovets, V. & N. Pokhilenko. 2004. Lithospheric mapping beneath the North American plate. Lithos, 77:873-922.

Gurney, J.J. 1991. Diamonds deliver the dirt. Nature, 353:601-602.

Heaman, L.M. 1989. The nature of the subcontinental mantle from Sr-Nd-Pb isotopic studies on kimberlitic perovskite. Earth and Planetary Science Letters, 92:323-334.

Heaman, L.M. & Kjarsgaard, B.A. 2000. Timing of Eastern North American kimberlite magmatism: continental extension of the Great Meteor Hotspot Track? Earth and Planetary Science Letters, 178:253-268.

Heaman, L.M., Kjarsgaard, B.A. & Creaser, R.A. 2003. The timing of kimberlite magmatism in North America: implications for global kimberlite genesis and diamond exploration. Lithos, 71:153-184.

Heaman, L.M., Kjarsgaard, B.A & Creaser R.A. 2004. The temporal evolution of North American kimberlites. Lithos, 76:377-397.

Holmden, C.E., Creaser, R.A., Muehlenbachs, K., Bergstrom, S.A. & Leslie S.A. 1996. Isotopic and elemental systematics of Sr and Nd in 454 Ma biogenic apatites: implications for paleoseawater studies. Earth and Planetary Science Letters, 142:425-437.

Jaffey, A.H., Flynn, K.F., Glendenin, L.E., Bentley, W.C. & Essling, A.M. 1971. Precise measurement of half-lives and specific activities of ^{235}U and ^{238}U. Physics Review, C4:1989-1906.

Kong, J.M., Boucher, D.R., and Scott-Smith, B.H. 1999. Exploration and Geology of the Attawapiskat Kimberlites, James Bay Lowland, Northern Ontario, Canada. Proceedings of the 7th International kimberlite conference, pp.452-467.

Larsen, L.M., and Rex, D.C. 1992. A review of the 2500 Ma span of alkaline-ultramafic, potassic and carbonatitic magmatism in West Greenland. Lithos, 28:367-402.

Ludwig, K.R. 2003. Isoplot/Ex version 3.0; a geochronological toolkit for Microsoft Excel; Berkeley Geochronology Center Special Publication No. 1a; Berkeley, California.

Maas, R., Kamenetsky, C., Paton, C., and Sharygin, S. 2008. Low $^{87}Sr/^{86}Sr$ in Kimberlitic Perovskite- Further evidence for recycled oceanic crust as a possible source of kimberlites. 9th International Kimberlite Conference Extended Abstract No. 9IKC-A-00296.

McCandless, T.E. Kimberlites: mantle expressions of deep-seated subduction. 1999. *in* Gurney, J.J., Gurney, J.L., Pascoe, M.D. and Richardson, S.H. (editors). Proceeding of the 7th International Kimberlite Conference, Volume 2, pp. 545-549. Red Roof Publishers, Cape Town, South Africa.

Mitchell, R.H. 1986. Kimberlites. Plenum Press, New York

Morgan, W.J. 1983. Hotspot tracks and the early rifting of the Atlantic, Tectonophysics, 94:123-139.

Nowell, G.M., Pearson, D.G., Kempton, P.D., Noble, S.R. and Smith, C.B. 1999. Origins of kimberlites: a hafnium perspective. In: Gurney, J.J., Gurney, J.L., Pascoe, M.D. and Richardson, S.H. (eds) Proceedings of the VIIth International Kimberlite Conference. Cape Town, Red Roof Design, pp.616-624.

Paton, C., Hergt, J.M., Phillips, D., Woodhead, J.D. & Shee, S.R. 2007. New insights into the genesis of Indian kimberlites from the Dharwar craton via in situ Sr isotope analysis of groundmass perovskite. Geology, 35:1011-1014.

Phipps, S.E. 1988. Deep rifts as sources for alkaline intraplate magmatism in eastern North America. Nature, 334:27-31.

Ringwood, A.E. 1991. Phase transformations and their bearing on the constitution and dynamics of the mantle. Geochimica et Cosmochimica Acta, 55:2083-2110.

Sage, R.P. 1996. Kimberlites of the Lake Timiskaming Structural Zone. Ontario Geological Survey open file 5937, 435 p.p.

Schmidberger, S.S., Simonetti, A. & D. Francis. 2001. Sr-Nd-Pb isotope systematics of mantle xenoliths from Somerset Island kimberlites: Evidence for lithosphere stratification beneath Arctic Canada. Geochimica et Cosmochimica Acta, 65:4243-4255.

Schmidberger, S.S., Simonetti, A., and Francis, D. 2003. Small-scale Sr-isotope investigation of clinopyroxenes from peridotite xenoliths by laser ablation MC-ICP-MS- Implications for mantle metasomatism. Chemical Geology, 199:317-329.

Scully, K.R., Canil, D. & D.J. Schulze. 2004. The lithospheric mantle of the Archean Superior Province as imaged by garnet xenocryst geochemistry. Chemical Geology, 207:189-221.

Sharp, W.E. 1974. A plate tectonic origin for diamond-bearing kimberlite. Earth and Planetary Science Letters, 21:351-354.

Sleep, N.H. 1990. Monteregian hotspot track: A long-lived mantle plume. Journal of Geophysical Research, 95:21983-21990.

Smith, C.B. 1983. Pb, Sr, and Nd isotopic evidence for sources of African Cretaceous kimberlite. Nature, 304:51-54.

Sol, S., Thomson, C.J., Kendall, J.M., White, D., VanDecar, J.C. & I. Asudeh. 2002. Seismic tomographic images of the cratonic upper mantle beneath the Western Superior Province of the Canadian Shield- a remnant Archean slab? Physics of the Earth and Planetary Interiors, 134:53-69.

Stacey, J.S., and Kramers, J.D. 1975. Approximation of terrestrial Pb isotope evolution by a two stage model. Earth and Planetary Science Letters, 26:207-221.

Tainton, K.M. 1992. The petrogenesis of group 2 kimberlites and lamproites from the Northern Cape Province, South Africa. Ph.D. thesis, Cambridge.

Tappe, S., Foley, S.F., Jenner, G.A., Heaman, L.M., Kjarsgaard, B.A., Romer, R.L., Stracke, A., Joyce, N., and Hoefs, J. 2006. Genesis of ultramafic lamprophyres and carbonatites at Aillik Bay, Labrador: a consequence of incipient lithospheric thinning beneath the North Atlantic Craton. Journal of Petrology, 47(7):1261-1315.

van der Lee, S. 2001. Deep below North America. Science, 294:1297-1298.

Veksler, I, and Teptelev, M. 1990. Conditions for crystallization and concentration of perovskite-type minerals in alkaline magmas. Lithos, 26:177-189.

Webb, K.J., Scott-Smith, B.A., Paul, J.L., and Hetman, C.M. 2004. Geology of the Victor kimberlite, Attawapiskat, Northern Ontario, Canada: cross-cutting and nested craters. Lithos, 76:29-50.

Workman, R.K., and Hart, S.R. 2005. Major and trace element composition of the depleted MORB mantle (DMM). Earth and Planetary Science Letters, 231:53-72.

Woodhead, J.D., Phillips, D., Hergt, J.M. and Paton, C. 2008. African kimberlites revisited: in situ Sr-isotope analysis of groundmass perovskite. 9th International Kimberlite Conference Extended Abstracts No. 9IKC-A-00092.

Zurevinski, S.E., Heaman, L.M., Creaser, R.A., and Strand, P. 2008. The Churchill kimberlite field, NU, Canada: Petrography, Mineral Chemistry and Geochronology. Canadian Journal of Earth Sciences, 45(9):1039-1059.

Table 4-1. U-Pb Perovskite results for selected kimberlites

	Weight (μg)	U (ppm)	Th (ppm)	Pb (ppm)	Th/U	TCPb (pg)	$^{206}Pb/^{204}Pb$	$^{238}U/^{204}Pb$	$^{206}Pb/^{238}U$	Age (Ma) $^{206}Pb/^{238}U$
Churchill Province, Nunavut										
05FWR005-A-2	52	401	632	21	1.6	174	286.78±1.01	7547.83±29.06	0.0356±0.0001	225.3±0.6
04KD230-A-(S)	39	255	1760	24	6.9	91	256.30±2.02	6959.37±67.10	0.0342±0.0002	216.7±2.4
04KD230-A-1(L)	36	375	2419	40	6.5	134	247.60±2.94	6527.15±103.2	0.0351±0.0003	222.4±4.0
CD 009-2-(S)	37	91	4405	15	48.4	127	64.69±0.46	1670.66±14.85	0.0277±0.0003	176.1±3.2
CD 009 (L)	90	117	2276	14	19.5	322	81.77±0.34	2044.15±9.70	0.0310±0.0001	196.5±1.4
CD 024-2 26.0m	33	132	2222	40	16.8	500	34.92±0.08	545.25±3.69	0.0303±0.0004	192.4±4.8
Attawapiskat, Ontario										
Bravo	75	258	3725	47	14.4	772	63.12±0.27	1588.08±16.51	0.0281±0.0003	178.9±3.7
Charlie	95	191	3980	42	20.8	693	62.39±0.16	1660.46±16.41	0.0265±0.0003	168.4±3.4
Kirkland Lake, Ontario										
Buffonta	99	33	592	7	18.2	225	40.82±0.16	915.87±10.72	0.0245±0.0003	155.7±3.9
Buzz	178	41	300	5	7.4	396	47.14±0.17	1153.92±12.15	0.0249±0.0003	158.4±3.7
Diamond Lake (small)	125	55	707	10	12.8	444	43.05±0.11	984.92±9.99	0.0250±0.0003	159.1±3.8
Diamond Lake (large)	162	19	43	3	2.2	319	34.27±0.10	624.39±6.72	0.0254±0.0004	161.4±4.9
Morissette Creek	137	135	2104	27	15.6	1227	45.54±0.08	949.24±9.14	0.0254±0.0003	161.6±3.9
Timiskaming, Ontario										
Glinkers	48	133	2233	21	16.8	235	48.02±0.29	1442.61±18.11	0.0205±0.0002	130.9±3.1
Peddie	66	118	1179	16	10.0	357	52.29±0.16	1381.08±14.35	0.0245±0.0003	156.1±3.3
OPAP	35	37	790	9	21.4	110	35.82±0.47	762.06±15.62	0.0227±0.0004	144.9±5.4

Perovskite $^{238}U/^{204}Pb$ and $^{206}U/^{204}Pb$ ratios were corrected for fractionation, blank and spike.

Th concentration estimated from amount of ^{208}Pb and $^{206}Pb/^{238}U$ age.

$^{206}Pb/^{238}U$ Age uncertainties reported at 2 sigma

TCPb: Total Common Pb

Table 4- 2. Sr and Nd isotopic ratios for kimberlitic perovskite

		Age (Ma)	$^{87}Sr/^{86}Sr_{(i)}$	Sm (ppm)	Nd (ppm)	$^{147}Sm/^{144}Nd$	$^{143}Nd/^{144}Nd_{(c)}$	$^{143}Nd/^{144}Nd_{(i)}$	$\varepsilon Nd_{(0)}$	$\varepsilon Nd_{(T)}$
Churchill Province, Nunavut										
05FWR005-A-2		225.3*	0.70328±0.00002	286	1991	0.08697	0.51286±0.00001	0.51273±0.00001	4.3	7.4
04KD230-A-(S)		216.7*	0.70356±0.00002	447	3501	0.07714	0.51296±0.00001	0.51285±0.00002	6.3	9.6
04KD230-A-1(L)		222.4*	0.70359±0.00001	318	2444	0.07863	0.51276±0.00001	0.51265±0.00001	2.5	5.8
CD 009-2-(S)		196.5*	0.70346±0.00003	283	2571	0.06660	0.51283±0.00001	0.51275±0.00001	3.7	6.7
CD 009 (L)		196.5*	0.70327±0.00001	356	3156	0.06816	0.51302±0.00005	0.51294±0.00005	7.6	10.9
CD 024-2 26.0m		192.4*	0.70317±.000002	406	3510	0.06994	0.51241±0.00001	0.51232±0.00001	-4.5	-1.35
Attawapiskat, Ontario										
MacFayden		177.3**	0.70401±0.00006	4033	33770	0.07220	0.51298±0.00003	0.51290±0.00003	6.7	9.5
Bravo	WA	177.7**	0.70419±0.00004	175	1599	0.06610	0.51319±0.00002	0.51311±0.00002	10.7	13.7
Bravo-2	WA	177.7**	0.70413±0.00004	54	515	0.06350	0.51296±0.00002	0.51288±0.00002	6.3	9.3
Charlie		168.4	0.70413±0.00003	538	4428	0.07343	0.51280±0.00001	0.51272±0.00002	3.2	5.8
Kirkland Lake, Ontario										
Buffonta		154.1	0.70509±0.00003	348	2721	0.07732	0.51278±0.00002	0.51270±0.00003	2.8	5.2
Buzz	WA	158.4	0.70417±0.00005	254	1828	0.08411	0.51280±0.00001	0.51271±0.00002	3.2	5.5
Diamond Lake (small)	WA	160.0	0.70451±0.00003	269	2062	0.07898	0.51279±0.00002	0.51268±0.00001	2.9	5.3
Diamond Lake (large)	WA	160.0	0.70451±0.00004	108	709	0.09182	0.51277±0.00001	0.51270±0.00002	2.7	4.8
Morissette Creek		161.6	0.70421±0.00003	521	3827	0.08227	0.512918±0.00001	0.51283±0.00002	5.5	7.8
Tandem		164.6**	0.70501±0.00005	21	202	0.06200	0.51276±0.00008	0.51269±0.00008	2.3	5.1
Timiskaming, Ontario										
Glinkers	WA	133.3	0.70364±0.00004	524	4900	0.06460	0.51286±0.00001	0.51281±0.00001	4.4	6.7
OPAP		144.9	0.70338±0.00003	115	1159	0.06005	0.51304±0.00002	0.51298±0.00002	7.9	10.39
MacLean		141.9**	0.70337±0.00002	317	2959	0.06490	0.51300±0.00001	0.51294±0.00001	7.1	9.48
Peddie	WA	154.5	0.70457±0.00003	449	3466	0.07830	0.51294±0.00002	0.51286±0.00003	6	8.3

*Zurevinski et al. 2008, **Heaman and Kjarsgaard 2000

$\lambda^{147}Sm = 6.54 \times 10^{-12}\ y^{-1}$; $^{143}Nd/^{144}Nd_{(CHUR)} = 0.512638$, $^{147}Sm/^{144}Nd_{(CHUR)} = 0.1967$

WA = Weighted Average $^{206}Pb/^{238}U$ age (see text for details)

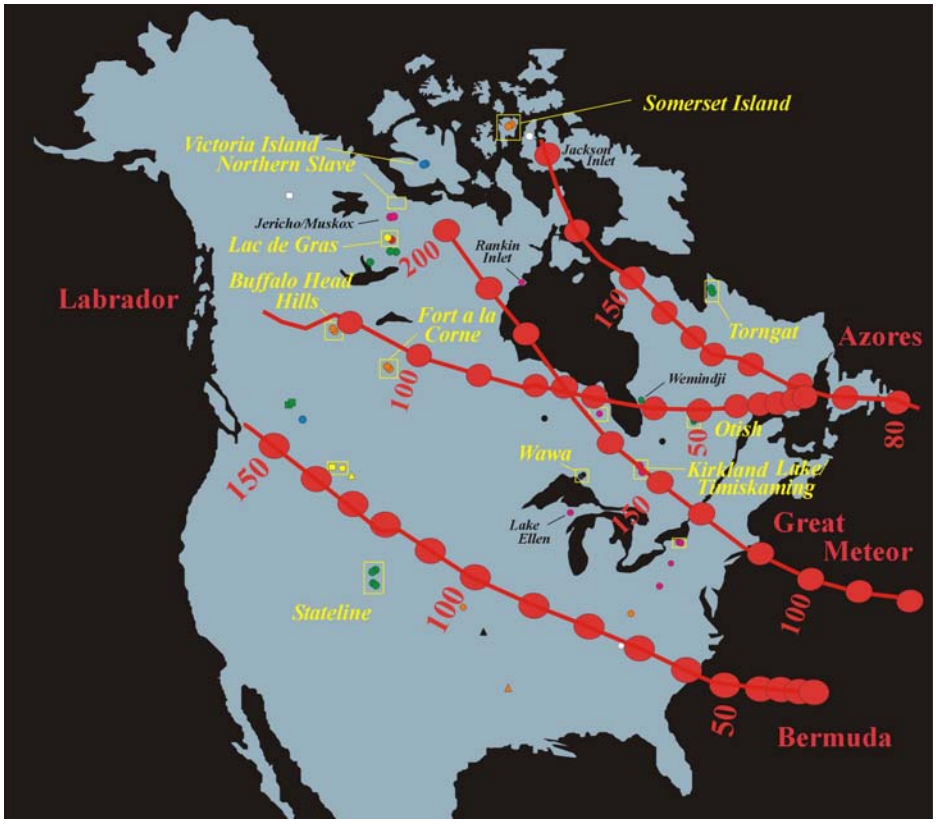

Figure 4-1. Map of North America showing the distribution of kimberlite clusters and fields, and the timing and location of various hotspot tracks (Tertiary: yellow; Cretaceous: orange; Jurassic: purple; Permian: blue; Paleozoic/Eocambrian: green) (after Heaman et al. 2003).

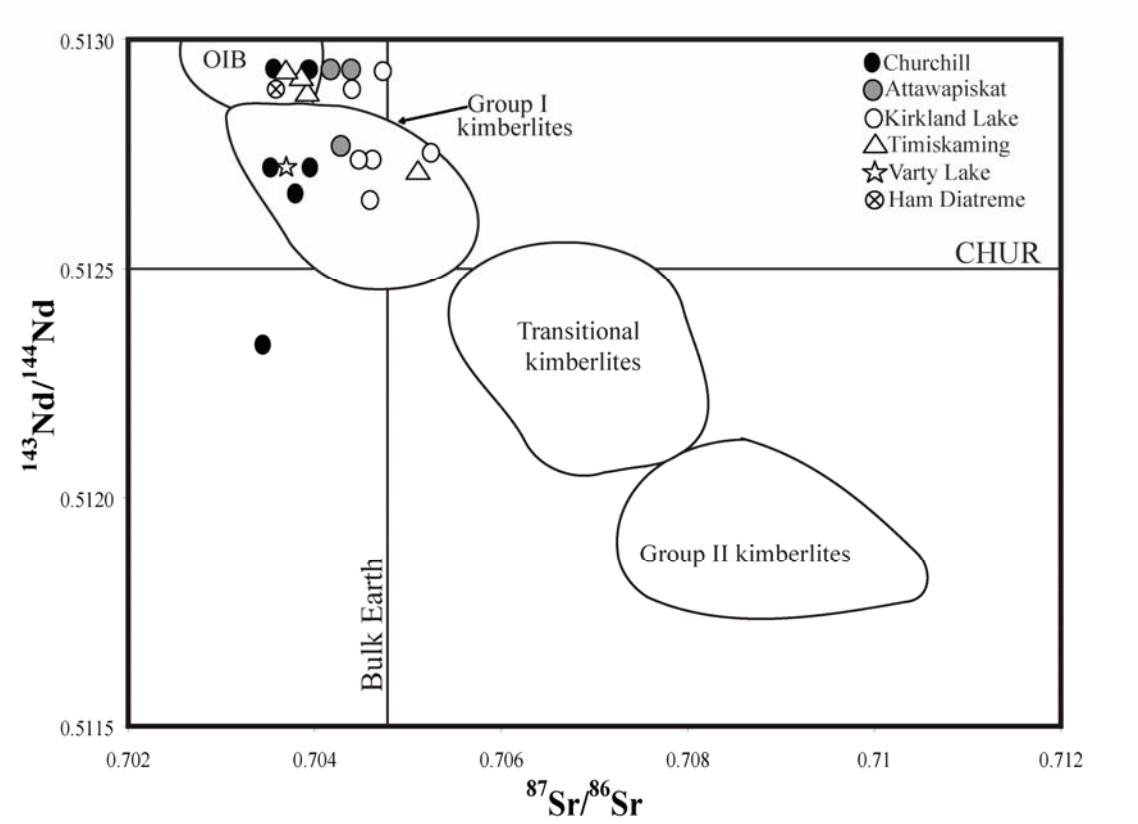

Figure 4-2. Nd-Sr isotope correlation diagram from kimberlitic perovskite. Fields for OIBs, Group I and II kimberlites are from Smith (1983), Fraser and Hawkesworth (1992), Tainton (1992), Nowell et al. (1999) and Becker and LeRoex (2006). Data from Varty Lake and Ham Diatreme from Heaman (1989). The values for Bulk Earth and Chondrite Uniform Reservoir (CHUR) are those for 150 Ma ago, assuming present day ratios of $^{87}Sr/^{86}Sr_{(Bulk\ Earth)} = 0.7045$; $^{87}Rb/^{86}Sr_{(Bulk\ Earth)} = 0.083(\lambda = 1.42 \times 10^{-11}\ y^{-1})$; and $^{143}Nd/^{144}Nd_{(CHUR)} = 0.512638$; $^{147}Sm/^{144}Nd_{(CHUR)} = 0.1967$ ($\lambda = 6.54 \times 10^{-12}\ y^{-1}$).

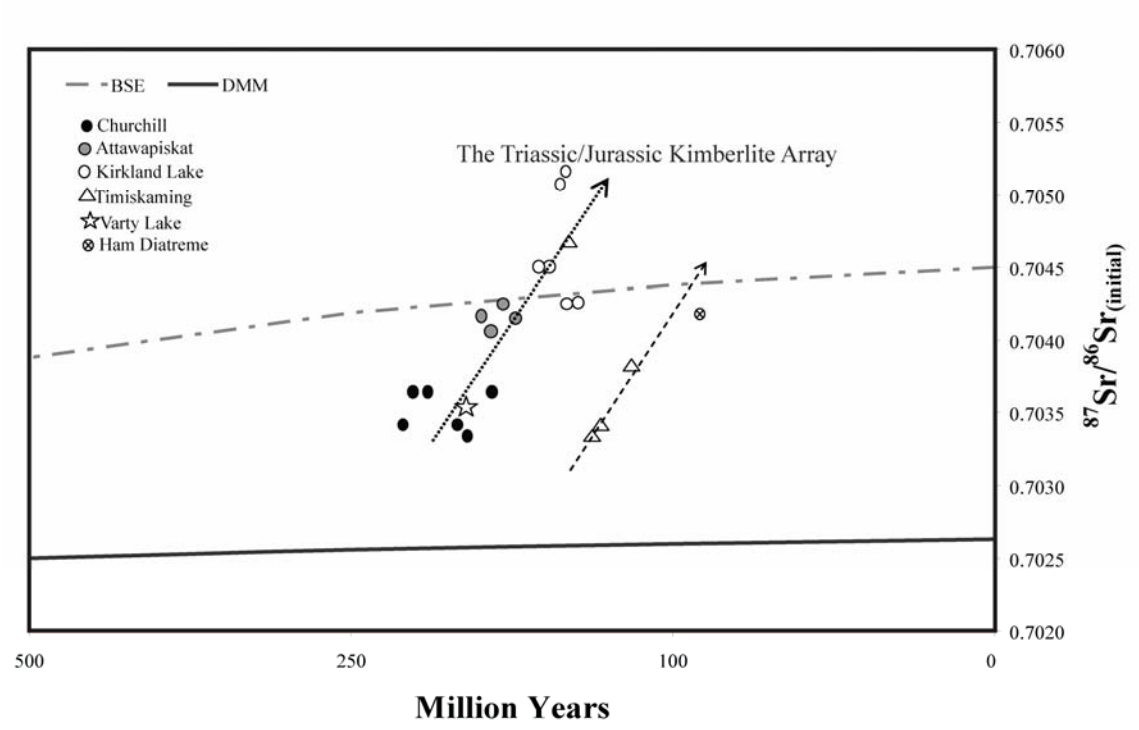

Figure 4-3. Sr versus time plotted with the Sr evolutionary lines of Depleted MORB Mantle (DMM) and Bulk Silicate Earth (BSE). Varty Lake and Ham Diatreme data from Heaman (1989).

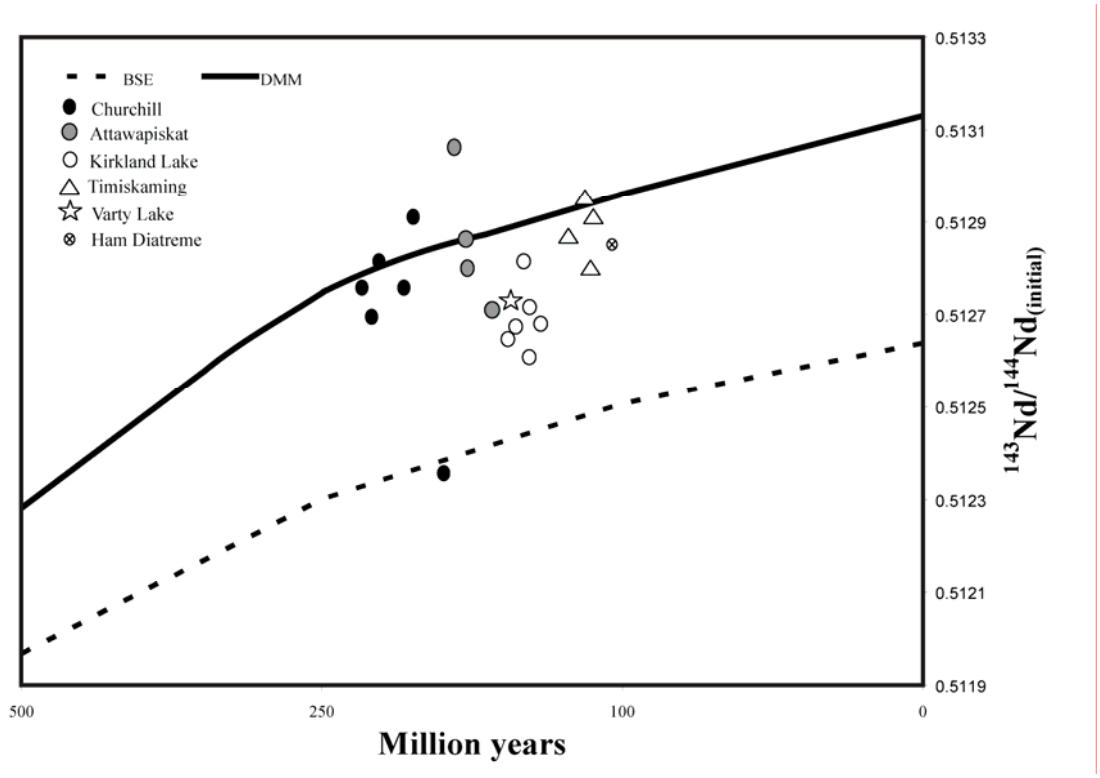

Figure 4-4. Nd versus time plotted with the Nd evolutionary lines of Depleted MORB Mantle (DMM) and Bulk Silicate Earth (BSE). Varty Lake and Ham Diatreme data from Heaman (1989).

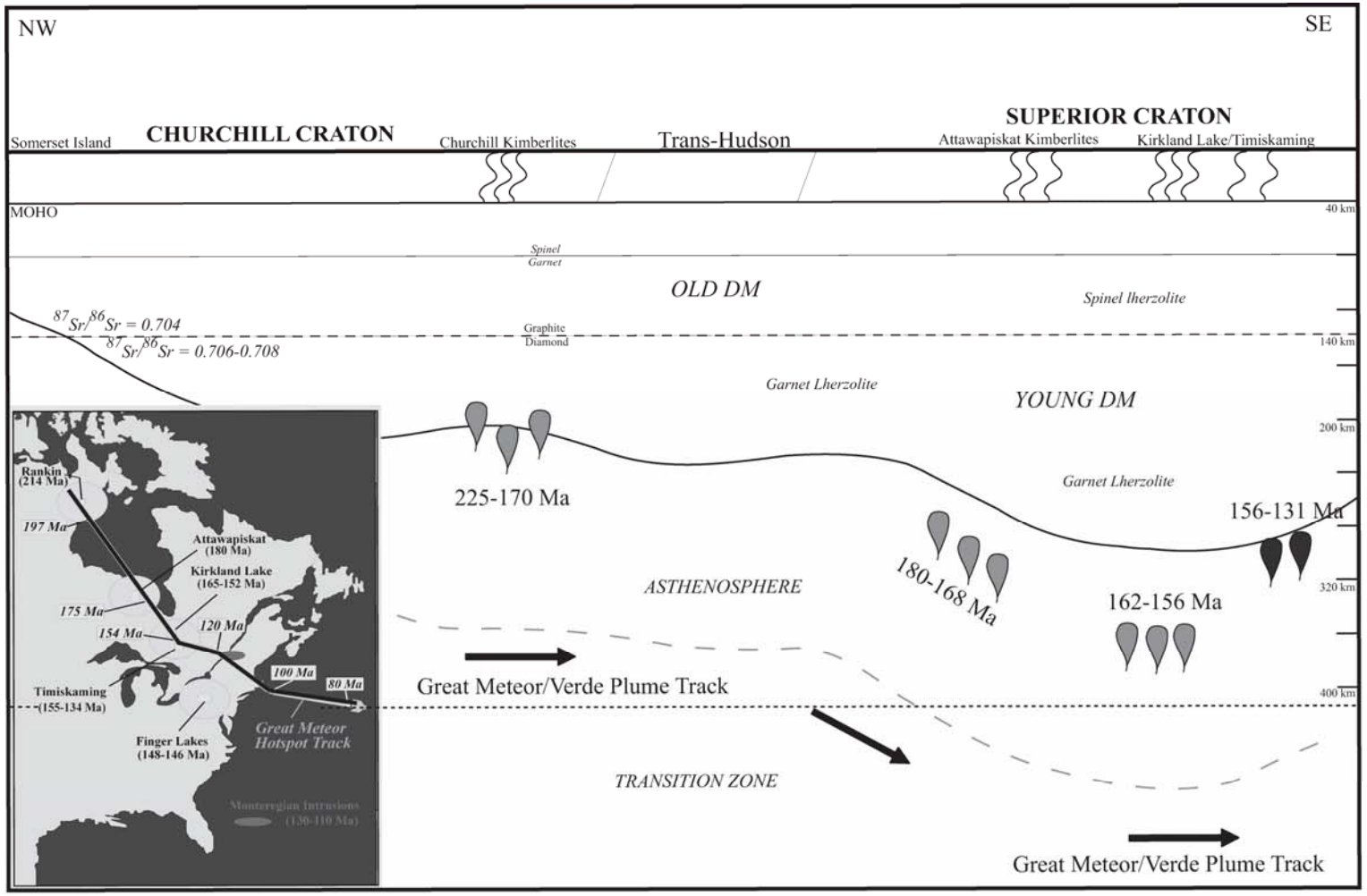

Figure 4-5. A proposed model of the upper mantle from Somerset Island, Nunavut through to Timiskaming, Ontario. DM=depleted mantle.

Chapter 5

Conclusion

The recent discoveries of kimberlitic rocks and accompanying xenoliths of variable age in North America allow for investigation of deep mantle processes beneath the North American continent through time. There are three main objectives in this multi-disciplinary study: 1) to classify each kimberlite field; 2) to investigate possible sources of kimberlite magma for North American kimberlites and 3) to evaluate tectonic models for the generation of kimberlite magma. Two main study areas were chosen, the Churchill kimberlite field, Nunavut and the Lac de Gras kimberlite field (the Diavik kimberlites), NWT, along with other known kimberlite fields (Attawapiskat, Kirkland Lake and Timiskaming) occurring along the proposed Great Meteor Hotspot Track (Heaman and Kjarsgaard 2000). The kimberlites were emplaced into stable Archean cratons, however, the Diavik kimberlites (Lac de Gras, NWT) contain economic diamond deposits, while the Churchill kimberlites discovered to date are generally diamond-poor. The overall goal of this study was to assist in determining the geotectonic processes responsible for the generation of kimberlite magmas, and whether or not different mantle processes are responsible for the generation of different kimberlite provinces.

The Churchill kimberlites have been formally classified in this study as sparsely macrocrystal oxide-rich carbonate hypabyssal kimberlite, with varying amounts of phlogopite, serpentine, monticellite and carbonate. The Churchill kimberlites are classified as archetypal Group I kimberlites on the basis of two generations of olivine, the presence of magnesian ilmenite, two generations of phlogopite, REE-poor perovskite is present and the spinel compositions follow the Magmatic Trend #1 of Mitchell and Clarke (1976). Sr isotopic composition of perovskite from Churchill kimberlites also supports the Group I classification. Evolved members of the Churchill kimberlites are also present. Hypabyssal kimberlite (HK) dominates in the Churchill field, therefore, are interpreted to belong to either the root zone of a kimberlite cluster or represent intrusive dykes or sills of a kimberlite complex. This could be an indication of erosional levels or of magmatic processes. The emplacement ages of eighty five percent of the known kimberlites in the Churchill field were determined in this study (12 U-Pb

perovskite and 15 Rb-Sr phlogopite), adding significantly to the geochronological database of North American kimberlites. The ages indicate that magmatism spanned ~55 Ma through the Middle Triassic to the Middle Jurassic (225-170 Ma), a very long period of kimberlite magmatism for a single field. Three magmatic "pulses" have been identified at 170-175 Ma, 181-204 Ma and 219-225 Ma. There are cases of inherited perovskite occurring in some Churchill kimberlites, which is interpreted as older kimberlite entrained in younger kimberlite, a scenario which could happen where there are multiple pulses of magmatism over an extended period of time.

The Diavik kimberlites are a cluster of more than 60 kimberlites, where there are pipes of similar emplacement ages in close proximity to each other that are both highly diamondiferous and diamond-poor. The objectives of the Diavik study were to establish the mineralogical and geochemical nature of the kimberlites and evaluate any diagnostic features that would distinguish the diamond-bearing economic pipes from the non-economic kimberlite on the property. Petrographic results from the Diavik kimberlites show that volcaniclastic kimberlite (VK) and resedimented volcaniclastic kimberlite (RVK) dominate, with lesser hypabyssal kimberlite (HK) and a few occurrences of tuffisitic kimberlite (TK). Geochemical results revealed that economic kimberlites have a more primitive signature, while non-economic kimberlites have a more evolved signature, resembling ultrabasic rock types. Diavik kimberlites display the LREE enriched patterns typical of worldwide kimberlite occurrences, but reveal a large intrafield range of REE contents. Mineralogy and geochemical bulk rock samples of the Diavik kimberlite show similarity to Group I kimberlites worldwide, however, whole rock isotopes show that the kimberlites have more of a transitional signature. Economic kimberlites have a slightly more radiogenic isotopic signature, possibly reflecting a source characteristic of the kimberlite magma. Two emplacement ages were determined for A154S and A841 (55.8 Ma and 56.7 Ma, respectively) and this slightly extends the previous emplacement age range of the Diavik kimberlites.

The evolution of Eastern North American kimberlite magmatism has been the focus of recent studies where different tectonic models responsible for the generation of kimberlite

magmas have been proposed (e.g. Phipps 1988; McCandless 1999; Heaman and Kjarsgaard 2000). Results from a Sr isotopic perovskite study presented here further prove the usefulness of the technique (Heaman 1989). The initial $^{87}Sr/^{86}Sr$ ratios of primary kimberlite magma can be used as a proxy for the nature of the mantle source region of a kimberlite melt. Heaman and Kjarsgaard (2000) postulated that the NW-SE corridor of Triassic to Cretaceous kimberlite magmatism in eastern Canada, which progressively youngs for more than 2000 kms, is likely the continental expression of magmatism linked to the Great Meteor plume mantle hotspot track. With the exception of three young kimberlites from the Timiskaming field, the perovskite results from this study show that the $^{87}Sr/^{86}Sr_{initial}$ ratios progressively increase along this ~2000-km-long corridor of near continuous Triassic/Jurassic kimberlite magmatism. This may be explained from either a single or multiple mantle plume hotspot track(s), responsible for the generation of kimberlite melts, as proposed by Heaman and Kjarsgaard (2000). The Churchill, Attawapiskat, and Kirkland Lake/Timiskaming kimberlite fields have unique isotopic compositions that indicate a distinct mantle source for each. The Churchill kimberlites reveal a depleted mantle source, and a more primitive source is indicated for the Attawapiskat and Kirkland Lake/Timiskaming kimberlite fields. Based on the study of these kimberlite fields, there is evidence for multiple mantle sources for Group I kimberlites.

References

Heaman, L.M. 1989. The nature of the subcontinental mantle from Sr-Nd-Pb isotopic studies on kimberlitic perovskite. Earth and Planetary Science Letters 92, 323-334.

Heaman, L.M. & Kjarsgaard, B.A. 2000. Timing of Eastern North American kimberlite magmatism: continental extension of the Great Meteor Hotspot Track? Earth and Planetary Science Letters 178, 253-268.

McCandless, T.E. Kimberlites: mantle expressions of deep-seated subduction. 1999. *in* Gurney, J.J., Gurney, J.L., Pascoe, M.D. and Richardson, S.H. (editors). Proceeding of the 7th International Kimberlite Conference, Volume 2, pp. 545-549: Red Roof Publishers, Cape Town, South Africa.

Mitchell, R.H. and Clarke, D.B. 1976. Oxide and sulphide mineralogy of the Peuyuk kimberlite, Somerset Island, N.W.T., Canada. Contributions to Mineralogy and Petrology**,** 56: 157-172.

Phipps, S.E. 1988. Deep rifts as sources for alkaline intraplate magmatism in eastern North America. Nature 334, 27-31.

Smith, C.B. 1983. Pb, Sr, and Nd isotopic evidence for sources of African Cretaceous kimberlite. Nature 304, 51-54.

APPENDIX I

The Diavik Kimberlite Field

Mineral Key for Diavik Petrography

Ap	Apatite
Bad	Baddeleyite
Cal-P	Calcite (primary)
Cal-P	Calcite (secondary)
Chl	Chlorite
Crustal	Crustal
Ilm	Ilmenite
Mg	Magnetite
Mtc	Monticellite
Mud	Mud
Ol	Olivine
Oxide	Oxide
Phl	Phlogopite
Prv	Perovskite
Rt	Rutile
Spl	Spinel
Srp	Serpentine

Sample Identification: 98-A2-07
Depth: 151.0m

Classification: TK

Summary: Altered crustal-rich segregationary textured tuffisitic kimberlite.

Colour: brown
Clay Minerals: alteration
Xenolith Abundance: [40%] lithic angular
Xenolith Size: < 3mm
Xenolith Reaction: bleached rims
Olivine Replacement: Cal, clay, pseudomorphic replacement
Pelletal Lapilli: n/a
Autoliths: n/a
Primary Carbonate: n/a
Kimberlitic Textures: Most textures are masked by alterations, segregationary texture

Modal Mineralogy:

[10%] Phenocrystal Ol- partially veined to completely pseudomorphic replacement, anhedral to subhedral habit
Large flow-banded Phl, anhedral [5%]

Modal Mineralogy/Matrix Ratio: 55/45

Matrix/Groundmass (in order of abundance):

Cal-S, Clay, Srp

Textures/Additional Information:

- Segregationary textures with Cal-S

- All primary matrix/groundmass is petrographically indistinguishable due to the alteration of the kimberlite

---

Sample Identification: 00-A4-05
Depth: 138.4m

Classification: HK

Summary: Macrocrystic, calcite segregationary-textured olivine-rich magmatic kimberlite.

Colour: grey
Clay Minerals: alteration
Xenolith Abundance: mantle [<5%], lithic [10%]
Xenolith Size: 0.1-1 mm
Xenolith Reaction: bleached rims on the lithic, n/a for the mantle
Olivine Replacement: Srp veins
Pelletal Lapilli: n/a
Autoliths: n/a
Primary Carbonate: probable
Kimberlitic Textures: Cal segregationary textures (with some Srp), cumulate textures, macrocrystic

Modal Mineralogy:

[15%] Macrocrystal Ol with Srp veins (anhedral habit)
[10%] Subhedral Ol phenocrysts with thick kelyphite rims

Modal Mineralogy/Matrix Ratio: 40/60

Matrix/Groundmass (in order of abundance):

Cal-P rhombs present in the Cal segregationary, Sp cumulates, Subhedral Prv, Srp, Clay, Chl

Textures/Additional Information:

- Mantle xenoliths classified as dunite
- Chl alteration found in the groundmass
- Colourless Cal-P matrix

Sample Identification: 00-A4-05
Depth: 139.2m

Classification: HK

Summary: Reasonably fresh macrocrystal olivine spinel hypabyssal kimberlite, exhibiting calcite segregationary textures.

Colour: green/dark grey
Clay Minerals: n/a
Xenolith Abundance: lithic [10%]
Xenolith Size: n/a
Xenolith Reaction: n/a
Olivine Replacement: Srp rims and veins
Pelletal Lapilli: n/a

Autoliths: n/a
Primary Carbonate: present in groundmass
Kimberlitic Textures: oxide cumulates, flow banding, Cal segregationary, macrocrystal

Modal Mineralogy:

[15%] Euhedral to subhedral phenocrystal Ol with only Srp rims
[10%] Anhedral macrocrystal Ol with Srp veining
[<5%] (trace) CPX, anhedral, altered
[<5%] (trace) Phl with flow banding (slight alteration between cleavage planes)
+/- OPX to be confirmed by microprobe

Modal Mineralogy/Matrix Ratio: 50/50

Matrix/Groundmass (in order of abundance):

Cal (present as segregationary textured groundmass), euhedral Sp, Prv (large cubic euhedral, red-brown transparent in colour), Phl

Textures/Additional Information:

- many of the Ol macrocrysts have thick kelyphite rims
- Prv is large and easily identified in thin section
- Colourless Cal matrix

Sample Identification: 00-A4-05
Depth: 139.0m

Classification: HK

Summary: A serpentine and primary calcite segregationary-textured spinel-rich hypabyssal kimberlite.

Colour: grey/green
Clay Minerals: clay
Xenolith Abundance: lithic [5%]
Xenolith Size: <1 mm
Xenolith Reaction: n/a
Olivine Replacement: Srp and Cal veins
Pelletal Lapilli: n/a
Autoliths: n/a
Primary Carbonate: matrix
Microlitic Textures: n/a
Kimberlitic Textures: segregationary textures, necklace textures

Modal Mineralogy:

[15%] Subhedral (+/- fragmental) Ol phenocrysts, Srp veins
[10%] Anhedral Ol macrocrysts, altered rims and Srp veins
[10%] Anhedral Ol macrocrysts, fragmental with altered rims and Srp veins

Modal Mineralogy/Matrix Ratio: 40/60

Matrix/Groundmass (in order of abundance):

Cal, Srp, Necklace Sp, Sp (euhedral), Prv

Textures/Additional Information:

- Matrix and groundmass is altered to Srp/Clay, therefore, primary mineralogy is very difficult to distinguish

---

Sample Identification: 00-A4-05
Depth: 179m

Classification: HK

Summary: Heavily altered sparsely macrocrystal olivine, spinel-rich hypabyssal kimberlite.

Colour: green/grey
Clay Minerals: alteration
Xenolith Abundance: lithic [40%]
Xenolith Size: 1mm-2cm
Xenolith Reaction: bleached rims
Olivine Replacement: Chl/Srp
Pelletal Lapilli: n/a
Autoliths: n/a
Primary Carbonate: n/a
Kimberlitic Textures: macrocryst-poor, segregationary textures with Srp and Chl

Modal Mineralogy:

[25%] Phenocrystal and microphenocrystal Ol (pseudomorphic replacement)
[10%] Macrocrystal Ol with Srp veins and rims
[<5%] Macrocrystal and phenocrystal CPX/OPX, with prominent cleavage

Modal Mineralogy/Matrix Ratio: 80/20

Matrix/Groundmass (in order of abundance):

Cal-S segregations
Sp- very abundant, sizes and habits vary throughout the matrix
Prv- distributed randomly throughout the section, brown-orange, thick dark rims, euhedral to subhedral

Textures/Additional Information:

- Thick kelyphite rims on macrocrystal Ol
- Late stage fractures infilled with Cal
- Secondary Cal segregations (mosaic-style)
- Suitable for Sp and Prv mineral analysis

Sample Identification: 02-A5-02-04
Depth: 127.2m

Classification: HK

Summary: Extremely altered, crustal-rich macrocrystal hypabyssal kimberlite.

Colour: grey
Clay Minerals: n/a
Xenolith Abundance: lithic [15%]
Xenolith Size: n/a
Xenolith Reaction: n/a
Olivine Replacement: Cal, Srp
Pelletal Lapilli: n/a
Autoliths: n/a
Primary Carbonate: n/a
Kimberlitic Textures: minor flow alignment, oxide cumulate, macrocrystal

Modal Mineralogy:

[15%] Macrocrystal Ol, subhedral to anhedral habit, pseudomorphic replacement to Cal
[10%] Phenocrystal Ol, euhedral to subhedral habit, pseudomorphic replacement to Cal and Srp
[5%] Oxide phenocrysts (Sp), very coarse grained

Modal Mineralogy/Matrix Ratio: 45/55

Matrix/Groundmass (in order of abundance):

Srp, Cal, Sp, Prv, +/- Rt

Textures/Additional Information:

- In parts of the thin section there is a minor flow alignment with some macrocrystal Ol
- Thin section not suitable for microprobe analysis, due to extensive alteration and crustal contamination

---

Sample Identification: 02-A5-02-04
Depth: 127.8m

Classification: HK

Summary: Macrocrystal flow-aligned, mud-rich, hypabyssal kimberlite exhibiting extreme alteration.

Colour: brown/black
Clay Minerals: matrix (late-stage)
Xenolith Abundance: trace lithic [<5%]
Xenolith Size: n/a
Xenolith Reaction: bleached rims
Olivine Replacement: Cal, Srp (veins to pseudomorphic replacement)
Pelletal Lapilli: n/a
Autoliths: n/a
Primary Carbonate: n/a
Kimberlitic Textures: segregationary textures, oxide-rich, flow alignment, atoll

Modal Mineralogy:

[25%] Phenocrystal Ol, subhedral habit, pseudomorphic replacement to Cal
[20%] Macrocrystal Ol, anhedral habit, pseudomorphic replacement to Cal
[10%] Phenocrystal Phl laths, flow banding textures

Modal Mineralogy/Matrix Ratio: 60/40

Matrix/Groundmass (in order of abundance):

Cal-S, Very abundant Sp, Phl laths (fragmental), Srp, Ap, Ilm, +/-Prv, trace atoll Sp

Textures/Additional Information:

- Segregationary texture appears to be a secondary fracture with Cal infilled.
- Flow alignment occurs with both the macrocrysts and phenocrysts of Ol and Phl

---

Sample Identification: 02-A5-02-04
Depth: 128.4m

Classification: HK

Summary: Extremely altered, crustal contaminated, macrocrystal olivine hypabyssal kimberlite exhibiting flow alignment.

Colour: grey
Clay Minerals: n/a
Xenolith Abundance: lithic [30%]
Xenolith Size: up to 2 cm
Xenolith Reaction: n/a
Olivine Replacement: Cal pseudomorphs
Pelletal Lapilli: n/a
Autoliths: n/a
Primary Carbonate: n/a
Kimberlitic Textures: flow alignment, segregationary textures, macrocrystal

Modal Mineralogy:

[20%] Macrocrystal Ol, rounded anhedral habit, pseudomorphic replacement by Cal
[20%] Phenocrystal and microphenocrystal subhedral Ol, pseudomorphic replacement by Cal
[5%] Phl laths exhibiting alteration between the cleavage planes

Modal Mineralogy/Matrix Ratio: 75/25

Matrix/Groundmass (in order of abundance):

Srp, Chl, and Cal mesostasis.
Sp, Phl, and lesser Ilm accessory minerals

Textures/Additional Information:

- All Ol has been pseudomorphed by cryptocrystalline secondary Cal
- Large angular fragments of crustal material, devoid of alteration rims

---

Sample Identification: 94-A5-1
Depth: 148.5m

Classification: HK

Summary: Calcite segregationary textured, crustal rich, oxide hypabyssal kimberlite.

Colour: brown/grey
Clay Minerals: matrix
Xenolith Abundance: lithic [15%]
Xenolith Size: <1 mm
Xenolith Reaction: n/a
Olivine Replacement: Srp veins
Pelletal Lapilli: n/a
Autoliths: n/a
Primary Carbonate: matrix/groundmass mineralogy
Kimberlitic Textures: Cal segregationary, atoll, macrocrystal

Modal Mineralogy:

[20%] Phenocrystal Ol, euhedral habit, Srp veins and rims
[15%] Macrocrystal Ol, subhedral- anhedral habit, some fragmental, Srp veins and rims
[<5%] (trace) CPX phenocryst
[<5%] (trace) Phl phenocrysts (possibly lithic)

Modal Mineralogy/Matrix Ratio: 60/40

Matrix/Groundmass (in order of abundance):

Cal-P, Cal-S, Sp (all sizes, microphenocrystal Sp and atoll), Prv, Srp, Ap, Phl, +/-CPX

Textures/Additional Information:

- Cal segregationary textures
- Abundant atoll Sp
- Thin section poorly cut

Sample Identification: 94-A5-1
Depth: 149m

Classification: HK

Summary: Uniform-textured spinel-rich hypabyssal kimberlite with abundant crustal material.

Colour: grey
Clay Minerals: n/a
Xenolith Abundance: lithic [15%]
Xenolith Size: 1-3 mm
Xenolith Reaction: n/a
Olivine Replacement: Srp veins
Pelletal Lapilli: n/a
Autoliths: n/a
Primary Carbonate: groundmass
Kimberlitic Textures: uniform textures

Modal Mineralogy:

[25%] Euhedral to subhedral Ol phenocrysts and microphenocrysts with altered rims
[15%] Rounded anhedral Ol, altered rims and veins

Modal Mineralogy/Matrix Ratio: 55/45

Matrix/Groundmass (in order of abundance):

Cal, Sp (very abundant) (all sizes, mainly euhedral), Prv, Srp, Chl, +/- Phl

Textures/Additional Information:

- Relatively "fresh" unaltered kimberlite
- Abundant crustal material
- Excellent thin section for EMPA
- Colourless Cal matrix

Sample Identification: 94-A5-1
Depth: 149.3 m

Classification: HK

Summary: Sparsely macrocrystic spinel-rich olivine hypabyssal kimberlite.

Colour: grey
Clay Minerals: n/a
Xenolith Abundance: lithic [20%]
Xenolith Size: n/a
Xenolith Reaction: bleached rims
Olivine Replacement: Srp rims and veins
Pelletal Lapilli: n/a
Autoliths: n/a
Primary Carbonate: matrix
Kimberlitic Textures: Atoll Sp, sparsely macrocrystic, uniform textures

Modal Mineralogy:

[20%] Phenocrystal Ol with Srp rims, some with Srp veins, mainly subhedral habit, lesser euhedral habit
[10%] Macrocrystal Ol with Srp veins, rounded anhedral habit
[<5%] Macrocrystal CPX, anhedral, slight alteration

Modal Mineralogy/Matrix Ratio: 55/45

Matrix/Groundmass (in order of abundance):

Cal, Sp (euhedral, some Atoll-textures), Phl (small, interstitial groundmass minerals), Ap (euhedral), +/-Prv (subhedral, slightly altered with thick dark rims)

Textures/Additional Information:

- Sparsely macrocrystic
- Uniform textures in the groundmass
- Sp is abundant in the groundmass mineralogy, shown to occur in a variety of sizes

---

Sample Identification: 94-A5-1
Depth: 150m

Classification: HK

Summary: Calcite segregationary textured, crustal-rich, oxide hypabyssal kimberlite.

Colour: brown
Clay Minerals: matrix
Xenolith Abundance: lithic [10%]
Xenolith Size: <1 mm
Xenolith Reaction: n/a
Olivine Replacement: Srp veining
Pelletal Lapilli: n/a
Autoliths: n/a
Primary Carbonate: groundmass/matrix
Kimberlitic Textures: segregationary textured groundmass

Modal Mineralogy:

[20%] Phenocrystal Ol, euhedral habit, Srp veins and thick dark rims
[15%] Macrocrystal Ol, subhedral habit, Srp veins and rims
[5%] Macrocrystal CPX, rounded anhedral habit, some alteration

Modal Mineralogy/Matrix Ratio: 50/50

Matrix/Groundmass (in order of abundance):

Cal-P and Cal-S, Sp (all sizes), Prv, Srp, Ap, Phl, +/-CPX

Textures/Additional Information:

- Cal segregations can be large and extreme in some areas of the thin section
- Some microphenocrystal minerals may be properly identified by EMPA
- Thick kelyphite rims on macrocrystal and phenocrystal Ol

Sample Identification: 97-A11-8
Depth: 113.4m

Classification: VK

Summary: Heavily altered, lithic-rich, juvenile lapilli-bearing volcaniclastic kimberlite.

Colour: dark brown
Clay Minerals: matrix
Xenolith Abundance: lithic [30%]
Xenolith Size: <0.5 mm
Xenolith Reaction: n/a
Olivine Replacement: Srp veins, pseudomorphic replacement with Cal
Pelletal Lapilli: n/a
Autoliths: n/a
Primary Carbonate: n/a
Kimberlitic Textures: Juvenile lapilli, matrix-supported

Modal Mineralogy:

[30%] Phenocrystal Ol, angular habit (or fragmental macrocrysts), varying degrees of alteration

[10%] Phenocrystal altered Phl, (alteration between cleavage planes)

Modal Mineralogy/Matrix Ratio: 70/30

Matrix/Groundmass (in order of abundance):

Clay, Cal, Srp, accessory Sp (in quite low abundance)

Textures/Additional Information:

- Unpolished thin section cut too thin
- Most of the primary mineralogy is difficult to distinguish due to the alteration of the kimberlite
- Juvenile lapilli irregular to lobate in habit
- Multiple occurrences of uncored Juvenile lapilli

Sample Identification: 97-A11-8
Depth: 114.5m

Classification: VK

Summary: Juvenile lapilli-bearing, clast-supported volcaniclastic kimberlite.

Colour: black/brown
Clay Minerals: alteration throughout section
Xenolith Abundance: lithic [20%], angular
Xenolith Size: n/a
Xenolith Reaction: n/a
Olivine Replacement: Srp/Clay
Pelletal Lapilli: n/a
Autoliths: n/a
Primary Carbonate: n/a
Kimberlitic Textures: clast-supported, juvenile lapilli

Modal Mineralogy:

[30%] Heavily altered, fragmental and rounded Ol macrocrysts, phenocrysts and microphenocrysts
[10%] Phl- anhedral (rounded)
[10%] CPX- anhedral (rounded)

Modal Mineralogy/Matrix Ratio: 70/30

Matrix/Groundmass (in order of abundance):

Mud, lesser rare Sp
The thin section matrix/groundmass mineralogy is petrographically indistinguishable.

Textures/Additional Information:

- Thin section is unpolished and cut unevenly
- Heavy clay/mud replacement/alteration
- Juvenile lapilli is rounded to irregular in habit, some are cored with Ol, some are uncored

Sample Identification: 97-A11-8
Depth: 116.4m

Classification: VK

Summary: Clast-supported juvenile lapilli-rich volcaniclastic kimberlite exhibiting a high degree of alteration.

Colour: grey/brown
Clay Minerals: occur in the matrix as replacement minerals
Xenolith Abundance: [20%] lithic, angular
Xenolith Size: range
Xenolith Reaction: n/a
Olivine Replacement: Srp rims and veins
Pelletal Lapilli: n/a
Autoliths: n/a
Primary Carbonate: n/a
Kimberlitic Textures: Juvenile lapilli, clast-supported, Srp mesostasis

Modal Mineralogy:

[20%] Macrocrystal Ol, angular and fragmental habit, veins of Srp present
[20%] Phenocrystal Ol, angular and fragmental habit, veins of Srp present

Modal Mineralogy/Matrix Ratio: 60/40

Matrix/Groundmass (in order of abundance):

Srp mesostasis, Mud/Clay, Ilm, Phl laths (brown in ppl, altered between cleavage planes)

Textures/Additional Information:

- Clast-supported
- High degree of alteration
- Juvenile lapilli are irregular with large kernals of Ol and phenocrysts of Ol surrounding the kernal in a random pattern

Sample Identification: 97-A11-8
Depth: 118.7m

Classification: RVK

Summary: Juvenile lapilli-bearing mud-rich resedimented volcaniclastic kimberlite.

Colour: dark brown
Clay Minerals: matrix
Xenolith Abundance: lithic [25%], angular to rounded habit
Xenolith Size: <3.5 mm
Xenolith Reaction: amorphous rims
Olivine Replacement: Srp veins
Pelletal Lapilli: n/a
Autoliths: n/a

Primary Carbonate: n/a
Kimberlitic Textures: Juvenile lapilli (15% modal), resedimentation

Modal Mineralogy:

Very difficult to distinguish, as everything is entirely pseudomorphed and replaced by mud/clay.

Modal Mineralogy/Matrix Ratio: 50/50

Matrix/Groundmass (in order of abundance):

Sp (small, euhedral). This is the only primary groundmass mineral that can be distinguished.

Textures/Additional Information:

- Thin section is full of alteration and replacement, and has abundant crustal material.

Sample Identification: 98-A21-16
Depth: 181m

Classification: VK (possible RVK)

Summary: A juvenile lapilli-bearing olivine volcaniclastic kimberlite.

Colour: brown
Clay Minerals: matrix/groundmass
Xenolith Abundance: lithic [25%]
Xenolith Size: 0.1-3 mm
Xenolith Reaction: n/a
Olivine Replacement: pseudomorphic replacement to Cal, Srp +/-Clay
Pelletal Lapilli: n/a
Autoliths: present
Primary Carbonate: n/a
Kimberlitic Textures: Spherical Juvenile lapilli, irregular Juvenile lapilli, flow banding, clast-supported

Modal Mineralogy:

[15%] Macrocrystal Ol, angular habit, pseudomorphic replacement to Cal-S
[15%] Phenocrystal Ol, angular to subhedral habit, pseudomorphic replacement to Cal-S
[10%] CPX, anhedral habit, rim alteration (probably kelyphite)
[10%] Phl, flow banding

Modal Mineralogy/Matrix Ratio: 75/25

Matrix/Groundmass (in order of abundance):

Clay, Srp, Cal-S, lesser Sp, lesser Ap, +/-Prv

Textures/Additional Information:

- Unpolished thin section
- Phenocrystal mineralogy is most likely fragmented macrocrysts

- Spherical and irregular Juvenile lapilli (cored and uncored)

Sample Identification: 97-A44-2
Depth: 172.0m

Classification: HK

Summary: Sparsely macrocrystic olivine-rich hypabyssal kimberlite with slight alteration.

Colour: brown/grey
Clay Minerals: alteration
Xenolith Abundance: lithic, [<10%], angular
Xenolith Size: up to 1.5 cm
Xenolith Reaction: bleached rims
Olivine Replacement: slight rim alteration, Srp/Cal/Chl
Pelletal Lapilli: n/a
Autoliths: n/a
Primary Carbonate: possibly in groundmass
Kimberlitic Textures: matrix-supported, necklace Sp, Atoll Sp

Modal Mineralogy:

[15%] Euhedral hopper-type Ol phenocrysts exhibiting very little alteration
[10%] Anhedral Ol macrocrysts with a thin rim alteration
Possible CPX phenocrysts, rounded with thin rim alteration [<5%]

Modal Mineralogy/Matrix Ratio: 40/60

Matrix/Groundmass (in order of abundance):

Cal-S, Large euhedral Sp, highly altered Phl, abundant large euhedral dark brown Prv, acicular Ap, anhedral Ilm, CPX

Textures/Additional Information:

- Secondary Cal infilling fractures
- Euhedral hopper-style Ol's are highly altered around the rim, and are left with a rounded unaltered core.
- Ol macrocrysts exhibit a thin kelyphite rim

Sample Identification: A154
Depth: 11? Unknown LH sample

Classification: VK

Summary: Crater facies kimberlite exhibiting relatively fresh mineralogy including abundant juvenile lapilli.

Colour: dark green/grey
Clay Minerals: present in the matrix, and as some replacement in macrocrystal minerals
Xenolith Abundance: lithic [10%]
Xenolith Size: 1-2 mm
Xenolith Reaction: clay

Olivine Replacement: Partial with Srp
Pelletal Lapilli: n/a
Autoliths: n/a
Primary Carbonate: matrix
Kimberlitic Textures: Juvenile lapilli, macrocrystal, flow-banding

Modal Mineralogy:

[20%] Ol: macrocrystal, Srp veining, rarely pseudomorphic replacement
[10%] Ilm: large anhedral macrocrysts
[10%] CPX: xenocrysts, anhedral habit

Modal Mineralogy/Matrix Ratio: 50/50

Matrix/Groundmass (in order of abundance):

Sp (euhedral, variation in size) [10%], possible Prv (confirm by EMPA), Cal (euhedral rhombs) [10%], Phl (flow banding) [5%]

Textures/Additional Information:

- Cal in matrix/groundmass
- Section is quite useful for EMPA (Ilm, Ol, Cal, Sp, Prv)
- Juvenile lapilli: (2-10mm) medium to coarse grained, some with large anhedral fresh Ol kernel surrounded by small euhedral fresh Ol, in a mud matrix interstitial to Sp and Prv. Some Juvenile lapilli are uncored. Habit is oblong.

Sample Identification: A154
Depth: 221m

Classification: VK

Summary: Altered crater facies kimberlite containing both autholithic material and juvenile lapilli textures. Too altered to confirm primary mineralogy.

Colour: grey/brown
Clay Minerals: yes
Xenolith Abundance: lithic, angular [30%]
Xenolith Size: n/a
Xenolith Reaction: n/a
Olivine Replacement: Srp, Cal
Pelletal Lapilli: n/a
Autoliths: Small (1-2 mm diameter)
Primary Carbonate: n/a
Kimberlitic Textures: Juvenile lapilli, autolith, macrocrystal, clast-supported

Modal Mineralogy:
[20%] Ol macrocrysts, rounded and partially serpentinized
[15%] Ol microphenocrysts and phenocrysts, subhedral habit
[5%] Phl: angular, bladed laths

Modal Mineralogy/Matrix Ratio: 70/30

Matrix/Groundmass (in order of abundance):

Mud, petrographically indistinguishable
Possible Prv: brown/orange, cubo-octahedral, zoning present
Sp

Textures/Additional Information:

- 100% serpentinized and chloritized (+/- Cal-S)
- late stage oxide cumulates within larger Ol macrocrysts
- a single large CPX megacryst
- Juvenile lapilli: uncored, small angular, serpentinized clasts distributed randomly in a mud matrix. Clasts composed of Sp, Ol, lesser Phl

---

Sample Identification: A154
Depth: 221m (b)

Classification: VK

Summary: Highly altered crater facies kimberlite.

Colour: brown/grey
Clay Minerals: yes
Xenolith Abundance: lithic [30%], angular
Xenolith Size: 2-5 mm
Xenolith Reaction: n/a
Olivine Replacement: Srp, clay, Cal-S
Pelletal Lapilli: n/a
Autoliths: n/a
Primary Carbonate: n/a
Kimberlitic Textures: Juvenile lapilli, globular segregationary textures, macrocrystal, cumulate Sp

Modal Mineralogy:

[30%] Ol macrocrysts, anhedral habit, serpentinized to pseudomorphic replacement
[10%] Phl: flow-banded, alteration between cleavage planes

Modal Mineralogy/Matrix Ratio: 70/30

Matrix/Groundmass (in order of abundance):

Mud, indistinguishable minerals
Oxide cumulates (Sp)

Textures/Additional Information:

- Most of the primary mineralogy is indistinguishable due to alteration of the kimberlite
- Giant CPX megacryst (still reasonably fresh, suitable for EMPA)
- CPX megacrysts exhibits strain lamellae
- Juvenile lapilli: Ol macrocrysts (pseudomorphic replacement, subhedral habit) in the middle surrounded by dark petrographically indistinguishable minerals within a thick lapilli.

Sample Identification: A154

Depth: 272m

Classification: VK

Summary: An altered crater facies kimberlite exhibiting juvenile lapilli and segregationary textures.

Colour: grey/green
Clay Minerals: secondary
Xenolith Abundance: [10%], lithic and mantle
Xenolith Size: 10 mm and 2 mm, resp.
Xenolith Reaction: typical rim replacement
Olivine Replacement: Srp veining and pseudomorphic replacement
Pelletal Lapilli: n/a
Autoliths: n/a
Primary Carbonate: n/a
Kimberlitic Textures: Cal secondary segregationary, Juvenile lapilli

Modal Mineralogy:

[15%] Ol: macrocrystal, euhedral to anhedral habit, Srp veins to pseudomorphic replacement
[15%] Ol: phenocrystal and microphenocrystal, euhedral to subhedral habit, partial Srp veins.
[5%] Ilm: macrocrystal, angular

Modal Mineralogy/Matrix Ratio: 45/55

Matrix/Groundmass (in order of abundance):

Clay, Sp (possible atoll), Sec. Cal.

Textures/Additional Information:

- All macrocrysts and microphenocrystal Ol are in their own juvenile lapillus, or are rimmed by an alteration of some kind
- Large lapillus have Ol (fresh) in the kernels and the matrix is oxide (Sp-rich) and appears dark and muddy. Matrix lapillus is very thin in comparison to the size of the kernels.

Sample Identification: A154-N
Depth: 294m

Classification: RVK

Summary: Altered mud-rich crater facies kimberlite containing 2 generations of Ol and the presence of Juvenile lapilli.

Colour: brown/green
Clay Minerals: matrix
Xenolith Abundance: lithic [15%]
Xenolith Size: ~1mm
Xenolith Reaction: altered rims, Chl +/-Srp
Olivine Replacement: Srp, Cal
Pelletal Lapilli: n/a
Autoliths: n/a
Primary Carbonate: n/a

Kimberlitic Textures: Juvenile lapillus- containing a few pseudomorphs/microphenocrysts (Cal alteration); abundant oxide cumulates

Modal Mineralogy:

[15%] Ol: macrocrysts are partially serpentinized, anhedral; microphenocrysts (euhedral) are pseudomorphs and some are hopper Ol.
[10%] Phl laths, varying degrees of alteration
[<5%] (trace) Ilm
[<5%] (trace) Gt, subhedral habit

Modal Mineralogy/Matrix Ratio: 50/50

Matrix/Groundmass (in order of abundance):

Mud and Srp-rich matrix, oxide minerals abundant throughout matrix

Textures/Additional Information:

- The largest Ol macrocrysts (3-6mm) have unaltered cores and very thick serpentinized rims.
- All of the microphenocrystal and groundmass minerals are pseudomorphs and are resedimented in mud.
- Large amorphous lithic fragments are present

Sample Identification: A154
Depth: 294 m (b)

Classification: VK

Summary: A fragmental Ol and CPX-bearing volcaniclastic kimberlite with a pronounced red staining.

Colour: brown/green
Clay Minerals: present
Xenolith Abundance: lithic [10%]
Xenolith Size: <1 mm
Xenolith Reaction: rim alteration (clay)
Olivine Replacement: Srp and secondary Cal
Pelletal Lapilli: n/a
Autoliths: n/a
Primary Carbonate: n/a
Kimberlitic Textures: Juvenile lapilli, oxide cumulate, globular segregationary textures

Modal Mineralogy:

[20%] Angular fragmental Ol (some Srp veins)
[5%] CPX, anhedral, partial altered, pronounced rim alteration
[5%] Phl, laths with altered rims and alteration between cleavage planes

Modal Mineralogy/Matrix Ratio: 40/60

Matrix/Groundmass (in order of abundance):

Matrix supported Cal and Srp mesostasis. Microphenocrystal anhedral Ol exhibiting Srp veins. Small anhedral heavily altered Phl, Spl (shown commonly as cumulate textures).

Textures/Additional Information:

- Possible perovskite in the matrix of the lapillus
- Single garnet identified in the section
- Red staining on many of the macrocrysts and microphenocrysts
- Single large 5mm long CPX partial megacryst, identified in the core of a lapilli. with large angular Ol kernels. PL is present on all size scales from phenocrystal to macrocrystal size. The lapillus is mud and oxide rich.

Sample Identification: A154
Depth: 315m

Classification: VK

Summary: A juvenile lapilli-rich volcaniclastic kimberlite exhibiting fresh macrocrystal and phenocrystal mineralogy.

Colour: grey/green
Clay Minerals: alteration- groundmass and matrix mineralogy
Xenolith Abundance: lithic [15%]
Xenolith Size: 1-2 mm
Xenolith Reaction: n/a
Olivine Replacement: Srp veining
Pelletal Lapilli: n/a
Autoliths: n/a
Primary Carbonate: n/a
Kimberlitic Textures: Juvenile lapilli, macrocrystal

Modal Mineralogy:

[10%] Anhedral to subhedral Ol- partially serpentinized to complete replacement
[10%] Phenocrystal Ol, euhedral to subhedral habit, varying degrees of alteration
[<5%] (trace) Phl, [<5%] (trace CPX)

Modal Mineralogy/Matrix Ratio: 45/55

Matrix/Groundmass (in order of abundance):

Mud-rich matrix, Sp: euhedral and very fine-grained

Textures/Additional Information:

- Abundant Juvenile lapilli
- Some of the primary mineralogy is petrographically indistinguishable due to the mud replacement of the kimberlite
- Some of the Juvenile lapilli are uncored, and contain relatively unaltered Ol phenocrysts

---

Sample Identification: A154-10
Depth: 315m

Classification: VK

Summary: Juvenile lapilli-bearing, clast-supported, extremely altered volcaniclastic kimberlite.

Colour: brown
Clay Minerals: alteration
Xenolith Abundance: lithic [15%], angular
Xenolith Size: 1-3 mm
Xenolith Reaction: n/a
Olivine Replacement: Srp veins
Pelletal Lapilli: n/a
Autoliths: n/a
Primary Carbonate: n/a
Kimberlitic Textures: Juvenile lapilli, clast-supported

Modal Mineralogy:

[15%] Phenocrystal Ol, Srp veins, subhedral habit
[10%] Macrocrystal Ol, fragmental habit
[5%] CPX, anhedral
[5%] Gt, +/-Phl

Modal Mineralogy/Matrix Ratio: 50/50

Matrix/Groundmass (in order of abundance):

Srp, Clay, Sp, Cal: The mineralogy is mainly secondary, therefore the primary mineralogy is petrographically indistinguishable.

Textures/Additional Information:

- Clast-supported
- Juvenile lapilli contains euhedral to subhedral Ol and CPX, some have "kernals" which are generally angular
- Juvenile lapilli are spherical to irregular in habit

Sample Identification: A154
Depth: 316m

Classification: VK

Summary: A juvenile lapilli-bearing olivine-rich volcaniclastic kimberlite.

Colour: green/brown
Clay Minerals: alteration
Xenolith Abundance: lithic fragmental [10%]
Xenolith Size: range
Xenolith Reaction: n/a
Olivine Replacement: partial Srp veining
Pelletal Lapilli: abundant
Autoliths: present in trace amt.
Primary Carbonate: yes
Kimberlitic Textures: Juvenile lapilli with Ol kernels, oxide cumulates, segregationary Cal, Cal veining/infilling fractures

Modal Mineralogy:

[25%] Anhedral Ol macrocrysts (some as P.L. kernels)
[10%] Phl laths (some exhibit flow banding) [trace]
[10%] Euhedral to subhedral microphenocrystal Ol, in a cryptocrystalline matrix

Modal Mineralogy/Matrix Ratio: 55/45

Matrix/Groundmass (in order of abundance):

Cal-S, euhedral Phl laths, Srp, Sp, possible Prv, primary Cal rhombs, Diop.

Textures/Additional Information:

- Heavy cumulate Sp found within altered Ol macrocrysts
- Some of the magmaclasts are very hard to define
- All of the clasts in the thin section are rimmed by Srp (secondary)
- Juvenile lapilli are elongate to irregular in habit

Sample Identification: A154-05
Depth: 316 m

Classification: VK

Summary: Juvenile lapilli-bearing volcaniclastic kimberlite exhibiting globular segregationary texture, along with the presence of garnet.

Colour: brown
Clay Minerals: alteration
Xenolith Abundance: lithic [10%]
Xenolith Size: microphenocrystal to phenocrystal
Xenolith Reaction: n/a
Olivine Replacement: Srp rims and veins
Pelletal Lapilli: n/a
Autoliths: n/a
Primary Carbonate: n/a
Kimberlitic Textures: flow banding, juvenile lapilli, globular segregations

Modal Mineralogy:

[15%] Phenocrystal Ol: also fragmental, mainly subhedral
[15%] Microphenocrystal Ol- completely pseudomorphed
[15%] Macrocrystal Ol- angular, also found as kernals in magmaclasts
[<5%] Anhedral Gt, [<5%] Phl exhibiting flow banding and some alteration around edges
+/- CPX, +/- OPX

Modal Mineralogy/Matrix Ratio: 65/35

Matrix/Groundmass (in order of abundance):

Srp + Chl mesostasis, Sp (very abundant in the lapillus)

Textures/Additional Information:

- Juvenile lapilli varies greatly in size from 0.1mm to 1cm
- Some lapilli are spherical, while some slightly take the shape of their Ol kernals
- The globular segregationary textures have randomly oriented phenocrysts and microphenocrysts of Ol within

---

Sample Identification: A154-105
Depth: 316m

Classification: RVK

Summary: Clast-supported, resedimented volcaniclastic kimberlite exhibiting strong evidence of movement. Thin section is too thick for further petrographic analysis.

Colour: dark brown
Clay Minerals: n/a
Xenolith Abundance: n/a
Xenolith Size: n/a
Xenolith Reaction: n/a
Olivine Replacement: n/a
Pelletal Lapilli: n/a
Autoliths: n/a
Primary Carbonate: n/a
Kimberlitic Textures: n/a

Modal Mineralogy:

Mineralogy is indistinguishable.

Matrix/Groundmass:

Mineralogy is indistinguishable.

Textures/Additional Information:

- Confirmation of RVK, thin section is too thick for petrographic purposes

---

Sample Identification: A154N-08
Depth: 325.24m

Classification: VK

Summary: Juvenile lapilli-rich, megacrystal Ol-bearing volcaniclastic kimberlite.

Colour: brown
Clay Minerals: alteration
Xenolith Abundance: mantle [5%], lithic [10%]
Xenolith Size: mantle: rounded, lithic: angular
Xenolith Reaction: n/a
Olivine Replacement: Srp veins
Pelletal Lapilli: n/a
Autoliths: present, identified as HK
Primary Carbonate: n/a
Kimberlitic Textures: Juvenile lapilli, Srp mesostasis, megacrystal

Modal Mineralogy:

[25%] Macrocrystal anhedral Ol, Srp veins and rims
[10%] Phenocrystal Ilm
[10%] Macrocrystal Ilm
[<5%] Megacrystal Ol, anhedral with an anhedral Ol inclusion

Modal Mineralogy/Matrix Ratio: 65/35

Matrix/Groundmass (in order of abundance):

Srp mesostasis, lesser Sp, Phl (lath), Ilm, CPX, +/-Prv (possible, needs to be confirmed by EMPA)

Textures/Additional Information:

- Juvenile lapilli: mainly fragmental Ol macrocrysts as kernals
- This section is mainly magmaclasts in a Srp mesostasis
- Autoliths appear to be HK, and are rare, small (0.3-0.5mm)
- Ilm is abundant as macrocrysts and phenocrysts

Sample Identification: A154-08
Depth: 325.24 m

Classification: VK

Summary: Juvenile lapilli-rich, spinel-rich volcaniclastic kimberlite exhibiting calcite segregationary texture.

Colour: grey
Clay Minerals: alteration
Xenolith Abundance: mantle [5%], lithic [5%]
Xenolith Size: from 0.1mm to 1 cm
Xenolith Reaction: n/a
Olivine Replacement: Srp veining
Pelletal Lapilli: n/a
Autoliths: trace (Sp-rich)
Primary Carbonate: groundmass
Kimberlitic Textures: Oxide cumulates, Juvenile lapilli: abundant [20-30 modal %], segregationary textures with Cal

Modal Mineralogy:

[25%] Phenocrystal Ol, unaltered, subhedral
[20%] Macrocrystal Ol, angular, fragmental, srp veining
[<5%] Phenocrystal Phl, laths, dark brown in ppl

Modal Mineralogy/Matrix Ratio: 60/40

Matrix/Groundmass (in order of abundance):

Abundant Cal (in Cal segregationary pools), Sp (euhedral), Ilm, Phl (within lapillus)

Textures/Additional Information:

- Juvenile lapilli has angular Ol kernals (fragments with small degree of alteration)
- Microphenocrystal Phl laths are also found in the lapillus
- Oxide cumulates areas of probable HK material

Sample Identification: A154N-08
Depth: 325.24m

Classification: VK

Summary: Juvenile lapilli-bearing, highly altered volcaniclastic kimberlite exhibiting globular segregationary textures.

Colour: grey/green
Clay Minerals: alteration in the groundmass mineralogy and the matrix
Xenolith Abundance: [10%] lithic, angular
Xenolith Size: ~2mm
Xenolith Reaction: n/a
Olivine Replacement: Srp, Chl: veins to pseudomorphic replacement
Pelletal Lapilli: n/a
Autoliths: n/a
Primary Carbonate: n/a
Kimberlitic Textures: Juvenile lapilli, globular segregationary textures

Modal Mineralogy:

[20%] Anhedral macrocrystal Ol, exhibiting heavily altered rims
[20%] Subhedral microphenocrystal and phenocrystal Ol, varying degrees of alteration
[<5%] (trace) CPX, anhedral, highly altered
[<5%] (trace) Phl, phenocrystal, fragmental, highly altered

Modal Mineralogy/Matrix Ratio: 60/40

Matrix/Groundmass (in order of abundance):

Sp (euhedral), Phl (fragmental) in a Srp mesostasis. Other groundmass mineralogy is indistinguishable due to this alteration.

Textures/Additional Information:

- Globular segregations are highly irregularly shaped, and consist of randomly oriented Ol phenocrysts and microphenocrysts
- Very similar to other thin sections at this depth
- Juvenile lapilli is highly irregular in shape, and mainly consists of a center Ol fragmental macrocrystal kernal

---

Sample Identification: A154-N-08
Depth: 325.25m

Classification: VK

Summary: Altered volcaniclastic kimberlite containing juvenile lapilli and exhibiting globular segregationary textures in a Srp mesostasis.

Colour: green/grey
Clay Minerals: alteration in the groundmass
Xenolith Abundance: [15%] lithic
Xenolith Size: varies
Xenolith Reaction: n/a
Olivine Replacement: Srp
Pelletal Lapilli: n/a
Autoliths: n/a
Primary Carbonate: n/a
Kimberlitic Textures: Juvenile lapilli (present up to 5 modal %), globular segregations, Srp mesostasis, flow banding

Modal Mineralogy:

[20%] Macrocrystal Ol, anhedral, Srp veins and rims
[20%] Phenocrystal and microphenocrystal Ol, anhedral, Srp veins and rims
[<5%] (trace) CPX, phenocrystal, rounded anhedral, altered rims
[<5%] (trace) Phl, high degree of alteration, flow banding

Modal Mineralogy/Matrix Ratio: 65/35

Matrix/Groundmass (in order of abundance):

Yellow (ppl) Srp-rich mesostasis with fragments of altered and pseudomorphed minerals. Sp (subhedral).

Textures/Additional Information:

- Juvenile lapilli has highly irregular forms, with angular fragments of Ol as the kernal in a mud-rich lapillus
- Slide is suitable for petrographic pictures

Sample Identification: A154N
Depth: 329m

Classification: VK

Summary: Juvenile lapilli-bearing volcaniclastic kimberlite exhibiting Srp segregationary textures.

Colour: reddish brown
Clay Minerals: matrix, pseudomorphs after Ol
Xenolith Abundance: lithic [25%], angular
Xenolith Size: n/a
Xenolith Reaction: n/a
Olivine Replacement: Mud/Srp veins
Pelletal Lapilli: abundant to ~50% modal
Autoliths: n/a
Primary Carbonate: n/a
Kimberlitic Textures: segregationary textures, Srp mesostasis

Modal Mineralogy:

Lapilli kernals of Ol and rarely CPX, Phl

Modal Mineralogy/Matrix Ratio: 50/50

Matrix/Groundmass (in order of abundance):

Srp mesostasis

Textures/Additional Information:

- The remainder of the macrocrysts and the groundmass is petrographically indistinguishable because of the alteration of the kimberlite.

Sample Identification: A154
Depth: 340' level, open pit

Classification: VK

Summary: Juvenile lapilli-bearing volcaniclastic kimberlite with serpentine segregationary textures.

Colour: grey brown
Clay Minerals: alteration
Xenolith Abundance: lithic [25%], angular to subangular
Xenolith Size: n/a
Xenolith Reaction: n/a
Olivine Replacement: mud/srp veins
Pelletal Lapilli: n/a
Autoliths: present <5% modal
Primary Carbonate: n/a
Kimberlitic Textures: Juvenile lapilli, segregationary Srp textures, flow banding

Modal Mineralogy:

[25%] Macrocrystal Ol, anhedral habit, Srp veins (fragmental Ol present)
[10%] Phenocrystal Ol, euhedral to subhedral habit
[5%] CPX, euhedral habit
[5%] Phenocrystal Phl, possibly lithic

Modal Mineralogy/Matrix Ratio: 70/30

Matrix/Groundmass (in order of abundance):

Srp, clay/mud, Chl, Sp (present in lapillus, and scattered throughout entire section)

Textures/Additional Information:

- Thin section is cut too thin
- Srp mesostasis
- Juvenile lapilli with subhedral macrocrystal Ol as the kernals, and a few that remain uncored

---

Sample Identification: 98-A180-2
Depth: 85.0 m

Classification: VK

Summary: A heavily altered volcaniclastic kimberlite exhibiting Juvenile lapilli and macrocrystal olivine set in a quenched microcrystalline matrix.

Colour: brown
Clay Minerals: present as alteration
Xenolith Abundance: lithic [<5%]
Xenolith Size: <2 mm
Xenolith Reaction: n/a
Olivine Replacement: clay and srp (moderate to pseudomorphic replacement)
Pelletal Lapilli: n/a
Autoliths: n/a
Primary Carbonate: n/a
Kimberlitic Textures: Juvenile lapilli, macrocrystal

Modal Mineralogy:

[15%] Pseudomorphed subhedral to anhedral Ol macrocrysts
[15%] Pseudomorphed subhedral to euhedral Ol phenocrysts
[<5%] Phl laths, with alteration between the cleavage planes
[<5%] Trace Ilm, [<5%] +/- CPX fragments

Modal Mineralogy/Matrix Ratio: 50/50

Matrix/Groundmass (in order of abundance):

Srp, Clay, Euhedral Sp, (found occurring in abundance within the Ol macrocrysts, therefore secondary; and also within the microcrystalline matrix of the Juvenile lapilli). Other matrix minerals are too difficult to distinguish due to their fine grained altered nature.

Textures/Additional Information:

- Unpolished section
- Possible Prv
- Heavy alteration in the matrix/groundmass, where most of the mineralogy is indistinguishable.
- Juvenile lapilli containing angular Ol phenocrysts in a light brown (ppl) microcrystalline matrix (+/- diop)

Sample Identification: 98-A180-2
Depth: 87m

Classification: RVK

Summary: A juvenile lapilli-bearing resedimented volcaniclastic kimberlite exhibiting flow textures with anhedral macrocrystal olivine set in a mud matrix.

Colour: brown
Clay Minerals: abundant alteration
Xenolith Abundance: lithic, angular and fragmental [10%]
Xenolith Size: 0.5-5 mm
Xenolith Reaction: cryptocrystalline rim alteration
Olivine Replacement: completely pseudomorphed to clay and Srp
Pelletal Lapilli: n/a

Autoliths: n/a
Primary Carbonate: n/a
Kimberlitic Textures: Juvenile lapilli, flow banding, mesostasis, oxide cumulate

Modal Mineralogy:

[15%] Macrocrystal anhedral Ol with Srp veining
[15%] Phenocrystal and microphenocrystal subhedral Ol, subhedral habit
[10%] Macrocrystal anhedral CPX, slightly altered
[5%] Phl laths
[5%] Ilm, rounded anhedral habit

Modal Mineralogy/Matrix Ratio: 60/40

Matrix/Groundmass (in order of abundance):

Srp and Clay mesostasis, Sp, Phl, Ol, CPX, Cal-S

Textures/Additional Information:

- Extremely large crustal fragment present, 2 cm long, 3 mm wide
- All crustal fragments are extremely altered
- Juvenile lapilli, up to 8mm in diameter, with phenocrystic Ol +/- Diop
- Flow banding in altered Phl
- Srp and clay mesostasis

Sample Identification: 99-A180-07
Depth: 98 m

Classification: VK

Summary: An altered volcaniclastic kimberlite exhibiting juvenile lapilli and partially-to fully pseudomorphed olivine macrocrysts and phenocrysts.

Colour: brown/grey
Clay Minerals: alteration
Xenolith Abundance: lithic [<10%]
Xenolith Size: 0.5-1 mm
Xenolith Reaction: n/a
Olivine Replacement: partially to fully pseudomorphed, clay
Pelletal Lapilli: n/a
Autoliths: n/a
Primary Carbonate: n/a
Kimberlitic Textures: Juvenile lapilli, macrocrystal, Srp mesostasis

Modal Mineralogy:

[20%] Subhedral Ol macrocrysts, partially to fully pseudomorphed
[15%] Subhedral Ol phenocrysts, partially to fully pseudomorphed
[<5%] +/- CPX macrocrysts (heavily altered)

Modal Mineralogy/Matrix Ratio: 50/50

Matrix/Groundmass (in order of abundance):

Abundant Srp and clays, Rare Sp in the groundmass, Phl fragments and altered laths

Textures/Additional Information:

- Some Ol phenocrysts are interpreted as fragments of broken macrocrystal Ol
- Fine grained minerals in the matrix are indistinguishable due to the alteration of the thin section
- Juvenile lapilli- microlitic textures present as the matrix of the lapillus, irregular to lobate in habit

---

Sample Identification: 99-A180-10
Depth: 225.7m

Classification: TKB

Summary: Clast-supported, pelletal lapilli-bearing tuffisitic kimberlite breccia.

Colour: brown
Clay Minerals: alteration
Xenolith Abundance: lithic [20%]
Xenolith Size: 1-3mm
Xenolith Reaction: bleached rims
Olivine Replacement: Srp, Clay, Chl, Cal-S (veins to pseudomorphic replacement)
Pelletal Lapilli: present in moderate abundance (15% modal)
Autoliths: present in low abundance (5% modal)
Primary Carbonate: n/a
Kimberlitic Textures: autolith, pelletal-lapilli, clast-supported

Modal Mineralogy:

[15%] Macrocrystal Ol, fragmental, anhedral (rounded)
[15%] Phenocrystal Ol, fragmental, subhedral- varying degrees of alteration
[<5%] (trace) CPX, anhedral and heavily altered
[<5%] (trace) Phl, most likely lithic

Modal Mineralogy/Matrix Ratio: 60/40

Matrix/Groundmass (in order of abundance):

Cal-S, Clay/mud, Srp, Chl, Sp (scattered throughout and abundant in lapillus)

Textures/Additional Information:

- Clast-supported
- Secondary fractures infilled with Cal-S
- Pelletal lapillus is lesser oxide abundant that other Diavik TKBs

---

Sample Identification: A418-21
Depth: 377m

Classification: VK

Summary: Clast-supported juvenile lapilli-bearing volcaniclastic kimberlite.

Colour: grey/lgt brown
Clay Minerals: alteration
Xenolith Abundance: lithic [30%], angular
Xenolith Size: 1-4 mm
Xenolith Reaction: bleached thick, amorphous rims
Olivine Replacement: Srp, Cal
Pelletal Lapilli: n/a
Autoliths: present (5% modal)
Primary Carbonate: n/a
Microlitic Textures: n/a
Kimberlitic Textures: Clast-supported, juvenile lapilli

Modal Mineralogy:

[20%] Macrocrystal angular Ol, varying degrees of alteration
[20%] Subhedral phenocrystal and microphenocrystal Ol, varying degrees of alteration
[10%] Angular macrocrystal CPX
[5%] Flow-banded Phl

Modal Mineralogy/Matrix Ratio: 85/15

Matrix/Groundmass (in order of abundance):

Clay/Mud, Sp (euhedral), Srp, Chl, Phl, CPX

Textures/Additional Information:

- Autolithic material (sm. Phenocrystal and microphenocrystal Ol) are unaltered
- Secondary fractures are infilled with Cal
- Juvenile lapilli are cored with Ol fragments, and are mainly the shape of their kernal
- Mud-rich

Sample Identification: A418-21
Depth: 380.0m

Classification: VK

Summary: Fragmental, juvenile lapilli-bearing volcaniclastic kimberlite breccia.

Colour: brown/grey
Clay Minerals: matrix
Xenolith Abundance: lithic [15%]
Xenolith Size: <2mm
Xenolith Reaction: small, thin, bleached rims
Olivine Replacement: veins (Srp) and thin rims
Pelletal Lapilli: n/a
Autoliths: n/a
Primary Carbonate: n/a
Kimberlitic Textures: Juvenile lapilli (Ol kernals), angular fragmental, flow-banding

Modal Mineralogy:

[50%] Macrocrystal and phenocrystal Ol (extremely angular fragments), with varying degrees of alteration.
[10%] Flow-banded Phl, quite possibly lithic

Modal Mineralogy/Matrix Ratio: 75/25

Matrix/Groundmass (in order of abundance):

Some mud/clay, fragments of macro/pheno Ol, Sp, Phl, Srp and Chl

Textures/Additional Information:

- Tiny microphenocrystal size of magmaclasts of juvenile lapilli
- Secondary fractures are infilled with Cal-S
- Select juvenile lapilli are uncored

Sample Identification: 02-A840-03
Depth: 130m

Classification: VK

Summary: Juvenile lapilli-rich volcaniclastic kimberlite exhibiting Srp segregationary textures.

Colour: grey
Clay Minerals: alteration in groundmass
Xenolith Abundance: lithic [25%], angular
Xenolith Size: 1-2 mm
Xenolith Reaction: n/a
Olivine Replacement: pseudomorphic replacement with Srp and Clay
Pelletal Lapilli: n/a
Autoliths: n/a
Primary Carbonate: n/a
Kimberlitic Textures: Juvenile lapilli, flow banding, segregationary textures

Modal Mineralogy:

[20%] Macrocrystal Ol, fragmental and anhedral, rim alteration
[20%] Phenocrystal Ol, fragmental, subhedral, rim alteration
[5%] CPX, anhedral
[5%] Phl, flow-banded
[<5%] (trace) Gt, subhedral

Modal Mineralogy/Matrix Ratio: 80/20

Matrix/Groundmass (in order of abundance):

Srp and Clay, Sp (especially in lapillus), Phl

Textures/Additional Information:

- Juvenile lapillus: some have a macrocrystal fragment of Ol as a kernal, some have phenocrystal euhedral Ol as a 2 kernal
- Slightly elongate and irregular sizes: large kernal is often completely pseudomorphed
- Srp segregationary textures

Sample Identification: 99-A841-03
Depth: 119.8m

Classification: VK (probable RVK)

Summary: Clast-supported mud-rich olivine volcaniclastic kimberlite.

Colour: brown/green
Clay Minerals: alteration in mud-rich segments
Xenolith Abundance: rare angular lithic fragments [5%]
Xenolith Size: n/a
Xenolith Reaction: n/a
Olivine Replacement: Srp veining to pseudomorphic replacement
Pelletal Lapilli: n/a
Autoliths: n/a
Primary Carbonate: n/a
Kimberlitic Textures: Juvenile lapilli, macrocrystal, mud-rich, clast-supported

Modal Mineralogy:

[25%] Large anhedral fragmental Ol, partially serpentinized to fully pseudomorphed (1-6mm)
[20%] Angular phenocrystal Ol, partially serpentinized to pseudomorphic replacement
[10%] Anhedral CPX, rims of grains are altered, cores remain unaltered

Modal Mineralogy/Matrix Ratio: 60/40

Matrix/Groundmass (in order of abundance):

Mud-rich oxide matrix (Sp), with very tiny microphenocrystal Ol which are fully pseudomorphed to clay/mud/chl/srp.

Textures/Additional Information:

- Clast supported, (high possibility of RVK)
- Infilled fractures (secondary Cal) throughout thin section
- Section cut too thick in some areas for proper petrographic methods
- Juvenile lapilli- irregular forms with small CPX and Ol randomly distributed in a mud-rich matrix.

Sample Identification: A841-07
Depth: 129.5m

Classification: VK

Summary: Altered juvenile lapilli-bearing volcaniclastic kimberlite exhibiting globular segregationary textures.

Colour: brown
Clay Minerals: alteration
Xenolith Abundance: lithic [20%]
Xenolith Size: angular, 0.5-1.5 mm
Xenolith Reaction: n/a

Olivine Replacement: Srp veining to pseudomorphic replacement
Pelletal Lapilli: n/a
Autoliths: n/a
Primary Carbonate: n/a
Kimberlitic Textures: Juvenile lapilli, globular segregationary textures, mesostasis

Modal Mineralogy:

[15%] Macrocrystal anhedral Ol, exhibiting varying degrees of alteration
[15%] Phenocrystal Ol, anhedral to subhedral, varying degrees of alteration
[5%] Phl, lath-shaped, alteration around edges of grain
[5%] CPX, fragmental, highly altered +/- OPX?

Modal Mineralogy/Matrix Ratio: 60/40

Matrix/Groundmass (in order of abundance):

Srp and Chl mesostasis
Sp (euhedral), varying sizes and habits

Textures/Additional Information:

- Secondary fractures are infilled by secondary Cal
- Irregular shapes and habit of juvenile lapilli in the kimberlite
- Remainder of the matrix and groundmass mineralogy is petrographically indistinguishable due to the alteration of the kimberlite
- Cored and uncored juvenile lapilli are present

Sample Identification: A841-07
Depth: 129.5m

Classification: VK

Summary: Juvenile lapilli-bearing volcaniclastic kimberlite.

Colour: grey
Clay Minerals: present in the lapilli
Xenolith Abundance: lithic [10%]
Xenolith Size: n/a
Xenolith Reaction: n/a
Olivine Replacement: Srp, Chl
Pelletal Lapilli: present (~15% modal abundance)
Autoliths: 5 micro autoliths present
Primary Carbonate: n/a
Kimberlitic Textures: necklace and cumulate textures with Sp, juvenile lapilli, autoliths

Modal Mineralogy:

[20%] Macrocrystal anhedral Ol, varying degrees of alteration
[20%] Phenocrystal euhedral to subhedral Ol, varying degrees of alteration
[20%] Macrocrystal and fragmental CPX, severe alteration

Modal Mineralogy/Matrix Ratio: 70/30

Matrix/Groundmass (in order of abundance):

Abundant Cal-S in the groundmass, Phl (rounded fragments), Sp cumulates and partial necklace textures

Textures/Additional Information:

- Juvenile lapilli has either anhedral Ol or anhedral CPX as the kernal
- The lapillus contains euhedral hopper-type Ol in a mud/clay matrix
- Juvenile lapilli are slightly elongate, exhibiting curvi-linear shapes
- Primary mineralogy is difficult to distinguish in the matrix due to alteration
- Uncored Juvenile lapilli are present in low abundance

Sample Identification: A841
Depth: 130.1m

Classification: VK

Summary: Matrix-supported, lithic-rich volcaniclastic kimberlite, exhibiting juvenile lapilli.

Colour: brown
Clay Minerals: alteration in groundmass
Xenolith Abundance: lithic [25%]
Xenolith Size: 0.5-4 mm
Xenolith Reaction: n/a
Olivine Replacement: Srp, Clay/mud
Pelletal Lapilli: a few occurrences
Autoliths: n/a
Primary Carbonate: n/a
Kimberlitic Textures: Juvenile lapilli, matrix-supported, flow banding, lithic rich, cumulate textures

Modal Mineralogy:

[20%] Macrocrystal Ol, varying degrees of alteration, rounded and fragmental habit
[<5%] Phl, alteration between cleavage planes, flow banding

Modal Mineralogy/Matrix Ratio: 50/50

Matrix/Groundmass (in order of abundance):

Sp, Mud/Clay, +/-Phl, +/-Ol microphenocrysts (pseudomorphic replacement)

Textures/Additional Information:

- Secondary fractures infilled by Cal
- Oxide cumulate zones around large macrocrysts
- Juvenile lapilli are slightly elongate, and are both cored and uncored

---

Sample Identification: A841-07
Depth: 130.5m

Classification: VK

Summary: Juvenile lapilli-bearing matrix-supported volcaniclastic kimberlite.

Colour: grey
Clay Minerals: matrix
Xenolith Abundance: lithic [15%]
Xenolith Size: <3mm, angular
Xenolith Reaction: bleached rims
Olivine Replacement: Cal pseudomorphic replacement, Srp veins
Pelletal Lapilli: n/a
Autoliths: n/a
Primary Carbonate: n/a
Kimberlitic Textures: Juvenile lapilli, matrix-supported

Modal Mineralogy:

[15%] Macrocrystal Ol, angular fragmental, varying degrees of alteration
[15%] Phenocrystal Ol, angular fragmental, varying degrees of alteration
[<5%] (trace) CPX, anhedral, highly altered
[<5%] (trace) Phl, phenocrystal, alteration between cleavage planes and rim alteration

Modal Mineralogy/Matrix Ratio: 55/45

Matrix/Groundmass (in order of abundance):

Clay, Srp, Sp (euhedral to subhedral- abundant in Juvenile lapilli), Cal-S, CPX, Ap, +/-Prv (to be confirmed by EMPA)

Textures/Additional Information:

- Juvenile lapilli: large subhedral clasts of Phl, Ol, CPX, and lapillus is Sp-rich
- Some of the smaller Juvenile lapilli: the kernals and clasts can be well rounded to angular fragments, to euhedral clasts
- Juvenile lapilli is both cored and uncored

Sample Identification: A841-07
Depth: 135.9m

Classification: VK (possibly RVK)

Summary: Heavily altered, juvenile lapilli-bearing, highly fractured and clast-supported volcaniclastic kimberlite.

Colour: brown
Clay Minerals: alteration within the groundmass
Xenolith Abundance: lithic [15%]
Xenolith Size: angular, fine-grained
Xenolith Reaction: bleached rims
Olivine Replacement: Srp veins
Pelletal Lapilli: n/a
Autoliths: n/a
Primary Carbonate: n/a
Microlitic Textures: n/a
Kimberlitic Textures: Juvenile lapilli, clast-supported, fractured

Modal Mineralogy:

Petrographically indistinguishable due to alteration of the kimberlite.

Modal Mineralogy/Matrix Ratio: 50/50

Matrix/Groundmass (in order of abundance):

Some Phl, Sp in a Cal-Srp matrix.
Most primary mineralogy of the groundmass is petrographically indistinguishable due to the alteration of the kimberlite.

Textures/Additional Information:

- Poorly cut thin section or varying thickness
- Thin section is unpolished

Sample Identification: A841-07
Depth: 139.1m

Classification: VK

Summary: Heavily altered, juvenile lapilli-bearing volcaniclastic kimberlite exhibiting microlitic textures throughout the groundmass.

Colour: dark brown
Clay Minerals: alteration
Xenolith Abundance: lithic [10%]
Xenolith Size: n/a
Xenolith Reaction: n/a
Olivine Replacement: Srp veining to pseudomorphs
Pelletal Lapilli: n/a
Autoliths: n/a
Primary Carbonate: possible in the groundmass/matrix
Kimberlitic Textures: Juvenile lapilli, globular segregations (both highly irregular shapes), Srp mesostasis, cumulates

Modal Mineralogy:

[25%] Euhedral phenocrystal Ol, heavy Srp alteration
[15%] Anhedral macrocrystal Ol, some fragmental
[5%] Phenocrystal Phl with heavy alteration between the cleavage planes
[<5%] (trace) CPX phenocrysts, heavily altered

Modal Mineralogy/Matrix Ratio: 60/40

Matrix/Groundmass (in order of abundance):

Srp mesostasis
Sp cumulates within the globular segregations and the lapilli.

Textures/Additional Information:

- Microlitic textures in the groundmass throughout the whole thin section

- Primary mineralogy in the groundmass is very hard to distinguish due to the alteration of the kimberlite
- Juvenile lapilli is both cored (with macrocrystal Ol fragments) and uncored (with multiple Ol phenocrysts and Ol microphenocrysts)
- Juvenile lapilli is irregular in habit, oblong

Sample Identification: 99-A841-05
Depth: 166.8m

Classification: VK

Summary: Juvenile lapilli-bearing olivine-rich volcaniclastic kimberlite exhibiting serpentine segregationary textures.

Colour: black/dark green
Clay Minerals: alteration
Xenolith Abundance: lithic angular [10%]
Xenolith Size: n/a
Xenolith Reaction: n/a
Olivine Replacement: Srp, mud/clay
Pelletal Lapilli: [10-15%] Ol kernels
Autoliths: rare {1} small (0.1mm)
Primary Carbonate: n/a
Kimberlitic Textures: Juvenile lapilli, necklace textures, autoliths, segregationary Srp textures.

Modal Mineralogy:

[30%] Megacrystal and macrocrystal Ol, anhedral habit, and/or fragmental with Srp veins
[10%] Phenocrystal and microphenocrystal Ol with thick distinct black rims (kelyphite)

Modal Mineralogy/Matrix Ratio: 50/50

Matrix/Groundmass (in order of abundance):

Srp segregationary textures, Sp cumulates in the groundmass, necklace Sp and possible Prv textures

Textures/Additional Information:

- Undulatory extinction on the macrocrystal Ol indicating strain
- Ol suitable for microprobe analyses
- Juvenile lapilli: angular Ol fragment as the kernel, with small Diop + Ol (anhedral) in a mud-rich matrix
- Groundmass mineralogy is difficult to distinguish due to the serpentinization of the groundmass

---

Sample Identification: 99-A841-05
Depth: no depth indicated

Classification: VK

Summary: Juvenile lapilli-bearing segregationary-textured volcaniclastic kimberlite.

Colour: brown
Clay Minerals: matrix
Xenolith Abundance: lithic [15%]
Xenolith Size: <2 mm
Xenolith Reaction: bleached rims
Olivine Replacement: Srp veins
Pelletal Lapilli: n/a
Autoliths: n/a
Primary Carbonate: n/a
Kimberlitic Textures: Juvenile lapilli, Srp segregationary textures

Modal Mineralogy:

[15%] Phenocrystal Ol, fragmental, Srp veins to pseudomorphic replacement, subhedral to euhedral
[10%] Macrocrystal Ol, fragmental, Srp veins, subhedral
[10%] CPX fragmental (probably macrocrystal), heavy alteration

Modal Mineralogy/Matrix Ratio: 50/50

Matrix/Groundmass (in order of abundance):

Cal-S, Srp (segregationary textures), Clay, Mud, Sp (euhedral, cubic)

Textures/Additional Information:

- Juvenile lapilli have abundant oxides in the lapillus
- Lots of angular, bleached, heavily altered lithic fragments, all sizes up to 2mm
- Cored and uncored Juvenile lapilli are present, most are elongate and irregular in habit
- Primary mineralogy in the groundmass is difficult to distinguish due to the extensive alteration, serpentinization, and clay replacement of the kimberlite

---

Sample Identification: 04-A1039-01
Depth: 69.2 m

Classification: TK (or TKB)

Summary: This thin section has mainly large lithic fragments present (>10 cm!), therefore a full petrographic report is not available.

Colour:
Clay Minerals:
Xenolith Abundance:
Xenolith Size:
Xenolith Reaction:
Olivine Replacement:
Pelletal Lapilli:
Autoliths:
Primary Carbonate:
Kimberlitic Textures: Pelletal lapilli

Modal Mineralogy:

Petrographically indistinguishable, due to large crustal fragment and thickness of section.

Modal Mineralogy/Matrix Ratio: 50/50

Matrix/Groundmass (in order of abundance):

Oxide rich matrix, surrounded by 99% mud!

Textures/Additional Information:

- This thin section is >90% crustal material, identifiable as granite and granodiorite. Please see the closest drill sample for a full petrographic report.
- Thin section is cut too thick

Sample Identification: 05-A1039 NE-01
Depth: 72m

Classification: TKB

Summary: Pelletal lapilli-bearing, mud-rich tuffisitic kimberlite breccia.

Colour: dark brown
Clay Minerals: entire slide
Xenolith Abundance: lithic [20%]
Xenolith Size: 2-3 mm, <0.5 mm
Xenolith Reaction: n/a
Olivine Replacement: pseudomorphic replacement to clay
Pelletal Lapilli: modally 10% abundant
Autoliths: n/a
Primary Carbonate: n/a
Kimberlitic Textures: Pelletal lapilli, fragmental

Modal Mineralogy:

[30%] Rounded and angular, mainly fragmental, macrocrystal, phenocrystal, microphenocrystal Ol with pseudomorphic replacement to clay

Modal Mineralogy/Matrix Ratio: 50/50

Matrix/Groundmass (in order of abundance):

Clay, Srp, Chl, Some Sp (in pelletal lapilli), Phl (heavily altered and rounded)

Textures/Additional Information:

- Thin section is unpolished because of clay alteration of kimberlite
- Primary mineralogy is impossible to distinguish
- Thin section Box 4,11 (A1039 NE-01, 72m) is identical to this section, with the exception of greater abundance of pelletal lapilli [15% modal]

Sample Identification: 05-A1039 NE-01
Depth: 74.5m

Classification: HK

Summary: Macrocrystal, uniform textured, heavily altered spinel hypabyssal kimberlite.

Colour: grey
Clay Minerals: n/a
Xenolith Abundance: trace [<5%] lithic
Xenolith Size: <1mm
Xenolith Reaction: none
Olivine Replacement: Cal
Pelletal Lapilli: n/a
Autoliths: n/a
Primary Carbonate: groundmass/matrix
Kimberlitic Textures: Necklace with Sp, Atoll Sp, accicular (quenching), uniform

Modal Mineralogy:

[25%] Phenocrystal Ol, some fragmental, subhedral, Srp rims, mainly pseudomorphic replacement with Cal
[15%] Macrocrystal Ol, some fragmental, anhedral, many pseudomorphs of Cal
Trace [<5%] Phl, fragmental, high degree of alteration

Modal Mineralogy/Matrix Ratio: 50/50

Matrix/Groundmass (in order of abundance):

Abundant Sp (euhedral cubic), Atoll Sp, accicular Ap, euhedral to subhedral brown Prv, +/- Phl, +/-Cal-P, Srp and Chl.

Textures/Additional Information:

- Uniform textures are seen in the matrix/groundmass
- Some secondary fractures in the thin section are infilled with Cal-S
- Thin section is highly oxide-abundant

Sample Identification: 04A1039-01
Depth: 67m

Classification: TK

Summary: Serpentine-rich segregationary textured, macrocryst-poor tuffisitic kimberlite.

Colour: green/brown
Clay Minerals: alteration in groundmass
Xenolith Abundance: lithic [15%]
Xenolith Size: 1-1.5 mm
Xenolith Reaction: Srp rims
Olivine Replacement: clay/mud/Chl, veins to pseudomorphic replacement
Pelletal Lapilli: present as 5 modal %
Autoliths: n/a
Primary Carbonate: n/a
Kimberlitic Textures: Pelletal lapilli, angular CPX (possibly OPX) kernal, fine-grained oxide-rich lapillus, segregationary textures with Srp and Cal

Modal Mineralogy:

[10%] Macrocrystal Ol, anhedral habit, pseudomorphic replacement
[15%] Phenocrystal and microphenocrystal Ol (subhedral habit) rimmed by Srp

[5%] Angular CPX, heavily altered throughout grains

Modal Mineralogy/Matrix Ratio: 45/55

Matrix/Groundmass (in order of abundance):

Srp, Sp, Cal, +/-Prv (to be confirmed by EMPA)

Textures/Additional Information:

- Thin section mineralogy is very altered and primary mineralogy is indistinguishable.
- Macrocrystal poor thin section
- Microlitic textures in the groundmass
- Pelletal lapilli are rare in this section

Sample Identification: 02-A1245-2
Depth: 45.5m

Classification: RVK

Summary: Mud-rich RVK with angular clasts and fragments (clast-supported).

Colour: brown
Clay Minerals: abundant
Xenolith Abundance: lithic [15%], angular
Xenolith Size: 1-5 mm
Xenolith Reaction: mud rims
Olivine Replacement: pseudomorphic replacement with mud/clay, +/-Chl
Pelletal Lapilli: n/a
Autoliths: n/a
Primary Carbonate: n/a
Kimberlitic Textures: RVK-very fragmental, evidence of movement, clast-supported, flow banding, Juvenile lapilli

Modal Mineralogy:

[50%] Angular pseudomorphs after Ol- slight flow alignment (evidence of movement, and redistributions)

Modal Mineralogy/Matrix Ratio: 65/35

Matrix/Groundmass (in order of abundance):

Mud matrix, lesser Sp, lesser CPX

Textures/Additional Information:

- Clast-supported
- Most macrocrysts are broken angular fragments
- The rest of the kimberlite mineralogy is petrographically indistinguishable due to the alteration of the kimberlite and mud replacement
- Juvenile lapilli are highly irregular in habit, and are mainly uncored

Sample Identification: 02-A1245-2
Depth: 45.5m

Classification: RVK

Summary: Clay-rich, clay-supported resedimented volcaniclastic kimberlite.

Colour: brown
Clay Minerals: matrix
Xenolith Abundance: lithic [10%]
Xenolith Size: 1-2 mm
Xenolith Reaction: n/a
Olivine Replacement: n/a
Pelletal Lapilli: n/a
Autoliths: n/a
Primary Carbonate: n/a
Kimberlitic Textures: resedimented, mud-supported, Juvenile lapilli

Modal Mineralogy:

[40%] Angular Ol macrocrysts, fragmental, rims and veins are serpentinized
(Phenocrystal Ol is interpreted to be fragments of macrocrystal Ol)
[<5%] (trace) CPX
[<5%] (trace) Gt

Modal Mineralogy/Matrix Ratio: 60/40

Matrix/Groundmass (in order of abundance):

Clay, Microphenocrystal Ol (pseudomorphic replacement with Clay),
Sp: small euhedral, not abundant

Textures/Additional Information:

- Clay-rich
- Clay-supported
- Extreme alteration, the primary mineralogy is petrographically indistinguishable
- Juvenile lapilli is both cored and uncored, and highly irregular in habit

Sample Identification: 02-A1245-2
Depth: 55.1m

Classification: RVK

Summary: Juvenile lapilli-bearing fragmental olivine, clay-rich resedimented volcaniclastic kimberlite.

Colour: brown
Clay Minerals: matrix
Xenolith Abundance: lithic [20%]
Xenolith Size: angular 1-2 mm
Xenolith Reaction: n/a
Olivine Replacement: Srp rims, kelyphite rims
Pelletal Lapilli: n/a

Autoliths: n/a
Primary Carbonate: n/a
Kimberlitic Textures: fragmental, flow-banding, juvenile lapilli

Modal Mineralogy:

[25%] Macrocrystal Ol, highly fragmented, alteration on rims
[25%] Phenocrystal Ol, highly fragmented, alteration on rims
[<5%] (trace) Megacrystal CPX
[<5%] (trace) Phl flow-banding, and heavy alteration

Modal Mineralogy/Matrix Ratio: 80/20

Matrix/Groundmass (in order of abundance):

Clay, Srp, Sp, Chl, Cal-S, +/-Prv

Textures/Additional Information:

- Thin section cut too thick (67.5m)
- Secondary fractures infilled with Cal-S
- Juvenile lapilli is approximately 15% modal, oblong habit, cored and uncored

---

Sample Identification: 02-A1245-2
Depth: 67.5m & 69.0m

Classification: RVK

Summary: Fragmental olivine, mud-rich resedimented volcaniclastic kimberlite.

Colour: brown
Clay Minerals: matrix
Xenolith Abundance: lithic [15%]
Xenolith Size: angular 1-2 mm
Xenolith Reaction: n/a
Olivine Replacement: Srp rims, clay rims
Pelletal Lapilli: n/a
Autoliths: n/a
Primary Carbonate: n/a
Kimberlitic Textures: fragmental, flow-banding

Modal Mineralogy:

[25%] Macrocrystal Ol, highly fragmented, alteration on rims
[25%] Phenocrystal Ol, highly fragmented, alteration on rims
[<5%] (trace) Megacrystal CPX
[<5%] (trace) Phl flow-banding, and heavy alteration

Modal Mineralogy/Matrix Ratio: 75/25

Matrix/Groundmass (in order of abundance):

Clay, Srp, Sp, Chl, Cal-S, +/-Prv

Textures/Additional Information:

- Thin section cut too thick (67.5m)
- Secondary fractures infilled with Cal-S
- Possible presence of Juvenile lapilli, thin section is too thick to confirm
- Evidence of movement (flow-banding)

Sample Identification: 03-A1620-02
Depth: 69.5m

Classification: VK

Summary: Juvenile-lapilli poor, moderately altered volcaniclastic kimberlite.

Colour: brown
Clay Minerals: matrix
Xenolith Abundance: lithic (trace) [<5%]
Xenolith Size: small, <1mm
Xenolith Reaction: n/a
Olivine Replacement: Srp and Cal, pseudomorphic replacement
Pelletal Lapilli: n/a
Autoliths: n/a
Primary Carbonate: n/a
Kimberlitic Textures: Fragmental, uniform textures, flow banding

Modal Mineralogy:

[15%] Ol phenocrysts and microphenocrysts, altered veins and rims
[10%] Ol macrocrysts, pseudomorphic replacement to Cal, Srp, anhedral
[<5%] (trace) CPX, [<5%] (trace) Phl (flow banding), [<5%] (trace) Sp (coarse)

Modal Mineralogy/Matrix Ratio: 45/55

Matrix/Groundmass (in order of abundance):

Clay, Srp, Sp: euhedral, Sm. Phl: heavy alteration

Textures/Additional Information:

- Oxide cumulates
- Partial necklace textures
- Flow-banded Phl
- Groundmass mineralogy is petrographically indistinguishable as a result of alteration of kimberlite
- Juvenile lapilli is highly irregular in habit, and is entirely uncored

---

Sample Identification: 03-A1620-02
Depth: 71m

Classification: RVK

Summary: Clast-supported, mud-rich resedimented volcaniclastic kimberlite.

Colour: brown/black
Clay Minerals: alteration in the groundmass mineralogy

Xenolith Abundance: [25%] lithic
Xenolith Size: ~1mm
Xenolith Reaction: indistinguishable due to resedimentation
Olivine Replacement: varies from Srp veining to complete pseudomorphs
Pelletal Lapilli: n/a
Autoliths: n/a
Primary Carbonate: n/a
Kimberlitic Textures: Flow banding (Phl), clast-supported, highly angular fragmental macrocrystal mineralogy

Modal Mineralogy:

[35%] Ol, CPX, Phl: angular fragmental, set in a clay/mud matrix/groundmass. Too difficult to identify as macrocrystal or phenocrystal due to the fragmentation, as well as the alteration.

Modal Mineralogy/Matrix Ratio: 60/40

Matrix/Groundmass (in order of abundance):

Mud/Clay, lesser Srp and Chl.

Textures/Additional Information:

- Primary mineralogy is petrographically indistinguishable due to the resedimentation and subsequent alteration of the entire kimberlite
- Primary textures are also difficult/impossible to identify
- Juvenile lapilli is uncored

Sample Identification: 04-A1621-01
Depth: 50.2m

Classification: RVK

Summary: Mud-rich matrix-supported resedimented volcaniclastic kimberlite.

Colour: brown/green
Clay Minerals: matrix
Xenolith Abundance: n/a
Xenolith Size: n/a
Xenolith Reaction: n/a
Olivine Replacement: Cal + Mud pseudomorphic replacement
Pelletal Lapilli: n/a
Autoliths: n/a
Primary Carbonate: n/a
Kimberlitic Textures: Matrix-supported, juvenile lapilli, atoll Sp

Modal Mineralogy:

[35%] Macrocrystal anhedral Ol, pseudomorphic replacement to Cal
[10%] Large atoll Sp
The remainder of the modal mineralogy is petrographically indistinguishable due to the resedimentation of the kimberlite.

Modal Mineralogy/Matrix Ratio: 45/55

Matrix/Groundmass (in order of abundance):

Mud-rich matrix, with the exception of atoll Sp. The remainder of the mineralogy is petrographically indistinguishable.

Textures/Additional Information:

- Juvenile lapilli: with large euhedral Ol in them
- Thin section unpolished, due to heavy clay alteration

Sample Identification: ABZ-7a [1]
Depth: unknown

Classification: RVK

Summary: Extremely altered RVK exhibiting segregationary textures with Cal and clay.

Colour: brown
Clay Minerals: abundant
Xenolith Abundance: lithic, up to [25%]
Xenolith Size: n/a
Xenolith Reaction: n/a
Olivine Replacement: Chl, mud, Cal, clay
Pelletal Lapilli: n/a
Autoliths: n/a
Primary Carbonate: n/a
Kimberlitic Textures: segregationary textures with Cal and clay/mud

Modal Mineralogy:

Everything is too altered to distinguish any primary or secondary mineralogy.

Modal Mineralogy/Matrix Ratio: 50/50

Matrix/Groundmass (in order of abundance):

Small anhedral CPX

Textures/Additional Information:

- Sample is resedimented with mud and clays
- Evidence of movement
- Fragmental and flow-aligned

Sample Identification: ABZ-7a [2]
Depth: unknown

Classification: VK

Summary: Macrocryst-poor heavily altered volcaniclastic kimberlite.

Colour: brown
Clay Minerals: alteration

Xenolith Abundance: lithic 10%
Xenolith Size: <0.5mm
Xenolith Reaction: n/a
Olivine Replacement: Srp, Cal
Pelletal Lapilli: n/a
Autoliths: n/a
Primary Carbonate: n/a
Kimberlitic Textures: Flow banded Phl, segregationary textured Cal, Atoll Sp, irregular Juvenile lapilli with a dark mud/clay matrix

Modal Mineralogy:

[35%] Ol anhedral phenocrysts and microphenocrysts, partially serpentinized., to fully pseudomorphed
[10%] Small fragmental Phl phenocrysts, flow-banded with alteration between cleavage planes
CPX [<5%] phenocrysts (subhedral and green in ppl)

Modal Mineralogy/Matrix Ratio: 60/40

Matrix/Groundmass (in order of abundance):

Clay, Small Phl microphenocrysts, CPX, Sp (with partial atoll), Sp (fragmental), +/- Rt, Prv (subhedral with dark brown rims)

Textures/Additional Information:

- Prv useful for emplacement age
- All sizes and habits of Sp-group minerals are present
- One single irregular Juvenile lapilli

Sample Identification: ABZ-7a [3]
Depth: unknown

Classification: VK

Summary: Juvenile lapilli-rich, lithic-rich olivine volcaniclastic kimberlite.

Colour: brown
Clay Minerals: alteration
Xenolith Abundance: lithic, rounded [15%]
Xenolith Size: n/a
Xenolith Reaction: n/a
Olivine Replacement: clay, Cal
Pelletal Lapilli: n/a
Autoliths: n/a
Primary Carbonate: n/a
Kimberlitic Textures: Juvenile lapilli-rich: surrounded by Cal segregations. Flow banding in mica, and partial necklace textures with Sp.

Modal Mineralogy:

[20%] Anhedral to subhedral Ol macrocrysts (pseudomorphed replacement)
[10%]Large flow-banded Phl macrocrysts, likely lithic
[<5%]Anhedral CPX phenocrysts

Modal Mineralogy/Matrix Ratio: 50/50

Matrix/Groundmass (in order of abundance):

Cal-S, Clay, euhedral to anhedral Sp (in partial necklace textures, not very abundant <5% of groundmass), Small Phl laths, possible Prv to be confirmed by microprobe

Textures/Additional Information:

- some lithic fragments cannot be identified
- Cal segregationary textures throughout
- Juvenile lapilli are cored

Sample Identification: Anik-01
Depth: 232.74m

Classification: VK

Summary: Clast-supported juvenile lapilli-bearing tuffisitic kimberlite.

Colour: brown
Clay Minerals: alteration
Xenolith Abundance: [20%] lithic, angular
Xenolith Size: 0.1-2mm
Xenolith Reaction: n/a
Olivine Replacement: Srp veining to pseudomorphic replacement
Pelletal Lapilli: n/a
Autoliths: n/a
Primary Carbonate: n/a
Kimberlitic Textures: Clast-supported, flow-banding, lithic-rich, juvenile lapilli, globular segregations, cumulate

Modal Mineralogy:

[20%] Phenocrystal Ol, angular, anhedral to subhedral
[15%] Macrocrystal Ol, angular (fragmental) anhedral
[5%] Phenocrystal Phl, flow banding
[5%] Phenocrystal CPX, various degrees of alteration

Modal Mineralogy/Matrix Ratio: 60/40

Matrix/Groundmass (in order of abundance):

Clay, euhedral Sp (some areas are cumulates), Phl, CPX, Srp

Textures/Additional Information:

- Kernals of the cored juvenile lapilli are angular Ol fragmented macrocrysts
- Globular segregationary textures are present with mud/clay in the groundmass
- The extremely variable alteration is notable, especially in the Ol macrocrysts and phenocrysts

---

Sample Identification: Anik-01

Depth: no depth given

Classification: VK

Summary: Juvenile lapilli-rich volcaniclastic kimberlite.

Colour: brown
Clay Minerals: identified in the matrix
Xenolith Abundance: lithic [10%], subangular
Xenolith Size: ~1mm
Xenolith Reaction: n/a
Olivine Replacement: Srp veins and rims
Pelletal Lapilli: n/a
Autoliths: n/a
Primary Carbonate: n/a
Kimberlitic Textures: juvenile lapilli

Modal Mineralogy:

[25%] Macrocrystal Ol, fragmental anhedral habit, some with Srp veins
[15%] Phenocrystal Ol, subrounded habit, Srp veins
[5%] CPX, rim alteration, subhedral habit
[5%] Phl, rounded lath-shaped, varying degrees of alteration

Modal Mineralogy/Matrix Ratio: 60/40

Matrix/Groundmass (in order of abundance):

Clay.
Besides Sp, the rest of the matrix/groundmass mineralogy is petrographically indistinguishable, due to the alteration of the kimberlite.

Textures/Additional Information:

- Juvenile lapilli: clasts are normally cored Ol surrounded by a very fine-grained matrix
- Heavily altered kimberlite
- Juvenile lapilli are subrounded in habit

Sample Identification: C27-3
Depth: 111.9m

Classification: VK

Summary: Juvenile lapilli-rich, olivine volcaniclastic kimberlite.

Colour: dark brown
Clay Minerals: matrix
Xenolith Abundance: [15%] lithic
Xenolith Size: 1mm average
Xenolith Reaction: n/a
Olivine Replacement: pseudomorphic replacement to Cal-S, Clay
Pelletal Lapilli: n/a
Autoliths: n/a
Primary Carbonate: n/a

Kimberlitic Textures: Juvenile lapilli, necklace Sp, cumulate Sp

Modal Mineralogy:

[30%] Phenocrystal Ol, anhedral habit, pseudomorphic replacement
[10%] Macrocrystal Ol, anhedral habit, pseudomorphic replacement
[5%] Euhedral Gt, red in ppl, alteration on rims

Modal Mineralogy/Matrix Ratio: 60/40

Matrix/Groundmass (in order of abundance):

Srp, Clay, Cal-S, lesser Phl, lesser Sp, lesser CPX, lesser Gt (fragment)

Textures/Additional Information:

- Unpolished thin section
- Juvenile lapilli, many phenocrystal kernals and fragments
- Highly irregular, globular forms of juvenile lapilli

Sample Identification: 94-C42-2
Depth: 66.5m

Classification: TKB

Summary: Highly fractured tuffisitic kimberlite breccia exhibiting globular segregationary textures in the matrix.

Colour: brown
Clay Minerals: groundmass
Xenolith Abundance: lithic [15%]
Xenolith Size: 0.5-1 mm
Xenolith Reaction: n/a
Olivine Replacement: pseudomorphic replacement with Cal
Pelletal Lapilli: n/a
Autoliths: n/a
Primary Carbonate: n/a
Kimberlitic Textures: globular segregationary

Modal Mineralogy:

[20%] Angular, fragmental Macrocrystal Ol (pseudomorphic replacement to Cal)
[20%] Angular, fragmental Phenocrystal Ol (pseudomorphic replacement to Cal)
[10%] Phl, probably lithic, slight rim alteration

Modal Mineralogy/Matrix Ratio: 65/35

Matrix/Groundmass (in order of abundance):

Clay, Srp, Cal-S, Sp (variety of sizes), Prv

Textures/Additional Information:

- Recrystallization along secondary fractures within the slide

- No magmaclasts present
- Phenocrystal mineralogy is most likely fractured macrocrysts

---

Sample Identification: 95-C53-2
Depth: 49m

Classification: VK (or RVK)

Summary: Juvenile lapilli-bearing, highly fragmental, altered volcaniclastic kimberlite exhibiting globular segregationary textures.

Colour: brown
Clay Minerals: matrix
Xenolith Abundance: lithic [10%], angular
Xenolith Size: <1 mm
Xenolith Reaction: n/a
Olivine Replacement: veining to pseudomorphic replacement to Cal-S
Pelletal Lapilli: n/a
Autoliths: n/a
Primary Carbonate: n/a
Kimberlitic Textures: Juvenile lapilli, globular segregationary, fractured

Modal Mineralogy:

[15%] Angular fragmental Ol macrocrysts, pseudomorphic replacement with Cal and Srp
[15%] Angular fragmental Ol phenocrysts, pseudomorphic replacement with Cal and Srp
[15%] Angular fragmental Ol microphenocrystal, pseudomorphic replacement with Clay
[5%] Phenocrystal Phl, possible lithic, highly altered

Modal Mineralogy/Matrix Ratio: 60/40

Matrix/Groundmass (in order of abundance):

Cal-S, Clay, Srp, Phl, lesser Sp (euhedral)

Textures/Additional Information:

- Juvenile lapilli is cored and uncored
- Primary mineralogy is difficult to distinguish due to the alteration and replacement of the kimberlite
- Secondary fractures (late stage) are infilled with Cal-S
- Juvenile lapilli have highly irregular habits, and range in size from 1-3mm

---

Sample Identification: DD
Depth: 39.5m

Classification: VK

Summary: An olivine-rich, juvenile lapilli-bearing volcaniclastic kimberlite.

Colour: brown
Clay Minerals: present as alteration
Xenolith Abundance: lithic, fragmental [10-15%]

Xenolith Size: angular, 0.5-3 mm
Xenolith Reaction: n/a
Olivine Replacement: Srp-Cal-clay
Pelletal Lapilli: n/a
Autoliths: n/a
Primary Carbonate: n/a
Kimberlitic Textures: Juvenile lapilli, abundant and a range of sizes

Modal Mineralogy:

[25%] Anhedral Ol macrocrysts, Srp veining
[15%] Anhedral Ol phenocrysts, cryptocrystalline rims and Srp veining
[10%]CPX, anhedral and strain features
Possible OPX microphenocrysts

Modal Mineralogy/Matrix Ratio: 65/35

Matrix/Groundmass (in order of abundance):

Cal-S, Clay, Abundant oxides and Sp in the groundmass, mainly euhedral. All other groundmass mineralogy is indistinguishable.

Textures/Additional Information:

- Small lithic fragments are angular while larger lithic fragments are rounded
- Many fractures infilled with secondary late-stage Cal
- Juvenile lapilli is mostly cored, with a oxide-rich lapillus
- Highly altered thin section

Sample Identification: DVK 78-1
Depth: 57m

Classification: TK

Summary: Extremely altered, serpentine-rich tuffisitic kimberlite exhibiting microlitic textures in the groundmass.

Colour: brown
Clay Minerals: groundmass
Xenolith Abundance: lithic [10%], angular
Xenolith Size: ~1 mm
Xenolith Reaction: n/a
Olivine Replacement: pseudomorphic replacement to Cal
Pelletal Lapilli: modally 5% abundant
Autoliths: n/a
Primary Carbonate: n/a
Kimberlitic Textures: Pelletal lapilli, microlitic textures, Srp mesostasis

Modal Mineralogy:

[15%] Phenocrystal Ol, anhedral habit, pseudomorphic replacement to Cal
[10%] Macrocrystal Ol, anhedral habit, pseudomorphic replacement to Cal

Modal Mineralogy/Matrix Ratio: 25/75

Matrix/Groundmass (in order of abundance):

Srp/Clay mesostasis, Sp

Textures/Additional Information:

- Impossible to identify the primary mineralogy of the groundmass/matrix due to the alteration and replacement of the kimberlite
- Sparsely macrocrystic
- Pelletal lapilli are in very low abundance in the kimberlite
- Pelletal lapilli are cored with a Ol fragment (pseudomorphic replacement with Cal, Srp)

Sample Identification: 04GTH83
Depth: 37.8m

Classification: VK

Summary: Juvenile lapilli-bearing mud-rich volcaniclastic kimberlite.

Colour: brown
Clay Minerals: matrix/groundmass
Xenolith Abundance: lithic [15%], angular
Xenolith Size: <2mm
Xenolith Reaction: n/a
Olivine Replacement: rim alterations, pseudomorphic replacement
Pelletal Lapilli: n/a
Autoliths: n/a
Primary Carbonate: n/a
Kimberlitic Textures: Juvenile lapilli (cored and uncored), cumulate

Modal Mineralogy:

[25%] Altered angular Ol in juvenile lapillus, varying degrees of alteration
[15%] Euhedral phenocrystal and microphenocrystal Ol, severe rim alteration

Modal Mineralogy/Matrix Ratio: 55/45

Matrix/Groundmass (in order of abundance):

Clay, Srp, Sp, +/- Prv (to be confirmed by EMPA), Ap, Cal-S, altered Phl fragments

Textures/Additional Information:

- Entire section is basically juvenile lapilli in a Cal-S/clay matrix with scattered Sp
- Some lapilli is Sp-rich
- Cored and uncored lapilli
- Oxide cumulate textures are common throughout slide
- Rim alterations on the Ol are kelyphite

Sample Identification: 04GTH83
Depth: 344.5m

Classification: HK in contact with autolithic VK

Summary: Macrocrystic olivine hypabyssal kimberlite in contact with a reasonably fresh, large autolithic volcaniclastic kimberlite.

Colour: autolith: brown/grey HK: dark grey/black
Clay Minerals: autolith
Xenolith Abundance: HK- mantle (3), lithic [<5%]
Xenolith Size: 1-2mm average
Xenolith Reaction: n/a
Olivine Replacement: n/a
Pelletal Lapilli: n/a
Autoliths: heterolithic HK breccia
Primary Carbonate: n/a
Kimberlitic Textures: Autolithic, undulose extinction (i.e. strain textures), Juvenile lapilli

Modal Mineralogy:

HK: Euhedral to subhedral Ol phenocrysts, very little alteration [20%]
Anhedral Ol macrocrysts [10-15%] (some are fragmental)
Anhedral CPX macrocrysts, light green in ppl [<5%]
Autolith: Angular fragmental Ol macrocrysts and phenocrysts with Srp veins and rims [20%]; Angular, fragmental highly altered Phl laths [10%]

Matrix/Groundmass (in order of abundance):

HK: Sp and Ilm are extremely abundant in a mesostasis of Srp and lesser mud
Autolith: Cal and Clay with lesser Sp and Ilm

Textures/Additional Information:

- Contact is uneven, not sharp and autoliths of HK are shown in the autolith of VK
- HK mantle xenoliths exhibit undulose extinction, therefore strain
- The VK breccia fragments are extremely strained, and the minerals have chewed up rims

---

Sample Identification: 04GTH83
Depth: 344.5m

Classification: Contact of HK and autolithic VK

Summary: Juvenile lapilli-bearing large autolith of VK in macrocrystal olivine hypabyssal kimberlite.

Colour: grey (VK), dark grey (HK)
Clay Minerals: alteration in the VK
Xenolith Abundance: VK lithic [10%]; HK lithic [5%]
Xenolith Size: angular, size varies widely
Xenolith Reaction: bleached rims
Olivine Replacement: rim alteration and some veining
Pelletal Lapilli: n/a
Autoliths: n/a
Primary Carbonate: n/a
Microlitic Textures: n/a

Kimberlitic Textures: Juvenile lapilli (VK)- mainly anhedral Ol macrocryst fragments as the kernal, with a fine-grained mud and euhedral to subhedral microphenocrysts. Kernals are not necessarily centralized.

Modal Mineralogy:

HK- [20%] Subhedral microphenocrystal Ol, slight Srp veining + rim alteration
[20%] Subhedral phenocrystal Ol, rim alteration
[10%] Anhedral macrocrystal Ol
[5%] Anhedral macrocrystal CPX, slight alteration
[<5%] Subhedral-anhedral Phl macrocrysts (trace)

Matrix/Groundmass (in order of abundance):

HK- Sp (euhedral), Ilm (anhedral), possible Prv
VK- Cal +Sp in the groundmass

Textures/Additional Information:

- Sharp contact between the HK and the VK
- The VK is one giant autolith (this is known from analysis of the drill core), with smaller scale autoliths of HK, making it very complicated
- Some of the autoliths in the VK have small, euhedral hopper-style Ol

---

Sample Identification: 04GTH83
Depth: 344.5m

Classification: Giant autolith of VK

Summary: Relatively unaltered clast-supported dark brown volcaniclastic kimberlite.

Colour: dark brown
Clay Minerals: matrix
Xenolith Abundance: lithic, trace <5%
Xenolith Size: angular, <1mm
Xenolith Reaction: n/a
Olivine Replacement: slight Srp fracture and veins in phenocrystal Ol
Pelletal Lapilli: n/a
Autoliths: present in abundance
Primary Carbonate: n/a
Microlitic Textures: n/a
Kimberlitic Textures: clast-supported, autoliths (small) microphenocrysts set in a mud or dark brown mesostasis (Sp abundant)

Modal Mineralogy:

[40%] Euhedral to subhedral phenocrystal Ol with minimal Srp veining
[5%] Anhedral fragmental Ol- unaltered

Modal Mineralogy/Matrix Ratio: 50/50

Matrix/Groundmass (in order of abundance):

Srp/clay groundmass, Sp (rare), accicular trace Ap

Textures/Additional Information:

- Sp is abundant in autoliths
- Ol is very suitable for microprobe

Sample Identification: 04GTH83
Depth: 344.5m

Classification: VK (autolithic)

Summary: Clast-supported, juvenile lapilli-rich tuffisitic kimberlite.

Colour: brown
Clay Minerals: matrix and groundmass replacements
Xenolith Abundance: lithic [15%]
Xenolith Size: 1-2 mm
Xenolith Reaction: n/a
Olivine Replacement: Dark amorphous kelyphite rims to pseudomorphic replacement
Pelletal Lapilli: abundant (approx. 10 modal%)
Autoliths: n/a
Primary Carbonate: n/a
Kimberlitic Textures: clast-supported, juvenile lapilli

Modal Mineralogy:

[20%] Macrocrystal Ol, angular fragmental, fresh
[15%] Phenocrystal Ol, some fresh (subhedral to euhedral), some rounded anhedral pseudomorphs
+/- Phl, +/-Ilm, +/-CPX, +/-Gt

Modal Mineralogy/Matrix Ratio: 50/50

Matrix/Groundmass (in order of abundance):

Srp, Chl, Sp(all euhedral, variety of sizes)

Textures/Additional Information:

- Juvenile lapilli: extremely angular Ol fragments in a thick lapillus which contains phenocrystal slightly more rounded Ol
- One occurrence of a large CPX megacryst as a kernal in a 2 cm in diameter magmaclast. The lapillus is mainly Ol phenocrysts and microphenocrysts random in a mud matrix
- There is both cored and uncored, irregular habit juvenile lapilli

---

Sample Identification: 04GTH83
Depth: no depth

Classification: VK

Summary: Juvenile lapilli-bearing volcaniclastic kimberlite with calcite segregationary textures.

Colour: grey/brown
Clay Minerals: matrix mineralogy
Xenolith Abundance: lithic [15%]
Xenolith Size: <1mm average
Xenolith Reaction: n/a
Olivine Replacement: rims to pseudomorphic replacement (Srp+Cal)
Pelletal Lapilli: n/a
Autoliths: n/a
Primary Carbonate: n/a
Kimberlitic Textures: Juvenile lapilli, globular segregationary textures with Cal

Modal Mineralogy:

[45%] Ol phenocrysts and macrocrysts, fragmental, various forms, varying degrees of alteration
[5%] Phl phenocrysts, highly altered and rounded

Modal Mineralogy/Matrix Ratio: 65/35

Matrix/Groundmass (in order of abundance):

Sp, Cal, Clay (Sp is most abundant in the lapillus)

Textures/Additional Information:

- Globular segregationary textures are Sp-rich and have highly irregular shapes
- Juvenile lapilli are both cored and uncored
- Juvenile lapilli are irregular in habit

Sample Identification: 03T7E-03
Depth: 37.5m

Classification: VK (mVK)

Summary: Mud-rich, juvenile lapilli rich, macrocrystal poor volcaniclastic kimberlite.

Colour: dark brown
Clay Minerals: matrix
Xenolith Abundance: lithic [20%], rounded
Xenolith Size: 1-3mm
Xenolith Reaction: n/a
Olivine Replacement: pseudomorphic replacement to Cal, Srp and Clay
Pelletal Lapilli: n/a
Autoliths: n/a
Primary Carbonate: n/a
Kimberlitic Textures: Juvenile lapilli, flow banding, atoll, necklace, clast-supported

Modal Mineralogy:

[30%] Phenocrystal Ol, subhedral to anhedral habit, pseudomorphic replacement to Cal
[10%] Macrocrystal Ol, anhedral habit, pseudomorphic replacement to Cal, Srp and Clay
[10%] Extremely altered, anhedral habit, CPX, large macrocrystal and megacrystal fragments
[10%] Phl, probably lithic, flow banding, alteration between cleavage planes, flow banding is some

Modal Mineralogy/Matrix Ratio: 80/20

Matrix/Groundmass (in order of abundance):

Clay/mud, Sp, Cal-S

Textures/Additional Information:

- The primary mineralogy of the entire slide is very difficult to distinguish because of the alteration and replacement of the kimberlite
- Unpolished section
- Cored and uncored Juvenile lapilli
- Atoll Sp is the kernal of a small Juvenile lapilli

Sample Identification: 03-T19-04
Depth: 85.5m

Classification: HK

Summary: Altered, sparsely macrocrystic, lithic-rich oxide hypabyssal kimberlite.

Colour: brown
Clay Minerals: alteration in matrix
Xenolith Abundance: lithic [10%]
Xenolith Size: 1 mm
Xenolith Reaction: n/a
Olivine Replacement: Srp veins to complete pseudomorphs
Pelletal Lapilli: n/a
Autoliths: present as 5% modal
Primary Carbonate: n/a
Kimberlitic Textures: sparsely macrocrystic, necklace textures, cumulate textures, atoll Sp textures

Modal Mineralogy:

[30%] Phenocrystal Ol, veins to pseudomorphic replacement, subhedral
[10%] Macrocrystal Ol, veins to pseudomorphic replacement, anhedral (rounded)
[10%] Phenocrystal Phl with significant flow banding, slight alterations
[5%] CPX, anhedral

Modal Mineralogy/Matrix Ratio: 65/35

Matrix/Groundmass (in order of abundance):

Srp, clay, Chl, Cal-S, Sp (necklace, cumulate and atoll textures), Phl, Prv, Ap

Textures/Additional Information:

- Oxides are found to occur in association with pseudomorphed Ol
- Secondary fractures infilled with Cal-S
- Prv suitable for U-Pb dating

Sample Identification: 94-T31-1
Depth: 26.5m

Classification: HK

Summary: Altered HK with extreme necklace textures around phenocrystal and microphenocrystal mineralogy.

Colour: green/grey
Clay Minerals: alteration of phenocrysts
Xenolith Abundance: lithic [10%]
Xenolith Size: <1 mm
Xenolith Reaction: bleached Srp and Chl rims
Olivine Replacement: Clay/Srp
Pelletal Lapilli: n/a
Autoliths: n/a
Primary Carbonate: n/a
Kimberlitic Textures: necklace, oxide cumulates, segregationary textures with Cal, macrocryst-poor

Modal Mineralogy:

[30%] Ol phenocrysts and microphenocrysts, pseudomorphic replacement with Clay-Srp+/-Chl, rounded anhedral

Modal Mineralogy/Matrix Ratio: 40/60

Matrix/Groundmass (in order of abundance):

Srp+Chl+Cal, Sp (in both coarse necklace textures and independently), Atoll Sp

Textures/Additional Information:

- Extreme necklace textures
- The rest of the mineralogy is petrographically indistinguishable due to the alteration of the kimberlite
- Sp is suitable for compositional analysis via EMPA

Sample Identification: 94-T31-1
Depth: 26.5m

Classification: HK

Summary: Extremely altered, macrocryst-poor, matrix-supported phlogopite olivine hypabyssal kimberlite.

Colour: grey
Clay Minerals: n/a
Xenolith Abundance: lithic, angular, trace [<5%]
Xenolith Size: n/a
Xenolith Reaction: n/a
Olivine Replacement: Srp rims and veins
Pelletal Lapilli: n/a
Autoliths: n/a
Primary Carbonate: groundmass/matrix
Kimberlitic Textures: necklace textures with Sp and Prv, atoll Sp, matrix-supported

Modal Mineralogy:

[30%] Phenocrystal Ol, subhedral, pseudomorphed and commonly rimmed by a necklace of Sp +/- Prv
[10%] Macrocrystal Ol, anhedral, pseudomorphed and cryptocrystalline

Modal Mineralogy/Matrix Ratio: 45/55

Matrix/Groundmass (in order of abundance):

Cal, Srp, euhedral Sp, [5%] atoll Sp, Ap, Phl (small laths with alteration between the cleavage planes), Prv (light brown euhedral)

Textures/Additional Information:

- Extreme necklace textures throughout entire section
- Matrix-supported
- Macrocryst-poor
- Prv is anhedral (rounded) and many occur with a thick dark rim, therefore may not be suitable for emplacement ages

---

Sample Identification: 94-T31-1
Depth: 27m

Classification: HK

Summary: Macrocryst-poor, serpentine-rich hypabyssal kimberlite, exhibiting extreme alteration and a mud-rich matrix.

Colour: brown
Clay Minerals: matrix as alteration
Xenolith Abundance: lithic [5%], angular
Xenolith Size: ~1mm
Xenolith Reaction: n/a
Olivine Replacement: Pseudomorphic replacement by Cal
Pelletal Lapilli: n/a
Autoliths: possible (1 single occurrence)
Primary Carbonate: n/a
Kimberlitic Textures: macrocryst-poor, matrix-supported

Modal Mineralogy:

[25%] Phenocrystal Ol, anhedral, pseudomorphic replacement with Cal
[10%] Macrocrystal Ol, anhedral, pseudomorphic replacement with Cal

Modal Mineralogy/Matrix Ratio: 40/60

Matrix/Groundmass (in order of abundance):

Clay, Abundant Sp: coarse, euhedral; Cal-S, Srp, Chl, +/- Prv.
Most of the primary mineralogy is petrographically indistinguishable due to the alteration of the kimberlite.

Textures/Additional Information:

- Macrocrystal Ol and phenocrystal Ol exhibit microcrystalline rims
- Macrocryst-poor, matrix-supported, mud-rich
- Thick, dark matrix- petrographically indistinguishable

Sample Identification: 94-T31-1
Depth: 29m

Classification: HK

Summary: Extremely altered, macrocryst-poor serpentine and oxide-rich hypabyssal kimberlite.

Colour: black/grey
Clay Minerals: n/a
Xenolith Abundance: n/a
Xenolith Size: n/a
Xenolith Reaction: n/a
Olivine Replacement: Cal
Pelletal Lapilli: n/a
Autoliths: n/a
Primary Carbonate: groundmass/matrix mineralogy
Kimberlitic Textures: Atoll Sp, partial Sp necklaces, macrocryst-poor

Modal Mineralogy:

[35%] Phenocrystal Ol, pseudomorphed to Cal, anhedral to subhedral. In addition, some are rimmed with thick Srp.
[20%] Macrocrystal Ol, pseudomorphed to Cal, anhedral.

Modal Mineralogy/Matrix Ratio: 55/45

Matrix/Groundmass (in order of abundance):

Euhedral Sp, Atoll Sp, Srp-rich groundmass +/- Cal, possible euhedral-subhedral brown/orange perovskite, Ap

Textures/Additional Information:

- Multiple generations of Srp in and interstitial to the groundmass and matrix mineralogy.
- It is difficult to distinguish some of the primary mineralogy due to the extensive alteration of the kimberlite.

Sample Identification: 93-T32-01
Depth: 97.8 m

Classification: RVK

Summary: A mud-rich resedimented volcaniclastic kimberlite with indistinguishable mineralogy and 15% lithic fragments.

Colour: dark brown
Clay Minerals: majority of section [80%]
Xenolith Abundance: lithic [15%]

Xenolith Size: 1-2 mm
Xenolith Reaction: n/a
Olivine Replacement: pseudomorphed, clay
Pelletal Lapilli: n/a
Autoliths: n/a
Primary Carbonate: n/a
Kimberlitic Textures: segregationary textures

Modal Mineralogy:

[25%] Subhedral to anhedral Ol microphenocrysts, pseudomorphic replacement
[10%] Anhedral Ol macrocrysts, pseudomorphic replacement with clay

Modal Mineralogy/Matrix Ratio: 50/50

Matrix/Groundmass (in order of abundance):

Mud with segregationary textures

Textures/Additional Information:

- Thin section mineralogy is indistinguishable (both the modal minerals and the matrix/groundmass)
- Unpolished section

Sample Identification: 93-T32-01
Depth: 100 m

Classification: RVK

Summary: A mud-rich resedimented volcaniclastic kimberlite containing completely altered minerals, most of which are indistinguishable.

Colour: brown
Clay Minerals: alteration [80%]
Xenolith Abundance: lithic [10%]
Xenolith Size: 1-2 mm
Xenolith Reaction: n/a
Olivine Replacement: pseudomorphed to clay + Srp
Pelletal Lapilli: n/a
Autoliths: n/a
Primary Carbonate: n/a
Microlitic Textures: n/a
Kimberlitic Textures: Juvenile lapilli, difficult to discern from remaining sample

Modal Mineralogy:

[35 %] Subhedral Ol macrocrysts and phenocrysts, pseudomorphic replacement
[<5%] CPX, altered rims and highly fractured
[<5%] Phl, very dark brown in ppl, heavily altered to clay

Modal Mineralogy/Matrix Ratio: 55/45

Matrix/Groundmass (in order of abundance):

Muddy matrix, containing Cal/clay/Srp

Textures/Additional Information:

- Unpolished thick section
- heavily fractured sample
- most primary mineralogy is indistinguishable

Sample Identification: 93-T32-01
Depth: 100.2m

Classification: VK

Summary: Juvenile lapilli-bearing, clast-supported volcaniclastic kimberlite.

Colour: brown
Clay Minerals: alteration in matrix mineralogy
Xenolith Abundance: lithic [15%]
Xenolith Size: 1-3 mm
Xenolith Reaction: n/a
Olivine Replacement: Srp veins and fractures to complete pseudomorphic replacement
Pelletal Lapilli: n/a
Autoliths: n/a
Primary Carbonate: n/a
Microlitic Textures: n/a
Kimberlitic Textures: necklace Sp textures, Juvenile lapilli, clast-supported

Modal Mineralogy:

[30%] Macrocrystal angular and fragmental Ol, veins to pseudomorphic replacement with Srp
[10%] Phenocrystal angular and fragmental Ol, veins to pseudomorphic replacement with Srp

Modal Mineralogy/Matrix Ratio: 55/45

Matrix/Groundmass (in order of abundance):

Clay, Srp, Sp (atoll and necklace textures), Chl
The rest of the mineralogy is petrographically indistinguishable due to the extreme alteration of the kimberlite.

Textures/Additional Information:

- Clast-supported
- Select juvenile lapilli are spherical and contain an subhedral Ol kernal surrounded by a fine-grained mud-rich lapillus. The lapilli throughout the thin section are of varying thicknesses
- Other juvenile lapilli are slightly irregular with 2 kernals

---

Sample Identification: T33
Depth: 76 m

Classification: HK

Summary: A highly altered, sparsely macrocrystic, segregationary textured oxide-rich hypabyssal kimberlite.

Colour: grey
Clay Minerals: n/a
Xenolith Abundance: n/a
Xenolith Size: n/a
Xenolith Reaction: n/a
Olivine Replacement: Srp and Cal, partial to completely pseudomorphed
Pelletal Lapilli: n/a
Autoliths: n/a
Primary Carbonate: present in groundmass mineralogy
Kimberlitic Textures: Cal segregationary, Atoll Sp, necklace textures

Modal Mineralogy:

[35%] Completely pseudomorphed anhedral to subhedral macrocrystal Ol
[5%]Anhedral Ilm, alteration at rims of grains

Modal Mineralogy/Matrix Ratio: 40/60

Matrix/Groundmass (in order of abundance):

Primary Cal rhombs, necklace textures with Sp, Atoll Sp, Phl, Prv, Chl, Srp

Textures/Additional Information:

- Extreme alteration prevents distinguishing primary mineralogy
- The Phl present in the thin section could be lithic fragments
- The matrix mineralogy is all present in a Cal-Srp-Chl mesostasis

---

Sample Identification: T33
Depth: 79.8 m

Classification: HK

Summary: Extremely altered sparsely macrocrystic hypabyssal kimberlite, exhibiting calcite segregationary textures.

Colour: green/brown
Clay Minerals: n/a
Xenolith Abundance: trace lithic [5%]
Xenolith Size: ~2 mm
Xenolith Reaction: n/a
Olivine Replacement: Srp, Cal – phenocrysts only
Pelletal Lapilli: n/a
Autoliths: n/a
Primary Carbonate: n/a
Kimberlitic Textures: Cal segregationary, secondary Cal veins/infilled fractures

Modal Mineralogy:

[25%] Anhedral pseudomorphed macrocrystal Ol
[15%] Macrocrystal Phl, alteration present on rim
[10%] Anhedral phenocrystal Ol, ranging from Srp veins to completely pseudomorphed

[5%]Ilm phenocrysts, [trace]

Modal Mineralogy/Matrix Ratio: 60/40

Matrix/Groundmass (in order of abundance):

Cal-S, Atoll Sp, necklace textured Sp + Prv, Phl

Textures/Additional Information:

- Some matrix mineralogy too small to identify without the probe.
- Extremely altered, difficult to determine primary mineralogy
- Extremely large atoll Sp
- Sp and Prv cumulate zones are very present
- Thin section suitable for the probe

Sample Identification: T33
Depth: 81m

Classification: HK

Summary: Extremely altered dark brown phenocrystic hypabyssal kimberlite, featuring necklace textures of Sp surrounding Ol phenocrysts.

Colour: brown
Clay Minerals: n/a
Xenolith Abundance: n/a, trace lithic fragments [5%]
Xenolith Size: n/a
Xenolith Reaction: n/a
Olivine Replacement: Srp, Cal, Chl, mud
Pelletal Lapilli: possible
Autoliths: n/a
Primary Carbonate: +/- Cal rhombs
Kimberlitic Textures: Cal-Srp segregationary textures, necklace oxide/Sp, Atoll Sp

Modal Mineralogy:

[35%] Euhedral Ol phenocrysts, partial to pseudomorphic replacement
[10%] Phl laths, alteration between cleavage planes

Modal Mineralogy/Matrix Ratio: 50/50

Matrix/Groundmass (in order of abundance):

Srp, Cal-S, abundant Sp (atoll, necklace), Ap, Ilm, Prv

Textures/Additional Information:

- Too altered to distinguish the macros (too few) and the phenocrysts
- Prv confirmed
- Essentially macrocryst-free thin section

Sample Identification: T33

Depth: 110 m

Classification: HK

Summary: A matrix supported, segregationary textured, oxide hypabyssal kimberlite, exhibiting extreme necklace textures.

Colour: grey
Clay Minerals: alteration (macrocrystal Ol)
Xenolith Abundance: lithic [<5%]
Xenolith Size: range in sizes, fragmental
Xenolith Reaction: n/a
Olivine Replacement: Srp, clay
Pelletal Lapilli: present
Autoliths: n/a
Primary Carbonate: n/a
Microlitic Textures: present, unknown mineralogy
Kimberlitic Textures: Matrix supported, Cal segregationary textures (in sections), necklace textures with Sp, Sp atoll textures

Modal Mineralogy:

[25%] Anhedral partially serpentinized Ol macrocrysts
[25%] Euhedral to subhedral Ol phenocrysts (pseudomorphic replacement)

Modal Mineralogy/Matrix Ratio: 55/45

Matrix/Groundmass (in order of abundance):

Cal (sec), Ap (acicular), Sp, Prv, Srp

Textures/Additional Information:

- Cumulate textures with the Sp group minerals
- Extreme necklace textures with the oxide group minerals
- Accicular Ap is present, interpreted to represent quenching of groundmass
- Excellent thin section for EMPA of Sp group

Sample Identification: T-146
Depth: unknown

Classification: HK

Summary: An extremely altered macrocrystic phlogopite oxide hypabyssal kimberlite exhibiting slight flow banding.

Colour: brown
Clay Minerals: present as alteration minerals
Xenolith Abundance: lithic xenoliths [50%]
Xenolith Size: entire range
Xenolith Reaction: rim
Olivine Replacement: completely pseudomorphs, Cal- Srp
Pelletal Lapilli: n/a
Autoliths: n/a

Primary Carbonate: segregations
Kimberlitic Textures: necklace textures Sp surrounding various phenocrysts

Modal Mineralogy:

[10%] Macrocrystic + phenocrystic Ol pseudomorphs, anhedral to subhedral
[5%] Altered Phl laths

Modal Mineralogy/Matrix Ratio: 65/35

Matrix/Groundmass (in order of abundance):

Srp- rich matrix, Atoll Sp, Clay

Textures/Additional Information:

- Possibility of Prv
- Primary mineralogy too difficult to distinguish due to alteration of kimberlite

---

Sample Identification: 95-T237
Depth: 29.7m

Classification: HK

Summary: Sparsely macrocrystic calcite hypabyssal kimberlite exhibiting a cryptocrystalline groundmass.

Colour: grey
Clay Minerals: alteration in the macrocrystal mineralogy
Xenolith Abundance: lithic (trace) [<5%]
Xenolith Size: n/a
Xenolith Reaction: n/a
Olivine Replacement: Cal pseudomorphic replacement
Pelletal Lapilli: n/a
Autoliths: n/a
Primary Carbonate: groundmass mineralogy
Kimberlitic Textures: aphanitic; sparsely macrocrystic, accicular, cryptocrystalline groundmass

Modal Mineralogy:

[50%] Phenocrystal and microphenocrystal Ol, varying degrees of habit and alteration
[<5%] Macrocrystal (2!) anhedral (rounded) Ol, pseudomorphic replacement to Cal
[<5%] Macrocrystal (1!) anhedral CPX, extremely altered

Modal Mineralogy/Matrix Ratio: 65/35

Matrix/Groundmass (in order of abundance):

Extremely fine-grained Srp and Cal groundmass.
Euhedral Sp [20%] and possible Prv (to be confirmed by EMPA), accicular Ap.

Textures/Additional Information:

- Only 3 macrocrysts in entire section, therefore interpreted as essentially aphanitic

- Accicular growth of Ap is an indication of quenching crystallization

---

Sample Identification: 95-T237-01
Depth: 31m

Classification: HK

Summary: Extremely altered, macrocryst-poor, calcite-rich hypabyssal kimberlite exhibiting segregationary textures with Cal.

Colour: grey
Clay Minerals: n/a
Xenolith Abundance: n/a
Xenolith Size: n/a
Xenolith Reaction: n/a
Olivine Replacement: Pseudomorphic replacement with Cal and Srp
Pelletal Lapilli: n/a
Autoliths: n/a
Primary Carbonate: n/a
Kimberlitic Textures: segregationary textures with Cal, Atoll Sp, necklace textures, oxide cumulates

Modal Mineralogy:

[20%] Phenocrystal Ol, pseudomorphic replacement with Cal
[10%] Phl phenocrysts, extremely altered
[10%] Macrocrystal Ol, pseudomorphic replacement with Cal

Modal Mineralogy/Matrix Ratio: 40/60

Matrix/Groundmass (in order of abundance):

Cal, Sp (atoll), Prv, Ap, Phl (small bladed, altered), Cal segregationary textures

Textures/Additional Information:

- Very low crustal contamination
- Increased amt of Phl phenocrysts for Diavik HK
- Very poorly polished sections
- The necklace textures have very fine-grained oxides

Sample Identification: 95-T237-01
Depth: 31m

Classification: HK

Summary: Extremely altered sparsely macrocrystic, matrix-supported spinel olivine hypabyssal kimberlite.

Colour: grey/brown

Clay Minerals: n/a
Xenolith Abundance: lithic [10%]
Xenolith Size: 1-2mm
Xenolith Reaction: n/a
Olivine Replacement: Pseudomorphic replacement by Cal
Pelletal Lapilli: n/a
Autoliths: n/a
Primary Carbonate: Possible in groundmass
Kimberlitic Textures: necklace, atoll, macrocrystal-poor, matrix-supported

Modal Mineralogy:

[30%] Subhedral Ol phenocrysts- pseudomorphic replacement by Cal-S
[10%] Subhedral Ol macrocrysts- pseudomorphic replacement by Cal-S

Modal Mineralogy/Matrix Ratio: 50/50

Matrix/Groundmass (in order of abundance):

Sp (variety of sizes scattered throughout the groundmass, mainly euhedral), Atoll Sp, Srp, Cal, euhedral Ap, +/-Prv

Textures/Additional Information:

- Extreme alteration
- Macrocryst-poor, matrix-supported
- Atoll Sp have larger moats that normally observed in atoll Sp in magmatic kimberlite

---

Summary of Petrographic Analysis
Diavik Kimberlites

Kimberlite A2

One thin section was studied with this particular drill hole (151.0m). This kimberlite is classified as an altered, crustal-rich tuffisitic kimberlite exhibiting calcite segregationary textures. This sample exhibits a very high degree of alteration, proving it very difficult to distinguish the primary mineralogy of the kimberlite (containing approximately 40% crustal fragments).

Kimberlite A4

Four thin sections were studied, varying from depths of 138.4m to 179m. All samples are classified as either macrocrystic or sparsely macrocrystic, spinel-rich hypabyssal kimberlite exhibiting calcite and serpentine segregationary textures. The samples exhibit a range of alteration, from moderate (Srp veining, secondary calcite in the matrix) to extremely altered (pseudomorphic replacement of entire macrocrystal and phenocrystal population). The extremely altered HK also contains a high abundance of crustal material.

Kimberlite A5

Seven thin sections were found to be suitable for petrographic analyses. The depth range of the samples is from 127 to 150m. All samples are classified as a calcite oxide macrocrystal

hypabyssal kimberlite, exhibiting both segregationary textures (with calcite) and uniform textures. The samples have low to moderate alteration, and high abundances of lithic fragments (similar to other Diavik hypabyssal kimberlite samples studied).

Kimberlite A11

Four thin sections were studied, varying from depths of 113.4m to 119m. Three samples are classified as volcaniclastic kimberlite, and one as resedimented volcaniclastic kimberlite. All of the kimberlites are clast-supported, and are heavily altered, with the primary mineralogy being completely masked by the alteration and replacement minerals. Juvenile lapilli is present in all samples, as irregular forms that are both cored and uncored.

Kimberlite A44

A single thin section at a depth of 172m was available for petrographic purposes. Kimberlite A44 is classified as a sparsely macrocrystic olivine-rich hypabyssal kimberlite exhibiting very little alteration.

Kimberlite A154

A total of 17 thin sections were studied, ranging from depths of 110m to approximately 250m. Both drill core and open pit samples were utilized for petrography. All samples are classified as volcaniclastic kimberlite, with four particular samples being further classified as resedimented volcaniclastic kimberlite (RVK). The kimberlite is olivine and mud rich (oVK and mVK, respectively). Juvenile lapilli is abundant in the A154 kimberlite, present as both cored and uncored, and spherical to elongate in habit. Mantle xenoliths are known to be abundant in the A154 kimberlite, however, few are identifiable at the microscopic level. Lithic fragments are commonly found occurring in the kimberlite, varying greatly in size and form. The A154 kimberlite exhibits a wide variation in alteration. Pyrope garnet is found to be a commonly occurring accessory mineral in the A154 kimberlite samples.

Kimberlite A180

Four thin sections were found to be suitable for petrographic analyses, with depths varying from 85m to 226m. The A180 kimberlite is separated into two classifications: volcaniclastic kimberlite at depths from 85m to 100m, and tuffisitic kimberlite breccia (226m). All samples are very heavily altered, and most of the primary mineralogy is indistinguishable by petrographic methods. The volcaniclastic samples have abundant juvenile lapilli, and are most commonly macrocrystal olivine-bearing (oVK). The tuffisitic kimberlite breccia contains pelletal lapilli and is clast-supported. The pelletal lapilli have macrocrystal olivine (anhedral habit) as the kernal.

Kimberlite A418

Two thin sections were found to be suitable for petrographic analysis, with depths of 377m and 380m. Both sections are classified as volcaniclastic kimberlite (VK). The kimberlite is highly fragmental, and contains numerous magmaclasts of juvenile lapilli which are mostly uncored. Phlogopite is identified in the kimberlite, exhibiting flow-banding textures (interpreted as plastic deformation). The A418 kimberlite is clast-supported and has a moderate degree of alteration.

Kimberlite A840

A single thin section at a depth of 130m was used for petrography. The kimberlite is formally classified as a juvenile lapilli-bearing volcaniclastic kimberlite, exhibiting segregationary textures with serpentine, as well as flow-banding textures with phlogopite mica.

Kimberlite 841

A total of nine thin sections, with depths ranging from 119m to 167m were utilized for petrography. All samples are classified as volcaniclastic kimberlite (VK), with one sample further classified as resedimented volcaniclastic kimberlite (RVK). The samples are found to be moderately to heavily altered. All samples from kimberlite 841 contain both cored and uncored juvenile lapilli. Select samples exhibit globular segregationary textures with serpentine and clay, as well as necklace and cumulate textures with spinel-group minerals.

Kimberlite A1039

Four thin sections were studied, with a depth range of 67m to 75m. Kimberlite A1039 varies greatly with increasing depth. At 67m and 69.2m, the kimberlite is classified as a tuffisitic kimberlite (TK). Pelletal lapilli are abundant, and both samples are extremely altered masking any primary mineralogy. At 72m, the kimberlite is classified as tuffisitic kimberlite breccia (TKB), due to the angular and fragmental nature of the minerals and clasts, as well as the aggressive clay replacement of the rock. At 75m, the kimberlite is classified as a sparsely macrocrystic, oxide-rich hypabyssal kimberlite. The variation observed in this set of samples from kimberlite A1039 does not necessarily imply genetic changes with depth, as it could be large autolithic material that was sampled, or a more complex situation involving kimberlitic dykes and sills.

Kimberlite A1245

Four thin sections were chosen for petrography, with depths ranging from 45.5m to 70m. All samples are classified as volcaniclastic kimberlite (VK), and two are further sub-classified as resedimented volcaniclastic kimberlite (RVK). All samples are clay-rich and highly altered (masking most primary mineralogy). Juvenile is present in moderate abundances, as both core and uncored, rounded and irregular in habit. Macrocrystal and phenocrystal mineralogy (mostly olivine, therefore can be properly classified as oVK), is highly fragmental and displays pseudomorphic replacement with serpentine, secondary calcite and clay. Some phlogopite exhibits flow banding, interpreted as a plastic deformation texture. Samples from kimberlite A1245 are crustal-rich.

Kimberlite A1620

Two thin sections were available, with depths of 69.5m and 71.0m. The samples are formally classified as volcaniclastic kimberlite and resedimented volcaniclastic kimberlite, respectively. Both are extremely altered, and contain a very low abundance of magmaclasts. Phlogopite is abundant in both samples, and commonly displays flow banding. Olivine macrocrysts are highly fragmental.

Kimberlite A1621

One single sample of kimberlite A1621 was available at a depth of 50.2m. The kimberlite is classified as a mud-rich, matrix-supported resedimented volcaniclastic kimberlite (RVK). Juvenile lapilli is present, lobate, and cored with macrocrystal olivine that has undergone varying degrees of alteration, ranging from rare serpentine veins to pseudomorphic replacement with serpentine and secondary calcite.

Kimberlite ABZ

Three thin sections from kimberlite ABZ were chosen for petrographic analyses, with unknown depths. The kimberlite is classified as mud-rich volcaniclastic kimberlite (mVK) and one section is further classified to a resedimented volcaniclastic kimberlite (RVK). All thin

sections display extreme alteration, and most of the primary mineralogy is replaced with clay and mud. Juvenile lapilli are present in moderate abundance, and are elongate and cored with olivine and clinopyroxene.

Kimberlite ANIK

Two samples at a depth of 232.74m was available from ANIK. The kimberlite is classified as an olivine-rich volcaniclastic kimberlite (oVK). Both samples are extremely altered kimberlite, with high abundances of clay and serpentine found in the matrix as replacement. The juvenile lapilli is abundant and cored with fragments of olivine macrocrysts.

Kimberlite DD

One single sample was available at a depth of 39.5m (No further thin sections could be successfully cut due to the clay alteration and replacement of the kimberlite). This sample is classified as an olivine-rich, juvenile lapilli-bearing volcaniclastic kimberlite (oVK).

Kimberlite GTH

Six samples of kimberlite GTH were studied with depths ranging from 37.8m to 344.5m. The sample at 37.8m is classified as a mud-rich volcaniclastic kimberlite (mVK) that contains both cored and uncored abundant juvenile lapilli. This sample is heavily altered. The samples at greater depths are classified as macrocrystal olivine hypabyssal kimberlite in contact with an altered large, autolithic volcaniclastic kimberlite. The juvenile lapilli in the autolithic volcaniclastic kimberlite are cored with fresh macrocrystal olivine.

Kimberlite T19

A single sample of kimberlite T19 (depth, 85.5m) was studied (No further thin sections could be successfully cut due to alteration of the kimberlite). This sample is classified as a heavily altered, sparsely macrocrystic, crustal-rich oxide hypabyssal kimberlite. The oxides within this sample displayed cumulate, atoll and necklace textures with the macrocrystal population of the kimberlite.

Kimberlite T31

Four samples of kimberlite T31 were studied with a small depth range of 26.5m to 29m. The kimberlite is classified as extremely altered, sparsely macrocrystic, serpentine oxide hypabyssal kimberlite. The samples are matrix-supported and contained a notable abundance of phlogopite.

Kimberlite T32

Three samples of kimberlite at depths ranging from 97.8m to 100.2m were utilized for petrography. One sample is classified as an olivine-bearing volcaniclastic kimberlite, and the two remaining samples are further classified as resedimented volcaniclastic kimberlite. All samples are found to be clast-supported with a clay matrix. Juvenile lapilli are present, exhibiting spherical and lobate form. The samples are very altered, proving it very difficult to discern any of the primary mineralogy (especially in the matrix of the kimberlite).

Kimberlite T33

Four samples were studied from kimberlite T33, with a depth range of 76m to 110m. The kimberlite is classified as a highly altered, sparsely macrocrystic, oxide hypabyssal kimberlite exhibiting segregationary textures with serpentine and calcite. The calcite displays rhombic form, providing evidence for the presence of primary calcite. The spinel group minerals are

found to occur in extreme necklace textures, surrounding the entire macrocrystal and phenocrystal population of the kimberlite. Perovskite is also notably abundant in the matrix of this kimberlite.

Kimberlite T146

A single sample of kimberlite T146 was available for study (unknown depth). This sample is classified as an extremely altered, macrocrystal phlogopite oxide hypabyssal kimberlite exhibiting slight flow orientation.

Kimberlite T237

Three samples with a limited depth range of 29.7m to 31m were utilized. The samples are collectively classified as an extremely altered, sparsely macrocrystic, matrix-supported oxide olivine hypabyssal kimberlite, exhibiting calcite segregationary textures.
This kimberlite is considered to be essentially aphanitic, due to the extremely low abundance of macrocrystal minerals.

Kimberlite T7E

Due to the extreme alteration and replacement (clay) of kimberlite T7E, only one thin section was able to be prepared (unpolished) (37.5m). This kimberlite is classified as a mud-rich, juvenile lapilli-rich, macrocrystal-poor volcaniclastic kimberlite (oVK). The juvenile lapilli are found to be both cored and uncored.

Kimberlite C53

Due to the extreme alteration and replacement of kimberlite C53, only a few sections were able to be prepared (unpolished) (49m). Kimberlite C53 is classified as a juvenile lapilli-bearing, highly fragmental, altered volcaniclastic kimberlite exhibiting globular segregationary textures.

Kimberlite DVK

One single sample was available for petrographic purposes (due to alteration and replacement with clay) (57m). Kimberlite DVK is classified as an extremely altered, serpentine-rich tuffisitic kimberlite (TK) exhibiting microlitic textures in the groundmass. Pelletal lapilli is rare, found to occur in <5% modal abundance.

Kimberlite C42

One single sample was available for petrographic purposes (due to alteration and replacement with clay) (66.5m). This kimberlite is classified as a highly fractured, tuffisitic kimberlite breccia (TKB) exhibiting globular segregationary textures in the matrix. No magmaclasts are found to be present in this sample.

Kimberlite A21

One single sample was available for petrographic study (due to alteration and replacement with clay) (181.0m). This kimberlite is classified as a juvenile lapilli-bearing, flow-banded, olivine volcaniclastic kimberlite (oVK). The minerals and clasts are surrounded in a mesostasis of serpentine and clay.

Kimberlite C27

One single sample was available for petrographic study (due to alteration and replacement with clay) (111.9m). Kimberlite C27 is classified as a juvenile lapilli-bearing, olivine volcaniclastic

kimberlite (oVK). The juvenile lapilli are highly irregular (globular) forms. The oxide minerals in the matrix are found to exhibit both necklace and cumulate textures.

Petrographic Images: Diavik kimberlites
Slide #1

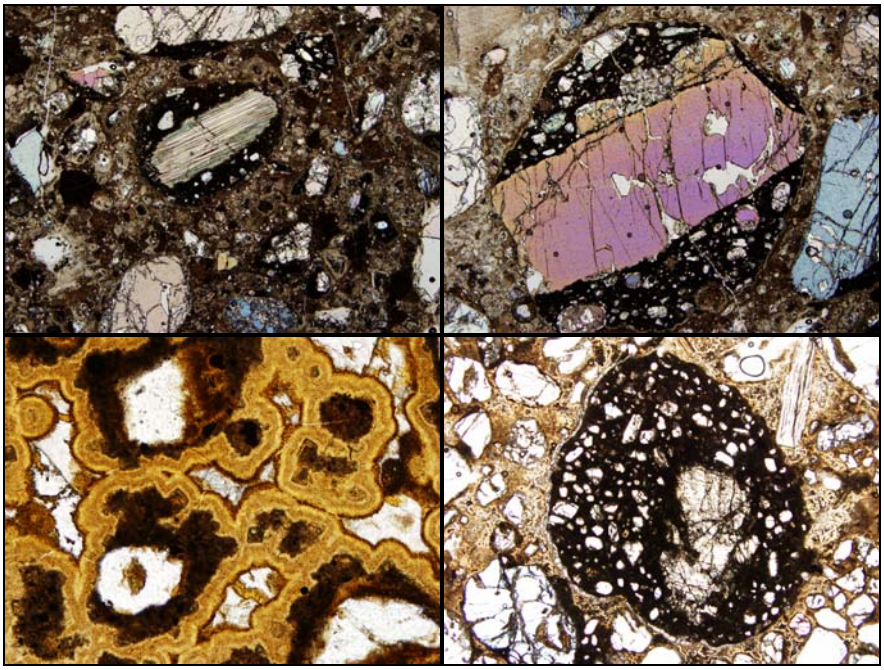

Top-Left: Diavik kimberlite A5, Field of view = 8mm, Cross polarized light

Description: Magmaclast containing altered phlogopite core. Moderately altered olivine in a serpentine and calcite groundmass.

Top-Right: Diavik kimberlite A5, Field of view = 8mm, Cross polarized light

Description: Magmaclast containing fragmental clinopyroxene core. Moderately altered olivines and oxides in a calcite groundmass.

Bottom-Left: Diavik kimberlite A154S, Field of view = 1mm, Plane polarized light

Description: Serpentine segregationary textures surrounding olivine pseudomorphs. Secondary calcite is interstitial to the serpentine.

Bottom-Right: Diavik kimberlite A154S, Field of view = 1mm, Plane polarized light

Description: Small autoliths found in a moderately altered kimberlite. Kimberlite matrix includes anhedral, serpentinized microphenocrystal olivine grains in a mud/clay and secondary calcite groundmass. Altered phlogopite laths are also present in the kimberlite matrix. The autolith contains a highly altered clinopyroxene fragments along with moderately fresh microphenocrystal olivines in an oxide matrix.

Petrographic Images: Diavik kimberlites
Slide #2

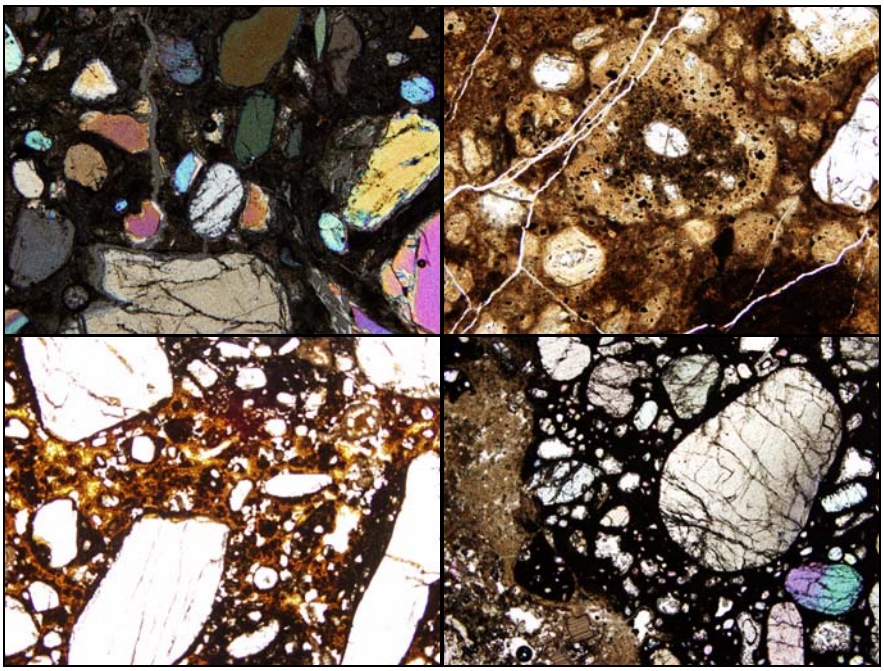

Top-Left: Diavik kimberlite A418, Field of view = 2.1mm, Cross polarized light

Description: Hypabyssal kimberlite showing various microphenocrystal and phenocrystal olivines. Some olivines are euhedral and show no signs of alteration, others are fragmental, anhedral and subhedral. Matrix and groundmass is dominated by oxides. A fracture running through the image has been infilled with secondary calcite.

Top-Right: Diavik kimberlite A841, Field of view = 2.1 mm, Plane polarized light

Description: Highly altered kimberlite showing altered magmaclast with olivine core. The larger spinel group minerals appear to be more abundant in the magmaclast. Most of the matrix and groundmass is serpentinized and pseudomorphed with clay.

Bottom-Left: Diavik kimberlite A841, Field of view = 2.1 mm, Plane polarized light

Description: Larger altered and fractured olivine phenocrysts surrounded by a matrix of fragmental olivine and phlogopite. Heavy serpentinization of the groundmass in segregationary textures with abundant spinels and oxides.

Bottom-Right: Diavik kimberlite GTH, Field of view = 4mm, Cross polarized light

Description: Contact of volcaniclastic kimberlite with hypabyssal kimberlite. Anhedral olivines are present as phenocrysts, microphenocrysts and fragments.

Diavik Kimberlites: Whole Rock Geochemistry

	SiO_2	Al_2O_3	$Fe_2O_{3(T)}$	MnO	MgO	CaO	Na_2O	K_2O	TiO_2	P_2O_5	LOI	Total
	%	%	%	%	%	%	%	%	%	%	%	%
Detection Limit	0.01	0.01	0.01	0.001	0.01	0.01	0.01	0.01	0.001	0.01		0.01
Method	FUS-ICP	FUS-ICP	FUS-ICP	FUS-ICP	FUS-ICP	FUS-ICP	FUS-ICP	FUS-ICP	FUS-ICP	FUS-ICP	FUS-ICP	FUS-ICP
ABZ-7a	46.26	6.94	6.25	0.12	16.66	4.93	0.19	3.23	0.959	0.45	14.36	100.30
A418-21 377m	38.29	2.05	7.73	0.11	40.48	3.05	0.13	0.53	0.438	0.16	7.346	100.30
94C42-2 89.50m	43.40	7.70	5.81	0.10	13.10	5.79	0.19	3.56	0.853	0.33	17.71	98.53
94C42-2 179m	44.47	8.11	5.81	0.10	12.97	5.45	0.31	3.29	0.790	0.33	18.40	100.00
00A4-05 179m	31.59	2.14	7.79	0.16	34.61	8.15	0.17	1.08	0.504	0.69	12.90	99.77
00A4-05 138.4m	29.70	2.03	6.60	0.14	27.89	15.23	0.17	2.45	0.424	0.58	14.62	99.85
00A4-05 139.0m	33.76	2.74	6.56	0.15	28.96	10.13	0.22	2.59	0.422	0.68	12.88	99.09
00A4-05 139.20m	32.73	2.33	7.59	0.15	33.12	10.16	0.13	1.49	0.469	0.60	11.81	100.60
94-A5-01 60.50m	35.50	4.73	6.16	0.28	16.18	11.46	0.15	2.18	0.442	0.64	21.27	98.99
94-A5-01 53.10m	29.76	4.77	6.88	0.15	24.38	14.03	0.48	2.26	0.528	0.68	14.69	98.61
94-A5-01 150.10m	27.31	2.77	7.21	0.15	27.41	14.84	0.10	1.7	0.532	0.70	15.96	98.69
94-A5-01 149.30m	44.46	7.91	5.61	0.10	13.21	5.50	0.28	3.23	0.685	0.33	18.10	99.40
94-A5-01 148.40m	31.08	3.50	8.92	0.19	28.41	10.29	0.10	1.71	0.717	0.90	13.19	99.02
03A1620-02 71.0m	42.62	5.03	6.38	0.10	25.50	3.71	0.10	1.46	0.387	0.34	15.02	100.70
94-T31-1 29.0m	29.85	4.67	10.12	0.23	25.96	9.94	0.06	2.57	0.868	0.93	13.73	98.92
98 A21-16 181.0m	42.04	4.89	6.33	0.10	25.42	2.84	0.09	0.65	0.406	0.20	17.24	100.20
04 GTH83 351.86m	32.32	3.12	6.66	0.13	31.20	7.16	0.12	1.99	0.679	0.71	16.11	100.20
DVK 78-1 57.0m	35.29	4.39	7.82	0.22	15.60	12.16	0.22	2.22	0.517	0.66	19.93	99.03
03T19-04 85.50m	46.54	6.92	5.76	0.09	14.36	4.76	0.17	3.58	0.558	0.37	17.40	100.50
02A1245-2 69.50m	40.92	4.68	6.00	0.11	27.83	4.02	0.13	1.07	0.276	0.30	14.66	100.00
05A1039 74.50m	40.99	5.77	7.38	0.11	21.66	4.54	0.19	2.50	0.505	0.49	15.93	100.10
05A1039 78.40m	39.57	5.51	7.85	0.12	21.20	4.99	0.18	1.62	0.487	0.48	17.61	99.61
A841-07 130.60m	33.59	3.93	7.13	0.20	29.58	8.98	0.09	0.88	0.532	0.17	13.70	98.79
99A180-07 98.0m	40.29	4.51	6.22	0.11	26.04	4.81	0.11	1.12	0.354	0.11	16.81	100.50

Diavik Kimberlites: Whole Rock Geochemistry

	SiO_2 %	Al_2O_3 %	$Fe_2O_{3(T)}$ %	MnO %	MgO %	CaO %	Na_2O %	K_2O %	TiO_2 %	P_2O_5 %	LOI %	Total %
Detection Limit	0.01	0.01	0.01	0.001	0.01	0.01	0.01	0.01	0.001	0.01		0.01
Method	FUS-ICP	FUS-ICP	FUS-ICP	FUS-ICP	FUS-ICP	FUS-ICP	FUS-ICP	FUS-ICP	FUS-ICP	FUS-ICP	FUS-ICP	FUS-ICP
99A841-03 119.8m	38.81	4.34	7.06	0.09	29.31	4.05	0.13	0.68	0.62	0.28	15.13	100.5
98A180-02 85.00m	40.70	4.87	5.83	0.08	23.65	4.79	0.17	1.15	0.37	0.34	16.69	98.65
97A44-2 172.0m	30.20	5.49	8.48	0.20	25.06	12.89	0.30	2.66	0.77	1.03	11.68	98.72
98-A2-07 151.0m	38.50	6.31	6.92	0.12	19.31	8.73	0.13	1.02	0.60	0.37	17.53	99.53
95 T237-01 31.00m	19.24	3.53	6.73	0.26	14.60	26.66	0.18	2.60	0.66	2.74	21.60	98.79
95 T237-01 29.70m	20.17	3.98	6.97	0.31	14.38	24.96	0.17	2.07	0.67	1.52	23.39	98.58
97 A11-08 116.40m	37.97	3.34	6.75	0.13	32.11	4.70	0.08	1.10	0.33	0.15	13.80	100.5
98 A11-08 118.7m	36.20	2.90	6.33	0.17	30.94	6.39	0.09	0.77	0.31	0.29	15.43	99.82
99 A11-08 114.5m	35.33	2.57	5.52	0.26	29.84	5.83	0.10	0.61	0.25	0.22	18.40	98.92
99A180-10 225.70m	39.27	2.71	6.58	0.11	31.33	3.29	0.10	0.76	0.23	0.25	15.56	100.2
T33 76.0m	35.74	5.28	8.72	0.18	25.00	10.93	0.31	3.42	0.70	0.4	9.11	99.79
T33 79.8m	32.85	5.18	8.49	0.18	26.54	12.45	0.18	3.36	0.72	0.77	7.89	98.61
T33 81.0m	33.20	5.22	9.13	0.18	26.77	10.09	0.18	2.67	0.73	0.64	10.08	98.88
T33 110.0m	27.29	3.32	7.96	0.18	16.86	18.47	0.13	0.84	0.64	0.71	22.63	99.03
A154 221m	38.21	2.65	6.44	0.10	35.42	2.31	0.13	0.91	0.33	0.14	13.13	99.77
A154 316.0m	36.30	2.08	5.97	0.12	37.87	3.00	0.28	1.42	0.37	0.17	11.50	99.08
A154 272m	35.50	2.13	6.12	0.13	30.53	4.51	0.06	0.65	0.33	0.17	19.76	99.89
A154 294m	36.08	1.99	7.24	0.12	35.71	4.93	0.10	1.38	0.35	0.22	11.85	99.98

Diavik Kimberlites: Whole Rock Geochemistry

	Sc	Be	V	Cr	Co	Ni	Cu	Zn	Ga	Ge	As	Rb	Sr
	ppm	ppm	ppm	ppm	ppm	ppm	ppm	ppm	ppm	ppm	ppm	ppm	ppm
Detection Limit	1	1	5	20	1	20	10	30	1	0.5	5	1	2
Method	FUS-ICP	FUS-ICP	FUS-ICP	FUS-MS	FUS-MS	FUS-MS	FUS-MS	FUS-MS	FUS-MS	FUS-MS	FUS-MS	FUS-MS	FUS-ICP
ABZ-7a	14	2	151	690	41	380	50	80	11	1.1	8	126	735
A418-21 377m	8	< 1	49	1580	106	1580	30	60	4	0.8	< 5	34	346
94C42-2 89.50m	11	2	159	590	39	410	40	70	12	0.6	7	127	700
94C42-2 179m	11	2	161	600	39	380	40	80	12	0.7	< 5	120	702
00A4-05 179m	11	1	81	1620	82	1210	50	50	5	0.8	< 5	88	1341
00A4-05 138.4m	10	1	154	1350	67	980	40	50	4	0.9	8	158	2021
00A4-05 139.0m	10	1	219	1070	55	790	40	60	5	0.9	11	172	1650
00A4-05 139.20m	11	2	121	1460	73	1070	40	60	5	0.9	< 5	129	1403
94-A5-01 60.50m	10	2	108	760	60	910	40	60	8	0.7	11	108	988
94-A5-01 53.10m	13	2	99	1070	55	620	50	60	8	0.7	< 5	136	1870
94-A5-01 150.10m	13	1	129	1120	58	710	50	100	7	0.8	7	126	1719
94-A5-01 149.30m	11	2	157	550	36	360	40	70	12	0.7	5	120	707
94-A5-01 148.40m	16	2	109	1360	65	770	60	60	8	1	< 5	135	1594
03A1620-02 71.0m	9	1	90	870	61	920	30	60	8	0.9	8	79	632
94-T31-1 29.0m	23	2	162	1080	68	600	60	80	9	1.1	6	353	1620
98 A21-16 181.0m	8	1	87	820	63	1010	30	60	7	0.8	6	48	361
04 GTH83 351.86m	10	1	95	1190	64	920	40	50	5	0.6	6	108	939
DVK 78-1 57.0m	12	2	105	1040	57	730	50	50	6	0.6	8	122	1257
03T19-04 85.50m	12	2	138	510	33	360	30	70	10	1	10	130	652
02A1245-2 69.50m	8	1	68	1270	63	970	20	80	7	0.6	9	58	555
05A1039 74.50m	10	2	100	770	54	730	50	60	10	0.7	< 5	109	749
05A1039 78.40m	10	1	93	780	58	760	50	60	9	0.8	< 5	88	751
A841-07 130.60m	19	< 1	76	5470	101	1310	30	60	5	1	< 5	63	381
99A180-07 98.0m	9	1	92	1090	64	970	30	60	7	0.8	7	70	425

Diavik Kimberlites: Whole Rock Geochemistry

	Sc	Be	V	Cr	Co	Ni	Cu	Zn	Ga	Ge	As	Rb	Sr
	ppm	ppm	ppm	ppm	ppm	ppm	ppm	ppm	ppm	ppm	ppm	ppm	ppm
Detection Limit	1	1	5	20	1	20	10	30	1	0.5	5	1	2
Method	FUS-ICP	FUS-ICP	FUS-ICP	FUS-MS	FUS-MS	FUS-MS	FUS-MS	FUS-MS	FUS-MS	FUS-MS	FUS-MS	FUS-MS	FUS-ICP
99A841-03 119.8m	9	1	96	1370	83	1190	40	70	7	0.7	10	49	441
98A180-02 85.00m	9	1	98	1120	50	770	30	50	7	0.7	5	69	541
97A44-2 172.0m	18	2	72	1200	68	640	90	70	11	0.9	< 5	188	1400
98-A2-07 151.0m	13	2	117	1110	58	740	50	80	10	0.7	6	110	638
95 T237-01 31.00m	15	2	101	960	42	420	180	50	8	0.7	25	213	3177
95 T237-01 29.70m	16	2	194	970	49	390	110	60	9	1.1	22	414	2599
97 A11-08 116.40m	9	< 1	65	1470	82	1310	30	50	5	0.7	10	56	524
98 A11-08 118.7m	8	< 1	58	1340	84	1350	30	50	5	0.6	7	44	482
99 A11-08 114.5m	6	< 1	47	1100	78	1300	20	50	4	0.7	14	41	397
99A180-10 225.70m	6	< 1	48	1310	89	1520	20	60	5	1.1	< 5	53	401
T33 76.0m	18	< 1	73	910	47	520	30	50	8	1.4	< 5	136	1434
T33 79.8m	19	1	149	970	46	530	60	< 30	8	1.2	6	179	1593
T33 81.0m	19	1	93	990	54	580	60	60	7	1.1	< 5	93	1271
T33 110.0m	17	1	111	830	44	460	60	30	6	< 0.5	< 5	60	2078
A154 221m	8	< 1	33	1010	56	920	20	30	4	0.5	< 5	54	236
A154 316.0m	8	< 1	54	1200	51	870	20	< 30	3	< 0.5	< 5	66	282
A154 272m	7	< 1	36	920	54	910	20	< 30	3	0.7	< 5	45	223
A154 294m	8	< 1	42	1170	70	1200	30	50	3	0.7	< 5	67	433

Diavik Kimberlites: Whole Rock Geochemistry

	Y	Zr	Nb	Mo	Ag	In	Sn	Sb	Cs	Ba	La	Ce	Pr
	ppm	ppm	ppm	ppm	ppm	ppm	ppm	ppm	ppm	ppm	ppm	ppm	ppm
Detection Limit	0.5	4	0.2	2	0.5	0.1	1	0.2	0.1	3	0.05	0.05	0.01
Method	FUS-MS	FUS-ICP	FUS-MS	FUS-MS	FUS-MS	FUS-MS	FUS-MS	FUS-MS	FUS-MS	FUS-ICP	FUS-MS	FUS-MS	FUS-MS
ABZ-7a	15.9	120	142	< 2	< 0.5	< 0.1	2	0.3	5.6	2136	143	243	24.4
A418-21 377m	4	25	61.9	< 2	3.3	< 0.1	3	0.5	0.8	696	45.3	74.8	7.38
94C42-2 89.50m	15.7	112	95	11	0.7	< 0.1	< 1	< 0.2	3.5	1507	87	148	15
94C42-2 179m	16.1	108	93.3	3	< 0.5	< 0.1	< 1	< 0.2	3.9	1481	83.3	143	14.6
00A4-05 179m	7.3	53	202	< 2	< 0.5	< 0.1	< 1	0.3	0.9	2863	192	316	30.7
00A4-05 138.4m	7	61	157	4	< 0.5	< 0.1	< 1	0.4	1.8	3262	174	266	25.3
00A4-05 139.0m	8	65	145	6	< 0.5	< 0.1	< 1	0.6	1.9	2314	205	302	27.3
00A4-05 139.20m	7.3	61	170	< 2	< 0.5	< 0.1	< 1	0.3	1.6	2239	201	312	29.3
94-A5-01 60.50m	13.8	83	150	< 2	< 0.5	< 0.1	< 1	0.5	2.5	1197	165	251	23.4
94-A5-01 53.10m	11.7	77	236	< 2	< 0.5	< 0.1	< 1	0.4	6.5	3989	225	346	31.7
94-A5-01 150.10m	13.3	68	232	< 2	< 0.5	< 0.1	< 1	0.4	2.6	3183	251	384	35.5
94-A5-01 149.30m	16.6	108	92.2	3	< 0.5	< 0.1	1	< 0.2	4	1501	91.2	154	15.6
94-A5-01 148.40m	11.8	80	314	< 2	< 0.5	< 0.1	< 1	0.3	2.6	4441	285	467	41.9
03A1620-02 71.0m	10.2	73	92.5	< 2	< 0.5	< 0.1	< 1	0.6	2.7	1744	101	168	16.6
94-T31-1 29.0m	15	94	209	< 2	< 0.5	< 0.1	< 1	0.4	11.5	3632	308	584	55.9
98 A21-16 181.0m	8.7	55	62.5	2	< 0.5	< 0.1	< 1	0.4	2.3	730	54.8	90.1	9.06
04 GTH83 351.86m	7.5	51	114	< 2	< 0.5	< 0.1	< 1	0.5	1.6	1573	92.7	162	15.4
DVK 78-1 57.0m	9.3	68	176	3	< 0.5	< 0.1	< 1	0.4	2.1	1768	179	301	29.4
03T19-04 85.50m	15.4	109	118	< 2	< 0.5	< 0.1	1	0.3	4	2186	123	195	18.5
02A1245-2 69.50m	8.4	60	67.9	5	< 0.5	< 0.1	< 1	0.4	1.8	1151	68.9	115	11.4
05A1039 74.50m	9.5	88	114	< 2	< 0.5	< 0.1	1	0.3	2	944	106	185	18.6
05A1039 78.40m	10.1	81	124	< 2	< 0.5	< 0.1	1	1.1	2	740	107	184	18.6
A841-07 130.60m	6.2	38	79.5	2	0.9	< 0.1	< 1	0.6	2.5	722	55.2	92.1	9.08
99A180-07 98.0m	10.8	84	85.6	3	< 0.5	< 0.1	< 1	0.5	3.1	684	76.3	131	13.3

Diavik Kimberlites: Whole Rock Geochemistry

	Y	Zr	Nb	Mo	Ag	In	Sn	Sb	Cs	Ba	La	Ce	Pr
	ppm	ppm	ppm	ppm	ppm	ppm	ppm	ppm	ppm	ppm	ppm	ppm	ppm
Detection Limit	0.5	4	0.2	2	0.5	0.1	1	0.2	0.1	3	0.05	0.05	0.01
Method	FUS-MS	FUS-ICP	FUS-MS	FUS-MS	FUS-MS	FUS-MS	FUS-MS	FUS-MS	FUS-MS	FUS-ICP	FUS-MS	FUS-MS	FUS-MS
99A841-03 119.8m	9.6	53	82.6	< 2	< 0.5	< 0.1	< 1	0.3	2.3	963	60.5	104	10.5
98A180-02 85.00m	11.2	94	83.7	< 2	< 0.5	< 0.1	< 1	0.4	2.9	1017	73.8	126	13
97A44-2 172.0m	12.8	95	277	< 2	< 0.5	< 0.1	< 1	0.4	2.5	3758	229	412	39.4
98-A2-07 151.0m	14.1	81	110	< 2	< 0.5	< 0.1	< 1	0.4	2.7	2113	79.5	136	13.8
95 T237-01 31.00m	13.2	71	449	< 2	< 0.5	< 0.1	< 1	0.4	2.3	4833	300	415	35.3
95 T237-01 29.70m	14.5	79	419	< 2	1.1	< 0.1	< 1	0.5	9	8896	286	389	34.5
97 A11-08 116.40m	6.6	55	85.5	< 2	< 0.5	< 0.1	< 1	0.5	1.7	1003	67.2	114	11.4
98 A11-08 118.7m	6.3	49	79.2	< 2	< 0.5	< 0.1	< 1	0.5	1.5	835	64.7	111	11
99 A11-08 114.5m	5.2	37	63.3	< 2	< 0.5	< 0.1	< 1	0.9	1.6	851	54.5	92	9.1
99A180-10 225.70m	5.5	42	63.7	< 2	< 0.5	< 0.1	< 1	0.7	1.6	1406	55.9	96.3	9.53
T33 76.0m	12.2	86	215	< 2	< 0.5	< 0.1	< 1	0.3	1.5	2533	213	358	35.4
T33 79.8m	11.3	73	231	< 2	< 0.5	< 0.1	< 1	0.4	1.6	2538	229	386	38
T33 81.0m	12.2	87	252	< 2	< 0.5	< 0.1	< 1	0.2	0.9	2436	227	389	38.7
T33 110.0m	10.7	77	221	< 2	< 0.5	< 0.1	< 1	0.6	1	2852	222	375	37.2
A154 221m	3.9	26	56.8	< 2	< 0.5	< 0.1	< 1	< 0.2	1.3	609	39.3	65.3	6.24
A154 316.0m	3.5	21	78.4	< 2	< 0.5	< 0.1	< 1	< 0.2	1.1	892	60	97	9.19
A154 272m	4.4	28	60.1	< 2	< 0.5	< 0.1	< 1	< 0.2	1.2	347	44.6	74.8	7.19
A154 294m	3.2	21	72.5	< 2	< 0.5	< 0.1	< 1	< 0.2	1.1	1055	57.8	94.2	8.84

Diavik Kimberlites: Whole Rock Geochemistry

	Nd	Sm	Eu	Gd	Tb	Dy	Ho	Er	Tm	Yb	Lu	Hf	Ta
	ppm	ppm	ppm	ppm	ppm	ppm	ppm	ppm	ppm	ppm	ppm	ppm	ppm
Detection Limit	0.05	0.01	0.005	0.01	0.01	0.01	0.01	0.01	0.005	0.01	0.002	0.1	0.01
Method	FUS-MS	FUS-MS	FUS-MS	FUS-MS	FUS-MS	FUS-MS	FUS-MS	FUS-MS	FUS-MS	FUS-MS	FUS-MS	FUS-MS	FUS-MS
ABZ-7a	75.9	8.84	2.19	5.17	0.66	3.17	0.57	1.54	0.213	1.34	0.186	3.1	10.4
A418-21 377m	22.6	2.49	0.615	1.36	0.16	0.78	0.14	0.37	0.056	0.35	0.047	0.7	4.95
94C42-2 89.50m	48.4	6.41	1.51	4.03	0.58	3.1	0.56	1.57	0.229	1.41	0.201	2.9	6.61
94C42-2 179m	47.6	6.49	1.51	4.32	0.61	3.07	0.55	1.51	0.225	1.4	0.196	2.8	6.65
00A4-05 179m	92.4	9.07	2.29	4.21	0.4	1.72	0.26	0.66	0.083	0.44	0.054	1.2	9.69
00A4-05 138.4m	75.6	7.58	1.88	3.31	0.35	1.58	0.25	0.64	0.083	0.46	0.057	1.3	7.67
00A4-05 139.0m	80.3	7.87	1.97	3.29	0.39	1.84	0.3	0.77	0.101	0.59	0.075	1.7	6.82
00A4-05 139.20m	86.4	8.34	2.1	3.49	0.38	1.72	0.28	0.69	0.092	0.52	0.064	1.4	8.13
94-A5-01 60.50m	70.1	7.55	1.86	3.89	0.54	2.61	0.47	1.27	0.18	1.13	0.152	2.1	7.7
94-A5-01 53.10m	92.8	9.34	2.38	4.28	0.53	2.57	0.43	1.11	0.144	0.84	0.114	1.9	11.1
94-A5-01 150.10m	104	10.5	2.64	4.82	0.62	2.87	0.48	1.24	0.159	0.93	0.13	1.6	12.1
94-A5-01 149.30m	50.4	6.74	1.55	4.28	0.64	3.29	0.6	1.62	0.235	1.44	0.207	2.9	6.23
94-A5-01 148.40m	122	11.6	2.93	4.65	0.59	2.77	0.46	1.16	0.148	0.84	0.109	1.9	15
03A1620-02 71.0m	50.6	5.64	1.32	2.85	0.4	2	0.36	0.99	0.136	0.87	0.135	2	5.4
94-T31-1 29.0m	173	17.1	4.21	7.02	0.77	3.54	0.59	1.49	0.192	1.08	0.141	2.4	18.7
98 A21-16 181.0m	29.3	3.65	0.849	2.19	0.32	1.68	0.32	0.89	0.128	0.79	0.114	1.4	3.83
04 GTH83 351.86m	47.2	5.19	1.25	2.64	0.34	1.67	0.29	0.73	0.101	0.6	0.081	1.4	8.28
DVK 78-1 57.0m	90.6	9	2.29	4.11	0.45	2.1	0.34	0.88	0.119	0.7	0.088	1.7	10.7
03T19-04 85.50m	56.8	6.75	1.7	3.9	0.57	3.05	0.55	1.51	0.215	1.35	0.197	2.8	6.76
02A1245-2 69.50m	35.5	3.99	0.907	2.56	0.33	1.58	0.27	0.76	0.109	0.67	0.099	1.7	4.15
05A1039 74.50m	60.1	6.98	1.68	4.06	0.46	2.07	0.35	0.91	0.12	0.73	0.1	2.3	7
05A1039 78.40m	58.9	6.77	1.63	3.86	0.45	1.99	0.34	0.91	0.121	0.72	0.1	2.2	7.07
A841-07 130.60m	28.7	3.12	0.83	1.92	0.26	1.16	0.21	0.6	0.084	0.52	0.077	0.9	6.16
99A180-07 98.0m	43.1	4.9	1.15	3.11	0.39	1.91	0.36	1.01	0.145	0.91	0.135	2.3	4.79

Diavik Kimberlites: Whole Rock Geochemistry

	Nd	Sm	Eu	Gd	Tb	Dy	Ho	Er	Tm	Yb	Lu	Hf	Ta
	ppm	ppm	ppm	ppm	ppm	ppm	ppm	ppm	ppm	ppm	ppm	ppm	ppm
Detection Limit	0.05	0.01	0.005	0.01	0.01	0.01	0.01	0.01	0.005	0.01	0.002	0.1	0.01
Method	FUS-MS	FUS-MS	FUS-MS	FUS-MS	FUS-MS	FUS-MS	FUS-MS	FUS-MS	FUS-MS	FUS-MS	FUS-MS	FUS-MS	FUS-MS
99A841-03 119.8m	34.2	4.01	1.02	2.65	0.35	1.78	0.33	0.9	0.129	0.79	0.115	1.5	6.64
98A180-02 85.00m	41.3	4.91	1.13	3.13	0.41	2.04	0.37	1.08	0.156	0.95	0.139	2.4	4.67
97A44-2 172.0m	122	11.7	3.08	6.44	0.67	2.74	0.45	1.14	0.149	0.86	0.103	2.4	17.8
98-A2-07 151.0m	45.2	5.7	1.46	3.82	0.49	2.53	0.46	1.26	0.178	1.11	0.163	2.2	7.24
95 T237-01 31.00m	100	9.56	2.47	4.52	0.57	2.64	0.44	1.1	0.139	0.79	0.107	1.9	13.9
95 T237-01 29.70m	97.8	9.65	2.51	4.84	0.6	2.67	0.46	1.18	0.154	0.85	0.108	2	13.3
97 A11-08 116.40m	35.4	3.84	0.952	2.1	0.24	1.19	0.21	0.61	0.085	0.51	0.077	1.5	5.25
98 A11-08 118.7m	34.6	3.68	0.906	2.08	0.24	1.2	0.21	0.55	0.078	0.49	0.072	1.3	5.05
99 A11-08 114.5m	28	3	0.73	1.69	0.2	0.96	0.18	0.51	0.073	0.45	0.063	1.1	3.9
99A180-10 225.70m	29.1	3.14	0.696	1.56	0.19	1	0.18	0.48	0.069	0.43	0.059	1.1	3.53
T33 76.0m	108	11.5	2.68	6.05	0.57	2.37	0.37	0.97	0.133	0.83	0.11	2.2	13.5
T33 79.8m	117	12.3	2.83	6.05	0.54	2.28	0.36	0.92	0.129	0.81	0.104	1.8	14.6
T33 81.0m	118	12.5	2.87	6.44	0.58	2.44	0.39	1.01	0.14	0.86	0.109	2.1	14.4
T33 110.0m	115	12.1	2.78	6.42	0.54	2.2	0.33	0.79	0.106	0.66	0.086	1.8	14
A154 221m	19.2	2.42	0.541	1.34	0.16	0.76	0.12	0.33	0.047	0.31	0.042	0.7	3.32
A154 316.0m	28.1	3.21	0.741	1.73	0.18	0.75	0.12	0.31	0.04	0.24	0.029	0.6	4.67
A154 272m	22.1	2.7	0.612	1.58	0.18	0.86	0.15	0.4	0.056	0.34	0.045	0.8	3.77
A154 294m	27.1	3.06	0.716	1.64	0.17	0.72	0.11	0.28	0.038	0.23	0.032	0.6	4.31

Diavik Kimberlites: Whole Rock Geochemistry

	W	Tl	Pb	Bi	Th	U
	ppm	ppm	ppm	ppm	ppm	ppm
Detection Limit	0.5	0.05	5	0.1	0.05	0.01
Method	FUS-MS	FUS-MS	FUS-MS	FUS-MS	FUS-MS	FUS-MS
ABZ-7a	178	0.45	12	< 0.1	19.7	3.36
A418-21 377m	204	0.12	< 5	< 0.1	5.6	1.32
94C42-2 89.50m	73	0.36	6	< 0.1	13.2	4.46
94C42-2 179m	62.7	0.47	6	< 0.1	14.5	4.23
00A4-05 179m	58.7	0.18	12	< 0.1	19.4	3.41
00A4-05 138.4m	56.5	0.29	16	0.1	16.4	3.65
00A4-05 139.0m	39.1	0.26	31	0.3	14.5	4.77
00A4-05 139.20m	47.8	0.23	13	0.1	17.1	3.26
94-A5-01 60.50m	26.3	0.4	9	< 0.1	17.6	10.3
94-A5-01 53.10m	48.3	0.32	14	< 0.1	24.4	3.78
94-A5-01 150.10m	32.6	0.31	14	< 0.1	28.3	4.77
94-A5-01 149.30m	24.4	0.52	8	< 0.1	14.2	3.91
94-A5-01 148.40m	29.1	0.36	14	0.1	31.5	4.62
03A1620-02 71.0m	31.4	0.35	7	< 0.1	13.2	2.87
94-T31-1 29.0m	28.7	0.36	17	0.2	45.4	4.29
98 A21-16 181.0m	18.3	0.34	7	< 0.1	7.87	2.51
04 GTH83 351.86m	36.1	0.28	6	< 0.1	11	2.11
DVK 78-1 57.0m	19.3	0.22	7	< 0.1	15.5	3.25
03T19-04 85.50m	12.4	0.57	10	< 0.1	18.6	2.79
02A1245-2 69.50m	17.1	0.45	7	< 0.1	12.3	3.22
05A1039 74.50m	9	0.49	12	0.1	18.4	3.62
05A1039 78.40m	2.2	0.56	13	0.2	17.7	3.36
A841-07 130.60m	140	0.51	< 5	< 0.1	9.33	1.88
99A180-07 98.0m	9.6	0.36	7	< 0.1	14.1	2.83

Diavik Kimberlites: Whole Rock Geochemistry

	W	Tl	Pb	Bi	Th	U
	ppm	ppm	ppm	ppm	ppm	ppm
Detection Limit	0.5	0.05	5	0.1	0.05	0.01
Method	FUS-MS	FUS-MS	FUS-MS	FUS-MS	FUS-MS	FUS-MS
99A841-03 119.8m	23.1	0.45	5	< 0.1	11.4	3.8
98A180-02 85.00m	4	0.21	< 5	< 0.1	13.8	2.79
97A44-2 172.0m	26.6	0.4	17	0.8	39.4	5.75
98-A2-07 151.0m	5	0.46	8	< 0.1	15	4.29
95 T237-01 31.00m	5.3	0.42	27	0.2	38.5	7.82
95 T237-01 29.70m	7.7	0.33	25	< 0.1	39.6	6.61
97 A11-08 116.40m	18	0.18	< 5	< 0.1	11.3	1.97
98 A11-08 118.7m	12.3	0.2	< 5	< 0.1	10.8	1.88
99 A11-08 114.5m	14.8	0.47	5	< 0.1	8.49	1.56
99A180-10 225.70m	10.6	0.2	5	< 0.1	8.51	1.44
T33 76.0m	14.6	0.07	9	< 0.1	25.3	2.94
T33 79.8m	16.8	0.06	15	< 0.1	24.9	5.82
T33 81.0m	11.1	0.13	9	< 0.1	26.9	4.37
T33 110.0m	4.2	0.16	6	< 0.1	24.1	4.35
A154 221m	11.4	0.1	< 5	< 0.1	5.36	1.42
A154 316.0m	17.1	< 0.05	< 5	< 0.1	7.82	1.71
A154 272m	4.2	0.07	< 5	< 0.1	5.95	1.58
A154 294m	20.7	0.17	5	< 0.1	7.33	1.59

Diavik Olivine Microprobe Analyses

	T33 (M)	T33 (M)	T33 (M)	T33 (M)	T33 (M)	T33 (M)	T33 (P)	T33 (P)	T33 (M)	T33 (M)
SiO_2	41.04	40.86	40.76	41.25	40.60	41.31	40.83	40.76	40.60	40.63
TiO_2	0.01	0.03	0.02	0.01	0.02	0.00	0.01	0.03	0.02	0.02
Al_2O_3	0.01	0.01	0.02	0.00	0.01	0.00	0.00	0.02	0.00	0.17
Cr_2O_3	0.03	0.04	0.07	0.06	0.07	0.07	0.08	0.02	0.07	0.14
FeO	10.38	9.85	9.64	9.44	9.22	8.75	8.85	9.82	9.11	9.04
MnO	0.27	0.10	0.11	0.12	0.12	0.10	0.12	0.13	0.12	0.12
MgO	49.29	49.39	48.85	49.74	49.13	50.13	49.17	49.04	49.03	48.95
NiO	0.40	0.36	0.37	0.39	0.39	0.39	0.36	0.32	0.40	0.37
CaO	0.05	0.06	0.08	0.08	0.07	0.09	0.09	0.03	0.05	0.17
TOTAL	101.48	100.70	99.91	101.08	99.61	100.85	99.52	100.16	99.41	99.62
Si	0.9958	0.9962	1.0006	0.9998	0.9982	1.0004	1.0027	0.9983	0.9996	0.9989
Ti	0.0003	0.0005	0.0003	0.0001	0.0004	0.0000	0.0003	0.0006	0.0004	0.0003
Al	0.0001	0.0003	0.0006	0.0000	0.0002	0.0001	0.0001	0.0005	0.0000	0.0050
Cr	0.0006	0.0008	0.0014	0.0011	0.0013	0.0014	0.0016	0.0004	0.0014	0.0028
Fe(ii)	0.2105	0.2007	0.1978	0.1913	0.1895	0.1772	0.1817	0.2011	0.1876	0.1859
Mn	0.0056	0.0021	0.0023	0.0024	0.0024	0.0021	0.0025	0.0027	0.0024	0.0024
Mg	1.7830	1.7951	1.7879	1.7972	1.8009	1.8100	1.8002	1.7906	1.7999	1.7942
Ni	0.0078	0.0070	0.0072	0.0075	0.0077	0.0077	0.0070	0.0062	0.0080	0.0073
Ca	0.0014	0.0015	0.0021	0.0020	0.0018	0.0024	0.0023	0.0008	0.0013	0.0045
TOTAL	3.0050	3.0042	3.0002	3.0015	3.0024	3.0013	2.9985	3.0014	3.0006	3.0014
Endmembers										
Fo	89.19	89.85	89.93	90.27	90.37	90.99	90.72	89.78	90.45	90.50
Fa	10.53	10.04	9.95	9.61	9.51	8.91	9.15	10.08	9.43	9.38
Tp	0.28	0.11	0.12	0.12	0.12	0.11	0.13	0.14	0.12	0.12

M= Macrocryst, P= Phenocryst, F= Fragment, MP= Microphenocryst, MF= Macrocrystal Fragment

Diavik Olivine Microprobe Analyses

	T33 (M)	T33 (M)	T33 (M)	T33 (M)	T33 (M)	T33 (M)	T33 (M)	T33 (M)	T33 (M)	T33 (M)
SiO_2	40.81	40.76	40.86	40.81	40.42	40.71	40.89	40.16	40.21	40.77
TiO_2	0.02	0.03	0.01	0.00	0.00	0.01	0.02	0.00	0.02	0.00
Al_2O_3	0.00	0.01	0.00	0.00	0.03	0.00	0.00	0.00	0.00	0.00
Cr_2O_3	0.05	0.05	0.07	0.05	0.09	0.07	0.05	0.06	0.08	0.08
FeO	9.22	9.08	8.95	8.88	8.83	9.08	9.02	8.97	8.81	8.68
MnO	0.10	0.13	0.10	0.13	0.13	0.13	0.13	0.13	0.14	0.10
MgO	48.96	49.18	49.32	49.57	48.78	48.87	48.86	48.32	48.27	49.42
NiO	0.37	0.35	0.38	0.40	0.35	0.40	0.38	0.37	0.39	0.41
CaO	0.08	0.07	0.05	0.08	0.07	0.08	0.07	0.09	0.08	0.09
TOTAL	99.60	99.65	99.73	99.91	98.69	99.34	99.43	98.10	97.98	99.54
Si	1.0028	1.0006	1.0013	0.9989	1.0012	1.0027	1.0055	1.0019	1.0034	1.0006
Ti	0.0003	0.0005	0.0001	0.0000	0.0000	0.0001	0.0004	0.0001	0.0004	0.0000
Al	0.0000	0.0003	0.0001	0.0000	0.0008	0.0000	0.0000	0.0000	0.0000	0.0000
Cr	0.0010	0.0010	0.0013	0.0009	0.0017	0.0014	0.0009	0.0012	0.0015	0.0015
Fe(ii)	0.1894	0.1865	0.1834	0.1817	0.1828	0.1869	0.1855	0.1870	0.1837	0.1780
Mn	0.0021	0.0026	0.0020	0.0027	0.0027	0.0027	0.0027	0.0027	0.0029	0.0022
Mg	1.7936	1.8001	1.8021	1.8086	1.8013	1.7946	1.7910	1.7972	1.7957	1.8083
Ni	0.0073	0.0069	0.0075	0.0079	0.0069	0.0079	0.0076	0.0075	0.0077	0.0081
Ca	0.0020	0.0019	0.0014	0.0022	0.0019	0.0020	0.0019	0.0024	0.0022	0.0023
TOTAL	2.9984	3.0003	2.9992	3.0028	2.9995	2.9984	2.9955	2.9998	2.9976	3.0010
Endmembers										
Fo	90.35	90.50	90.67	90.75	90.66	90.44	90.49	90.45	90.59	90.94
Fa	9.54	9.37	9.23	9.12	9.20	9.42	9.37	9.41	9.27	8.95
Tp	0.11	0.13	0.10	0.14	0.14	0.13	0.14	0.13	0.15	0.11

Diavik Olivine Microprobe Analyses

	T33 (M)	T33 (M)	T33 (M)	T33 (M)	T33 (M)	T33 (M)	T33 (M)	T33 (M)	T33 (M)	T33 (M)
SiO_2	40.74	40.74	40.91	40.87	40.28	40.11	40.52	40.70	40.48	40.30
TiO_2	0.01	0.01	0.01	0.01	0.01	0.00	0.02	0.03	0.01	0.01
Al_2O_3	0.01	0.01	0.01	0.00	0.00	0.00	0.00	0.00	0.00	0.00
Cr_2O_3	0.08	0.08	0.07	0.07	0.04	0.06	0.05	0.04	0.06	0.09
FeO	8.91	9.02	8.73	9.01	9.22	9.06	9.06	9.23	9.07	8.96
MnO	0.11	0.11	0.12	0.10	0.12	0.11	0.12	0.15	0.14	0.11
MgO	49.68	49.20	49.72	49.61	48.55	48.34	48.99	49.09	48.59	48.40
NiO	0.38	0.40	0.45	0.39	0.38	0.31	0.35	0.39	0.36	0.38
CaO	0.10	0.05	0.06	0.07	0.05	0.05	0.06	0.07	0.07	0.09
TOTAL	100.02	99.61	100.08	100.13	98.65	98.03	99.16	99.70	98.78	98.34
Si	0.9966	1.0004	0.9989	0.9984	1.0001	1.0010	0.9997	0.9998	1.0027	1.0027
Ti	0.0001	0.0001	0.0001	0.0002	0.0002	0.0000	0.0004	0.0006	0.0001	0.0001
Al	0.0002	0.0001	0.0002	0.0001	0.0000	0.0000	0.0000	0.0000	0.0000	0.0000
Cr	0.0015	0.0016	0.0014	0.0013	0.0008	0.0011	0.0009	0.0008	0.0013	0.0018
Fe(ii)	0.1823	0.1852	0.1783	0.1841	0.1913	0.1890	0.1869	0.1896	0.1879	0.1864
Mn	0.0022	0.0023	0.0025	0.0020	0.0025	0.0023	0.0024	0.0031	0.0028	0.0024
Mg	1.8118	1.8010	1.8099	1.8069	1.7968	1.7986	1.8021	1.7976	1.7945	1.7953
Ni	0.0075	0.0079	0.0088	0.0077	0.0076	0.0063	0.0069	0.0078	0.0072	0.0076
Ca	0.0027	0.0013	0.0015	0.0018	0.0014	0.0013	0.0016	0.0018	0.0019	0.0023
TOTAL	3.0051	2.9999	3.0017	3.0025	3.0007	2.9997	3.0011	3.0011	2.9984	2.9986
Endmembers										
Fo	90.76	90.57	90.92	90.66	90.26	90.38	90.49	90.32	90.39	90.49
Fa	9.13	9.31	8.96	9.24	9.61	9.50	9.39	9.53	9.46	9.39
Tp	0.11	0.12	0.13	0.10	0.12	0.12	0.12	0.15	0.14	0.12

Diavik Olivine Microprobe Analyses

	T33 (M)	**T33 (M)**	**T33 (F)**	**T33 (M)**	**T33 (M)**	**T33 (M)**	**T33 (M)**	**T33 (M)**	**T33 (M)**	**T33 (M)**
SiO_2	40.62	40.66	40.99	40.67	40.77	40.21	40.39	40.73	40.71	40.25
TiO_2	0.00	0.01	0.00	0.00	0.01	0.00	0.00	0.03	0.02	0.01
Al_2O_3	0.00	0.01	0.00	0.04	0.00	0.00	0.00	0.00	0.01	0.02
Cr_2O_3	0.08	0.04	0.07	0.06	0.07	0.08	0.08	0.08	0.07	0.05
FeO	8.63	7.86	8.91	9.65	9.55	9.18	8.96	8.93	8.71	8.55
MnO	0.11	0.15	0.12	0.13	0.13	0.13	0.09	0.14	0.11	0.17
MgO	48.81	49.00	49.78	48.80	48.43	48.17	48.35	49.11	48.88	48.47
NiO	0.39	0.31	0.41	0.36	0.33	0.36	0.41	0.40	0.38	0.25
CaO	0.08	0.17	0.07	0.07	0.07	0.07	0.08	0.13	0.09	0.25
TOTAL	98.72	98.20	100.36	99.78	99.36	98.20	98.36	99.53	98.96	98.02
Si	1.0046	1.0077	0.9988	0.9999	1.0053	1.0028	1.0044	1.0013	1.0046	1.0040
Ti	0.0000	0.0001	0.0001	0.0000	0.0002	0.0000	0.0000	0.0006	0.0003	0.0002
Al	0.0000	0.0004	0.0000	0.0011	0.0000	0.0000	0.0000	0.0000	0.0002	0.0006
Cr	0.0015	0.0007	0.0014	0.0012	0.0014	0.0015	0.0016	0.0015	0.0014	0.0010
Fe(ii)	0.1784	0.1628	0.1815	0.1983	0.1970	0.1914	0.1862	0.1835	0.1797	0.1784
Mn	0.0024	0.0032	0.0024	0.0027	0.0026	0.0027	0.0019	0.0028	0.0022	0.0036
Mg	1.7998	1.8104	1.8083	1.7885	1.7806	1.7908	1.7924	1.7999	1.7984	1.8024
Ni	0.0078	0.0062	0.0080	0.0071	0.0066	0.0072	0.0082	0.0079	0.0075	0.0049
Ca	0.0021	0.0046	0.0017	0.0019	0.0019	0.0019	0.0021	0.0033	0.0024	0.0067
TOTAL	2.9967	2.9962	3.0022	3.0008	2.9956	2.9983	2.9968	3.0007	2.9968	3.0018
Endmembers										
Fo	90.87	91.60	90.77	89.89	89.92	90.22	90.50	90.62	90.81	90.83
Fa	9.01	8.24	9.11	9.97	9.95	9.64	9.40	9.24	9.07	8.99
Tp	0.12	0.16	0.12	0.14	0.13	0.14	0.10	0.14	0.11	0.18

Diavik Olivine Microprobe Analyses

	T33 (P)	**T33 (P)**	**T33 (P)**	**T33 (P)**	**T33 (P)**	**T33 (P)**	**T33 (M)**	**T33 (M)**	**T33 (M)**	**T33 (M)**
SiO_2	40.13	40.70	40.48	40.15	40.29	40.09	40.09	40.77	40.95	41.13
TiO_2	0.00	0.00	0.01	0.01	0.02	0.02	0.01	0.00	0.03	0.01
Al_2O_3	0.00	0.00	0.00	0.00	0.00	0.00	0.01	0.00	0.01	0.00
Cr_2O_3	0.04	0.06	0.08	0.06	0.04	0.02	0.04	0.05	0.05	0.05
FeO	8.83	8.97	8.74	9.71	9.25	9.44	8.96	9.07	9.35	9.24
MnO	0.10	0.10	0.12	0.10	0.10	0.12	0.13	0.10	0.10	0.08
MgO	48.60	49.63	47.98	48.17	48.01	47.93	48.28	48.96	49.12	48.99
NiO	0.40	0.37	0.38	0.39	0.36	0.34	0.35	0.37	0.38	0.37
CaO	0.07	0.07	0.06	0.05	0.07	0.06	0.07	0.04	0.05	0.06
TOTAL	98.17	99.91	97.86	98.64	98.15	98.04	97.93	99.35	100.03	99.93
Si	0.9997	0.9966	1.0099	0.9992	1.0051	1.0023	1.0016	1.0033	1.0022	1.0065
Ti	0.0000	0.0001	0.0002	0.0002	0.0004	0.0004	0.0002	0.0000	0.0005	0.0002
Al	0.0001	0.0000	0.0000	0.0000	0.0000	0.0000	0.0002	0.0000	0.0002	0.0000
Cr	0.0008	0.0011	0.0015	0.0011	0.0007	0.0005	0.0007	0.0010	0.0010	0.0009
Fe(ii)	0.1840	0.1837	0.1823	0.2020	0.1930	0.1974	0.1871	0.1866	0.1914	0.1890
Mn	0.0021	0.0021	0.0026	0.0021	0.0022	0.0026	0.0028	0.0020	0.0020	0.0017
Mg	1.8051	1.8119	1.7848	1.7874	1.7856	1.7868	1.7982	1.7960	1.7920	1.7872
Ni	0.0079	0.0074	0.0077	0.0078	0.0072	0.0069	0.0071	0.0073	0.0074	0.0074
Ca	0.0017	0.0019	0.0017	0.0014	0.0019	0.0017	0.0018	0.0011	0.0013	0.0015
TOTAL	3.0015	3.0047	2.9907	3.0014	2.9961	2.9986	2.9996	2.9973	2.9980	2.9944
Endmembers										
Fo	90.65	90.70	90.61	89.75	90.14	89.93	90.45	90.49	90.26	90.36
Fa	9.24	9.19	9.26	10.14	9.75	9.94	9.41	9.40	9.64	9.55
Tp	0.11	0.11	0.13	0.11	0.11	0.13	0.14	0.10	0.10	0.08

Diavik Olivine Microprobe Analyses

	A44 (M)	**A44 (M)**	**A44 (M)**	**A44 (M)**	**A44 (M)**	**A44 (M)**	**A44 (M)**	**A44 (M)**	**A44 (M)**	**A44 (M)**
SiO_2	40.46	40.51	40.73	40.55	41.01	39.99	40.23	40.42	41.17	40.74
TiO_2	0.02	0.03	0.02	0.01	0.02	0.02	0.03	0.03	0.02	0.00
Al_2O_3	0.01	0.14	0.03	0.04	0.00	0.00	0.00	0.00	0.00	0.00
Cr_2O_3	0.05	0.06	0.06	0.05	0.03	0.00	0.05	0.03	0.06	0.04
FeO	9.00	9.06	8.81	8.98	9.16	9.17	9.46	7.44	7.98	7.67
MnO	0.18	0.14	0.15	0.16	0.14	0.17	0.20	0.15	0.13	0.15
MgO	48.44	48.80	49.26	48.88	49.54	48.75	48.26	49.37	50.15	50.20
NiO	0.21	0.17	0.18	0.19	0.13	0.17	0.15	0.27	0.39	0.31
CaO	0.18	0.19	0.17	0.17	0.16	0.17	0.18	0.14	0.07	0.13
TOTAL	98.54	99.11	99.41	99.05	100.19	98.44	98.56	97.85	99.96	99.22
Si	1.0048	1.0004	1.0014	1.0016	1.0012	0.9956	1.0012	1.0037	1.0023	0.9988
Ti	0.0003	0.0006	0.0004	0.0002	0.0004	0.0004	0.0006	0.0005	0.0003	0.0000
Al	0.0002	0.0041	0.0009	0.0012	0.0000	0.0000	0.0000	0.0000	0.0000	0.0001
Cr	0.0009	0.0012	0.0011	0.0010	0.0005	0.0001	0.0010	0.0006	0.0012	0.0007
Fe(ii)	0.1869	0.1870	0.1811	0.1855	0.1871	0.1909	0.1968	0.1545	0.1624	0.1572
Mn	0.0038	0.0030	0.0031	0.0033	0.0029	0.0035	0.0043	0.0031	0.0027	0.0031
Mg	1.7933	1.7965	1.8057	1.8002	1.8034	1.8098	1.7907	1.8277	1.8202	1.8349
Ni	0.0041	0.0034	0.0036	0.0038	0.0026	0.0035	0.0031	0.0054	0.0077	0.0060
Ca	0.0048	0.0050	0.0046	0.0046	0.0042	0.0045	0.0047	0.0036	0.0018	0.0034
TOTAL	2.9992	3.0013	3.0018	3.0016	3.0023	3.0083	3.0024	2.9991	2.9986	3.0042
Endmembers										
Fo	90.39	90.43	90.74	90.51	90.47	90.30	89.90	92.06	91.68	91.97
Fa	9.42	9.41	9.10	9.33	9.38	9.53	9.88	7.78	8.18	7.88
Tp	0.19	0.15	0.16	0.17	0.15	0.18	0.21	0.16	0.14	0.16

Diavik Olivine Microprobe Analyses

	A44 (M)	**A44 (M)**	**A44 (M)**	**A44 (M)**	**A44 (M)**	**A44 (M)**	**A44 (M)**	**A44 (M)**	**A44 (M)**	**A44 (M)**
SiO_2	39.80	40.65	41.29	40.73	40.30	40.18	40.98	40.69	41.02	40.57
TiO_2	0.04	0.00	0.00	0.00	0.01	0.01	0.01	0.01	0.01	0.02
Al_2O_3	0.00	0.01	0.00	0.00	0.00	0.01	0.01	0.00	0.01	0.01
Cr_2O_3	0.05	0.03	0.06	0.07	0.04	0.03	0.04	0.03	0.06	0.05
FeO	9.47	9.16	8.55	8.45	7.78	7.74	7.75	8.34	7.78	7.90
MnO	0.16	0.13	0.12	0.12	0.15	0.15	0.12	0.11	0.12	0.15
MgO	48.22	49.61	50.05	49.47	49.02	48.61	49.76	49.70	50.37	50.08
NiO	0.14	0.16	0.38	0.36	0.30	0.27	0.38	0.36	0.36	0.28
CaO	0.20	0.17	0.04	0.06	0.12	0.13	0.08	0.04	0.10	0.12
TOTAL	98.09	99.91	100.47	99.26	97.72	97.14	99.14	99.27	99.82	99.16
Si	0.9962	0.9962	1.0022	1.0010	1.0036	1.0063	1.0050	0.9993	0.9997	0.9964
Ti	0.0008	0.0000	0.0000	0.0001	0.0003	0.0002	0.0003	0.0002	0.0002	0.0004
Al	0.0001	0.0003	0.0000	0.0000	0.0000	0.0001	0.0002	0.0000	0.0002	0.0002
Cr	0.0010	0.0005	0.0011	0.0014	0.0007	0.0007	0.0009	0.0005	0.0012	0.0010
Fe(ii)	0.1983	0.1877	0.1734	0.1736	0.1620	0.1621	0.1588	0.1712	0.1585	0.1623
Mn	0.0035	0.0027	0.0024	0.0024	0.0032	0.0032	0.0026	0.0022	0.0025	0.0032
Mg	1.7996	1.8127	1.8108	1.8126	1.8198	1.8150	1.8190	1.8196	1.8301	1.8338
Ni	0.0029	0.0032	0.0073	0.0071	0.0060	0.0054	0.0076	0.0072	0.0070	0.0054
Ca	0.0053	0.0045	0.0010	0.0015	0.0031	0.0036	0.0021	0.0010	0.0026	0.0031
TOTAL	3.0077	3.0079	2.9983	2.9997	2.9988	2.9967	2.9963	3.0012	3.0020	3.0057
Endmembers										
Fo	89.92	90.50	91.15	91.15	91.68	91.65	91.85	91.30	91.91	91.72
Fa	9.91	9.37	8.73	8.73	8.16	8.19	8.02	8.59	7.96	8.12
Tp	0.17	0.13	0.12	0.12	0.16	0.16	0.13	0.11	0.13	0.16

Diavik Olivine Microprobe Analyses

	A44 (M)	**A44 (M)**	**A44 (P)**	**A44 (P)**	**A44 (P)**	**A44 (P)**	**A44 (P)**	**A44 (P)**	**A5 (M)**	**A5 (M)**
SiO_2	40.58	40.56	40.91	40.93	41.05	41.02	41.38	41.13	40.68	41.00
TiO_2	0.01	0.03	0.02	0.00	0.01	0.01	0.01	0.01	0.02	0.01
Al_2O_3	0.01	0.00	0.00	0.00	0.01	0.00	0.04	0.00	0.55	0.00
Cr_2O_3	0.02	0.02	0.05	0.07	0.04	0.06	0.04	0.05	0.08	0.05
FeO	8.92	8.85	7.59	7.76	7.58	7.83	8.03	7.90	8.75	8.04
MnO	0.18	0.16	0.09	0.12	0.09	0.10	0.12	0.12	0.11	0.16
MgO	48.99	48.91	50.20	50.14	49.95	50.27	48.73	50.32	49.57	50.15
NiO	0.19	0.16	0.35	0.35	0.33	0.38	0.42	0.37	0.42	0.23
CaO	0.18	0.18	0.04	0.06	0.04	0.05	0.08	0.11	0.21	0.12
TOTAL	99.07	98.87	99.26	99.41	99.10	99.72	98.85	100.00	100.39	99.77
Si	1.0020	1.0029	1.0011	1.0010	1.0053	1.0005	1.0175	1.0010	0.9916	1.0006
Ti	0.0001	0.0005	0.0003	0.0000	0.0002	0.0002	0.0001	0.0002	0.0003	0.0002
Al	0.0002	0.0001	0.0000	0.0000	0.0001	0.0000	0.0011	0.0000	0.0159	0.0000
Cr	0.0004	0.0003	0.0010	0.0013	0.0008	0.0011	0.0008	0.0010	0.0016	0.0010
Fe(ii)	0.1841	0.1830	0.1552	0.1586	0.1553	0.1596	0.1650	0.1607	0.1783	0.1642
Mn	0.0037	0.0034	0.0019	0.0025	0.0019	0.0021	0.0024	0.0025	0.0022	0.0033
Mg	1.8032	1.8030	1.8314	1.8283	1.8239	1.8277	1.7861	1.8257	1.8011	1.8249
Ni	0.0038	0.0032	0.0069	0.0068	0.0064	0.0075	0.0084	0.0072	0.0083	0.0045
Ca	0.0049	0.0048	0.0012	0.0015	0.0011	0.0013	0.0021	0.0028	0.0054	0.0032
TOTAL	3.0024	3.0012	2.9992	2.9999	2.9951	3.0000	2.9835	3.0011	3.0048	3.0018
Endmembers										
Fo	90.57	90.63	92.10	91.90	92.07	91.87	91.43	91.80	90.89	91.59
Fa	9.25	9.20	7.81	7.97	7.84	8.02	8.45	8.08	9.00	8.24
Tp	0.19	0.17	0.10	0.12	0.09	0.11	0.12	0.12	0.11	0.17

Diavik Olivine Microprobe Analyses

	A5 (M)	**A5 (M)**	**A5 (M)**	**A5 (M)**	**A5 (M)**	**A5 (M)**	**A5 (M)**	**A5 (M)**	**A5 (P)**	**A5 (P)**
SiO_2	41.19	41.18	40.66	40.70	40.38	40.21	40.39	40.67	40.82	40.82
TiO_2	0.02	0.02	0.01	0.01	0.00	0.02	0.01	0.00	0.02	0.02
Al_2O_3	0.30	0.01	0.02	0.03	0.07	0.13	0.11	0.02	0.06	0.00
Cr_2O_3	0.06	0.09	0.05	0.08	0.06	0.05	0.05	0.08	0.03	0.05
FeO	8.08	8.50	8.94	9.46	9.21	8.05	10.01	7.99	8.52	8.49
MnO	0.14	0.12	0.11	0.10	0.12	0.11	0.20	0.14	0.11	0.10
MgO	50.21	49.90	48.87	48.89	48.43	48.22	48.00	48.81	49.51	49.17
NiO	0.34	0.35	0.39	0.41	0.40	0.39	0.13	0.41	0.38	0.39
CaO	0.08	0.07	0.10	0.08	0.08	0.07	0.26	0.08	0.05	0.06
TOTAL	100.40	100.24	99.15	99.75	98.74	97.26	99.15	98.20	99.51	99.09
Si	0.9985	1.0019	1.0028	1.0001	1.0016	1.0068	1.0020	1.0082	1.0009	1.0047
Ti	0.0003	0.0004	0.0002	0.0001	0.0000	0.0003	0.0001	0.0000	0.0004	0.0003
Al	0.0087	0.0003	0.0006	0.0009	0.0020	0.0040	0.0032	0.0006	0.0018	0.0000
Cr	0.0011	0.0016	0.0010	0.0015	0.0011	0.0010	0.0010	0.0015	0.0007	0.0009
Fe(ii)	0.1637	0.1730	0.1843	0.1944	0.1910	0.1686	0.2076	0.1656	0.1746	0.1747
Mn	0.0028	0.0024	0.0023	0.0020	0.0024	0.0024	0.0042	0.0030	0.0023	0.0020
Mg	1.8147	1.8101	1.7971	1.7913	1.7907	1.7996	1.7751	1.8037	1.8094	1.8042
Ni	0.0067	0.0069	0.0078	0.0081	0.0080	0.0078	0.0026	0.0082	0.0076	0.0078
Ca	0.0019	0.0019	0.0027	0.0022	0.0022	0.0020	0.0068	0.0020	0.0013	0.0016
TOTAL	2.9983	2.9986	2.9989	3.0007	2.9990	2.9924	3.0026	2.9928	2.9989	2.9961
Endmembers										
Fo	91.60	91.17	90.59	90.12	90.25	91.32	89.34	91.45	91.09	91.08
Fa	8.26	8.71	9.29	9.78	9.63	8.55	10.45	8.40	8.79	8.82
Tp	0.14	0.12	0.12	0.10	0.12	0.12	0.21	0.15	0.12	0.10

Diavik Olivine Microprobe Analyses

	A5 (P)	**A5 (M)**	**A5 (M)**	**A5 (M)**	**A5 (M)**	**A5 (M)**	**A5 (M)**	**A5 (M)**	**A5 (M)**	**A5 (MP)**
SiO_2	40.83	39.89	39.98	41.02	41.18	40.58	40.65	40.30	40.45	40.94
TiO_2	0.01	0.01	0.02	0.02	0.01	0.00	0.00	0.00	0.04	0.02
Al_2O_3	0.01	0.01	0.00	0.00	0.01	0.00	0.05	0.08	0.02	0.00
Cr_2O_3	0.01	0.03	0.01	0.01	0.03	0.03	0.03	0.08	0.03	0.06
FeO	8.57	8.79	8.61	8.68	8.90	7.91	7.82	7.73	7.93	8.19
MnO	0.13	0.11	0.11	0.12	0.10	0.14	0.08	0.11	0.10	0.12
MgO	49.18	47.98	48.35	49.61	49.54	48.94	48.94	49.55	48.88	49.54
NiO	0.39	0.36	0.39	0.40	0.38	0.41	0.34	0.30	0.37	0.37
CaO	0.03	0.03	0.03	0.04	0.04	0.07	0.04	0.06	0.02	0.08
TOTAL	99.15	97.20	97.49	99.90	100.18	98.07	97.95	98.21	97.84	99.31
Si	1.0045	1.0028	1.0015	1.0021	1.0037	1.0069	1.0083	0.9982	1.0055	1.0041
Ti	0.0002	0.0002	0.0003	0.0004	0.0002	0.0000	0.0000	0.0000	0.0007	0.0003
Al	0.0002	0.0002	0.0000	0.0000	0.0001	0.0000	0.0013	0.0024	0.0006	0.0001
Cr	0.0001	0.0006	0.0003	0.0003	0.0006	0.0006	0.0006	0.0015	0.0006	0.0011
Fe(ii)	0.1762	0.1848	0.1804	0.1773	0.1813	0.1640	0.1622	0.1600	0.1648	0.1679
Mn	0.0028	0.0023	0.0023	0.0024	0.0020	0.0029	0.0017	0.0023	0.0021	0.0025
Mg	1.8036	1.7984	1.8055	1.8071	1.8003	1.8100	1.8097	1.8295	1.8114	1.8116
Ni	0.0077	0.0073	0.0078	0.0078	0.0074	0.0082	0.0068	0.0060	0.0073	0.0073
Ca	0.0008	0.0007	0.0007	0.0010	0.0011	0.0018	0.0010	0.0015	0.0006	0.0020
TOTAL	2.9960	2.9973	2.9987	2.9984	2.9968	2.9945	2.9917	3.0014	2.9938	2.9970
Endmembers										
Fo	90.97	90.58	90.81	90.96	90.76	91.55	91.69	91.85	91.56	91.40
Fa	8.89	9.31	9.07	8.92	9.14	8.30	8.22	8.03	8.33	8.47
Tp	0.14	0.12	0.11	0.12	0.10	0.15	0.09	0.11	0.10	0.13

Diavik Olivine Microprobe Analyses

	A5 (MP)	**A5 (MP)**	**A5 (MP)**	**A5 (MP)**	**A5 (P)**	**A5 (P)**	**A5 (P)**	**A5 (P)**	**A5 (P)**	**A5 (P)**
SiO_2	40.88	39.80	40.79	40.81	41.19	41.24	41.31	41.49	41.81	42.37
TiO_2	0.02	0.02	0.03	0.05	0.04	0.04	0.03	0.00	0.00	0.00
Al_2O_3	0.01	0.00	0.00	0.03	0.15	0.00	0.01	0.00	0.00	0.01
Cr_2O_3	0.05	0.03	0.00	0.03	0.03	0.03	0.04	0.02	0.04	0.03
FeO	8.06	9.04	9.77	10.01	8.02	8.08	8.12	7.54	7.69	7.44
MnO	0.12	0.19	0.22	0.20	0.11	0.09	0.11	0.07	0.09	0.08
MgO	50.09	47.62	48.31	48.60	50.75	50.44	50.69	50.32	50.39	50.56
NiO	0.39	0.14	0.06	0.07	0.36	0.37	0.34	0.39	0.38	0.38
CaO	0.09	0.24	0.38	0.35	0.04	0.05	0.07	0.03	0.04	0.04
TOTAL	99.70	97.09	99.58	100.14	100.69	100.33	100.70	99.86	100.43	100.90
Si	0.9990	1.0044	1.0067	1.0025	0.9955	1.0005	0.9988	1.0077	1.0100	1.0162
Ti	0.0003	0.0005	0.0006	0.0009	0.0007	0.0007	0.0005	0.0000	0.0000	0.0000
Al	0.0003	0.0000	0.0001	0.0008	0.0043	0.0000	0.0002	0.0000	0.0000	0.0003
Cr	0.0010	0.0007	0.0000	0.0006	0.0006	0.0005	0.0007	0.0004	0.0008	0.0006
Fe(ii)	0.1647	0.1908	0.2017	0.2056	0.1622	0.1638	0.1641	0.1531	0.1553	0.1491
Mn	0.0024	0.0041	0.0046	0.0042	0.0022	0.0019	0.0023	0.0015	0.0018	0.0015
Mg	1.8248	1.7915	1.7777	1.7799	1.8288	1.8240	1.8270	1.8217	1.8144	1.8081
Ni	0.0076	0.0029	0.0012	0.0015	0.0070	0.0072	0.0066	0.0077	0.0075	0.0073
Ca	0.0023	0.0064	0.0101	0.0092	0.0011	0.0012	0.0017	0.0008	0.0009	0.0010
TOTAL	3.0024	3.0012	3.0027	3.0051	3.0025	2.9997	3.0020	2.9929	2.9906	2.9842
Endmembers										
Fo	91.61	90.19	89.60	89.46	91.75	91.67	91.65	92.18	92.03	92.31
Fa	8.27	9.61	10.17	10.33	8.14	8.23	8.23	7.75	7.88	7.61
Tp	0.12	0.21	0.23	0.21	0.11	0.09	0.12	0.07	0.09	0.08

Diavik Olivine Microprobe Analyses

	A5 (P)	**GTH (M)**	**GTH (M)**	**GTH (M)**	**GTH (M)**	**GTH (M)**	**GTH (M)**	**GTH (M)**	**GTH (M)**	**GTH (M)**
SiO_2	41.10	41.08	41.17	41.14	40.57	40.43	40.97	41.18	40.59	40.93
TiO_2	0.01	0.01	0.00	0.01	0.02	0.02	0.03	0.02	0.03	0.04
Al_2O_3	0.00	0.00	0.00	0.00	0.00	0.00	0.00	0.00	0.00	0.00
Cr_2O_3	0.03	0.04	0.04	0.03	0.04	0.05	0.03	0.04	0.02	0.01
FeO	7.37	8.56	8.58	8.53	8.47	8.86	9.10	8.93	10.47	10.79
MnO	0.10	0.12	0.11	0.10	0.10	0.07	0.12	0.09	0.11	0.10
MgO	50.37	49.97	49.69	50.11	48.98	48.11	49.25	49.37	48.60	48.68
NiO	0.35	0.36	0.39	0.36	0.38	0.37	0.32	0.36	0.34	0.34
CaO	0.03	0.02	0.02	0.03	0.04	0.05	0.04	0.04	0.04	0.03
TOTAL	99.35	100.16	99.99	100.31	98.60	97.95	99.86	100.02	100.20	100.92
Si	1.0033	1.0003	1.0038	1.0001	1.0036	1.0081	1.0030	1.0052	0.9971	0.9989
Ti	0.0001	0.0002	0.0000	0.0001	0.0003	0.0004	0.0005	0.0003	0.0005	0.0008
Al	0.0000	0.0000	0.0000	0.0000	0.0000	0.0000	0.0000	0.0000	0.0000	0.0000
Cr	0.0005	0.0008	0.0007	0.0006	0.0007	0.0009	0.0005	0.0008	0.0003	0.0001
Fe(ii)	0.1505	0.1744	0.1749	0.1734	0.1752	0.1848	0.1862	0.1822	0.2150	0.2201
Mn	0.0020	0.0024	0.0024	0.0021	0.0022	0.0015	0.0025	0.0018	0.0024	0.0021
Mg	1.8331	1.8141	1.8064	1.8160	1.8062	1.7881	1.7973	1.7965	1.7801	1.7715
Ni	0.0069	0.0070	0.0076	0.0070	0.0076	0.0073	0.0063	0.0071	0.0067	0.0067
Ca	0.0009	0.0006	0.0005	0.0008	0.0010	0.0012	0.0011	0.0010	0.0012	0.0008
TOTAL	2.9972	2.9997	2.9963	3.0002	2.9968	2.9923	2.9973	2.9950	3.0034	3.0011
Endmembers										
Fo	92.32	91.12	91.06	91.19	91.06	90.57	90.50	90.71	89.12	88.85
Fa	7.58	8.76	8.82	8.71	8.83	9.36	9.38	9.20	10.77	11.04
Tp	0.10	0.12	0.12	0.11	0.11	0.07	0.13	0.09	0.12	0.11

Diavik Olivine Microprobe Analyses

	GTH (M)	GTH (M)	GTH (M)	GTH (M)	GTH (M)	GTH (M)	GTH (M)	GTH (M)	GTH (M)	GTH (M)
SiO_2	40.77	40.90	40.79	41.40	40.75	40.86	40.77	40.97	40.93	40.88
TiO_2	0.04	0.06	0.02	0.02	0.01	0.01	0.02	0.02	0.03	0.02
Al_2O_3	0.00	0.00	0.00	0.00	0.00	0.00	0.00	0.00	0.00	0.00
Cr_2O_3	0.01	0.02	0.03	0.04	0.02	0.02	0.03	0.04	0.10	0.01
FeO	10.80	10.71	8.22	8.20	9.09	8.39	8.66	9.14	9.31	8.40
MnO	0.14	0.09	0.09	0.10	0.10	0.11	0.11	0.11	0.11	0.11
MgO	48.52	48.63	49.21	50.49	49.40	49.51	49.18	49.48	49.17	49.90
NiO	0.35	0.34	0.40	0.40	0.36	0.34	0.35	0.36	0.28	0.33
CaO	0.02	0.04	0.02	0.03	0.00	0.05	0.05	0.04	0.04	0.03
TOTAL	100.65	100.77	98.77	100.69	99.74	99.30	99.17	100.16	99.95	99.68
Si	0.9983	0.9993	1.0054	1.0012	0.9989	1.0029	1.0032	1.0004	1.0019	0.9997
Ti	0.0007	0.0010	0.0003	0.0003	0.0003	0.0002	0.0004	0.0004	0.0005	0.0003
Al	0.0000	0.0000	0.0000	0.0000	0.0000	0.0001	0.0000	0.0000	0.0000	0.0000
Cr	0.0002	0.0003	0.0006	0.0008	0.0004	0.0004	0.0006	0.0007	0.0019	0.0002
Fe(ii)	0.2212	0.2188	0.1694	0.1658	0.1863	0.1722	0.1782	0.1866	0.1905	0.1717
Mn	0.0028	0.0019	0.0018	0.0020	0.0022	0.0023	0.0023	0.0024	0.0023	0.0023
Mg	1.7708	1.7715	1.8084	1.8202	1.8054	1.8118	1.8043	1.8014	1.7941	1.8193
Ni	0.0070	0.0066	0.0080	0.0079	0.0070	0.0067	0.0069	0.0070	0.0055	0.0065
Ca	0.0006	0.0009	0.0005	0.0009	0.0000	0.0014	0.0012	0.0010	0.0009	0.0009
TOTAL	3.0016	3.0004	2.9944	2.9990	3.0006	2.9980	2.9972	2.9999	2.9976	3.0008
Endmembers										
Fo	88.77	88.92	91.35	91.56	90.55	91.22	90.90	90.51	90.30	91.27
Fa	11.09	10.98	8.56	8.34	9.34	8.67	8.98	9.38	9.59	8.62
Tp	0.14	0.10	0.09	0.10	0.11	0.11	0.12	0.12	0.11	0.11

Diavik Olivine Microprobe Analyses

	GTH (M)	**GTH (M)**	**GTH (M)**	**GTH (M)**	**GTH (M)**	**GTH (M)**	**GTH (MP)**	**GTH (MP)**	**GTH (MP)**	**GTH (MP)**
SiO_2	40.86	40.90	40.96	40.85	40.45	40.58	40.53	40.53	40.45	40.56
TiO_2	0.02	0.03	0.02	0.01	0.00	0.02	0.01	0.00	0.04	0.03
Al_2O_3	0.00	0.00	0.00	0.00	0.00	0.00	0.00	0.00	0.00	0.00
Cr_2O_3	0.01	0.02	0.02	0.02	0.02	0.01	0.00	0.05	0.01	0.03
FeO	8.18	8.39	8.20	8.26	11.77	11.77	11.69	8.68	11.33	10.49
MnO	0.12	0.12	0.10	0.10	0.16	0.16	0.14	0.11	0.13	0.12
MgO	49.71	49.56	49.47	49.58	47.49	47.78	47.37	49.07	48.13	48.52
NiO	0.33	0.34	0.36	0.32	0.21	0.22	0.25	0.39	0.36	0.34
CaO	0.03	0.04	0.01	0.03	0.04	0.02	0.03	0.05	0.06	0.04
TOTAL	99.26	99.40	99.14	99.16	100.14	100.55	100.01	98.87	100.51	100.14
Si	1.0023	1.0028	1.0053	1.0031	0.9996	0.9984	1.0021	1.0011	0.9951	0.9972
Ti	0.0003	0.0006	0.0004	0.0002	0.0000	0.0003	0.0002	0.0000	0.0007	0.0006
Al	0.0000	0.0000	0.0000	0.0000	0.0000	0.0000	0.0000	0.0000	0.0000	0.0000
Cr	0.0002	0.0003	0.0004	0.0003	0.0004	0.0002	0.0000	0.0009	0.0002	0.0006
Fe(ii)	0.1677	0.1720	0.1682	0.1697	0.2433	0.2422	0.2417	0.1793	0.2331	0.2157
Mn	0.0025	0.0025	0.0020	0.0020	0.0033	0.0033	0.0028	0.0023	0.0027	0.0024
Mg	1.8178	1.8115	1.8104	1.8149	1.7493	1.7524	1.7459	1.8071	1.7653	1.7786
Ni	0.0066	0.0068	0.0072	0.0062	0.0043	0.0044	0.0050	0.0078	0.0071	0.0068
Ca	0.0007	0.0009	0.0002	0.0007	0.0009	0.0004	0.0008	0.0013	0.0017	0.0011
TOTAL	2.9980	2.9974	2.9942	2.9972	3.0011	3.0016	2.9985	2.9997	3.0058	3.0030
Endmembers										
Fo	91.44	91.22	91.40	91.36	87.65	87.71	87.71	90.87	88.22	89.07
Fa	8.43	8.66	8.49	8.54	12.19	12.12	12.14	9.01	11.65	10.80
Tp	0.13	0.12	0.10	0.10	0.17	0.17	0.14	0.12	0.14	0.12

Diavik Olivine Microprobe Analyses

	GTH (MF)	GTH (MF)	GTH (MF)	GTH (MF)	GTH (MF)	GTH (MF)	GTH (MF)	GTH (M)	GTH (M)	GTH (M)
SiO_2	40.38	40.68	40.66	40.77	40.15	39.64	41.24	39.60	40.60	40.41
TiO_2	0.05	0.02	0.04	0.02	0.03	0.02	0.03	0.01	0.02	0.02
Al_2O_3	0.00	0.01	0.00	0.00	0.04	0.00	0.01	0.00	0.00	0.01
Cr_2O_3	0.00	0.01	0.00	0.01	0.02	0.01	0.02	0.00	0.04	0.04
FeO	10.63	10.47	10.64	10.58	10.02	10.05	7.99	10.33	9.59	9.31
MnO	0.14	0.15	0.17	0.15	0.13	0.13	0.08	0.16	0.12	0.12
MgO	48.29	48.45	48.38	48.55	48.61	47.41	50.80	48.01	48.91	48.62
NiO	0.31	0.34	0.30	0.31	0.35	0.36	0.30	0.29	0.33	0.34
CaO	0.03	0.04	0.06	0.05	0.04	0.03	0.01	0.06	0.08	0.06
TOTAL	99.83	100.16	100.25	100.43	99.38	97.66	100.47	98.45	99.69	98.93
Si	0.9966	0.9995	0.9992	0.9994	0.9935	0.9984	0.9982	0.9913	0.9988	1.0005
Ti	0.0009	0.0004	0.0007	0.0004	0.0005	0.0005	0.0005	0.0002	0.0003	0.0004
Al	0.0000	0.0002	0.0000	0.0000	0.0010	0.0000	0.0001	0.0000	0.0000	0.0004
Cr	0.0000	0.0002	0.0000	0.0002	0.0003	0.0002	0.0003	0.0000	0.0008	0.0008
Fe(ii)	0.2194	0.2151	0.2185	0.2168	0.2074	0.2117	0.1616	0.2161	0.1974	0.1926
Mn	0.0029	0.0030	0.0035	0.0032	0.0026	0.0028	0.0017	0.0033	0.0025	0.0025
Mg	1.7765	1.7748	1.7723	1.7741	1.7930	1.7802	1.8329	1.7917	1.7941	1.7946
Ni	0.0062	0.0067	0.0059	0.0062	0.0069	0.0073	0.0059	0.0059	0.0066	0.0068
Ca	0.0007	0.0011	0.0015	0.0012	0.0011	0.0008	0.0003	0.0015	0.0021	0.0015
TOTAL	3.0032	3.0009	3.0016	3.0014	3.0064	3.0019	3.0014	3.0100	3.0026	3.0001
Endmembers										
Fo	88.88	89.05	88.87	88.97	89.52	89.25	91.82	89.09	89.98	90.20
Fa	10.98	10.79	10.96	10.87	10.35	10.61	8.10	10.75	9.90	9.68
Tp	0.14	0.15	0.17	0.16	0.13	0.14	0.08	0.16	0.13	0.12

Diavik Olivine Microprobe Analyses

	GTH (M)	GTH (M)	GTH (M)	GTH (M)	GTH (M)	GTH (P)	GTH (P)	GTH (MP)	GTH (MP)	GTH (MP)
SiO_2	40.56	40.18	40.90	40.87	41.14	40.75	40.89	39.50	39.85	39.04
TiO_2	0.00	0.02	0.02	0.01	0.19	0.03	0.02	0.02	0.03	0.05
Al_2O_3	0.01	0.00	0.00	0.01	0.14	0.00	0.00	0.01	0.01	0.00
Cr_2O_3	0.02	0.07	0.05	0.06	0.00	0.06	0.04	0.07	0.06	0.02
FeO	9.36	9.30	9.24	9.11	2.60	9.11	9.04	8.50	9.19	9.38
MnO	0.10	0.11	0.11	0.12	0.27	0.11	0.11	0.12	0.13	0.14
MgO	49.13	48.47	49.41	49.66	53.79	49.68	49.54	48.03	48.12	47.22
NiO	0.37	0.34	0.34	0.38	0.04	0.36	0.35	0.38	0.33	0.34
CaO	0.07	0.08	0.07	0.09	1.38	0.04	0.04	0.18	0.11	0.09
TOTAL	99.62	98.56	100.14	100.30	99.56	100.12	100.01	96.80	97.82	96.28
Si	0.9977	0.9990	0.9996	0.9974	0.9947	0.9959	0.9995	0.9986	0.9987	0.9958
Ti	0.0001	0.0004	0.0004	0.0002	0.0035	0.0005	0.0004	0.0003	0.0005	0.0010
Al	0.0001	0.0000	0.0000	0.0002	0.0040	0.0000	0.0000	0.0002	0.0003	0.0000
Cr	0.0004	0.0013	0.0009	0.0011	0.0000	0.0011	0.0009	0.0013	0.0011	0.0003
Fe(ii)	0.1926	0.1933	0.1889	0.1859	0.0526	0.1861	0.1848	0.1796	0.1925	0.2000
Mn	0.0022	0.0022	0.0022	0.0025	0.0056	0.0023	0.0022	0.0025	0.0028	0.0030
Mg	1.8016	1.7967	1.8006	1.8070	1.9388	1.8101	1.8053	1.8101	1.7976	1.7958
Ni	0.0073	0.0069	0.0067	0.0074	0.0007	0.0070	0.0068	0.0077	0.0066	0.0070
Ca	0.0019	0.0022	0.0017	0.0022	0.0358	0.0010	0.0009	0.0048	0.0030	0.0025
TOTAL	3.0039	3.0021	3.0012	3.0040	3.0356	3.0040	3.0007	3.0051	3.0031	3.0054
Endmembers										
Fo	90.25	90.18	90.40	90.56	97.08	90.57	90.62	90.86	90.20	89.84
Fa	9.65	9.70	9.49	9.32	2.64	9.31	9.27	9.01	9.66	10.01
Tp	0.11	0.11	0.11	0.13	0.28	0.11	0.11	0.12	0.14	0.15

Diavik Olivine Microprobe Analyses

	GTH (M)	GTH (M)	GTH (M)	GTH (MF)	GTH (MF)	GTH (MF)	GTH (MF)	GTH (MF)	A5 (P)	A5 (P)
SiO_2	41.19	40.81	40.49	40.00	39.92	40.84	40.74	40.38	40.25	40.61
TiO_2	0.00	0.02	0.03	0.00	0.00	0.00	0.03	0.02	0.00	0.00
Al_2O_3	0.00	0.00	0.00	0.00	0.00	0.00	0.00	0.01	0.01	0.00
Cr_2O_3	0.04	0.05	0.03	0.03	0.03	0.03	0.05	0.08	0.05	0.03
FeO	7.52	7.71	7.68	7.55	7.39	8.13	8.17	8.73	8.84	8.09
MnO	0.11	0.14	0.10	0.10	0.11	0.09	0.11	0.12	0.13	0.13
MgO	51.18	51.27	50.95	49.13	48.94	50.58	50.34	49.78	49.83	50.25
NiO	0.37	0.36	0.35	0.29	0.32	0.35	0.33	0.39	0.37	0.32
CaO	0.02	0.03	0.01	0.03	0.03	0.06	0.04	0.15	0.05	0.11
TOTAL	100.43	100.38	99.64	97.14	96.73	100.09	99.79	99.65	99.54	99.54
Si	0.9961	0.9895	0.9887	1.0006	1.0021	0.9943	0.9948	0.9919	0.9897	0.9946
Ti	0.0000	0.0003	0.0006	0.0000	0.0000	0.0001	0.0005	0.0004	0.0000	0.0000
Al	0.0000	0.0000	0.0000	0.0000	0.0000	0.0000	0.0000	0.0003	0.0003	0.0000
Cr	0.0008	0.0010	0.0006	0.0007	0.0005	0.0006	0.0010	0.0016	0.0010	0.0006
Fe(ii)	0.1521	0.1563	0.1568	0.1579	0.1551	0.1655	0.1667	0.1794	0.1818	0.1657
Mn	0.0022	0.0028	0.0022	0.0020	0.0023	0.0019	0.0023	0.0024	0.0027	0.0028
Mg	1.8451	1.8529	1.8547	1.8320	1.8312	1.8360	1.8325	1.8230	1.8269	1.8350
Ni	0.0071	0.0070	0.0069	0.0059	0.0064	0.0069	0.0064	0.0077	0.0074	0.0064
Ca	0.0006	0.0007	0.0003	0.0009	0.0009	0.0016	0.0009	0.0038	0.0014	0.0029
TOTAL	3.0041	3.0104	3.0107	3.0000	2.9985	3.0070	3.0051	3.0106	3.0111	3.0079
Endmembers										
Fo	92.28	92.09	92.11	91.97	92.09	91.64	91.56	90.93	90.83	91.59
Fa	7.61	7.77	7.79	7.93	7.80	8.26	8.33	8.95	9.04	8.27
Tp	0.11	0.14	0.11	0.10	0.11	0.10	0.11	0.12	0.13	0.14

Diavik Olivine Microprobe Analyses

	A5 (M)	**A5 (M)**	**A5 (M)**	**A5 (M)**	**A5 (M)**	**A5 (M)**	**A5 (M)**	**A4 (P)**	**A4 (M)**	**A4 (M)**	**A4 (P)**
SiO_2	40.83	40.85	40.93	40.78	40.89	39.79	39.81	40.37	41.23	40.31	40.57
TiO_2	0.03	0.02	0.04	0.02	0.04	0.02	0.04	0.03	0.01	0.01	0.02
Al_2O_3	0.00	0.00	0.00	0.00	0.00	0.00	0.01	0.00	0.00	0.00	0.00
Cr_2O_3	0.05	0.05	0.01	0.03	0.03	0.01	0.00	0.05	0.04	0.06	0.06
FeO	7.51	7.29	7.35	7.36	7.29	9.58	9.50	8.97	7.20	8.99	9.90
MnO	0.09	0.08	0.07	0.09	0.09	0.12	0.14	0.10	0.09	0.16	0.14
MgO	51.07	51.08	51.50	51.09	51.09	48.27	48.58	50.33	51.51	49.44	48.33
NiO	0.38	0.40	0.38	0.39	0.39	0.31	0.34	0.40	0.34	0.14	0.29
CaO	0.04	0.03	0.02	0.03	0.04	0.02	0.03	0.06	0.01	0.09	0.10
TOTAL	100.00	99.79	100.29	99.79	99.85	98.11	98.46	100.30	100.42	99.19	99.40
Si	0.9924	0.9937	0.9910	0.9926	0.9941	0.9951	0.9924	0.9859	0.9954	0.9942	1.0022
Ti	0.0006	0.0003	0.0006	0.0003	0.0007	0.0005	0.0007	0.0006	0.0001	0.0002	0.0004
Al	0.0000	0.0000	0.0000	0.0000	0.0000	0.0000	0.0004	0.0000	0.0000	0.0001	0.0001
Cr	0.0010	0.0009	0.0002	0.0006	0.0006	0.0002	0.0000	0.0010	0.0007	0.0011	0.0012
Fe(ii)	0.1526	0.1484	0.1488	0.1498	0.1481	0.2003	0.1981	0.1832	0.1453	0.1853	0.2045
Mn	0.0019	0.0017	0.0014	0.0018	0.0019	0.0026	0.0029	0.0020	0.0019	0.0034	0.0029
Mg	1.8506	1.8526	1.8588	1.8539	1.8520	1.7996	1.8055	1.8325	1.8541	1.8180	1.7799
Ni	0.0074	0.0078	0.0074	0.0077	0.0075	0.0061	0.0067	0.0078	0.0065	0.0027	0.0057
Ca	0.0011	0.0008	0.0004	0.0007	0.0010	0.0004	0.0009	0.0015	0.0001	0.0023	0.0025
TOTAL	3.0076	3.0063	3.0087	3.0075	3.0059	3.0047	3.0076	3.0145	3.0042	3.0073	2.9993
Endmembers											
Fo	92.29	92.51	92.52	92.44	92.51	89.87	89.99	90.82	92.65	90.60	89.57
Fa	7.61	7.41	7.41	7.47	7.40	10.00	9.87	9.08	7.26	9.24	10.29
Tp	0.09	0.08	0.07	0.09	0.10	0.13	0.14	0.10	0.09	0.17	0.14

Diavik Spinel Microprobe Analyses

	A154	A154	A154	A154	A154	A154	A154
SiO_2	0.00	0.00	0.00	0.00	0.00	0.00	0.00
TiO_2	2.95	3.53	4.84	3.21	3.34	2.71	3.09
Al_2O_3	5.93	6.45	5.22	12.80	12.78	14.31	13.69
Cr_2O_3	56.33	54.34	51.88	48.00	48.64	46.66	45.73
V_2O_3	0.00	0.00	0.00	0.00	0.00	0.00	0.00
FeO	20.69	21.56	23.52	19.77	19.94	19.86	20.31
MnO	0.50	0.46	0.54	0.36	0.30	0.41	0.45
MgO	12.36	13.42	13.82	13.67	14.64	14.34	14.34
CaO	0.03	0.02	0.03	0.05	0.05	0.04	0.04
ZnO	0.00	0.00	0.00	0.00	0.00	0.00	0.00
TOTAL	98.82	99.80	99.87	97.88	99.72	98.36	97.71
SiO_2	0.00	0.00	0.00	0.00	0.00	0.00	0.00
TiO_2	2.95	3.53	4.84	3.21	3.34	2.71	3.09
Al_2O_3	5.93	6.45	5.22	12.80	12.78	14.31	13.69
Cr_2O_3	56.33	54.34	51.88	48.00	48.64	46.66	45.73
V_2O_3	0.00	0.00	0.00	0.00	0.00	0.00	0.00
Fe_2O_3	5.31	6.96	8.76	5.25	6.24	6.57	7.11
FeO	15.91	15.29	15.63	15.04	14.32	13.94	13.95
MnO	0.50	0.46	0.54	0.36	0.30	0.41	0.45
MgO	12.36	13.42	13.82	13.67	14.64	14.34	14.34
CaO	0.03	0.02	0.03	0.05	0.05	0.04	0.04
ZnO	0.00	0.00	0.00	0.00	0.00	0.00	0.00
TOTAL	99.35	100.50	100.75	98.41	100.34	99.01	98.42
Formula							
Si	0.000	0.000	0.000	0.000	0.000	0.000	0.000
Ti	0.099	0.116	0.159	0.104	0.106	0.087	0.100
Al	0.311	0.332	0.269	0.651	0.635	0.716	0.691
Cr	1.980	1.874	1.791	1.637	1.621	1.567	1.548
V	0.000	0.000	0.000	0.000	0.000	0.000	0.000
Fe(ii)	0.769	0.787	0.859	0.713	0.703	0.705	0.728
Mn	0.019	0.017	0.020	0.013	0.011	0.015	0.016
Mg	0.820	0.873	0.900	0.879	0.921	0.908	0.915
Ca	0.002	0.001	0.002	0.002	0.003	0.002	0.002
Zn	0.000	0.000	0.000	0.000	0.000	0.000	0.000
TOTAL	4.000	4.000	4.000	4.000	4.000	4.000	4.000
Fe/Fe+Mg	0.48	0.47	0.48	0.44	0.43	0.43	0.44
Cr/Cr+Al	0.86	0.84	0.86	0.71	0.71	0.68	0.69
Mg:Fe	1.06	1.10	1.04	1.23	1.30	1.28	1.25
Ti/(Ti+Cr+Al)	0.04	0.04	0.07	0.04	0.04	0.03	0.04
Fe(ii)	0.592	0.558	0.571	0.543	0.505	0.495	0.499
Fe(iii)	0.177	0.228	0.288	0.171	0.198	0.210	0.229

Diavik Spinel Microprobe Analyses

	A154	A154	A154	A154	A154	A154	A154
SiO_2	0.00	0.00	0.00	0.00	0.00	0.00	0.00
TiO_2	3.20	3.36	3.13	6.71	3.71	3.50	4.93
Al_2O_3	12.50	12.67	12.47	7.51	11.53	8.25	6.34
Cr_2O_3	48.20	48.47	49.42	41.58	49.92	52.69	47.43
V_2O_3	0.00	0.00	0.00	0.00	0.00	0.00	0.00
FeO	20.07	19.74	19.96	26.38	20.51	21.42	26.14
MnO	0.38	0.30	0.37	0.62	0.41	0.47	0.56
MgO	13.58	14.26	14.14	14.72	14.64	13.00	12.99
CaO	0.01	0.02	0.01	0.02	0.03	0.05	0.04
ZnO	0.00	0.00	0.00	0.00	0.00	0.00	0.00
TOTAL	97.97	98.85	99.52	97.59	100.79	99.40	98.45
SiO_2	0.00	0.00	0.00	0.00	0.00	0.00	0.00
TiO_2	3.20	3.36	3.13	6.71	3.71	3.50	4.93
Al_2O_3	12.50	12.67	12.47	7.51	11.53	8.25	6.34
Cr_2O_3	48.20	48.47	49.42	41.58	49.92	52.69	47.43
V_2O_3	0.00	0.00	0.00	0.00	0.00	0.00	0.00
Fe_2O_3	5.44	5.64	5.77	12.05	6.42	6.01	10.49
FeO	15.17	14.67	14.76	15.53	14.72	16.00	16.69
MnO	0.38	0.30	0.37	0.62	0.41	0.47	0.56
MgO	13.58	14.26	14.14	14.72	14.64	13.00	12.99
CaO	0.01	0.02	0.01	0.02	0.03	0.05	0.04
ZnO	0.00	0.00	0.00	0.00	0.00	0.00	0.00
TOTAL	98.52	99.41	100.10	98.79	101.43	100.00	99.50
Formula							
Si	0.000	0.000	0.000	0.000	0.000	0.000	0.000
Ti	0.104	0.108	0.100	0.221	0.117	0.115	0.164
Al	0.636	0.637	0.624	0.388	0.571	0.424	0.331
Cr	1.646	1.634	1.659	1.440	1.658	1.816	1.659
V	0.000	0.000	0.000	0.000	0.000	0.000	0.000
Fe(ii)	0.725	0.704	0.709	0.966	0.721	0.781	0.967
Mn	0.014	0.011	0.013	0.023	0.015	0.017	0.021
Mg	0.874	0.906	0.895	0.961	0.917	0.845	0.857
Ca	0.000	0.001	0.000	0.001	0.001	0.002	0.002
Zn	0.000	0.000	0.000	0.000	0.000	0.000	0.000
TOTAL	4.000	4.000	4.000	4.000	4.000	4.000	4.000
Fe/Fe+Mg	0.45	0.43	0.44	0.50	0.43	0.48	0.53
Cr/Cr+Al	0.72	0.71	0.72	0.78	0.74	0.81	0.83
Mg:Fe	1.20	1.28	1.26	0.99	1.27	1.08	0.88
Ti/(Ti+Cr+Al)	0.04	0.04	0.04	0.10	0.05	0.04	0.07
Fe(ii)	0.548	0.523	0.525	0.569	0.518	0.584	0.618
Fe(iii)	0.176	0.181	0.184	0.397	0.203	0.197	0.349

Diavik Spinel Microprobe Analyses

	A154	A154	A154	A154	A154	A154	T33
SiO_2	0.00	0.00	0.00	0.00	0.00	0.00	0.00
TiO_2	12.52	4.75	3.64	3.49	3.73	5.36	1.94
Al_2O_3	9.37	8.40	9.87	10.63	12.10	5.31	7.24
Cr_2O_3	24.56	46.16	50.77	50.02	48.50	50.67	52.93
V_2O_3	0.00	0.00	0.00	0.00	0.00	0.00	0.00
FeO	36.61	24.87	21.19	20.76	20.45	23.89	23.51
MnO	0.61	0.47	0.43	0.45	0.33	0.55	0.34
MgO	16.54	13.09	14.31	13.50	14.57	11.31	14.58
CaO	0.03	0.07	0.05	0.05	0.05	0.13	0.11
ZnO	0.00	0.00	0.00	0.00	0.00	0.00	0.00
TOTAL	100.25	97.84	100.28	98.93	99.77	97.24	100.68
SiO_2	0.00	0.00	0.00	0.00	0.0	0.00	0.00
TiO_2	12.52	4.75	3.64	3.49	3.73	5.36	1.94
Al_2O_3	9.37	8.40	9.87	10.63	12.10	5.31	7.24
Cr_2O_3	24.56	46.16	50.77	50.02	48.50	50.67	52.93
V_2O_3	0.00	0.00	0.00	0.00	0.00	0.00	0.00
Fe_2O_3	19.28	9.25	7.19	5.87	6.42	5.51	12.15
FeO	19.25	16.54	14.72	15.47	14.66	18.93	12.57
MnO	0.61	0.47	0.43	0.45	0.33	0.55	0.34
MgO	16.54	13.09	14.31	13.50	14.57	11.31	14.58
CaO	0.03	0.07	0.05	0.05	0.05	0.13	0.11
ZnO	0.00	0.00	0.00	0.00	0.00	0.00	0.00
TOTAL	102.18	98.76	101.00	99.51	100.42	97.80	101.89
Formula							
Si	0.000	0.000	0.000	0.000	0.000	0.000	0.000
Ti	0.394	0.157	0.117	0.113	0.119	0.184	0.062
Al	0.462	0.436	0.495	0.541	0.603	0.285	0.364
Cr	0.812	1.609	1.708	1.708	1.622	1.825	1.788
V	0.000	0.000	0.000	0.000	0.000	0.000	0.000
Fe(ii)	1.280	0.917	0.754	0.750	0.723	0.910	0.840
Mn	0.022	0.018	0.016	0.016	0.012	0.021	0.012
Mg	1.031	0.860	0.908	0.869	0.919	0.768	0.929
Ca	0.001	0.003	0.002	0.002	0.002	0.006	0.005
Zn	0.000	0.000	0.000	0.000	0.000	0.000	0.000
TOTAL	4.000	4.000	4.000	4.000	4.000	4.000	4.000
Fe/Fe+Mg	0.55	0.51	0.45	0.46	0.44	0.54	0.47
Cr/Cr+Al	0.63	0.78	0.77	0.75	0.72	0.86	0.83
Mg:Fe	0.80	0.93	1.20	1.15	1.27	0.84	1.10
Ti/(Ti+Cr+Al)	0.23	0.07	0.05	0.04	0.05	0.08	0.02
Fe(ii)	0.673	0.610	0.524	0.559	0.519	0.721	0.450
Fe(iii)	0.606	0.307	0.230	0.191	0.204	0.189	0.390

Diavik Spinel Microprobe Analyses

	T33	T33	T33	T33	T33	T33	T33
SiO_2	0.00	0.00	0.00	0.00	0.00	0.00	0.00
TiO_2	0.95	1.67	1.46	5.76	3.98	4.91	5.55
Al_2O_3	7.68	22.62	27.46	6.05	7.99	5.86	4.71
Cr_2O_3	58.01	35.46	29.17	0.45	0.16	0.12	0.09
V_2O_3	0.00	0.00	0.00	0.00	0.00	0.00	0.00
FeO	19.35	23.15	22.71	64.61	65.74	65.41	66.81
MnO	0.37	0.29	0.28	0.61	0.53	0.63	0.65
MgO	14.34	17.20	18.35	18.92	15.84	15.61	15.49
CaO	0.21	0.27	0.13	0.08	0.60	0.40	0.26
ZnO	0.00	0.00	0.00	0.00	0.00	0.00	0.00
TOTAL	100.94	100.68	99.52	96.50	94.86	92.97	93.60
SiO_2	0.00	0.00	0.00	0.00	0.00	0.00	0.00
TiO_2	0.95	1.67	1.41	5.76	3.98	4.91	5.55
Al_2O_3	7.68	22.62	27.46	6.05	7.99	5.86	4.71
Cr_2O_3	58.01	35.46	29.17	0.45	0.16	0.12	0.09
V_2O_3	0.00	0.00	0.00	0.00	0.00	0.00	0.00
Fe_2O_3	8.17	13.90	14.97	62.41	61.07	60.30	60.81
FeO	12.00	10.64	9.23	8.44	10.78	11.15	12.09
MnO	0.37	0.29	0.28	0.61	0.53	0.63	0.65
MgO	14.34	17.20	18.35	18.92	15.84	15.61	15.49
CaO	0.21	0.27	0.13	0.08	0.60	0.40	0.26
ZnO	0.00	0.00	0.00	0.00	0.00	0.00	0.00
TOTAL	101.76	102.07	101.02	102.75	100.98	99.01	99.69
Formula							
Si	0.000	0.000	0.000	0.000	0.000	0.000	0.000
Ti	0.030	0.050	0.043	0.183	0.130	0.165	0.186
Al	0.386	1.051	1.254	0.301	0.408	0.308	0.248
Cr	1.957	1.105	0.893	0.015	0.005	0.004	0.003
V	0.000	0.000	0.000	0.000	0.000	0.000	0.000
Fe(ii)	0.691	0.763	0.736	2.283	2.385	2.441	2.494
Mn	0.013	0.010	0.009	0.022	0.019	0.024	0.025
Mg	0.912	1.011	1.060	1.192	1.024	1.039	1.031
Ca	0.010	0.011	0.005	0.004	0.028	0.019	0.012
Zn	0.000	0.000	0.000	0.000	0.000	0.000	0.000
TOTAL	4.000	4.000	4.000	4.000	4.000	4.000	4.000
Fe/Fe+Mg	0.43	0.43	0.40	0.65	0.69	0.70	0.70
Cr/Cr+Al	0.83	0.51	0.41	0.04	0.01	0.01	0.01
Mg:Fe	1.32	1.32	1.44	0.52	0.42	0.42	0.41
Ti/(Ti+Cr+Al)	0.01	0.02	0.01	0.36	0.23	0.34	0.42
Fe(ii)	0.428	0.351	0.301	0.299	0.391	0.417	0.452
Fe(iii)	0.262	0.412	0.434	1.984	1.993	2.024	2.042

Diavik Spinel Microprobe Analyses

	T33	T33	T33	T33	T33	T33	T33
SiO_2	0.00	0.00	0.00	0.00	0.00	0.00	0.00
TiO_2	6.10	5.61	4.76	1.04	1.17	1.53	1.23
Al_2O_3	7.44	7.03	7.83	6.64	7.33	17.02	6.16
Cr_2O_3	0.08	0.10	0.03	58.67	56.59	40.75	58.33
V_2O_3	0.00	0.00	0.00	0.00	0.00	0.00	0.00
FeO	65.47	64.32	63.65	18.48	20.17	23.60	19.09
MnO	0.62	0.66	0.62	0.34	0.35	0.34	0.40
MgO	16.94	17.57	17.43	14.89	14.15	15.50	14.01
CaO	0.10	0.13	0.50	0.26	0.19	0.30	0.12
ZnO	0.00	0.0	0.00	0.00	0.00	0.00	0.00
TOTAL	96.78	95.45	94.85	100.35	99.98	99.07	99.36
SiO_2	0.00	0.00	0.00	0.00	0.00	0.00	0.00
TiO_2	6.10	5.61	4.76	1.04	1.17	1.53	1.23
Al_2O_3	7.44	7.03	7.83	6.64	7.33	17.02	6.16
Cr_2O_3	0.08	0.10	0.03	58.67	56.59	40.75	58.33
V_2O_3	0.00	0.00	0.00	0.00	0.00	0.00	0.00
Fe_2O_3	59.41	60.29	60.68	8.46	8.88	13.30	7.77
FeO	12.01	10.06	9.04	10.86	12.17	11.63	12.09
MnO	0.62	0.66	0.62	0.34	0.35	0.34	0.40
MgO	16.94	17.58	17.43	14.89	14.15	15.50	14.01
CaO	0.10	0.13	0.50	0.26	0.19	0.30	0.12
ZnO	0.00	0.00	0.00	0.00	0.00	0.00	0.00
TOTAL	102.73	101.49	100.92	101.20	100.87	100.40	100.14
Formula							
Si	0.000	0.000	0.000	0.000	0.000	0.000	0.000
Ti	0.195	0.181	0.154	0.034	0.038	0.048	0.040
Al	0.373	0.355	0.396	0.336	0.373	0.828	0.317
Cr	0.003	0.003	0.001	1.991	1.930	1.330	2.013
V	0.000	0.000	0.000	0.000	0.000	0.000	0.000
Fe(ii)	2.328	2.307	2.287	0.663	0.728	0.815	0.697
Mn	0.022	0.024	0.023	0.012	0.013	0.012	0.015
Mg	1.074	1.123	1.116	0.953	0.910	0.954	0.912
Ca	0.005	0.006	0.023	0.012	0.009	0.013	0.006
Zn	0.000	0.000	0.000	0.000	0.000	0.000	0.000
TOTAL	4.000	4.000	4.000	4.000	4.000	4.000	4.000
Fe/Fe+Mg	0.68	0.67	0.67	0.41	0.44	0.46	0.43
Cr/Cr+Al	0.00	0.01	0.00	0.85	0.83	0.61	0.86
Mg:Fe	0.46	0.48	0.48	1.43	1.25	1.17	1.30
Ti/(Ti+Cr+Al)	0.34	0.33	0.27	0.01	0.01	0.02	0.01
Fe(ii)	0.427	0.361	0.325	0.390	0.440	0.402	0.441
Fe(iii)	1.900	1.945	1.962	0.273	0.287	0.413	0.255

Diavik Spinel Microprobe Analyses

	T33	T33	T33	T33	T33	T33	T33
SiO_2	0.00	0.00	0.00	0.00	0.00	0.00	0.00
TiO_2	6.20	1.55	1.40	1.12	0.98	1.46	1.11
Al_2O_3	9.70	7.82	25.14	6.84	7.52	24.25	9.24
Cr_2O_3	0.29	53.12	27.90	56.48	58.28	32.37	53.95
V_2O_3	0.00	0.00	0.00	0.00	0.00	0.00	0.00
FeO	60.66	21.25	22.92	20.35	18.61	22.81	20.13
MnO	0.65	0.34	0.27	0.39	0.40	0.31	0.35
MgO	17.88	14.19	17.44	13.78	14.26	16.49	14.19
CaO	0.20	0.25	1.68	0.39	0.18	0.30	0.24
ZnO	0.00	0.00	0.00	0.00	0.0	0.00	0.00
TOTAL	95.61	98.54	96.78	99.38	100.25	98.01	99.24
SiO_2	0.00	0.00	0.00	0.00	0.00	0.00	0.00
TiO_2	6.20	1.55	1.40	1.12	0.98	1.46	1.11
Al_2O_3	9.70	7.82	25.14	6.84	7.52	24.25	9.24
Cr_2O_3	0.29	53.12	27.90	56.48	58.28	32.37	53.95
V_2O_3	0.00	0.00	0.00	0.00	0.00	0.00	0.00
Fe_2O_3	55.80	10.23	17.06	9.10	7.45	13.26	8.95
FeO	10.45	12.04	7.57	12.16	11.90	10.87	12.07
MnO	0.65	0.34	0.27	0.39	0.40	0.31	0.35
MgO	17.88	14.19	17.44	13.78	14.26	16.49	14.19
CaO	0.20	0.25	1.68	0.39	0.18	0.30	0.24
ZnO	0.00	0.00	0.00	0.00	0.00	0.00	0.00
TOTAL	101.20	99.57	98.49	100.29	101.00	99.34	100.14
Formula							
Si	0.000	0.000	0.000	0.000	0.000	0.000	0.000
Ti	0.197	0.051	0.042	0.037	0.032	0.044	0.036
Al	0.484	0.401	1.186	0.351	0.381	1.149	0.469
Cr	0.010	1.829	0.883	1.944	1.981	1.029	1.836
V	0.000	0.000	0.000	0.000	0.000	0.000	0.000
Fe(ii)	2.148	0.774	0.767	0.741	0.669	0.767	0.725
Mn	0.023	0.013	0.009	0.014	0.015	0.011	0.013
Mg	1.129	0.921	1.041	0.895	0.914	0.988	0.911
Ca	0.009	0.012	0.072	0.018	0.008	0.013	0.011
Zn	0.000	0.000	0.000	0.000	0.000	0.000	0.000
TOTAL	4.000	4.000	4.000	4.000	4.000	4.000	4.000
Fe/Fe+Mg	0.65	0.45	0.42	0.45	0.42	0.43	0.44
Cr/Cr+Al	0.01	0.82	0.42	0.84	0.83	0.47	0.79
Mg:Fe	0.52	1.19	1.35	1.20	1.36	1.28	1.25
Ti/(Ti+Cr+Al)	0.28	0.02	0.02	0.01	0.01	0.01	0.01
Fe(ii)	0.370	0.439	0.254	0.443	0.428	0.366	0.435
Fe(iii)	1.778	0.335	0.513	0.298	0.241	0.400	0.289

Diavik Spinel Microprobe Analyses

	T33	T33	A44	A44	A44	A44	A44
SiO_2	0.00	0.00	0.00	0.00	0.00	0.00	0.00
TiO_2	1.90	1.02	2.28	2.47	8.08	7.42	1.54
Al_2O_3	10.56	6.10	28.52	6.82	20.11	18.0	46.40
Cr_2O_3	46.56	57.49	24.24	51.71	0.02	0.01	7.633
V_2O_3	0.00	0.00	0.00	0.00	0.00	0.00	0.00
FeO	24.18	18.86	24.15	23.75	48.72	49.38	21.31
MnO	0.35	0.39	0.28	0.34	0.45	0.56	0.16
MgO	14.16	13.56	18.64	14.08	19.97	19.96	20.48
CaO	0.15	0.12	0.42	0.06	0.13	1.58	0.04
ZnO	0.00	0.00	0.00	0.00	0.00	0.00	0.00
TOTAL	97.89	97.57	98.55	99.26	97.51	96.96	97.59
SiO_2	0.00	0.00	0.00	0.00	0.00	0.00	0.00
TiO_2	1.90	1.02	2.28	2.47	8.08	7.42	1.54
Al_2O_3	10.56	6.10	28.52	6.82	20.11	18.01	46.40
Cr_2O_3	46.56	57.49	24.24	51.71	0.02	0.01	7.633
V_2O_3	0.0	0.00	0.00	0.00	0.00	0.00	0.00
Fe_2O_3	12.67	7.61	16.70	11.55	41.67	45.58	14.06
FeO	12.77	12.00	9.12	13.35	11.22	8.36	8.65
MnO	0.35	0.39	0.28	0.34	0.45	0.56	0.16
MgO	14.16	13.56	18.64	14.08	19.97	19.96	20.48
CaO	0.15	0.12	0.42	0.06	0.13	1.58	0.04
ZnO	0.00	0.00	0.00	0.00	0.00	0.00	0.00
TOTAL	99.16	98.33	100.22	100.42	101.69	101.52	99.00
Formula							
Si	0.000	0.000	0.000	0.000	0.000	0.000	0.000
Ti	0.062	0.034	0.066	0.081	0.241	0.223	0.042
Al	0.538	0.320	1.303	0.350	0.940	0.848	1.981
Cr	1.592	2.023	0.743	1.778	0.001	0.000	0.219
V	0.000	0.000	0.000	0.000	0.000	0.000	0.000
Fe(ii)	0.875	0.702	0.783	0.864	1.616	1.651	0.646
Mn	0.013	0.015	0.009	0.013	0.015	0.019	0.005
Mg	0.913	0.900	1.078	0.913	1.181	1.190	1.106
Ca	0.007	0.006	0.017	0.003	0.006	0.068	0.002
Zn	0.000	0.000	0.000	0.000	0.000	0.000	0.000
TOTAL	4.000	4.000	4.000	4.000	4.000	4.000	4.000
Fe/Fe+Mg	0.48	0.43	0.42	0.48	0.57	0.58	0.36
Cr/Cr+Al	0.74	0.86	0.36	0.83	0.00	0.00	0.09
Mg:Fe	1.04	1.28	1.37	1.05	0.73	0.72	1.71
Ti/(Ti+Cr+Al)	0.02	0.01	0.03	0.03	0.20	0.20	0.01
Fe(ii)	0.462	0.447	0.296	0.486	0.373	0.281	0.263
Fe(iii)	0.412	0.254	0.487	0.377	1.243	1.372	0.383

Diavik Spinel Microprobe Analyses

	A44	A44	A44	A5	A5	A5	A5
SiO_2	0.00	0.00	0.00	0.00	0.00	0.00	0.00
TiO_2	2.38	1.56	1.33	8.89	9.29	8.47	8.81
Al_2O_3	6.67	38.76	42.88	16.35	15.42	13.68	16.69
Cr_2O_3	53.09	17.57	11.40	0.51	0.13	0.20	0.04
V_2O_3	0.00	0.00	0.00	0.00	0.00	0.00	0.00
FeO	23.05	22.00	20.47	56.19	56.98	56.97	55.04
MnO	0.33	0.20	0.20	0.53	0.52	0.52	0.62
MgO	14.66	20.09	20.59	12.88	14.22	12.82	15.05
CaO	0.04	0.04	0.25	0.06	0.09	0.07	0.37
ZnO	0.00	0.00	0.00	0.00	0.00	0.00	0.00
TOTAL	100.25	100.24	97.15	95.44	96.67	92.76	96.649
SiO_2	0.00	0.00	0.00	0.00	0.00	0.00	0.00
TiO_2	2.38	1.56	1.33	8.89	9.29	8.47	8.81
Al_2O_3	6.67	38.76	42.88	16.35	15.42	13.68	16.69
Cr_2O_3	53.09	17.57	11.40	0.51	0.13	0.20	0.04
V_2O_3	0.00	0.00	0.00	0.00	0.00	0.00	0.00
Fe_2O_3	11.48	14.55	14.59	38.53	41.00	41.09	41.00
FeO	12.72	8.89	7.34	21.52	20.09	19.99	18.14
MnO	0.31	0.20	0.20	0.53	0.52	0.52	0.62
MgO	14.66	20.09	20.59	12.88	14.22	12.82	15.05
CaO	0.04	0.04	0.25	0.06	0.09	0.07	0.37
ZnO	0.00	0.00	0.00	0.00	0.00	0.00	0.00
TOTAL	101.40	101.69	98.61	99.30	100.78	96.87	100.75
Formula							
Si	0.000	0.000	0.000	0.000	0.000	0.000	0.000
Ti	0.077	0.043	0.037	0.287	0.295	0.283	0.277
Al	0.338	1.672	1.858	0.828	0.768	0.717	0.822
Cr	1.804	0.508	0.331	0.017	0.004	0.007	0.001
V	0.000	0.000	0.000	0.000	0.000	0.000	0.000
Fe(ii)	0.828	0.673	0.629	2.020	2.014	2.119	1.923
Mn	0.012	0.006	0.006	0.019	0.019	0.020	0.022
Mg	0.939	1.096	1.129	0.825	0.896	0.850	0.938
Ca	0.002	0.002	0.010	0.003	0.004	0.003	0.017
Zn	0.000	0.000	0.000	0.000	0.000	0.000	0.000
TOTAL	4.000	4.000	4.000	4.000	4.000	4.000	4.000
Fe/Fe+Mg	0.46	0.38	0.35	0.70	0.69	0.71	0.67
Cr/Cr+Al	0.84	0.23	0.15	0.02	0.00	0.01	0.00
Mg:Fe	1.13	1.62	1.79	0.40	0.44	0.40	0.48
Ti/(Ti+Cr+Al)	0.03	0.01	0.01	0.25	0.27	0.28	0.25
Fe(ii)	0.457	0.272	0.225	0.773	0.710	0.744	0.634
Fe(iii)	0.371	0.400	0.404	1.246	1.303	1.375	1.289

Diavik Spinel Microprobe Analyses

	A5	A5	A5	GTH	GTH	GTH	GTH
SiO_2	0.00	0.00	0.00	0.00	0.00	0.00	0.00
TiO_2	9.07	8.33	9.27	5.34	19.38	22.42	21.78
Al_2O_3	15.55	16.72	15.31	7.64	10.86	11.03	10.89
Cr_2O_3	0.31	0.45	0.08	45.70	2.33	0.90	0.89
V_2O_3	0.00	0.00	0.00	0.00	0.00	0.00	0.00
FeO	56.33	54.11	56.73	24.43	43.70	38.19	41.13
MnO	0.52	0.53	0.60	0.51	0.71	0.80	0.66
MgO	14.43	13.66	14.70	14.51	18.94	22.49	22.77
CaO	0.11	0.16	0.28	0.51	0.25	0.27	0.48
ZnO	0.00	0.00	0.00	0.00	0.00	0.00	0.00
TOTAL	96.34	93.99	97.00	98.68	96.20	96.12	98.62
SiO_2	0.00	0.00	0.00	0.00	0.00	0.00	0.00
TiO_2	9.07	8.33	9.27	5.34	19.38	22.42	21.78
Al_2O_3	15.55	16.72	15.31	7.64	10.86	11.03	10.89
Cr_2O_3	0.31	0.45	0.08	45.70	2.33	0.90	0.89
V_2O_3	0.00	0.00	0.00	0.00	0.00	0.00	0.00
Fe_2O_3	40.98	38.70	41.78	11.02	25.84	22.91	26.48
FeO	19.45	19.28	19.13	14.51	20.44	17.57	17.29
MnO	0.52	0.53	0.60	0.51	0.71	0.80	0.66
MgO	14.43	13.66	14.70	14.51	18.94	22.49	22.77
CaO	0.11	0.16	0.28	0.51	0.25	0.27	0.48
ZnO	0.00	0.00	0.00	0.00	0.00	0.00	0.00
TOTAL	100.44	97.86	101.18	99.788	98.79	98.42	101.27
Formula							
Si	0.000	0.000	0.000	0.000	0.000	0.000	0.000
Ti	0.289	0.271	0.293	0.174	0.615	0.695	0.660
Al	0.775	0.852	0.758	0.391	0.540	0.536	0.517
Cr	0.010	0.015	0.003	1.568	0.078	0.029	0.028
V	0.000	0.000	0.000	0.000	0.000	0.000	0.000
Fe(ii)	1.992	1.955	1.992	0.886	1.541	1.317	1.385
Mn	0.019	0.019	0.021	0.019	0.025	0.028	0.023
Mg	0.910	0.880	0.920	0.939	1.191	1.383	1.367
Ca	0.005	0.007	0.013	0.024	0.011	0.012	0.021
Zn	0.000	0.000	0.000	0.000	0.000	0.000	0.000
TOTAL	4.000	4.000	4.000	4.000	4.000	4.000	4.000
Fe/Fe+Mg	0.68	0.68	0.68	0.48	0.56	0.48	0.50
Cr/Cr+Al	0.01	0.01	0.00	0.80	0.12	0.05	0.05
Mg:Fe	0.45	0.45	0.46	1.05	0.77	1.05	0.98
Ti/(Ti+Cr+Al)	0.26	0.23	0.27	0.08	0.49	0.55	0.54
Fe(ii)	0.688	0.697	0.672	0.527	0.721	0.606	0.583
Fe(iii)	1.304	1.258	1.320	0.359	0.820	0.711	0.802

Diavik Spinel Microprobe Analyses

	GTH	GTH	GTH	GTH	GTH	GTH	A4
SiO_2	0.00	0.00	0.00	0.00	0.00	0.00	0.00
TiO_2	3.94	3.99	3.71	22.37	20.81	21.10	2.11
Al_2O_3	6.68	9.68	8.57	9.95	11.10	11.83	11.55
Cr_2O_3	52.65	50.47	52.05	0.86	0.77	0.78	51.14
V_2O_3	0.00	0.00	0.00	0.00	0.00	0.00	0.00
FeO	22.61	22.27	21.42	41.48	44.36	43.45	20.84
MnO	0.37	0.31	0.31	0.68	0.65	0.59	0.46
MgO	13.40	13.32	12.88	22.80	21.51	20.20	14.50
CaO	0.37	0.22	0.27	0.50	0.40	0.25	0.17
ZnO	0.00	0.00	0.00	0.00	0.00	0.00	0.00
TOTAL	100.04	100.29	99.24	98.66	99.62	98.22	100.80
SiO_2	0.00	0.00	0.00	0.00	0.00	0.00	0.00
TiO_2	3.94	3.99	3.71	22.37	20.81	21.10	2.11
Al_2O_3	6.68	9.68	8.57	9.95	11.10	11.83	11.55
Cr_2O_3	52.65	50.47	52.05	0.86	0.77	0.78	51.14
V_2O_3	0.00	0.00	0.00	0.00	0.00	0.00	0.00
Fe_2O_3	7.90	6.48	5.72	26.52	28.34	24.99	8.35
FeO	15.49	16.43	16.27	17.61	18.85	20.96	13.32
MnO	0.37	0.31	0.31	0.68	0.65	0.59	0.46
MgO	13.40	13.32	12.88	22.80	21.51	20.20	14.50
CaO	0.37	0.22	0.27	0.50	0.40	0.25	0.17
ZnO	0.00	0.00	0.00	0.00	0.00	0.00	0.00
TOTAL	100.83	100.93	99.82	101.32	102.46	100.72	101.64
Formula							
Si	0.000	0.000	0.000	0.000	0.000	0.000	0.000
Ti	0.129	0.129	0.122	0.680	0.629	0.650	0.067
Al	0.342	0.489	0.441	0.474	0.526	0.571	0.572
Cr	1.809	1.711	1.795	0.027	0.024	0.025	1.698
V	0.000	0.000	0.000	0.000	0.000	0.000	0.000
Fe(ii)	0.822	0.798	0.781	1.401	1.491	1.488	0.732
Mn	0.014	0.011	0.011	0.023	0.022	0.020	0.016
Mg	0.868	0.851	0.838	1.373	1.289	1.234	0.908
Ca	0.017	0.010	0.013	0.022	0.017	0.011	0.008
Zn	0.000	0.000	0.000	0.000	0.000	0.000	0.000
TOTAL	4.000	4.000	4.000	4.000	4.000	4.000	4.000
Fe/Fe+Mg	0.48	0.48	0.48	0.50	0.53	0.54	0.44
Cr/Cr+Al	0.84	0.77	0.80	0.0	0.04	0.04	0.74
Mg:Fe	1.05	1.06	1.07	0.98	0.86	0.82	1.24
Ti/(Ti+Cr+Al)	0.05	0.05	0.05	0.57	0.53	0.52	0.02
Fe(ii)	0.563	0.589	0.593	0.598	0.634	0.718	0.468
Fe(iii)	0.258	0.209	0.187	0.806	0.858	0.770	0.264

Diavik Spinel Microprobe Analyses

	A5	A5	A5	A5	A5	A5	A5
SiO_2	0.00	0.00	0.00	0.00	0.00	0.00	0.00
TiO_2	8.34	8.99	8.31	8.98	9.04	8.16	8.91
Al_2O_3	16.05	15.06	17.83	16.12	16.16	18.12	15.20
Cr_2O_3	0.09	1.44	0.60	0.35	0.42	0.91	0.26
V_2O_3	0.00	0.00	0.00	0.00	0.00	0.00	0.00
FeO	53.01	56.06	55.28	56.64	56.45	53.68	55.25
MnO	0.56	0.55	0.52	0.50	0.50	0.50	0.49
MgO	14.91	14.55	14.94	13.09	14.85	15.79	13.64
CaO	0.39	0.20	0.15	0.10	0.12	0.15	0.14
ZnO	0.00	0.00	0.00	0.00	0.00	0.00	0.00
TOTAL	93.39	96.87	97.61	95.81	97.57	97.32	93.92
SiO_2	0.00	0.00	0.00	0.00	0.00	0.00	0.00
TiO_2	8.34	8.99	8.31	8.98	9.04	8.16	8.91
Al_2O_3	16.05	15.06	17.83	16.12	16.16	18.12	15.20
Cr_2O_3	0.09	1.44	0.60	0.35	0.42	0.91	0.26
V_2O_3	0.00	0.00	0.00	0.00	0.00	0.00	0.00
Fe_2O_3	40.23	41.01	40.63	39.22	41.29	40.50	39.55
FeO	16.81	19.15	18.71	21.34	19.28	17.23	19.65
MnO	0.56	0.55	0.52	0.50	0.50	0.50	0.49
MgO	14.91	14.55	14.94	13.09	14.85	15.79	13.64
CaO	0.39	0.20	0.15	0.10	0.12	0.15	0.14
ZnO	0.00	0.00	0.00	0.00	0.00	0.00	0.00
TOTAL	97.42	100.98	101.74	99.74	101.71	101.38	97.88
Formula							
Si	0.000	0.000	0.000	0.000	0.000	0.000	0.000
Ti	0.271	0.285	0.258	0.289	0.283	0.253	0.292
Al	0.816	0.748	0.868	0.813	0.793	0.879	0.780
Cr	0.003	0.048	0.020	0.012	0.014	0.030	0.009
V	0.000	0.000	0.000	0.000	0.000	0.000	0.000
Fe(ii)	1.913	1.976	1.909	2.028	1.965	1.847	2.010
Mn	0.020	0.020	0.018	0.018	0.018	0.017	0.018
Mg	0.959	0.914	0.920	0.835	0.922	0.969	0.885
Ca	0.018	0.009	0.007	0.005	0.005	0.007	0.007
Zn	0.000	0.000	0.000	0.000	0.000	0.000	0.000
TOTAL	4.000	4.000	4.000	4.000	4.000	4.000	4.000
Fe/Fe+Mg	0.66	0.68	0.67	0.70	0.68	0.65	0.69
Cr/Cr+Al	0.00	0.06	0.02	0.01	0.01	0.03	0.01
Mg:Fe	0.50	0.46	0.48	0.41	0.46	0.52	0.44
Ti/(Ti+Cr+Al)	0.24	0.26	0.22	0.25	0.25	0.21	0.26
Fe(ii)	0.606	0.675	0.647	0.764	0.672	0.593	0.715
Fe(iii)	1.306	1.300	1.262	1.263	1.293	1.253	1.244

Diavik Spinel Microprobe Analyses

	A5	A5	A5	A5	A5	A5	A5
SiO_2	0.00	0.00	0.00	0.00	0.00	0.00	0.00
TiO_2	9.04	9.08	8.36	8.83	8.73	8.56	8.32
Al_2O_3	14.02	15.82	16.01	14.70	15.81	15.57	20.11
Cr_2O_3	0.37	0.21	0.45	0.12	0.17	0.10	0.67
V_2O_3	0.00	0.00	0.00	0.00	0.00	0.00	0.00
FeO	58.8	57.20	55.37	55.73	54.29	53.29	53.78
MnO	0.55	0.55	0.53	0.61	0.51	0.55	0.49
MgO	13.96	12.80	14.98	15.12	14.67	15.04	10.92
CaO	0.11	0.11	0.09	0.26	0.09	0.25	0.32
ZnO	0.00	0.00	0.00	0.00	0.00	0.00	0.00
TOTAL	96.88	95.80	95.81	95.40	94.29	93.36	94.65
SiO_2	0.00	0.00	0.00	0.00	0.00	0.00	0.00
TiO_2	9.04	9.08	8.36	8.83	8.73	8.56	8.32
Al_2O_3	14.02	15.82	16.01	14.70	15.81	15.57	20.11
Cr_2O_3	0.37	0.21	0.45	0.12	0.17	0.10	0.67
V_2O_3	0.00	0.00	0.00	0.00	0.00	0.00	0.00
Fe_2O_3	43.00	39.37	41.63	42.47	40.12	40.42	33.12
FeO	20.07	21.77	17.90	17.50	18.18	16.91	23.97
MnO	0.55	0.55	0.53	0.61	0.51	0.55	0.49
MgO	13.96	12.80	14.98	15.12	14.67	15.04	10.92
CaO	0.11	0.11	0.09	0.26	0.09	0.25	0.32
ZnO	0.00	0.00	0.00	0.00	0.00	0.00	0.00
TOTAL	101.19	99.74	99.98	99.66	98.31	97.44	97.97
Formula							
Si	0.000	0.000	0.000	0.000	0.000	0.000	0.000
Ti	0.289	0.293	0.266	0.283	0.282	0.278	0.271
Al	0.702	0.801	0.797	0.737	0.800	0.793	1.025
Cr	0.012	0.007	0.015	0.004	0.006	0.003	0.023
V	0.000	0.000	0.000	0.000	0.000	0.000	0.000
Fe(ii)	2.088	2.054	1.956	1.983	1.950	1.925	1.945
Mn	0.020	0.020	0.019	0.022	0.019	0.020	0.018
Mg	0.884	0.820	0.943	0.959	0.939	0.969	0.704
Ca	0.005	0.005	0.004	0.012	0.004	0.012	0.015
Zn	0.000	0.000	0.000	0.000	0.000	0.000	0.000
TOTAL	4.000	4.000	4.000	4.000	4.000	4.000	4.000
Fe/Fe+Mg	0.70	0.72	0.65	0.67	0.67	0.66	0.73
Cr/Cr+Al	0.01	0.00	0.0	0.00	0.0	0.00	0.02
Mg:Fe	0.42	0.39	0.48	0.48	0.48	0.50	0.36
Ti/(Ti+Cr+Al)	0.28	0.26	0.24	0.27	0.25	0.25	0.20
Fe(ii)	0.713	0.782	0.633	0.623	0.653	0.611	0.867
Fe(iii)	1.374	1.272	1.323	1.360	1.296	1.314	1.077

Diavik Spinel Microprobe Analyses

	GTH	GTH	GTH	GTH	GTH	GTH
SiO_2	0.00	0.00	0.00	0.00	0.00	0.00
TiO_2	1.70	1.79	2.40	1.25	1.99	2.42
Al_2O_3	14.75	5.53	15.15	5.63	5.89	18.63
Cr_2O_3	43.15	55.59	38.75	59.58	54.23	31.48
V_2O_3	0.00	0.00	0.00	0.00	0.00	0.00
FeO	23.17	22.64	26.35	18.58	22.97	27.81
MnO	0.31	0.39	0.37	0.33	0.37	0.44
MgO	15.31	13.96	16.10	14.73	14.07	18.41
CaO	0.43	0.14	0.11	0.03	0.03	0.31
ZnO	0.00	0.00	0.00	0.00	0.00	0.00
TOTAL	98.86	100.07	99.27	100.14	99.58	99.53
SiO_2	0.00	0.00	0.00	0.00	0.00	0.00
TiO_2	1.70	1.79	2.40	1.25	1.99	2.42
Al_2O_3	14.75	5.53	15.15	5.63	5.89	18.63
Cr_2O_3	43.15	55.59	38.75	59.58	54.23	31.48
V_2O_3	0.00	0.00	0.00	0.00	0.00	0.00
Fe_2O_3	12.95	10.90	16.49	8.03	11.20	21.56
FeO	11.50	12.82	11.51	11.35	12.89	8.40
MnO	0.31	0.39	0.37	0.33	0.37	0.44
MgO	15.31	13.96	16.10	14.73	14.07	18.41
CaO	0.43	0.14	0.11	0.03	0.03	0.31
ZnO	0.00	0.00	0.00	0.00	0.00	0.00
TOTAL	100.16	101.16	100.92	100.95	100.70	101.69
Formula						
Si	0.000	0.000	0.000	0.000	0.000	0.000
Ti	0.053	0.059	0.075	0.041	0.065	0.073
Al	0.727	0.283	0.738	0.287	0.302	0.878
Cr	1.426	1.910	1.266	2.037	1.867	0.995
V	0.000	0.000	0.000	0.000	0.000	0.000
Fe(ii)	0.810	0.823	0.911	0.672	0.837	0.930
Mn	0.011	0.014	0.013	0.012	0.014	0.015
Mg	0.954	0.905	0.992	0.950	0.914	1.097
Ca	0.019	0.007	0.005	0.001	0.001	0.013
Zn	0.000	0.000	0.000	0.000	0.000	0.000
TOTAL	4.000	4.000	4.000	4.000	4.000	4.000
			4.000			
Fe/Fe+Mg	0.45	0.47	0.47	0.41	0.47	0.45
Cr/Cr+Al	0.66	0.87	0.63	0.87	0.86	0.53
Mg:Fe	1.17	1.09	1.08	1.41	1.09	1.18
Ti/(Ti+Cr+Al)	0.02	0.02	0.03	0.01	0.02	0.03
Fe(ii)	0.403	0.466	0.398	0.411	0.470	0.281
Fe(iii)	0.407	0.356	0.513	0.261	0.366	0.649

APPENDIX II

The Churchill Kimberlite Field, Nunavut

Churchill Kimberlite Field: Petrography
Mineral Key

Ap	Apatite
Bad	Baddeleyite
Cal	Calcite
Chl	Chlorite
Crustal	Crustal
Ilm	Ilmenite
Mtc	Monticellite
Mud	Mud
Ol	Olivine
Oxide	Oxide
Phl	Phlogopite
Prv	Perovskite
Rt	Rutile
Spl	Spinel
Srp	Serpentine
Zcn	Zirconolite

SAMPLE: **04-JBP-001 [04KD597-01]**
DEPTH: **58.2 m**

CLASSIFICATION: HK

SUMMARY: An oxide-rich phlogopite hypabyssal kimberlite.

Colour: Brown
Clay Minerals: alteration
Xenolith Abundance: crustal
Xenolith Size: <4mm, >4mm
Xenolith Reaction: moderate
Olivine Replacement: some Srp veining
Pelletal Lapilli: none
Autoliths: none
Primary Carbonate: matrix
Kimberlitic Textures: inequigranular, matrix-supported, sparsely macrocrystic, atoll Sp

MODAL MINERALOGY:

Ol Phenocrysts: euhedral to subhedral	60%
Phl Phenocrysts: euhedral	20%
Ol Macrocrysts: 3-6mm, anhedral	10%
Phl Macrocrysts: 2-4mm, subhedral	5%
Crustal	5%

MATRIX:

Major: Phl, Srp, Oxides (Spl), Cal-P
Minor: Cal, Ap
Trace: n/a

TEXTURES/ADDITIONAL INFORMATION:

- Minimal alteration throughout the slide.
- Atoll-textures are identified, abundant opaque Spl.
- Colourless Cal-P.
- Some Phl are distorted.

SAMPLE: **04-JDP-002 [04KD597-01]**
DEPTH: **17.7 m**

CLASSIFICATION: HK [altered]

SUMMARY: A serpentinized oxide-rich phlogopite hypabyssal kimberlite.

Colour: dark brown/black
Clay Minerals: alteration
Xenolith Abundance: crustal 5%
Xenolith Size: 4mm
Xenolith Reaction: rim
Pelletal Lapilli: none
Autoliths: none
Primary Carbonate: matrix
Kimberlitic Textures: uniform textured, matrix-supported, sparsely macrocrystic, inequigranular

MODAL MINERALOGY:

Ol phenocrysts: euhedral, serpentinized	55%
Phl macrocrysts: rounded	20%
Crustal: angular	20%
Ol macrocrysts: anhedral, resorption features, serpentinized	15%

MATRIX:

Major: Phl, Srp, Cal-P
Minor: Mtc, Prv, Oxides (Spl)
Trace: Cal-S

TEXTURES/ADDITIONAL INFORMATION:

- Sample is significantly serpentinized.
- Mtc is euhedral, and in some cases completely pseudomorphed by Cal-S.
- Prv is irregular and is rimmed by thick dark amorphous material.
- Opaques form necklace textures around phenocrystal Ol.

SAMPLE: **04-JBP-003 [04KD568-01]**
DEPTH: **12.1 m**

CLASSIFICATION: HK [altered]

SUMMARY: An oxide-rich hypabyssal kimberlite exhibiting a preferred flow orientation.

Colour: grey
Clay Minerals: alteration
Xenolith Abundance: Ilm
Xenolith Size: 4mm
Xenolith Reaction: none
Pelletal Lapilli: none
Autoliths: none
Primary Carbonate: matrix
Kimberlitic Textures: uniform textured, flow alignment

MODAL MINERALOGY:

Ol phenocrysts: euhedral, partially to fully serpentinized	60%
Phl phenocrysts: euhedral lath shaped	20%
Ol macrocrysts: subhedral to anhedral, serpentinized	10%
Ilm xenocrysts: rims of chlorite/clay	10%

MATRIX:

Major: Cal-P, Srp, Oxides (Spl)
Minor: Ap, Phl, Prv, Cal-S
Trace: n/a

TEXTURES/ADDITIONAL INFORMATION:

- Ol phenocrysts show a preferred orientation.
- Secondary carbonate veining is present.
- Abundant Spl.
- Colourless Cal-P.

SAMPLE: **04JBP-004 [04KD428-01]**
DEPTH: **30.6 m**

CLASSIFICATION: HK [altered]

SUMMARY: An oxide-rich hypabyssal kimberlite. *It is very difficult to distinguish primary mineralogy.

Colour: brown/green
Clay Minerals: alteration/matrix
Xenolith Abundance: crustal
Xenolith Size: n/a
Xenolith Reaction: rims
Pelletal Lapilli: none
Autoliths: none
Primary Carbonate: matrix?
Kimberlitic Textures: inequigranular, segregation textured, highly altered

MODAL MINERALOGY:

Ol phenocrysts: pseudomorphs, euhedral to subhedral	60%
Ol macrocrysts: pseudomorphs, anhedral	20%
Phl phenocrysts: rounded, alteration around rim	10%
Crustal: granite?	10%

MATRIX:

Major: Srp, Oxides (Spl), Cal-S or –P
Minor: Phl
Trace: Prv?

TEXTURES/ADDITIONAL INFORMATION:

- Section is extremely altered.
- Very difficult to distinguish minerals.
- Phl distortion.
- Inconclusive.
- Phenocrysts and macrocrysts are within a Srp and Cal mesostasis.

SAMPLE: 04JBP-005 [04KD428-01]
DEPTH: 43.3 m

CLASSIFICATION: HK [altered]

SUMMARY: An extremely altered hypabyssal kimberlite, containing abundant angular and partially digested country rock fragments.

Colour: green
Clay Minerals: alteration
Xenolith Abundance: crustal
Xenolith Size: n/a
Xenolith Reaction: n/a
Pelletal Lapilli: none
Autoliths: none
Primary Carbonate: matrix?
Kimberlitic Textures: inequigranular, segregationary textured, clast-supported

MODAL MINERALOGY:

Crustal: angular	50%
Ol phenocrysts: euhedral to subhedral, serpentinized	40%
Phl phenocrysts: rounded and altered between planes	5%
Ol macrocrysts: rounded and serpentinized	5%

MATRIX:

Major: Oxides (Spl), Srp, Cal-P or -S
Minor: n/a
Trace: n/a

TEXTURES/ADDITIONAL INFORMATION:

- Thin section is extremely altered, and it’s difficult to distinguish primary kimberlitic minerals.
- Inconclusive.

SAMPLE: 04JBP-006 [04KD428-01]

DEPTH: 68.2 m

CLASSIFICATION: HK [altered]

SUMMARY: A serpentine hypabyssal kimberlite, containing abundant crustal material.

Colour: brown/green
Clay Minerals: alteration
Xenolith Abundance: crustal 5%
Xenolith Size: n/a
Xenolith Reaction: n/a
Pelletal Lapilli: n/a
Autoliths: n/a
Primary Carbonate: n/a
Kimberlitic Textures: inequigranular, segregationary textured, sparsely macrocrystic

MODAL MINERALOGY:

Ol phenocrysts: anhedral and pseudomorphs	60%
Crustal: angular and partially digested	30%
Ol macrocrysts: rounded anhedral and pseudomorphs	10%

MATRIX:

Major: Oxides (Spl), Phl, Srp
Minor: Cal-P or -S
Trace: Prv

TEXTURES/ADDITIONAL INFORMATION:

- Extensively altered, difficult to distinguish primary mineralogy, therefore inconclusive.
- Irregular masses of Prv.

SAMPLE: 04JBP-012 [04KD217-01]
DEPTH: 59.9 m

CLASSIFICATION: HK

SUMMARY: A sparsely macrocrystic calcite hypabyssal kimberlite containing abundant Ol phenocrysts.

Colour: dark grey
Clay Minerals: none
Xenolith Abundance: none
Xenolith Size: n/a
Xenolith Reaction: n/a
Pelletal Lapilli: n/a
Autoliths: n/a
Primary Carbonate: matrix
Kimberlitic Textures: uniform textured, inequigranular, matrix-supported, sparsely macrocrystic, fresh

MODAL MINERALOGY:

Ol phenocrysts: subhedral to rounded anhedral	50%
Ol microphenocryst: euhedral to subhedral	30%
Ol macrocrysts: anhedral rounded	20%

MATRIX:

Major: Cal-P, Oxides (Spl)
Minor: Prv
Trace: Ap, Phl

TEXTURES/ADDITIONAL INFORMATION:

- Thin section is fresh and suitable from Microprobe.
- Some Ol tend to be very rounded, (both the macrocrysts and phenocrysts). Therefore the rounded Ol phenocrysts are most likely the product of dissaggregation of macrocrystal Ol.
- Very low degree of alteration.
- Primarily Cal-P in the matrix.
- Colourless Cal-P.

SAMPLE: **04JBP-013 [04KD230-01]**
DEPTH: **37.0 m**

CLASSIFICATION: HK [altered]

SUMMARY: A phlogopite hypabyssal kimberlite?

Colour: black brown
Clay Minerals: alteration
Xenolith Abundance: n/a
Xenolith Size: n/a
Xenolith Reaction: n/a
Pelletal Lapilli: n/a
Autoliths: n/a
Primary Carbonate: ?
Kimberlitic Textures: altered, segregationary textured, phenocrystic

MODAL MINERALOGY:

Ol phenocrysts: pseudomorphed, anhedral	60%
Phl phenocrysts: secondary?	40%

MATRIX:

Major: Cal P- or S, Phl, Srp
Minor: Chl
Trace: n/a

TEXTURES/ADDITIONAL INFORMATION:

- This thin section is heavily altered.
- Cannot easily distinguish between Cal-P and Cal-S.
- All primary minerals have been pseudomorphed by Srp, Chl and Cal-S.
- Considered to be inconclusive.

SAMPLE: **04-JBP-014 [04KD230-01]**
DEPTH: **21.3 m**

CLASSIFICATION: HK [altered]

SUMMARY: An altered monticellite? phlogopite hypabyssal kimberlite, with abundant secondary calcite veining.

Colour: grey
Clay Minerals: alteration
Xenolith Abundance: none
Xenolith Size: n/a
Xenolith Reaction: n/a
Pelletal Lapilli: n/a
Autoliths: n/a
Primary Carbonate: matrix?
Kimberlitic Textures: inequigranular, segregationary textured, sparsely macrocrystic, matrix supported

MODAL MINERALOGY:

Ol phenocrysts: mixed population- rounded and euhedral	60%
Ol macrocrysts: large anhedral with Srp veins	40%

MATRIX:

Major: Cal-P or S, Phl, Mtc, Oxides (Spl)
Minor: Prv, Ilm, Srp
Trace: Ap

TEXTURES/ADDITIONAL INFORMATION:

- Cal segregationary textures present.
- Mixed population of Ol phenocrysts.
- Ol phenocrysts and macrocrysts are relatively fresh, but the matrix is altered.
- Ap is of acicular radial habit.
- Most Mtc is identified by it's high relief and habit, however is pseudomorphed by Cal-S.
- Considered to be inconclusive.

SAMPLE: **04JBP-015 [04KD235-01]**
DEPTH: **54.9 m**

CLASSIFICATION: HK

SUMMARY: An oxide-rich hypabyssal kimberlite with abundant spinel and monticellite in the groundmass.

Colour: dark grey
Clay Minerals: none
Xenolith Abundance: none
Xenolith Size: n/a

Xenolith Reaction: n/a
Pelletal Lapilli: none
Autoliths: none
Primary Carbonate: matrix
Kimberlitic Textures: inequigranular, uniform textured, sparsely macrocrystic, matrix-supported

MODAL MINERALOGY:

Ol phenocrysts: euhedral to subhedral, Srp veining	60%
Ol macrocrysts: subhedral to anhedral, Srp veining	40%

MATRIX:

Major: Oxides (Spl), Cal-P, Ilm
Minor: Mtc, Prv
Trace: Ap

TEXTURES/ADDITIONAL INFORMATION:

- Macrocrystal Ol have a thick rim of amorphous material.
- Macrocrystic Ol contains abundant inclusions.
- Some of the opaques in the groundmass are euhedral (cubic, cuboctahedral) while some are completely rounded.
- Prv's seem to have zoning present and are relatively larger. (50-100um) There is a range in the size of Prv grains.

SAMPLE: **04JBP-016 [04KD235-01]**
DEPTH: **75.6 m**

CLASSIFICATION: HK

SUMMARY: An interesting sample, consisting of a monticellite oxide-rich hypabyssal kimberlite with a single megacrystal Ol.

Colour: brown/grey
Clay Minerals: alteration
Xenolith Abundance: none
Xenolith Size: n/a
Xenolith Reaction: n/a
Pelletal Lapilli: n/a
Autoliths: n/a
Primary Carbonate: matrix
Kimberlitic Textures: inequigranular, uniform textured, matrix-supported, phenocrystic

MODAL MINERALOGY:

Ol phenocrysts: euhedral to subhedral, partially serpentinized	90%
Ol megacrysts: one single anhedral, 2.5 cm diameter	10%

MATRIX:

Major: Cal, Oxides (Spl), Mtc, Srp

Minor: Chl, Ap
Trace: Prv?

TEXTURES/ADDITIONAL INFORMATION:

- Sample has a coarse matrix/groundmass, very suitable for probe work.
- Mtc is abundant and euhedral throughout the matrix.
- Phenocrystal Ol's exhibit a very thick rim of very fine groundmass material.
- The megacrystal Ol is approximately 2.5 cm in diameter, and exhibits serpentine veining.

SAMPLE: **CD 001**
DEPTH: **20.4m**

CLASSIFICATION: HK

SUMMARY: A sparsely macrocrystic, oxide-rich hypabyssal kimberlite.

Colour: lgt grey, brown
Clay Minerals: alteration
Xenolith Abundance: one large crustal
Xenolith Size: 1.5 cm
Xenolith Reaction: orange alteration?
Olivine Replacement: clay/Srp
Pelletal Lapilli: none
Autoliths: none
Primary Carbonate: none
Kimberlitic Textures: uniform textured, matrix-supported, sparsely macrocrystic, inequigranular

MODAL MINERALOGY:

Ol phenocrysts: pseudomorphs (Srp, clay)	55%
Ol macrocrysts: Srp veining	25%
Ilm xenocrysts: large anhedral	15%
Cpx: a few macrocrysts, quite altered	5%

MATRIX:

Major: Oxides (Spl), Phl
Minor: Prv, Cal-S, Ilm
Trace: Ap

TEXTURES/ADDITIONAL INFORMATION:

- Ap is acicular in the matrix.
- Prv is found forming necklace textures around Ol phenocrysts.
- Possible pseudomorphed Cal after Mtc.
- Ol macrocrysts are fresh, with some veining infilled with Srp.
- Ol phenocrysts are pseudomorphed by clay/Srp/Chl.

SAMPLE: **CD 001**

DEPTH: 39.53 m

CLASSIFICATION: HK [altered]

SUMMARY: A perovskite-rich spinel hypabyssal kimberlite.

Colour: brown/grey
Clay Minerals: alteration
Xenolith Abundance: none
Xenolith Size: n/a
Xenolith Reaction: n/a
Pelletal Lapilli: n/a
Autoliths: n/a
Primary Carbonate: matrix
Kimberlitic Textures: inequigranular, uniform textured, matrix-supported, sparsely macrocrystic

MODAL MINERALOGY:

Ol macrocrysts, phenocrysts, and microphenocrysts (pseudomorphs)	100%

MATRIX:

Major: Oxides (Spl), Phl, Cal-P or -S, Ilm, Prv
Minor: Cal-S, Ap, Srp, Chl
Trace: n/a

TEXTURES/ADDITIONAL INFORMATION:

- Thin section is extremely altered.
- Prv and oxides (Spl, Ilm) have a close association.
- Two distinct populations of Spl are present. Tiny euhedral cubes can be found within pseudomorphs after Ol. Larger Spl is found forming necklace textures with Prv.
- It is difficult to distinguish between Cal-P and Cal-S.

SAMPLE: CD 001
DEPTH: 73.58 m

CLASSIFICATION: HK [altered]

SUMMARY: A macrocryst-poor, phlogopite-rich, spinel hypabyssal kimberlite.

Colour: brown/grey
Clay Minerals: alteration
Xenolith Abundance: none
Xenolith Size: n/a
Xenolith Reaction: n/a
Pelletal Lapilli: n/a
Autoliths: n/a
Primary Carbonate: matrix
Kimberlitic Textures: inequigranular, uniform textured, matrix-supported, phenocrystic

MODAL MINERALOGY:

Ol phenocrysts: pseudomorphs, anhedral	80%
Phl phenocrysts: deformed, flow banding	15%
Ilm phenocrysts: anhedral	5%

MATRIX:

Major: Oxides (Spl), Phl, Cal-P or –S, Srp
Minor: Ilm
Trace: Prv

TEXTURES/ADDITIONAL INFORMATION:

- Slide is extremely altered. The matrix is primarily small lath shaped Phl and Cal-P or –S.
- There is some Cal segregationary textures present.
- Phl distortion.

SAMPLE: **CD 001**
DEPTH: **73.60m**

CLASSIFICATION: HK[altered]

SUMMARY: Segregationary-textured oxide-rich hypabyssal kimberlite with phenocrystal Ol in low abundance.

Colour: Light Brown
Clay Minerals: alteration clay minerals
Xenolith Abundance: crustal; 5%
Xenolith Size: 2mm
Xenolith Reaction: none present
Olivine Replacement: clay
Pelletal Lapilli: none
Autoliths: none
Primary Carbonate: none
Kimberlitic Textures: Spl necklace texture around Phl, atoll Spl, inequigranular, segregationary

MODAL MINERALOGY:

Ol phenocrysts: pseudomorphed	55%
Ilm phenocrysts: anhedral	15%
Phl phenocrysts: subhedral	30%

MATRIX:

Major: Oxides (Spl), Cal-S, Srp, Chl
Minor: Prv, Phl
Trace: Ap

TEXTURES/ADDITIONAL INFORMATION:

- Secondary crustal vein, infilled with Cal.
- Chlorite alteration through groundmass.
- Phl phenocrysts are flow-banded.

- Abundant secondary alterations are present, including secondary fracturing and veining. Extremely high concentrations of Sp and Ilm.

SAMPLE: **CD 001**
DEPTH: **81.96 m**

CLASSIFICATION: HK [altered]

SUMMARY: A sparsely macrocrystic, oxide- rich serpentine hypabyssal kimberlite.

Colour: Dk brown
Clay Minerals: alteration abundant
Xenolith Abundance: crustal
Xenolith Size: 3-8mm
Xenolith Reaction: cal
Olivine Replacement: clay/srp
Pelletal Lapilli: none
Autoliths: none
Primary Carbonate: none
Kimberlitic Textures: matrix-supported, sparsely macrocrystic, uniform textured, inequigranular

MODAL MINERALOGY:

Ol phenocrysts: pseudomorphed	30%
Ol macrocrysts: pseudomorphed	20%
Phl macrocrysts: well rounded	20%
Phl phenocrysts: lath shaped	15%
Ilm xenocrysts: anhedral	15%

MATRIX:

Major: Oxide (Spl), Srp
Minor: Prv, Cal-S
Trace: Ap

TEXTURES/ADDITIONAL INFORMATION:

- **S**ome Prv's display 2 zones.
- Prv's are euhedral cubic and display a thick amorphous rim.
- Spl is abundant and forms necklace textures around pseudomorphs after Ol.
- Phl macrocrysts are well rounded and display alteration between cleavages.
- Phl macrocrysts and phenocrysts can display kink banding, and are distorted.

SAMPLE: **CD 002**
DEPTH: **30.05 m**

CLASSIFICATION: HK

SUMMARY: An oxide-rich calcite phlogopite hypabyssal kimberlite.

Colour: brown/grey
Clay Minerals: alteration
Xenolith Abundance: none

Xenolith Size: n/a
Xenolith Reaction: n/a
Pelletal Lapilli: n/a
Autoliths: n/a
Primary Carbonate: matrix
Kimberlitic Textures: inequigranular, uniform textured, matrix-supported, sparsely macrocrystic

MODAL MINERALOGY:

Phl phenocrysts: rounded, alteration rims	50%
Phl macrocrysts: rounded, alteration rims	25%
Ol phenocrysts: pseudomorphs (Cal)	25%

MATRIX:

Major: Oxides (Spl), Ilm, Prv, Cal-P
Minor: Ap, Srp, Chl
Trace: Prv

TEXTURES/ADDITIONAL INFORMATION:

- There seem to be two generations of Prv, large and small. Necklace textures are common with both generations of this mineral.
- There is a relationship with the oxides and Prv, both commonly found together.

SAMPLE: **CD 002**
DEPTH: **34.38 m**

CLASSIFICATION: HK

SUMMARY: A monticellite? phlogopite hypabyssal kimberlite, exhibiting unique textures and ilmenite megacrysts. Perovskite is abundant in the matrix.

Colour: brown/grey
Clay Minerals: alteration
Xenolith Abundance: crustal
Xenolith Size: n/a
Xenolith Reaction: n/a
Pelletal Lapilli: n/a
Autoliths: n/a
Primary Carbonate: matrix
Kimberlitic Textures: inequigranular, uniform textured, matrix-supported, macrocrystic, megacrystic

MODAL MINERALOGY:

Ol microphenocrysts: euhedral to subhedral, alteration to Cal	25%
Phl phenocrysts: flow banding, phl distinct rims	25%
Ol phenocrysts: euhedral to subhedral, alteration to Cal, Srp	25%
Ilm megacrysts: large, 1.5 cm in diameter, euhedral	15%
Crustal: angular, up to 0.75 cm	10%

MATRIX:

Major: Oxides (Spl), Ilm, Phl, Mtc, Prv, Srp
Minor: Ap, Chl, Cal-P
Trace: n/a

TEXTURES/ADDITIONAL INFORMATION:

- Ilm megacrysts is euhedral.
- Slide has abundant necklace textures, with both Spl and Prv's.
- Ol is pseudomorphed by Cal and Srp (Chl)
- Prv is unusually abundant in this sample.
- Crustal material is angular.
- Much of the matrix is undistinguishable brown/green material.
- Tiny oxides are concentrated in specific zones.
- Prv is abundant and commonly completely surrounding Ilm in the matrix.

SAMPLE: **CD 003**
DEPTH: **12.79 m**

CLASSIFICATION: HK [altered]

SUMMARY: A phlogopite-rich hypabyssal kimberlite, displaying atoll- textured spinels.

Colour: brown/grey
Clay Minerals: alteration
Xenolith Abundance: none
Xenolith Size: n/a
Xenolith Reaction: n/a
Pelletal Lapilli: n/a
Autoliths: n/a
Primary Carbonate: matrix
Kimberlitic Textures: inequigranular, uniform textured, matrix-supported, sparsely macrocrystic

MODAL MINERALOGY:

Phl phenocrysts: lath-shaped, alteration rims, flow banding	40%
Ol phenocrysts: subhedral, pseudomorphed (Cal, Srp)	20%
Phl macrocrysts: alteration, rounded, alteration rims	20%
Ilm phenocrysts: rounded	10%
Crustal: angular	10%

MATRIX:

Major: Cal-P, Phl, Oxides (Spl), Srp
Minor: Ilm, Prv, Srp, Mtc
Trace: Ap, Chl

TEXTURES/ADDITIONAL INFORMATION:

- Oxides and Prv exhibit necklace textues (reaction mantles).
- Phl distortion.
- Some atoll-Spl are corroded.

SAMPLE: **CD 004**
DEPTH: **18.0 m**

CLASSIFICATION: HK [altered]

SUMMARY: An oxide-rich hypabyssal kimberlite, containing abundant crustal xenocrysts.

Colour: dark brown
Clay Minerals: alteration
Xenolith Abundance: crustal 15%
Xenolith Size: 1 cm diameter
Xenolith Reaction: n/a
Pelletal Lapilli: none
Autoliths: none
Primary Carbonate: none
Kimberlitic Textures: inequigranular, uniform texture, matrix-supported

MODAL MINERALOGY:

Ol phenocrysts: subhedral, pseudomorphed	50%
Ol macrocrysts: subhedral, pseudomorphed	30%
Crustal Xenocrysts: large, angular	20%

MATRIX:

Major: Oxides (Spl), Srp, Cal-P
Minor: Cal
Trace: n/a

TEXTURES/ADDITIONAL INFORMATION:

- Entirely dominated by Spl.
- Secondary Cal infilling fractures.

SAMPLE: **CD 004**
DEPTH: **36.97 m**

CLASSIFICATION: HK

SUMMARY: An oxide-rich macrocrystal hypabyssal kimberlite.

Colour: brown/grey
Clay Minerals: alteration
Xenolith Abundance: none
Xenolith Size: n/a
Xenolith Reaction: n/a
Pelletal Lapilli: n/a
Autoliths: n/a
Primary Carbonate: matrix
Kimberlitic Textures: inequigranular, uniform textured, macrocrystic, matrix-supported

MODAL MINERALOGY:

Ol phenocrysts: euhedral to subhedral, pseudomorphed (Srp)	60%
Ol macrocrysts: rounded anhedral, pseudomorphed (Srp)	20%
Crustal material:	20%

MATRIX:

Major: Phl, Srp, Cal-P, Oxides (Spl)
Minor: Prv, Ap
Trace: n/a

TEXTURES/ADDITIONAL INFORMATION:

- Oxides display necklace textures, reaction mantles.
- Most of the groundmass is amorphous (probably Srp).
- Phl is abundant in the matrix.
- Phl is poikiolitic in the matrix.

SAMPLE: **CD 006**
DEPTH: **38.57 m**

CLASSIFICATION: HK?

SUMMARY: An oxide-rich phlogopite hypabyssal kimberlite?

Colour: brown/grey
Clay Minerals: alteration
Xenolith Abundance: none
Xenolith Size: n/a
Xenolith Reaction: n/a
Pelletal Lapilli: n/a
Autoliths: n/a
Primary Carbonate: matrix
Kimberlitic Textures: inequigranular, uniform textured, phenocrystic (sparsely macrocrystic), matrix-supported.

MODAL MINERALOGY:

Phl phenocrysts: epitaxial overgrowths	60%
Ol phenocrysts: anhedral, pseudomorphs (Cal,Srp)	40%

MATRIX:

Major: Phl, Cal-P, Oxides (Spl)
Minor: Prv, Ilm
Trace: Ap

TEXTURES/ADDITIONAL INFORMATION:

- Epitaxial overgrowths. Amazing Phl macrocrysts: They appear to have begun crystallizing, then have been altered and subsequently rounded, and surrounded by small oxides, (opaques), then at this point continued growth into a lath shaped macrocrysts.
- Colourless Cal.

- As for classification, results are inconclusive.

SAMPLE: **CD 006**
DEPTH: **65.0 m**

CLASSIFICATION: HK [altered]

SUMMARY: A hypabyssal kimberlite exhibiting flow banded completely rounded macrocrysts (xenocrysts?) of Phl.

Colour: Brown
Clay Minerals: alteration (30%)
Xenolith Abundance: 10% crustal
Xenolith Size: 2-5 mm
Xenolith Reaction: cal
Olivine Replacement: Srp, completely pseudomorphed
Pelletal Lapilli: none
Autoliths: none
Primary Carbonate: none
Kimberlitic Textures: segregationary textures, matrix-supported, inequigranular

MODAL MINERALOGY:

Ol phenocrysts: euhedral to subhedral (pseudomorphed)	55%
Di phenocrysts: euhedral to subhedral (pseudomorphed)	15%
Phl macrocrysts: (completely rounded, alteration between sheets)	15%
Ilm macrocrysts and phenocrysts: anhedral	10%
Crustal: angular to rounded	5%

MATRIX:

Major: Cal-P, Oxides (Spl), Cal-S
Minor: Phl, Chl
Trace: Ap

TEXTURES/ADDITIONAL INFORMATION:

- Phl: alteration between sheets, completely rounded grains.
- Secondary Cal infilled in fractures.
- Spl forms necklace textures around Ol and Di phenocrysts.
- Phl shows flow banding features.
- Extreme alteration.
- Phl distortion.

SAMPLE: **CD 007**
DEPTH: **18.65 m**

CLASSIFICATION: HK?

SUMMARY: A matrix dominated calcite hypabyssal kimberlite (possibly carbonatite?)

Colour: brown/grey
Clay Minerals: alteration

Xenolith Abundance: none
Xenolith Size: n/a
Xenolith Reaction: n/a
Pelletal Lapilli: n/a
Autoliths: n/a
Primary Carbonate: matrix
Kimberlitic Textures: uniform textured, matrix-supported, phenocrystic, coarse matrix

MODAL MINERALOGY:

Ol phenocrystal: euhedral, Srp veining, alteration rims	40%
Phl phenocrystal: flow banding, lath shapes	30%
Ilm phenocrystal: anhedral, fractured	10%
Phl macrocrystal: flow banding, lath shapes, alteration	10%
Ol macrocrystal: anhedral, fractured, Srp veining	5%
Crustal:	5%

MATRIX:

Major: Cal-P, Oxides (Spl), Phl, Srp
Minor: Ilm
Trace: Prv

TEXTURES/ADDITIONAL INFORMATION:

- Matrix is Cal dominated. Cal forms crystals interstitial to the phenocrysts and macrocrysts.
- Thin section must be probed for Spl etc. for proper identification of rock.

SAMPLE: **CD 007**
DEPTH: **47.10 m**

CLASSIFICATION: HK

SUMMARY: A sparsely macrocrystic, calcite hypabyssal kimberlite (carbonatite?).

Colour: brown/grey
Clay Minerals: alteration
Xenolith Abundance: none
Xenolith Size: n/a
Xenolith Reaction: n/a
Pelletal Lapilli: n/a
Autoliths: n/a
Primary Carbonate: matrix
Kimberlitic Textures: inequigranular, uniform textured, matrix-supported, sparsely macrocrystic

MODAL MINERALOGY:

Ol microphenocrysts: euhedral to subhedral, Srp veining (possible fragments)	50%
Ol phenocrysts: euhedral to subhedral, slight Srp veining	35%
Ol macrocrysts: anhedral, fragmented	5%
Ilm phenocrysts: fractured and fracture fragments	5%
Phl phenocrysts: rounded laths, slight alteration on rim	5%

MATRIX:

Major: Cal-P, Oxides (Spl), Phl
Minor: Prv, Srp
Trace: n/a

TEXTURES/ADDITIONAL INFORMATION:

- Located at the edge of the thin section is a Cal-S vein. On the outer edge of the vein, the kimberlite is highly altered, including Srp pseudomorphs after Ol phenocrysts.
- Oxides form necklace textures around Ol microphenocrysts, phenocrysts and Phl phenocrysts.
- Prv seems to have 2 distinct populations, rare large cubic (zoned, including a dark core) Prv's and small dark rounded Prv's, the latter more abundant.

SAMPLE: **CD 007**
DEPTH: **78.64 m**

CLASSIFICATION: HK

SUMMARY: A macrocrystal calcite hypabyssal kimberlite, containing multiple xenoliths of unknown origin. (Probe to confirm).

Colour: grey
Clay Minerals: alteration
Xenolith Abundance: 7%
Xenolith Size: 0.5mm to 3cm diameter
Xenolith Reaction: thin rims
Pelletal Lapilli: n/a
Autoliths: n/a
Primary Carbonate: matrix, equant grains
Kimberlitic Textures: uniform textured, matrix-supported, macrocrystic, fresh.

MODAL MINERALOGY:

Ol macrocrystal: anhedral, Srp veining, alteration rims	40%
Ol phenocrystal: euhedral to subhedral, Srp veining	40%
Ilm phenocrystal: anhedral	10%
Ilm macrocrystal: anhedral, fractured	5%
Xenoliths: unknown origin	5%

MATRIX:

Major: Cal-P, Phl, Oxides (Spl)
Minor: Ap, Cal-S, Ilm
Trace: Prv?

TEXTURES/ADDITIONAL INFORMATION:

- Cal is very abundant in the matrix, and forms euhedral crystals, interlocking. This Cal is primary.
- Ol phenocrysts are mainly euhedral, with some rounded edges.
- Phl grains are lath-shaped with sharp edges. Grains are small and are found interstitial to the Cal within the matrix.

- Ap occurs in minor abundance in the matrix, and forms euhedral prisms.

SAMPLE: **CD 009**
DEPTH: **32.61 m**

CLASSIFICATION: HK [altered]

SUMMARY: Segregation textured hypabyssal kimberlite displaying completely pseudomorphed Ol. Entire thin section is altered and pseudomorphed after the primary minerals.

Colour: brown/green
Clay Minerals: none
Xenolith Abundance: Crustal 20%
Xenolith Size: 1-4mm
Xenolith Reaction: black thick rim
Olivine Replacement: Srp
Pelletal Lapilli: none
Autoliths: none
Primary Carbonate: matrix
Kimberlitic Textures: segregation textures, necklace textures, inequigranular

MODAL MINERALOGY:

Ol phenocrysts: pseudomorphs, subhedral	50%
Ilm phenocrysts: anhedral	20%
Ol macrocrysts: anhedral	15%
Crustal: angular	15%

MATRIX:

Major: Oxides (Spl), Cal-S, Ap, Srp
Minor: Prv, Phl, Cal-P
Trace: Chl

TEXTURES/ADDITIONAL INFORMATION:

- Spl display necklace textures, reaction mantles.
- Prv has been analysed via probe.
- Dominant segregationary texture present.
- Ap is found acicular and bladed in the matrix.

SAMPLE: **CD 009**
DEPTH: **33.11 m**

CLASSIFICATION: HK [altered]

SUMMARY: *This section contains a large Mnz grain which has been chemically dated via the microprobe. This is an altered phenocrystal hypabyssal spinel kimberlite.

Colour: brown
Clay Minerals: alteration
Xenolith Abundance: crustal 25%

Xenolith Size: 3cm
Xenolith Reaction: clay and chlorite
Olivine Replacement: serpentinite
Pelletal Lapilli: none
Autoliths: none
Primary Carbonate: none
Kimberlitic Textures: segregation textures, clast-supported, inequigranular

MODAL MINERALOGY:

Ol phenocrysts: subhedral	70%
Opaques	15%
Crustal: angular	15%

MATRIX:

Major: Oxides (Spl), Cal-S, Srp
Minor: Mtc, Prv
Trace: Ap

TEXTURES/ADDITIONAL INFORMATION:

- Ol is pseudomorphed.
- Spl are euhedral and appears to show atoll texture in some instances.
- Both Cal and Srp segregationary textures.
- Prv is abundant, large cubic, or cubo-octahedral light brown to orange, and also has a rim of optically undistinguishable material.
- Mtc is pseudomorphed by Cal-S. It has been identified by it's crystal habit and high relief in the thin section.

SAMPLE: **CD 009**
DEPTH: **34.14 m**

CLASSIFICATION: HK? [altered]

SUMMARY: Extremely altered hypabyssal kimberlite containing pseudomorphs after rounded Ol. The thin section is clast-supported, and has abundant crustal xenoliths.

Colour: Green
Clay Minerals: secondary alteration
Xenolith Abundance: crustal (10%)
Xenolith Size: 1 mm to 1 cm
Xenolith Reaction: Cal rim
Olivine Replacement: clay/Srp
Pelletal Lapilli: none
Autoliths: none
Primary Carbonate: matrix
Kimberlitic Textures: clast-supported, phenocrystic, uniform textured, inequigranular

MODAL MINERALOGY:

Ol phenocrysts: rounded (pseudomorphed)	70%
Ilm phenocrysts:	10%
Ol macrocrysts: rounded (pseudomorphed)	15%

Opaques: 5%

MATRIX/GROUNDMASS:

Major: Oxides (Spl), Srp
Minor: Phl, Prv, Chl, Cal-P
Trace: Ap

TEXTURES/ADDITIONAL INFORMATION:

- Clay/Srp pseudomorphs after Ol.
- Chlorite alteration around crustal material.
- Crustal material altered to various (clay, chlorite, cal).
- Phl is found as bladed and acicular.
- Necklace textures or reaction mantles, with Spl.

SAMPLE: CD 009
DEPTH: 44.31 m

CLASSIFICATION: Aphanitic HK

SUMMARY: Aphanitic hypabyssal kimberlite exhibiting secondary calcite and quartz veins, flow banding and preferred mineral orientation, containing abundant monticellite, apatite, perovskite and Cr-spinels.

Colour: Dk brown
Clay Minerals: none
Xenolith Abundance: none
Xenolith Size: none
Xenolith Reaction: none
Olivine Replacement: clay/serpentine
Pelletal Lapilli: none
Autoliths: none
Primary Carbonate: none, secondary
Kimberlitic Textures: aphanitic, flow banding, equigranular

MODAL MINERALOGY:

Cr-Spl: small euhedral to subhedral	30%
Prv: small cubic	15%
Ilm: anhedral	10%
Ap: small irregular grains	10%
Mtc: small euhedral grains	10%
Ol: pseudomorphs (serpentinite) phenocrysts	5%

MATRIX: n/a

TEXTURES/ADDITIONAL INFORMATION:

- Aphanitic
- Flow banding and preferred orientation of grains
- Some Qtz (secondary) infilling fractures
- Some Cal (secondary) infilling fractures

- Srp pseudomorphs after Ol are euhedral to subhedral, phenocrystic

---

SAMPLE: **CD 010**
DEPTH: **62.05 m**

CLASSIFICATION: HK [altered]

SUMMARY: A sparsely macrocrystic oxide-rich hypabyssal kimberlite.

Colour: brown/grey
Clay Minerals: alteration
Xenolith Abundance: none
Xenolith Size: n/a
Xenolith Reaction: n/a
Pelletal Lapilli: n/a
Autoliths: n/a
Primary Carbonate: matrix
Kimberlitic Textures: uniform textured, matrix-supported, sparsely macrocrystic, inequigranular

MODAL MINERALOGY:

Ol phenocrysts: euhedral, pseudomorphs (Srp, Cal)	60%
Ol macrocrysts: anhedral, Srp veining	20%
Crustal: angular	20%

MATRIX:

Major: Oxides (Spl), Cal-P, Phl
Minor: Prv, Ap
Trace: n/a

TEXTURES/ADDITIONAL INFORMATION:

- Ap appears to be euhedral (see circle on thin section).
- Necklace textures are prominent throughout thin section.
- Some of the phenocrysts may or may not be Ol, it is too difficult to distinguish due to alteration.
- Colourless Cal.
- Possible dissaggregation of macrocrysts.
- Larger rounded Ol macrocrysts are essentially alteration-free while matrix is heavily altered.

SAMPLE: **CD 010**
DEPTH: **80.3 m**

CLASSIFICATION: HK

SUMMARY: Macrocrystal oxide-rich hypabyssal kimberlite, exhibiting a uniform textured fresh groundmass.

Colour: brown
Clay Minerals: alteration

Xenolith Abundance: crustal 10%
Xenolith Size: 1cm avg
Xenolith Reaction: rim
Pelletal Lapilli: none
Autoliths: none
Primary Carbonate: none
Kimberlitic Textures: uniform matrix, sparsely macrocrystic, matrix supported, inequigranular

MODAL MINERALOGY:

Ol phenocrysts: euhedral to anhedral, fresh, thick amorphous rims	60%
Ol macrocrysts: anhedral, fresh to slight veining	30%
Phl: anhedral, corroded	5%
Crustal: angular to subangular	5%

MATRIX:

Major: Oxides (Spl), Cal-P, Srp
Minor: Ap
Trace: Prv

TEXTURES/ADDITIONAL INFORMATION:

- Cal makes up most of the groundmass.
- Extreme necklace textures shown with the Spl's.
- Colourless Cal.
- Some Ol grains exhibit an uneven birefringence, (a weak strain).

SAMPLE: **CD 010**
DEPTH: **86.00 m**

CLASSIFICATION: HK?

SUMMARY: *minerals must be analysed for further indication of a bona fide kimberlite.

Colour: brown/grey
Clay Minerals: alteration
Xenolith Abundance: none
Xenolith Size: n/a
Xenolith Reaction: n/a
Pelletal Lapilli: n/a
Autoliths: n/a
Primary Carbonate: matrix
Kimberlitic Textures: equigranular, matrix-supported, phenocrystic, uniform textured

MODAL MINERALOGY:

Ol phenocrysts: very rounded, pseudomorphed (Cal, Srp)	90%
Crustal: angular	10%

MATRIX:

Major: Oxide (Spl), Ap, Cal-S
Minor: Prv, Srp, Chl

Trace: ?

TEXTURES/ADDITIONAL INFORMATION:

- Oxides are very coarse, and large enough for EMPA.
- Necklace textures with fine grained oxides.
- Matrix minerals must be identified with EMPA.
- Srp and Chl matrix.
- Some corroded atoll textured Spls.

SAMPLE: CD 010
DEPTH: 91.1 m

CLASSIFICATION: HK [altered]

SUMMARY: A spinel-rich hypabyssal kimberlite.

Colour: dark brown
Clay Minerals: alteration
Xenolith Abundance: crustal 10%
Xenolith Size: 1-2 cm
Xenolith Reaction: rim
Pelletal Lapilli: none
Autoliths: none
Primary Carbonate: none
Kimberlitic Textures: equigranular, segregationary textured, matrix-supported, sparsely macrocrystic

MODAL MINERALOGY:

Ol phenocrysts: pseudomorphs (Srp)	60%
Ol macrocrysts: large anhedral, Srp veining	20%
Ilm: anhedral	10%
Crustal: subangular to angular	10%

MATRIX:

Major: Oxides (Spl), Cal-S or –S, Srp
Minor: Ap, Phl
Trace: Prv

TEXTURES/ADDITIONAL INFORMATION:

- Ol macrocrysts are fractured and display Srp veining, while the Ol phenocrysts are pseudomorphs after Ol, and the matrix is heavily altered.
- There is a very dominant Cal segregationary texture present.
- Some Spl are large enough to be counted within the modal mineralogy.
- Necklace textures around the Ol phenocrysts and macrocrysts is present throughout the entire thin section.
- Very difficult to distinguish between Cal-P and Cal-S.
- Some Spl are large and display atoll-textures.

SAMPLE: CD 013

DEPTH: 14.75 m

CLASSIFICATION: HK [altered]

SUMMARY: A spinel-rich hypabyssal kimberlite.

Colour: brown/grey
Clay Minerals: alteration
Xenolith Abundance: none
Xenolith Size: n/a
Xenolith Reaction: n/a
Pelletal Lapilli: n/a
Autoliths: n/a
Primary Carbonate: matrix
Kimberlitic Textures: inequigranular, segregationary textured, matrix-supported, sparsely macrocrystic

MODAL MINERALOGY:

Ol phenocrysts and macrocrysts: pseudomorphs 100%

MATRIX:

Major: Oxides (Spl), Srp, Chl, Cal-S
Minor: Phl, Ilm
Trace: Prv

TEXTURES/ADDITIONAL INFORMATION:

- Most Spl's in the section exhibit atoll-textures.
- Smaller oxides exhibit necklace textures around the Srp pseudomorphs after Ol.
- All Ol in the section is completely altered.
- Matrix is heavily altered, essentially a "pool" of Srp and Cal-S.

SAMPLE: CD 013
DEPTH: 19.31 m

CLASSIFICATION: HK

SUMMARY: A phlogopite calcite hypabyssal kimberlite containing a microxenolith population.

Colour: brown/grey
Clay Minerals: alteration
Xenolith Abundance: microxenoliths 10%
Xenolith Size: 0.5-3 mm
Xenolith Reaction: none, slight necklace textures
Pelletal Lapilli: n/a
Autoliths: n/a
Primary Carbonate: matrix
Kimberlitic Textures: inequigranular, uniform textured, matrix-supported, macrocrystic

MODAL MINERALOGY:

Ol microphenocrysts: fragmental, slight alteration to some	40%
Ol phenocrysts: euhedral to subhedral, Srp veining, Srp margins	30%
Ol macrocrysts: anhedral, some Srp veining	20%
Microxenoliths: appear to be Ol (must be probed)	10%

MATRIX:

Major: Oxides (Spl), Prv, Phl, Ilm Cal-P, Srp
Minor: Chl
Trace: Bad or Zcn, Ap

TEXTURES/ADDITIONAL INFORMATION:

- Atoll-textured Spl's are present, and abundant.
- The Prv in the matrix is cubic, and some of the population is fragmental.
- Bad/Zcn rods in the matrix must be confirmed with microprobe.
- Prv has a strong association with atoll-textured Spl's.

SAMPLE: **CD 013**
DEPTH: **19.89 m**

CLASSIFICATION: HK

SUMMARY: A relatively fresh sparsely macrocrystic, perovskite-rich, calcite hypabyssal kimberlite.

Colour: brown/grey
Clay Minerals: alteration
Xenolith Abundance: none
Xenolith Size: n/a
Xenolith Reaction: n/a
Pelletal Lapilli: n/a
Autoliths: n/a
Primary Carbonate: matrix
Kimberlitic Textures: inequigranular, uniform textured, matrix-supported, sparsely macrocrystic

MODAL MINERALOGY:

Ol microphenocrysts: probably fractured macro's and pheno's (anhedral, angular)	40%
Ol phenocrysts: euhedral to subhedral, Srp veining, thick alteration rims	40%
Ol macrocrysts: anhedral, well-rounded, pseudomorphs and fresh	10%
Ol microxenoliths: large (5mm), relatively unaltered	10%

MATRIX:

Major: Oxides (Spl), Cal-P, Srp
Minor: Ilm, Prv, Cal-S
Trace: Ap?

TEXTURES/ADDITIONAL INFORMATION:

- Ol macrocrysts display and uneven birefringence probably from a weak strain.
- Prv is abundant in matrix, and has a dark rim. It is euhedral (cubic), and light brown.

- Prv and Spl have a close association.

SAMPLE: **CD 013**
DEPTH: **20.10 m**

CLASSIFICATION: HK

SUMMARY: A relatively fresh magmatic hypabyssal kimberlite, exhibiting a large anhedral megacryst of Ol.

Colour: Brown
Clay Minerals: none
Xenolith Abundance: none
Xenolith Size: none
Xenolith Reaction: none
Olivine Replacement: Srp veining
Pelletal Lapilli: none
Autoliths: none
Primary Carbonate: none
Kimberlitic Textures: uniform textured, macrocrystic, matrix-supported, inequigranular

MODAL MINERALOGY:

Ol phenocrysts: euhedral to subhedral, slight Srp veining	55%
Ol macrocrysts: anhedral, some have extensive Srp veining	35%
Ol megacryst: anhedral 1.5 cm long	5%
Ilm phenocrysts: anhedral	<5%
Heterolithic Breccia	<1%

MATRIX:

Major: Oxides (Spl), Prv, Mtc?, Cal-P, Srp
Minor: Phl, Chl, Cal-S
Trace: Ap

TEXTURES/ADDITIONAL INFORMATION:

- Some of the Prv are large and zoning can be shown.
- Sp is uniform throughout the groundmass/matrix.
- Carbonates are interstitial in some areas, (possible fracture zones?)
- Mtc must be confirmed with the probe, due to small sizes (10-35 um)
- Colourless Cal.

SAMPLE: **CD 013**
DEPTH: **21.2 m**

CLASSIFICATION: TK?, possibly (more likely) transition zone between root and diatreme.

SUMMARY: This slide can be classified as transition zone between the root zone and diatreme. Pelletal lapillus is found to be 1.5 cm in diameter, however, no other diatreme-like features are identified in drill core/thin sections at the same depth.

Colour: brown
Clay Minerals: alteration
Xenolith Abundance: none
Xenolith Size: n/a
Xenolith Reaction: n/a
Olivine Replacement: Srp
Pelletal Lapilli: yes, 1.5 cm diameter
Autoliths: none
Primary Carbonate: none
Kimberlitic Textures: segregationary texture, phenocrystic

MODAL MINERALOGY:

Ol phenocrysts: euhedral to subhedral, serpentinized	65%
Ol macrocrysts: anhedral, serpentinized	30%
Ilm xenocrysts: anhedral	5%

MATRIX:

Major: Spl, Cal, mud
Minor: Prv, Rt, Chl
Trace: Phl

TEXTURES/ADDITIONAL INFORMATION:

- Pelletal lapillus contains a rounded kernel of Ol (pseudomorph).
- Within lapillus, concentric small euhedral Ol (pseudomorph)
- Flow alignment
- Secondary Cal-fluid crystallization through fractures.
- Heavily chloritized area of groundmass.

SAMPLE: **CD 013**
DEPTH: **30.97 m**

CLASSIFICATION: HK [altered]

SUMMARY: This thin section is extremely altered and it is very difficult to distinguish any of the macrocrysts and phenocrysts as they are pseudomorphed to Serpentine, Clays and Calcite. It appears it would be classified as a macrocrystal calcite hypabyssal kimberlite.

Colour: brown
Clay Minerals: alteration
Xenolith Abundance: crustal
Xenolith Size: n/a
Xenolith Reaction: n/a
Pelletal Lapilli: n/a
Autoliths: n/a
Primary Carbonate: matrix
Kimberlitic Textures: unavailable

MODAL MINERALOGY:

Ol phenocrysts: pseudomorphed	70%

Ol macrocrysts: pseudomorphed	30%

MATRIX:

Major: Spl?
Minor:
Trace:

TEXTURES/ADDITIONAL INFORMATION:

- Spl displays atoll- and necklace-textures, and is quite corroded. The matrix is made up of Srp and Chl.
- Secondary Cal veining.
- Ol is completely pseudomorphed by Srp.

SAMPLE: **CD 013**
DEPTH: **52.55 m**

CLASSIFICATION: HK, transition zone

SUMMARY: This slide consists of Ol phenocrysts and a few macrocrysts within a segregationary textured matrix. Some of the Ol phenocrysts are partially fresh, while the majority are pseudomorphs.

Colour: grey/brown
Clay Minerals: alteration
Xenolith Abundance: crustal, 5%
Xenolith Size: 1.5 cm
Xenolith Reaction: none
Olivine Replacement: Srp, clay
Pelletal Lapilli: none
Autoliths: none
Primary Carbonate: matrix
Kimberlitic Textures: inequigranular, globular segregationary textures, matrix supported

MODAL MINERALOGY:

Ol phenocrysts: euhedral to subhedral, pseudomorph	45%
Ol macrocrysts: subhedral to anhedral, pseudomorph	15%
Phl macrocrysts: rounded, alteration between cleavage planes	15%
Phl phenocrysts: rounded, alteration between cleavage planes	15%
Opaques (Ilm?), subhedral, fragments	10%

MATRIX:

Major: Oxides (Spl), Cal-P, Chl, Mud
Minor: Mtc, Phl
Trace: n/a

TEXTURES/ADDITIONAL INFORMATION:

- Spl exhibits necklace textures surrounded pseudomorphs after Ol.
- Cal + Mud segregationary textures present through the entire section.

SAMPLE: **CD 013**
DEPTH: **54.49 m**

CLASSIFICATION: HK

SUMMARY: A relatively fresh macrocryst-poor calcite hypabyssal kimberlite, rich in matrix perovskite.

Colour: brown/grey
Clay Minerals: alteration
Xenolith Abundance: none
Xenolith Size: n/a
Xenolith Reaction: n/a
Pelletal Lapilli: n/a
Autoliths: n/a
Primary Carbonate: matrix
Kimberlitic Textures: equigranular, matrix-supported, macrocryst-poor

MODAL MINERALOGY:

Ol microphenocrysts: possible fragments present, euhedral to subhedral	50%
Ol phenocrysts: fragmented, euhedral to subhedral	50%
Ol macrocrysts: one large macrocrysts/microxenolith?	<1%

MATRIX:

Major: Oxides (Spl), Prv, Cal-P, Srp
Minor: Phl, Ilm
Trace: n/a

TEXTURES/ADDITIONAL INFORMATION:

- Prv is extremely abundant in the matrix (20%).
- Oxides in the matrix are coarse, and ideal for the microprobe.
- Colourless Cal.
- Relative range in the size of Prv grains.
- Weakly zoned Prv.

SAMPLE: **CD 015**
DEPTH: **24.30 m**

CLASSIFICATION: HK [altered]

SUMMARY: A spinel-rich, macrocrystal calcite hypabyssal kimberlite.

Colour: dark grey
Clay Minerals: alteration
Xenolith Abundance: crustal
Xenolith Size: n/a
Xenolith Reaction: n/a
Pelletal Lapilli: n/a
Autoliths: n/a
Primary Carbonate: matrix

Kimberlitic Textures: inequigranular, uniform textures, matrix-supported, macrocrystic

MODAL MINERALOGY:

Ol phenocrysts: Srp/Clay pseudomorphs, thick amorphous rims	70%
Ol macrocrysts: Srp veins, anhedral and rounded	15%
Crustal: Cal-S	15%

MATRIX:

Major: Oxides (Spl), Cal-P, Srp
Minor: Cal-S, Prv, Phl
Trace: Chl

TEXTURES/ADDITIONAL INFORMATION:

- The Ol phenocrysts are highly altered or completely pseudomorphed, while the macrocrysts are reasonably fresh, while matrix is highly altered.
- Oxides form necklace textures, or reaction mantles.
- Colourless Cal.
- Relative range in size of Prv grains.

SAMPLE: **CD 015**
DEPTH: **unknown depth (unk1), 14.20m (2 thin sections were identical)**

CLASSIFICATION: HK [altered]

SUMMARY: A macrocrystal spinel-rich hypabyssal kimberlite containing CPX phenocrysts.

Colour: brown
Clay Minerals: none
Xenolith Abundance: none
Xenolith Size: n/a
Xenolith Reaction: n/a
Pelletal Lapilli: none
Autoliths: none
Primary Carbonate: none
Kimberlitic Textures: inequigranular, uniform textured, matrix supported

MODAL MINERALOGY:

Ol phenocrysts: euhedral to subhedral, pseudomorphs	40%
CPX macrocrysts, fragmental, alteration rims, subhedral	30%
Ilm phenocrysts: small rounded, alteration rims	20%
Phl phenocrysts: small rounded, alteration between cleavages	10%

MATRIX:

Major: Oxides (Spl), Cal-S, Srp
Minor: Prv, Phl
Trace: n/a

TEXTURES/ADDITIONAL INFORMATION:

- Some Cal segregationary textures throughout the section.
- Spl dominant.
- Phl distortion.
- Weakly zoned Prv.

SAMPLE: **CD 020**
DEPTH: **20.0 m**

CLASSIFICATION: HK

SUMMARY: A spinel-rich hypabyssal kimberlite exhibiting slight alteration.

Colour: dark brown
Clay Minerals: alteration
Xenolith Abundance: crustal 5%
Xenolith Size: 0.5cm
Xenolith Reaction: clay rim
Pelletal Lapilli: none
Autoliths: none
Primary Carbonate: matrix
Kimberlitic Textures: inequigranular, matrix-supported, uniform textured, macrocrystic

MODAL MINERALOGY:

Ol phenocrysts: euhedral to subhedral, Srp veining	60%
Ol macrocrysts: subhedral to anhedral, Srp veining	30%
CPX: small (1mm avg) rounded and altered, fractured	10%

MATRIX:

Major: Oxides (Spl), Mtc, Cal-P
Minor: Prv, Ap
Trace: Phl, Ilm

TEXTURES/ADDITIONAL INFORMATION:

- Ol phenocrysts display a thick black rim of amorphous material.
- Ol macrocrysts and phenocrysts commonly have Srp veining, sometimes infilled with Chl material.
- Small amounts of Cal segregationary textures are present. Colourless Cal.
- Groundmass is uniform and mainly Spl, most of which display cubic form.

SAMPLE: **CD 020**
DEPTH: **46.91 m**

CLASSIFICATION: HK

SUMMARY: A relatively fresh, sparsely macrocrystic, serpentine calcite hypabyssal kimberlite.

Colour: brown/grey
Clay Minerals: alteration

Xenolith Abundance: crustal
Xenolith Size: n/a
Xenolith Reaction: Cal-S
Pelletal Lapilli: n/a
Autoliths: n/a
Primary Carbonate: matrix
Kimberlitic Textures: inequigranular, sparsely macrocrystic, uniform textured, matrix-supported

MODAL MINERALOGY:

Ol microphenocrysts: full range of alteration present	55%
Ol phenocrysts: full range, thick amorphous rims, subhedral	35%
Ol macrocrysts: full range, anhedral, amorphous rims	10%

MATRIX:

Major: Oxides (Spl), Phl, Ap, Cal-P, Srp
Minor: Cal-S, Ilm, Prv
Trace: n/a

TEXTURES/ADDITIONAL INFORMATION:

- Ol phenocrysts and microphenocrysts have a very thick amorphous rim, and it is because of this rim that there true habit is undistinguishable.
- The Phl is large laths in the groundmass, sometimes poikiolitic.
- Atoll Spls are abundant, as well as necklace textures surrounding Ol phenocrysts.
- Colourless Cal.
- Prv is weakly zoned (darker cores).

SAMPLE: **CD 020**
DEPTH: **51.55**

CLASSIFICATION: HK?

SUMMARY: A relatively fresh sparsely macrocrystic phlogopite calcite hypabyssal kimberlite.

Colour: brown/grey
Clay Minerals: alteration
Xenolith Abundance: none
Xenolith Size: n/a
Xenolith Reaction: n/a
Pelletal Lapilli: n/a
Autoliths: Yes, Kimberlite groundmass
Primary Carbonate: matrix
Kimberlitic Textures: inequigranular, uniform textured, phenocrystic, matrix-supported

MODAL MINERALOGY:

Ol phenocrysts: euhedral to anhedral, Srp veining to fresh	80%
Autoliths of distinctly different altered kimberlite	10%
Crustal: angular	10%

MATRIX:

Major: Oxides (Spl), Phl, Srp, Ilm, Cal-P
Minor: Ap, Prv
Trace: n/a

TEXTURES/ADDITIONAL INFORMATION:

- Some of the oxides display atoll-textures.
- Colourless Cal.
- Ol phenocrysts are a mixture of separate mineral grains and fragmented Ol grains, possibly from macrocrystic Ol. This can be confirmed with microprobe.

SAMPLE: **CD 020**
DEPTH: **64.0 m**

CLASSIFICATION: HK?

SUMMARY: A spinel-rich phlogopite hypabyssal kimberlite with abundant calcite and apatite within the matix.

Colour: dark grey
Clay Minerals: slight alteration
Xenolith Abundance: crustal <5%
Xenolith Size: small
Xenolith Reaction: n/a
Pelletal Lapilli: none
Autoliths: none
Primary Carbonate: n/a
Kimberlitic Textures: uniform textured, matrix supported, sparsely macrocystic, equigranular.

MODAL MINERALOGY:

Ol phenocrysts: anhedral, both fresh and Srp veins	50%
Phl: lath shaped, slight alteration	50%

MATRIX:

Major: Cal-P, Prv, Ap, Oxides (Spl)
Minor: Mtc, Ilm, Srp
Trace: n/a

TEXTURES/ADDITIONAL INFORMATION:

- Thin section appears very fresh.
- Prv is very abundant, some grains show weak zoning.
- Colourless Cal.
- Abundant Spl.

SAMPLE: **CD 020**
DEPTH: **89.20 m**

CLASSIFICATION: HK

SUMMARY: A relatively fresh sample of calcite hypabyssal kimberlite, containing fresh olivine macrocrysts.

Colour: grey
Clay Minerals: alteration
Xenolith Abundance: none
Xenolith Size: n/a
Xenolith Reaction: n/a
Pelletal Lapilli: n/a
Autoliths: n/a
Primary Carbonate: matrix
Kimberlitic Textures: inequigranular, uniform texture, matrix-supported, sparsely macrocrystic

MODAL MINERALOGY:

Ol phenocrysts: subhedral, fresh, some Srp veining	80%
Ol macrocrysts: anhedral, fresh, some Srp veining	10%
Crustal: thick alteration rims, angular	10%

MATRIX:

Major: Mtc? Or Ap, Oxides (Spl), Cal-P
Minor: Prv, Ilm
Trace: n/a

TEXTURES/ADDITIONAL INFORMATION:

- Must microprobe to identify the main constituent of the groundmass/matrix. It is very difficult to distinguish between Ap and Mtc.
- Prv has thick dark amorphous rim.
- Ol's have very little Srp veining.
- Ol's display undulatory birefringence, indicating strain on the grains.
- Colourless Cal.

SAMPLE: **CD 021**
DEPTH: **30.77 m**

CLASSIFICATION: HK [altered]

SUMMARY: A macrocrystic serpentine calcite hypabyssal kimberlite. It is difficult to distinguish primary mineralogy of this thin section.

Colour: brown
Clay Minerals: alteration
Xenolith Abundance: none
Xenolith Size: n/a
Xenolith Reaction: n/a
Pelletal Lapilli: n/a
Autoliths: n/a
Primary Carbonate: matrix
Kimberlitic Textures: inequigranular, segregationary textured, matrix-supported, macrocrystic.

MODAL MINERALOGY:

Ol phenocrysts: pseudomorphs	70%
Ol macrocrysts: pseudomorphs	15%
Crustal: angular	10%
Phl phenocrysts: probably crustal	5%

MATRIX:

Major: Oxides (Spl), Srp, Cal-P, Cal-S, Phl
Minor: n/a
Trace: n/a

TEXTURES/ADDITIONAL INFORMATION:

- It is difficult to decifer Cal-P from Cal-S.
- The groundmass/matrix is very hard to distinguish in this section.
- Srp and Cal-S makes up most of the matrix

SAMPLE: CD 021
DEPTH: 47.75 m

CLASSIFICATION: HK [altered]

SUMMARY: A macrocrystal serpentine calcite hypabyssal kimberlite. Primary mineralogy is very difficult to distinguish.

Colour: brown
Clay Minerals: alteration
Xenolith Abundance: crustal
Xenolith Size: n/a
Xenolith Reaction: n/a
Pelletal Lapilli: n/a
Autoliths: n/a
Primary Carbonate: matrix
Kimberlitic Textures: inequigranular, matrix-supported, uniform textured, macrocrystal

MODAL MINERALOGY:

Primary mineralogy is very difficult to distinguish, it is estimated to be 70% phenocrystal Ol, 30% macrocrystal Ol.

MATRIX:

Major: Oxides(Spl), Oxides, Cal-P, Cal-S, Phl
Minor: Prv, Ap
Trace: n/a

TEXTURES/ADDITIONAL INFORMATION:

- It is difficult to distinguish between Cal-P and Cal-S. Nonetheless, the matrix is made up of a Cal-Srp “pool”.

SAMPLE: CD 021

DEPTH: **88.26 m**

CLASSIFICATION: HK

SUMMARY: This sample is a hypabyssal calcite serpentine kimberlite, containing a small mantle xenolith.

Colour: brown/grey
Clay Minerals: alteration
Xenolith Abundance: possible peridotite
Xenolith Size: 2-3 mm
Xenolith Reaction: Srp rim
Pelletal Lapilli: n/a
Autoliths: n/a
Primary Carbonate: matrix
Kimberlitic Textures: inequigranular, uniform textured, macrocrystal, necklace

MODAL MINERALOGY:

Ol phenocrysts: euhedral to anhedral, Srp veining	75%
Ol macrocrysts: anhedral, Srp veining, Srp rim	20%
Crustal:	5%

MATRIX:

Major: Oxides (Spl), Cal-P, Ilm, Srp
Minor: Phl, Prv
Trace: Cal-S

TEXTURES/ADDITIONAL INFORMATION:

- Ol phenocrysts are euhedral, and it appears that the “phenocrysts” which are anhedral, are fragments of Ol macrocrysts.
- Cal-P is colourless.
- Prv displays weak zoning.

SAMPLE: **CD 021**
DEPTH: **unk1 (unknown depth)**

CLASSIFICATION: HK [altered]

SUMMARY: A macrocrystal perovskite-rich hypabyssal kimberlite.

Colour: dark brown
Clay Minerals: alteration
Xenolith Abundance: crustal 15%
Xenolith Size: sm
Xenolith Reaction: rim
Pelletal Lapilli: none
Autoliths: none
Primary Carbonate: none
Kimberlitic Textures: inequigranular, uniform textured, matrix-supported, sparsely macrocrystic

MODAL MINERALOGY:

Ol phenocrysts: anhedral, pseudomorphed	50%
Ol macrocrysts: anhedral, pseudomorphed	20%
Crustal: angular fragments	20%
Phl:	10%

MATRIX:

Major: Cal, Oxides (Spl), Srp
Minor: Ap, Prv
Trace: n/a

TEXTURES/ADDITIONAL INFORMATION:

- Cal-P rich uniform textured oxide-rich groundmass.
- Rounded lath-shaped Phl phenocrysts, some exhibit serpentinization between cleavage planes.
- Heavy serpentinization after Ol, both phenocrystic and macrocrystic Ol.
- Brown and yellow alteration (Srp?)
- Spls form necklace textures surrounding serpentinized Ol.
- Relative range in the sizes of Prv xls.

SAMPLE: CD 024
DEPTH: 39.90 m

CLASSIFICATION: HK

SUMMARY: A Cal-segregationary textured magmatic hypabyssal kimberlite.

Colour: brown
Clay Minerals: alteration
Xenolith Abundance: none
Xenolith Size: n/a
Xenolith Reaction: n/a
Olivine Replacement: Srp after Ol
Pelletal Lapilli: none
Autoliths: none
Primary Carbonate: yes
Kimberlitic Textures: Cal segregationary, matrix-supported, inequigranular

MODAL MINERALOGY:

Ol phenocrysts: euhedral, subhedral, fresh	50%
Ol phenocrysts: euhedral, subhedral, pseudomorphed	45%
Opaques: small, lath shaped	5%

MATRIX:

Major: Oxides (Spl), Cal-P
Minor: Prv, Cal-S, Phl, Srp
Trace: possible Ap

TEXTURES/ADDITIONAL INFORMATION:

- 2 distinct populations of Ol, fresh and pseudomorphed (Srp).

- Both populations of Ol have many euhedral phenocrysts.
- The pseudomorphed Ol tend to be euhedral.
- Both populations of Ol are rimmed with a heavy thick alteration material.
- The Sp group appears to form a necklace texture around certain minerals.
- The Sp group appear to concentrate in small areas of the calcite segregations.
- There appears to be two distinct sizes of Spl's, small 0.05-0.1 mm and large 0.2-0.4 mm, both euhedral.

SAMPLE: **CD 024**
DEPTH: **46.74 m**

CLASSIFICATION: HK [altered]

SUMMARY: An oxide-rich serpentine calcite hypabyssal kimberlite. *However the primary mineralogy is difficult to examine due to the extreme alteration.

Colour: brown
Clay Minerals: alteration
Xenolith Abundance: none
Xenolith Size: n/a
Xenolith Reaction: n/a
Pelletal Lapilli: n/a
Autoliths: n/a
Primary Carbonate: matrix
Kimberlitic Textures: inequigranular, macrocryst-poor

MODAL MINERALOGY:

Cal-S Pseudomorphs after Ol 100%

MATRIX:

Major: Oxides (Spl), Cal-P, Srp
Minor: Cal-S
Trace: n/a

TEXTURES/ADDITIONAL INFORMATION:

- It is very difficult to distinguish between primary and secondary Cal.
- Matrix is amorphous.

SAMPLE: **CD 024**
DEPTH: **88.37 m**

CLASSIFICATION: HK

SUMMARY: An oxide-rich macrocrystal calcite serpentine hypabyssal kimberlite.

Colour: grey
Clay Minerals: alteration
Xenolith Abundance: crustal
Xenolith Size: 2 mm
Xenolith Reaction: none

Pelletal Lapilli: n/a
Autoliths: n/a
Primary Carbonate: matrix
Kimberlitic Textures: inequigranular, uniform textured, necklace textures, macrocrystal, matrix-supported

MODAL MINERALOGY:

Ol phenocrysts: pseudomorphs, or partial Srp veining, subhedral	80%
Ol macrocrysts: anhedral, well-rounded, partial Srp veining	15%
Crustal: angular	5%

MATRIX:

Major: Oxides (Spl), Cal-P, Srp
Minor: Ilm, Cal-S, Prv
Trace: Ap, Phl

TEXTURES/ADDITIONAL INFORMATION:

- Oxide minerals in the groundmass are corroded.
- Difficult to distinguish between primary and secondary Cal.
- Prv is anhedral, and has a thick black amorphous rim.

SAMPLE: CD 024
DEPTH: 127.4 m

CLASSIFICATION: HK

SUMMARY: This thin section is classified as a magmatic, segregationary textured hypabyssal kimberlite.

Colour: Brown
Clay Minerals: alteration after Ol
Xenolith Abundance: crustal
Xenolith Size: 2mm avg.
Xenolith Reaction: small rim
Olivine Replacement: Srp
Pelletal Lapilli: none
Autoliths: none
Primary Carbonate: none
Kimberlitic Textures: matrix-supported, Cal-segregationary, inequigranular, sparsely macrocrystic

MODAL MINERALOGY:

Ol phenocrysts: Srp after Ol phenocrysts	45%
Ol phenocrysts: fresh	35%
Ol macrocrysts: fresh	10%
Opaque large phenocrysts	5%
Crustal: difficult to interpret	5%

MATRIX:

Major: Oxides (Spl), Srp, Cal-P

Minor: Prv, Cal-S (or Mtc)
Trace: Ap

TEXTURES/ADDITIONAL INFORMATION:

- Ol macrocrysts are fresh and anhedral (completely rounded).
- Thin section is similar to CD 024 39.90 m
- Phenocrystic euhedral to subhedral Ol dominates the matrix supported section.

SAMPLE: **CD 024**
DEPTH: **unknown**

CLASSIFICATION: HK

SUMMARY: Hypabyssal kimberlite containing abundant Spl and Prv in matrix.

Colour: Brown/Black
Clay Minerals: little replacement
Xenolith Abundance: crustal
Xenolith Size: 3mm length avg
Xenolith Reaction: none or small calcite/clay rims
Olivine Replacement: a few phenocrysts
Pelletal Lapilli: none
Autoliths: none
Primary Carbonate: none
Kimberlitic Textures: magmatic, inequigranular, uniform texture, matrix-supported

MODAL MINERALOGY:

Ol phenocrysts: Srp veining, 0.5 mm-1.0 mm	25%
Ol macrocrysts: with Srp veining	25%
Ol phenocrysts: partially serpentinized	25%
Crustal:subangular	15%
Phl macrocysts: rounded and alteration rims	10%

MATRIX:

Major: Oxides **(**Spl), Prv, Srp
Minor: Cal-P, Phl
Trace: -

TEXTURES/ADDITIONAL INFORMATION:

- Ol macrocrysts and phenocrysts are randomly oriented throughout the thin section.
- Some Ol (macro and pheno) have a black isotropic amorphous rim.
- Ol phenocrysts are veined and some are fresh (fine grained).
- Phl grains are acicular and bladed, and sometimes corroded.
- There is an association between Prv and Spl.

SAMPLE: **CD 025**
DEPTH: **26.18 m**

CLASSIFICATION: HK [altered]

SUMMARY: A macrocrystal spinel-rich calcite kimberlite.

Colour: brown/grey/green
Clay Minerals: alteration
Xenolith Abundance: none
Xenolith Size: n/a
Xenolith Reaction: n/a
Pelletal Lapilli: n/a
Autoliths: n/a
Primary Carbonate: matrix
Kimberlitic Textures: n/a

MODAL MINERALOGY:

Unidentifiable, however macrocrysts dominate.

MATRIX:

Major: Spl, Cal-S
Minor: n/a
Trace: n/a

TEXTURES/ADDITIONAL INFORMATION:

- Thin section is important because it presents macrocrystal kimberlite.
- This thin section is highly altered, and it is difficult to identify the primary mineralogy.

SAMPLE: **CD 025**
DEPTH: **30.29 m**

CLASSIFICATION: HK [altered]

SUMMARY: A sparsely macrocrystic spinel-rich hypabyssal kimberlite.

Colour: brown
Clay Minerals: alteration
Xenolith Abundance: none
Xenolith Size: n/a
Xenolith Reaction: n/a
Pelletal Lapilli: n/a
Autoliths: n/a
Primary Carbonate: matrix
Kimberlitic Textures: n/a

MODAL MINERALOGY:

Cal-S, Clay and Srp pseudomorphs after Ol.

MATRIX:

Major: Oxides (Spl), Cal-S
Minor: Ilm
Trace: n/a

TEXTURES/ADDITIONAL INFORMATION:

- Atoll, necklace-textured spinels.
- This thin section is extremely altered, where all of the primary mineralogy is unidentifiable.

SAMPLE: **CD 025**
DEPTH: **51.5 m**

CLASSIFICATION: HK? [altered]

SUMMARY: Segregationary textures are evident, shown with Cal, and also with a mud matrix. There is the possibility of a transition zone between HK and TK.

Colour: brown
Clay Minerals: Various
Xenolith Abundance: 5%
Xenolith Size: 2-5 mm
Xenolith Reaction: none
Olivine Replacement: Srp
Pelletal Lapilli: none
Autoliths: none
Primary Carbonate: matrix
Kimberlitic Textures: matrix-supported, inequigranular, segregationary textured

MODAL MINERALOGY:

Crustal: angular to subangular	60%
Ol phenocrysts: pseudomorphed Srp	20%
Di phenocrysts?: pseudomorphed	20%

MATRIX:

Major: Spl, Ap, Cal-S
Minor: Cal-P, Phl
Trace: -

TEXTURES/ADDITIONAL INFORMATION:

- Quite possibly a transition zone, including some seggregationary mud matrix, with Cal and Ap matrix supported zones. HK---TK transition?
- Extremely altered section, no primary mineralogy remaining.

SAMPLE: **CD 025**
DEPTH: **85.30 m**

CLASSIFICATION: HK [altered]

SUMMARY: A segregationary oxide-rich hypabyssal kimberlite.

Colour: Lgt Brown
Clay Minerals: alteration, crustal material
Xenolith Abundance: crustal 5%

Xenolith Size: 10mm to 0.5cm
Xenolith Reaction: none
Olivine Replacement: clay/srp
Pelletal Lapilli: none
Autoliths: none
Primary Carbonate: none
Kimberlitic Textures: matrix-supported, sparsely macrocrystic, segregationary textured

MODAL MINERALOGY:

Ol phenocrysts: (Srp pseudomorphs)	25%
Opaques: Large (Ilm?)	25%
Crustal: angular	20%
Ol macrocrysts (Srp pseudomorphs)	15%
Phl phenocrysts: kink-banded	15%

MATRIX/GROUNDMASS:

Major: Oxides (Spl)
Minor: Prv, Cal-S, Phl, Ap
Trace: Mtc?

TEXTURES/ADDITIONAL INFORMATION:

- Necklace textures with Prv.
- Groundmass contains abundant Prv, Phl, and Ap.
- Abundant crustal material.
- Mtc is a possibility; it has been pseudomorphed by Cal-S.
- Corroded atoll-textured spinels.

SAMPLE: **CD 025**
DEPTH: **90.67 m**

CLASSIFICATION: HK

SUMMARY: A fresh macrocrystal oxide-rich serpentine apatite hypabyssal kimberlite.

Colour: brown/green
Clay Minerals: alteration
Xenolith Abundance: none
Xenolith Size: n/a
Xenolith Reaction: n/a
Pelletal Lapilli: n/a
Autoliths: n/a
Primary Carbonate: matrix
Kimberlitic Textures: segregationary textured, inequigranular.

MODAL MINERALOGY:

Ol phenocrysts: euhedral to subhedral, Srp veining	70%
Ol macrocrysts: anhedral, Srp veining, thick black rims, highly fractured	15%
Phl phenocrysts: probably secondary/crustal	10%
Crustal: angular to subangular	5%

MATRIX:

Major: Srp, Phl-P, Oxides (Spl), Ap, Cal-P
Minor: Mtc?, Prv
Trace: Phl-S

TEXTURES/ADDITIONAL INFORMATION:

- The matrix is coarse grained.
- The oxides/Spl display atoll-textures.
- The Prv is cubic and dk orange/brown.
- The Prv is ~20um-75um.
- There is Cal segregationary textures in parts of the thin section, and other parts of the thin section have abundant Ap and Phl in the matrix. Prv is found in both sections.
- Mtc, as in many other sections is hard to distinguish b/c of alteration to Cal. The euhedral form is found in the matix, however, appears to be Cal-S.

SAMPLE: CD 025
DEPTH: 119.9 m

CLASSIFICATION: HK [altered]

SUMMARY: A macrocryst-poor calcite hypabyssal kimberlite.

Colour: grey
Clay Minerals: alteration
Xenolith Abundance: none
Xenolith Size: n/a
Xenolith Reaction: n/a
Pelletal Lapilli: n/a
Autoliths: n/a
Primary Carbonate: matrix
Kimberlitic Textures: segregationary textured, phenocrystic, inequigranular
MODAL MINERALOGY:

Ol phenocrysts: pseudomorphs, subhedral	80%
Ol macrocrysts: pseudomorphs, anhedral	20%

MATRIX:

Major: Cal-P, Srp, Oxides (Spl), Cal-S
Minor: Prv, Chl
Trace: Ap

TEXTURES/ADDITIONAL INFORMATION:

- Oxide rich, Spl's display atoll-textures.
- Prv's form necklace textures around Ol phenocrysts.
- Prv's are anhedral, and commonly fragmented.
- Cal-P is the majority of the matrix.

SAMPLE: CD 026

DEPTH: 69.10 m

CLASSIFICATION: HK [altered]

SUMMARY: A calcite hypabyssal kimberlite containing abundant crustal xenoliths, and secondary calcite veining.

Colour: brown/grey
Clay Minerals: alteration
Xenolith Abundance: crustal
Xenolith Size: 2 cm
Xenolith Reaction: Cal-S rim
Pelletal Lapilli: n/a
Autoliths: n/a
Primary Carbonate: matrix
Kimberlitic Textures: inequigranular, uniform textured, sparsely macrocrystic

MODAL MINERALOGY:

Ol phenocrysts: Srp veining, euhedral to anhedral	60%
Crustal: angular, granodiorite	30%
Ol macrocrysts: anhedral, some pseudomorphs, resorption features	10%

MATRIX:

Major: Cal-P, Cal-S, Oxides, Srp
Minor: Phl, Prv, Ap
Trace: Chl

TEXTURES/ADDITIONAL INFORMATION:

- This thin section is altered, and many of the Ol phenocrysts and/or macrocrysts have fractured and are within the matrix.
- Mtc may have been present, but could be pseudomorphed by Cal-S. The euhedral habit is still very visible in the thin section.

SAMPLE: CD 026
DEPTH: 76.70 m

CLASSIFICATION: HK [altered]

SUMMARY: A calcite hypabyssal kimberlite exhibiting extreme calcite segregationary textures.

Colour: dark grey
Clay Minerals: entire
Xenolith Abundance: crustal
Xenolith Size: n/a
Xenolith Reaction: Cal
Pelletal Lapilli: none
Autoliths: none
Primary Carbonate: none
Kimberlitic Textures: segregationary textured,

MODAL MINERALOGY:

This slide is extremely altered, mineral identification cannot be completed.

MATRIX:

Major: n/a
Minor: n/a
Trace: n/a

TEXTURES/ADDITIONAL INFORMATION:

- Everything is pseudomorphs of Cal and Phl after ????.
- Mtc habit is possible in the matrix, however it has been pseudomorphed to Cal-S.

SAMPLE: CD 026
DEPTH: 81.77 m

CLASSIFICATION: HK [altered]

SUMMARY: A sparsely macrocrystic oxide-rich hypabyssal kimberlite containing a serpentine matrix.

Colour: brown/grey
Clay Minerals: alteration
Xenolith Abundance: none
Xenolith Size: n/a
Xenolith Reaction: n/a
Pelletal Lapilli: n/a
Autoliths: n/a
Primary Carbonate: matrix
Kimberlitic Textures: inequigranular, matrix-supported, uniform textured, sparsely macrocrystic

MODAL MINERALOGY:

Ol phenocrysts: euhedral to subhedral, pseudomorphed	60%
Crustal: angular	30%
Ol macrocrysts: rounded anhedral, pseudomorphed	10%

MATRIX:

Major: Srp, Opaques, Ilm, Cal-P (or –S?)
Minor: Prv, Ap
Trace: Phl

TEXTURES/ADDITIONAL INFORMATION:

- Thin section is extremely altered.
- Groundmass is very hard to distinguish.
- It is very difficult to distinguish between Cal-P and Cal-S.

SAMPLE: CD 026
DEPTH: 96.01m

CLASSIFICATION: HK

SUMMARY: A spinel-rich macrocrystic hypabyssal kimberlite.

Colour: brown
Clay Minerals: none
Xenolith Abundance: few crustal
Xenolith Size: none
Xenolith Reaction: none
Olivine Replacement: none
Pelletal Lapilli: none
Autoliths: none
Primary Carbonate: none
Kimberlitic Textures: uniform textured, matrix-supported, inequigranular

MODAL MINERALOGY:

Ol phenocrysts, anhedral, rounded, fresh	70%
Ol macrocrysts, anhedral, rounded, fresh	20%
Ol phenocrysts (pseudomorphed), anhedral	10%

MATRIX:

Major: Oxides (Spl), Srp
Minor: Prv
Trace: Ap, Cal-S

TEXTURES/ADDITIONAL INFORMATION:

- The "fresh" Ol macrocrysts and phenocrysts display some Srp veining.
- The Prv are large, cubic, and orange- brown.
- This thin section should be microprobed (Ol).
- Other than the oxides, the groundmass is undistinguishable (amorphous) therefore it is assumed to be Srp.

SAMPLE: CD 026
DEPTH: 99.40 m

CLASSIFICATION: HK

SUMMARY: A sparsely phenocrystic, spinel and calcite-rich hypabyssal kimberlite.

Colour: brown/grey
Clay Minerals: alteration
Xenolith Abundance: none
Xenolith Size: n/a
Xenolith Reaction: n/a
Pelletal Lapilli: n/a
Autoliths: n/a
Primary Carbonate: matrix
Kimberlitic Textures: equigranular, matrix-supported, sparsely phenocrystic

MODAL MINERALOGY:

Ol phenocrystal: euhedral to subhedral, pseudomorphed	80%
Crustal: angular	20%

MATRIX:

Major: Cal-P, Oxides (Spl), Ilm
Minor: Phl, Prv
Trace: Ap

TEXTURES/ADDITIONAL INFORMATION:

- Thin section is essentially aphanitic.
- Prv's exhibit zoning and thick rims.
- 1 macrocryst is found in the thin section, it is pseudomorphed and has a fracture/hole that is infilled with small fine grained opaques. These opaques are not the same size as the opaques found in the matrix of the thin section.

SAMPLE: **CD 029**
DEPTH: **35.58 m**

CLASSIFICATION: HK

SUMMARY: A sparsely macrocrystic, perovskite-rich calcite hypabyssal kimberlite.

Colour: brown/grey
Clay Minerals: alteration
Xenolith Abundance: none
Xenolith Size: n/a
Xenolith Reaction: n/a
Pelletal Lapilli: n/a
Autoliths: n/a
Primary Carbonate: matrix
Kimberlitic Textures: inequigranular, uniform textured, matrix-supported, sparsely macrocrystic.

MODAL MINERALOGY:

Ol phenocrysts: subhedral to anhedral, pseudomorphed	65%
Crustal:subangular	25%
Ol macrocrysts: anhedral, thick alteration rims, pseudomorphs	10%

MATRIX:

Major: Oxides (Spl), Ilm, Prv, Cal-P, Srp
Minor: Ap, Phl, Chl
Trace: Mtc?

TEXTURES/ADDITIONAL INFORMATION:

- Ol in the thin section is completely pseudomorphed.
- Prv in the thin section is large and zoned.
- Opaques in the thin section are anhedral and two sizes, 10 um and 50 um (approx).

- Opaques form necklace textures around pseudomorphs after Ol.
- Radial Ap's are present.

SAMPLE: **CD 029**
DEPTH: **56.98 m**

CLASSIFICATION: HK [altered]

SUMMARY: An macrocrystal phlogopite-rich hypabyssal kimberlite, with abundant perovskite in the groundmass.

Colour: brown/grey
Clay Minerals: alteration
Xenolith Abundance: none
Xenolith Size: n/a
Xenolith Reaction: n/a
Pelletal Lapilli: n/a
Autoliths: n/a
Primary Carbonate: matrix
Kimberlitic Textures: inequigranular, uniform textured, matrix-supported, sparsely macrocrystic

MODAL MINERALOGY:

Ol phenocrysts: Subhedral to anhedral, pseudomorphed	60%
Phl phenocrysts: Large (0.5-1 mm long) lath shaped	20%
Ol macrocrysts: anhedral rounded and pseudomorphed	20%

MATRIX:

Major: Srp, Cal-P, Phl, Oxides (Spl)
Minor: Prv, Ap
Trace: Ilm

TEXTURES/ADDITIONAL INFORMATION:

- Accicular Ap
- Phl phenocrysts have inclusions and have been extensively altered/corroded.
- Prv's are large 100 um avg, and are mainly anhedral.
- Two sizes of opaques. Smaller Spl form necklace textures.
- Clear close relationship of Spl and Prv.

SAMPLE: **CD 029**
DEPTH: **86.06 m**

CLASSIFICATION: HK [altered]

SUMMARY: An oxide-rich phlogopite hypabyssal kimberlite. This section contains abundant crustal material.

Colour: brown/grey
Clay Minerals: alteration

Xenolith Abundance: none
Xenolith Size: n/a
Xenolith Reaction: n/a
Pelletal Lapilli: n/a
Autoliths: n/a
Primary Carbonate: matrix
Kimberlitic Textures: inequigranular, uniform textured, matrix-supported, sparsely macrocrystic

MODAL MINERALOGY:

Ol phenocrysts: rounded and pseudomorphed	70%
Crustal:angular to rounded	20%
Ol macrocrysts: rounded and pseudomorphed	10%

MATRIX:

Major: Phl, Oxides (Spl), Cal-S
Minor: Ap, Ilm, Prv, Srp
Trace: n/a

TEXTURES/ADDITIONAL INFORMATION:

- Slide contains abundant crustal material.
- Slide contains a phlogopite-rich groundmass/matrix.

SAMPLE: **CWDH-3001-01**
DEPTH: **34.98 m**

CLASSIFICATION: HK [altered]

SUMMARY: A macrocryst-poor extremely altered hypabyssal kimberlite.

Colour: brown/grey
Clay Minerals: alteration
Xenolith Abundance: none
Xenolith Size: n/a
Xenolith Reaction: n/a
Pelletal Lapilli: n/a
Autoliths: n/a
Primary Carbonate: matrix
Kimberlitic Textures: segregationary textured, sparsely phenocrystic

MODAL MINERALOGY:

Ol phenocrysts: pseudomorphs	100%

MATRIX:

Major: Cal-P, Prv, Ilm, Oxides, Chl, Cal-S
Minor: Ap, Srp
Trace: Phl

TEXTURES/ADDITIONAL INFORMATION:

- Thin section is extremely altered.
- Very difficult to distinguish mineralogy.

SAMPLE: **CWDH-3003-01**
DEPTH: **22.49 m**

CLASSIFICATION: HK

SUMMARY: A spinel-rich calcite hypabyssal kimberlite, similar to the Jos kimberlite, Somerset Island.

Colour: brown/grey
Clay Minerals: alteration
Xenolith Abundance: none
Xenolith Size: n/a
Xenolith Reaction: n/a
Pelletal Lapilli: n/a
Autoliths: n/a
Primary Carbonate: matrix
Kimberlitic Textures: inequigranular, matrix-supported, course groundmass, uniform textured

MODAL MINERALOGY:

Ol phenocrysts: euhedral to subhedral, Srp veining, thick alteration rim	70%
Ol microphenocryst: euhedral to subhedral, fractures, pseudomorphed	25%
Ol macrocrysts: subhedral, Srp veining	5%

MATRIX:

Major: Oxides, Ilm, Cal-P
Minor: Prv?
Trace: n/a

TEXTURES/ADDITIONAL INFORMATION:

- Matrix is coarse grained.
- Cal-P is tabular, randomly oriented prisms.
- All Ol's have thick alteration rims.
- Spl (Oxides) are found as necklace textures and in cumulates.
- Opaques are fine-grained.

SAMPLE: **CWDH-3003-01**
DEPTH: **28.96 m**

CLASSIFICATION: HK

SUMMARY: A hypabyssal calcite kimberlite similar to the JOS kimberlite (Somerset Island), where the primary calcite forms tabular, randomly oriented prisms.

Colour: brown/grey
Clay Minerals: alteration
Xenolith Abundance: none

Xenolith Size: n/a
Xenolith Reaction: n/a
Pelletal Lapilli: n/a
Autoliths: n/a
Primary Carbonate: matrix
Kimberlitic Textures: inequigranular, matrix supported, uniform textured

MODAL MINERALOGY:

Ol phenocrysts: euhedral to subhedral, thick alteration rims	50%
Ol phenocrysts: subhedral to anhedral, pseudomorphs	30%
Ol macrocrysts: rounded subhedral to anhedral, Srp veining	10%
Ol microphenocrysts: appear to be fragments, pseudomorphed	10%

MATRIX:

Major: Oxides, Ilm, Cal-P
Minor: n/a
Trace: Prv

TEXTURES/ADDITIONAL INFORMATION:

- Extremely coarse matrix.
- Cal is primary and forms tabular, randomly oriented prisms.
- Macrocryst-poor.
- Opaques (Spl?) forms necklace textures and cumulates throughout the thin section.

SAMPLE: **CWDH-3003-01**
DEPTH: **44.24 m**

CLASSIFICATION: HK [altered]

SUMMARY: An opaque-rich phenocrystal hypabyssal kimberlite containing olivines exhibiting strain textures.

Colour: brown grey
Clay Minerals: alteration
Xenolith Abundance: none
Xenolith Size: n/a
Xenolith Reaction: n/a
Pelletal Lapilli: n/a
Autoliths: n/a
Primary Carbonate: matrix (secondary)
Kimberlitic Textures: inequigranular, uniform textured, phenocrystic, matrix-supported

MODAL MINERALOGY:

Ol phenocrystal: subhedral to anhedral, pseudomorphed	90%
Ol macrocrystal: anhedral, pseudomorphed	10%

MATRIX:

Major: Ilm, Oxides, Prv, Cal-S
Minor: Ap, Phl

Trace: n/a

TEXTURES/ADDITIONAL INFORMATION:

- Multiple fractures throughout thin sections infilled with microcrystalline Qtz.
- Thin section is altered.
- Ol have thick amorphous rim.
- Ol exhibit uneven birefringence (due to strain).
- Devoid of Prv.

Summary of Petrographic Analysis
Churchill Kimberlite Project

CWDH-3001-01

One thin section was studied with this particular drill hole (34.98 m). This was classified as a sparsely macrocrystic, segregationary-textured, calcite hypabyssal kimberlite. The degree of alteration of this sample was high.

CWDH-3003-01

The depth range of the samples studied was 22.49–44.24 m. With a very low degree of alteration, these samples were classified as sparsely macrocrystic, oxide-rich, calcite hypabyssal kimberlite. The key features were a coarse matrix, where calcite forms tabular randomly oriented prisms. Trace perovskite was identified.

04KD597-01

The depth range of the samples studied was 17.7-58.2 m. Alteration varied with depth, with the shallow sample being extensively altered, and the deeper sample relatively fresh. Overall, these samples were classified as sparsely macrocrystic, phlogopite serpentine hypabyssal kimberlite. Phlogopite phenocrysts were abundant, along with oxide minerals, primarily spinel-group minerals.

04KD568-01

One thin section was studied with this particular drill hole (12.1m). This was classified as a highly altered, serpentine-rich calcite hypabyssal kimberlite. This thin section exhibited a preferred flow orientation.

04KD428-01

The depth range of the samples studied was 30.6-68.2 m. These samples were extremely altered, and classification was inconclusive due to the extensive alteration. If one could speculate, the samples would be classified as serpentine-rich calcite hypabyssal kimberlite.

04KD217-01

One thin section was studied with this particular drill hole (59.9m). This was classified as a sparsely macrocyrstic calcite hypabyssal kimberlite. There was a very low degree of alteration with this sample, and disaggregated macrocrystic olivines were identified.

04KD230-01

The depth range of the samples studied was 21.3-37.0 m. These samples were extremely altered, and the primary mineralogy was difficult to identify. As a result classification was inconclusive. The matrix included abundant phlogopite, calcite (primary/secondary?) and abundant serpentine.

04KD235-01

The depth range of the samples studied was 54.9-75.6 m. The samples were all fresh, with minor amounts of alteration. The samples were altogether classified as a sparsely macrocrystic oxide-rich calcite hypabyssal kimberlite. In one thin section, a megacrysts of olivine was identified. There was a range in perovskite sizes identified in the matrix of all the samples.

CD 001

The depth range of the samples studied was 20.4-81.96 m. The samples exhibited moderate amounts of alteration, where the olivine phenocrysts were pseudomorphs, and the olivine macrocrysts remained fresh. The samples altogether were classified as sparsely macrocrystic oxide-rich serpentine calcite hypabyssal kimberlite. Phlogopite phenocrysts were found in some samples, while phlogopite laths were commonly found in the matrix of the samples.

CD 002

The depth range of the samples studied was 30.05-34.38 m. The samples were all fresh, with very little alteration present. They are altogether classified as macrocrystic oxide-rich monticellite phlogopite hypabyssal kimberlite. Primary calcite was abundant in the matrix of the samples, along with two generations of perovskite. The oxides and the perovskite grains were commonly associated with each other in the matrix of the kimberlite. Ilmenite megacrysts were identified in one of the thin sections.

CD 003

One thin section was studied with this particular drill hole (12.79m). The sample was heavily altered, with phlogopite, spinels and primary calcite as the main matrix minerals. The sample can be classified as phlogopite-rich hypabyssal kimberlite. Corroded atoll-textured spinels were identified as occurring in the matrix. Phlogopite grains were distorted and some grains exhibited flow banding.

CD 004

The depth range of the samples studied was 18.0-36.97 m. There was a moderate degree of alteration noted for the drill hole. The samples are altogether classified as oxide-rich calcite hypabyssal kimberlite. The matrix consisted of abundant spinel in a mesostasis of serpentine, chlorite and calcite.

CD 006

The depth range of the samples studied was 38.57-65.0 m. The samples exhibited extreme alteration, and identification of the primary mineralogy inconclusive. Minerals identified in the matrix included phlogopite, calcite and spinels. Epitaxial overgrowths were identified on a select few phlogopite phenocrysts.

CD 007

The depth range of the samples studied was 18.65-78.64 m. The samples overall exhibited a low degree of alteration, and were sparsely macrocrystic to macrocrystic. The majority of the matrix mineralogy consisted of large coarse primary calcite, with lesser phlogopite and oxides. This sample needs microprobe analyses of some of the primary mineralogy before it can be correctly classified as a *bona fide* magmatic kimberlite. (carbonatite?)

CD 009

The depth range of the samples studied was 32.61-44.31 m. Most of the samples were highly altered, however, the sample at 44.31 m was reasonably fresh. The samples can be altogether classified as a segregationary-textured aphanitic oxide-rich hypabyssal kimberlite. Matrix mineralogy was complex, including calcite (both primary and secondary), chlorite, spinel, monticellite, apatite, and serpentine.

CD 010

The depth range of the samples studied was 62.05-91.1 m. With the exception of one fresh sample, the remaining were heavily altered. Although further analysis (via microprobe) is required in order for classification of a *bona fide* hypabyssal kimberlite, temporary classification of the samples can be made. Altogether, the samples represent a macrocrystal oxide-rich calcite serpentine hypabyssal kimberlite. Corroded atoll-textured spinels are abundant in the matrix mineralogy.

CD 013

The depth range of the samples studied was 14.75-54.49 m. The degree of alteration changes with depth. Classification for these samples was difficult, as there is some indication of TK. Muddy matrix and pelletal lapilli are identified, along with abundant clays and serpentine. However, most of the samples would be classified as hypabyssal kimberlite. One explanation could be a transition zone between a diatreme and root zone, where characteristic features of both types are commonly found together.

CD 015

The depth range of the samples studied was from 14.20-24.30 m. These samples were all extremely altered, however, the macrocrysts were reasonably fresh while the phenocrysts were pseudomorphed. This section can altogether be classified as a macrocrystal calcite-rich serpentine hypabyssal kimberlite. Both primary and secondary calcite are found occurring in the matrix.

CD 020

The depth range of the samples studied was from 20.0-89.20 m. The samples had little to no alteration, and one sample contained some kimberlite autoliths. They can altogether be classified as a sparsely macrocrystic calcite-rich oxide hypabyssal kimberlite. Atoll-textured spinels were located in the matrix, along with apatite and serpentine.

CD 021

The depth range of the samples studied was from 30.77-88.26 m. The degree of alteration was high throughout the drill hole. Phlogopite was abundant in the matrix, along with calcite. It was very difficult to distinguish between primary and secondary calcite. The samples can altogether be classified as macrocrystal calcite hypabyssal kimberlite.

CD 024

The depth range of the samples studied was from 39.90-127.4 m. The alteration was only significant in one sample (around 50m). The macrocrysts were fresh, anhedral and rounded, while the phenocrysts were slightly altered and sparsely macrocrystic. The samples can altogether be classified as sparsely macrocrystic oxide-rich calcite hypabyssal kimberlite.

CD 025

The depth range of the samples studied was from 26.8-119.9 m. The degree of alteration varied with depth. The samples varied from sparsely macrocrystic to macrocrystic. Atoll-textured spinels, and necklace textures were common. Seggregationary (calcite) textures were noted at 3 depths (~50, 80, 90m). The samples can be classified as both segregationary textured calcite hypabyssal kimberlite, and oxide-rich calcite hypabyssal kimberlite.

CD 026

The depth range of the samples studied was from 69.10-99.40 m. The degree of alteration varies with depth. Both segregationary textures and uniform textures were identified. Abundant crustal material was found in these samples. The samples altogether can be classified as sparsely macrocrystic to macrocrystic oxide hypabyssal kimberlite.

CD 029

The depth range of the samples studied was 35.58-86.06 m. Low to moderate alteration was identified with the samples. The samples can be classified as sparsely macrocrystic to macrocrystic calcite-rich phlogopite oxide hypabyssal kimberlite. Abundant crustal material was identified in the thin sections.

Petrographic Images: Churchill kimberlite field
Slide #1

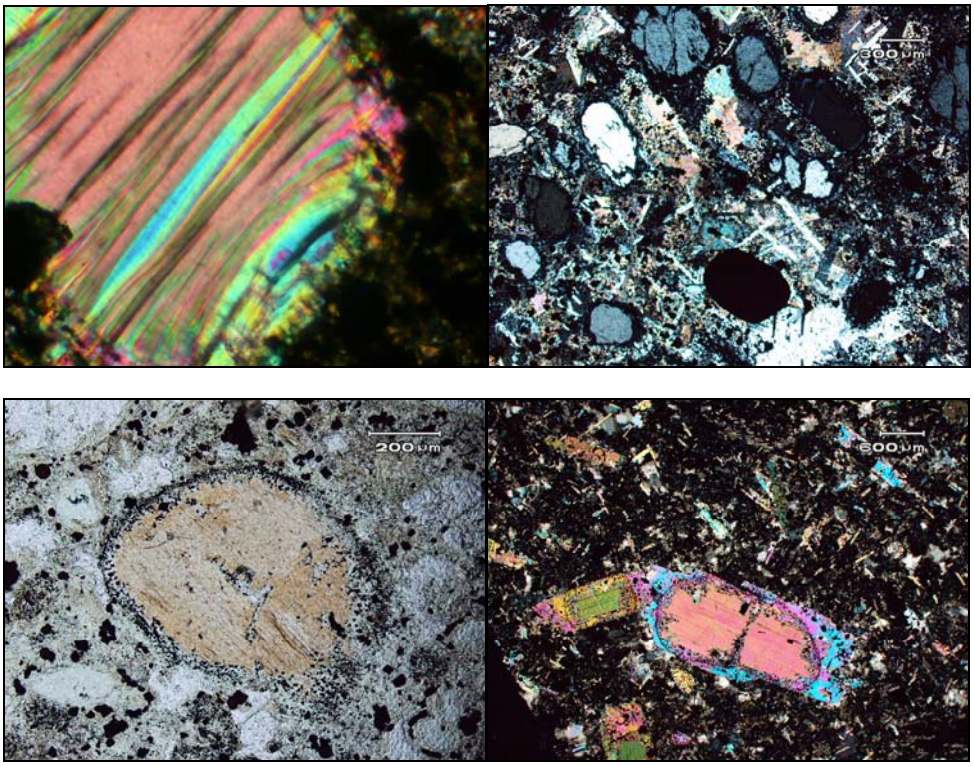

Top-Left: Churchill kimberlite CD01, 82m depth. FOV=1.8mm (cross polarized light)
Description: Rim alteration on phenocrystal phlogopite. Also note alteration between cleavage planes.

Top-Right: Churchill kimberlite 04KD230 21m depth, scale shown (cross polarized light)
Description: Anhedral microphenocrystal olivine in a matrix of phlogopite laths and oxides, interstitial calcite.

Bottom-Left: Churchill kimberlite CD02 35m depth, scale shown (plane polarized light)
Description: Altered rounded phlogopite rimmed with oxides in a necklace texture, characteristic of oxides in a kimberlite groundmass. Larger spinels are shown in the matrix of the kimberlite.

Bottom-Right: Churchill kimberlite CD06, 50m depth, scale shown (cross polarized light)
Description: Altered phlogopite laths showing necklace textures with oxides as well as epitaxial overgrowths. Matrix and groundmass contains abundant apatite and calcite.

Petrographic Images: Churchill kimberlite field
Slide #2

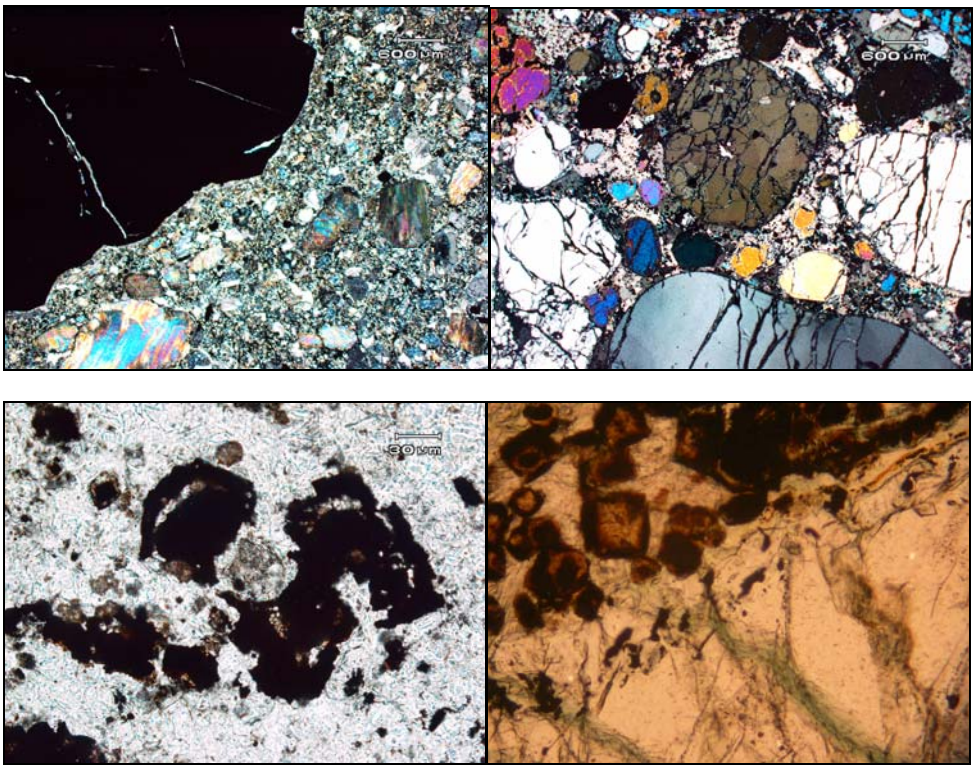

Top-Left: Churchill kimberlite CD02, 35m depth, scale shown (cross polarized light) Description: Large anhedral ilmenite macrocryst shown with a hypabyssal kimberlite matrix and groundmass consisting of altered microphenocrystal olivines, apatite, oxides, phlogopite and calcite.

Top-Right: Churchill kimberlite CD07, 79 depth, scale shown (cross polarized light) Description: Typical hypabyssal kimberlite showing different generations of olivine and varying degrees of alteration. Matrix and groundmass consists of spinels and oxides, and primary calcite.

Bottom-Left: Churchill kimberlite 04KD217, 60m depth, scale shown (plane polarized light) Description: Large atoll spinels shown with brown euhedral to anhedral perovskite. The two minerals are commonly found occurring with each other in the Churchill kimberlites.

Bottom-Right: Churchill kimberlite CD01, 61m depth, Field of view = 1mm (plane polarized light)Description: Euhedral cubic perovskite (brown) shown infilling a fracture of a macrocrystal olivine. Note the chlorite infilling the secondary fractures in the olivine grain.

Petrographic Images: Churchill kimberlite field
Slide #3

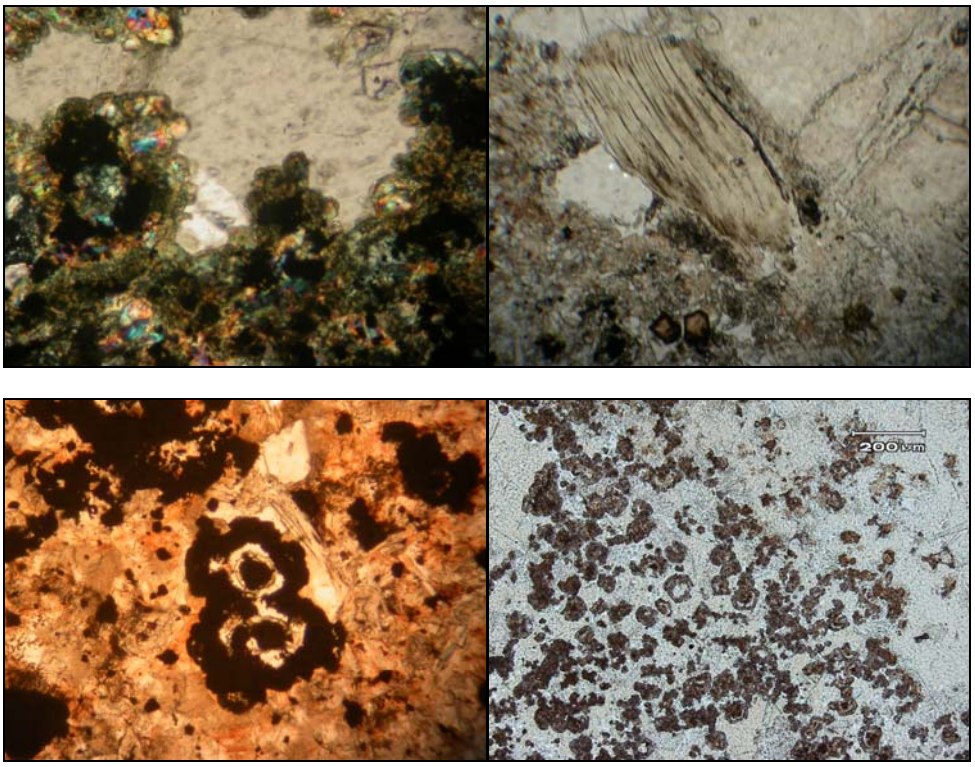

Top-Left: Churchill kimberlite CD09, 32m depth, FOV = 2.1mm (cross polarized light)
Description: Calcite segregationary textures shown. Note the large spinel group minerals present along with the serpentine and chlorite alteration in the matrix.

Top-Right: Churchill kimberlite CD24 40m depth, FOV = 2.1mm (plane polarized light)
Description: Altered phlogopite (flow banding) shown with large euhedral cubic perovskite. Note the alteration on the perovskite rims.

Bottom-Left: Churchill kimberlite CD25 55m depth, FOV= 1mm (plane polarized light)
Description: Atoll spinel with smaller spinel group minerals surrounding the atoll outer edge.

Bottom-Right: Churchill kimberlite CDWH3001 30m, Scale shown (plane polarized light)
Description: Perovskite cumulates (along with some spinel group minerals) in the matrix of a sparsely macrocrystic hypabyssal kimberlite. The groundmass consists almost entirely of apatite and calcite.

Churchill Kimberlite Olivine Analyses

Sample		SiO_2	TiO_2	Al_2O_3	Cr_2O_3	FeO	MnO	NiO	MgO	CaO	Na_2O	Oxide Total
SZ-CD20-1	P-C	41.100	0.009	0.031	0.028	8.840	0.110	0.369	49.350	0.077	0.022	99.936
SZ-CD20-2	P-C	41.080	0.000	0.029	0.055	8.610	0.113	0.376	49.020	0.084	0.025	99.392
SZ-CD20-3	P-C	41.100	0.013	0.069	0.048	9.030	0.111	0.372	48.860	0.077	0.046	99.726
SZ-CD20-4	P-C	41.030	0.019	0.025	0.076	8.890	0.117	0.362	48.950	0.076	0.040	99.585
SZ-CD20-5	P-C	41.070	0.025	0.040	0.076	9.220	0.109	0.380	48.960	0.080	0.048	100.008
SZ-CD20-6	P-C	41.090	0.000	0.023	0.040	9.060	0.108	0.366	49.120	0.060	0.023	99.890
SZ-CD20-7	P-C	40.850	0.010	0.042	0.030	9.050	0.113	0.361	48.850	0.059	0.040	99.405
SZ-CD20-8	P-C	40.740	0.020	0.013	0.068	8.860	0.112	0.371	49.030	0.070	0.037	99.321
SZ-CD20-9	P-C	41.000	0.000	0.018	0.016	8.830	0.122	0.379	49.140	0.065	0.021	99.591
SZ-CD20-10	P-C	40.970	0.000	0.036	0.083	9.420	0.112	0.382	48.700	0.087	0.055	99.845
SZ-CD20-11	P-C	40.820	0.010	0.065	0.048	9.340	0.123	0.373	48.780	0.091	0.060	99.710
SZ-CD20-12	P-C	41.030	0.000	0.041	0.054	9.390	0.119	0.378	48.470	0.092	0.029	99.603
SZ-CD20-13	MA	40.740	0.032	0.000	0.040	8.750	0.106	0.364	48.780	0.053	0.023	98.888
SZ-CD20-14	MA	40.710	0.021	0.029	0.060	8.640	0.105	0.378	49.000	0.074	0.054	99.071
SZ-CD20-15	P-R	41.780	0.000	0.000	0.000	2.250	0.160	0.116	53.800	0.377	0.021	98.504
SZ-CD20-16	P-R	42.050	0.000	0.000	0.000	2.260	0.135	0.134	53.740	0.333	0.014	98.666
SZ-CD20-17	P-R	10.150	0.068	0.105	0.124	22.080	0.157	0.612	39.360	0.167	0.093	72.916
SZ-CD20-18	P-R	41.340	0.015	0.051	0.056	9.170	0.108	0.376	48.770	0.087	0.040	100.013
SZ-CD20-19	P-R	40.860	0.023	0.038	0.060	9.110	0.117	0.384	48.850	0.079	0.033	99.554
SZ-CD20-20	P-R	39.970	0.027	0.059	0.080	8.920	0.119	0.366	48.880	0.106	0.057	98.584
SZ-CD24-1	P	41.050	0.000	0.027	0.034	9.220	0.120	0.361	49.180	0.061	0.030	100.083
SZ-CD24-2	P	40.970	0.026	0.034	0.020	9.100	0.109	0.366	48.750	0.084	0.025	99.484
SZ-CD24-3	P	41.330	0.034	0.025	0.033	8.960	0.130	0.378	48.860	0.080	0.025	99.855
SZ-CD24-4	P	41.320	0.009	0.021	0.015	8.530	0.126	0.390	48.910	0.067	0.036	99.424
SZ-CD24-5	P	41.210	0.014	0.058	0.061	8.570	0.107	0.393	48.810	0.067	0.063	99.353
SZ-CD24-6	P	41.040	0.022	0.021	0.034	8.920	0.121	0.368	49.260	0.072	0.028	99.886
SZ-CD24-7	P	41.020	0.040	0.020	0.118	9.680	0.121	0.364	48.240	0.085	0.026	99.714
SZ-CD24-8	P	41.350	0.023	0.047	0.070	9.650	0.105	0.367	48.450	0.089	0.040	100.191

P-C: Phenocryst core; P-R: Phenocryst Rim; P: Phenocryst; MA: Macrocryst; ME: Megacryst; OPX: Orthopyroxene inclusion

Churchill Kimberlite Olivine Analyses

Sample		SiO_2	TiO_2	Al_2O_3	Cr_2O_3	FeO	MnO	NiO	MgO	CaO	Na_2O	Oxide Total
SZ-CD24-9	P	40.900	0.021	0.029	0.051	9.050	0.123	0.371	48.470	0.087	0.025	99.127
SZ-CD24-10	P	40.970	0.000	0.027	0.018	8.980	0.109	0.380	48.300	0.092	0.035	98.911
SZ-CD24-11	P	42.000	0.000	0.000	0.000	2.520	0.145	0.119	53.660	0.414	0.000	98.858
SZ-CD24-12	P	42.010	0.010	0.015	0.022	2.450	0.146	0.115	53.430	0.392	0.000	98.590
SZ-CD24-13	P	41.660	0.000	0.014	0.044	2.330	0.129	0.179	52.310	0.394	0.009	97.069
SZ-CD24-14	P	40.570	0.010	0.012	0.056	9.290	0.108	0.356	47.760	0.111	0.029	98.302
SZ-CD24-15	P	40.340	0.000	0.023	0.030	10.270	0.111	0.290	47.680	0.071	0.040	98.855
SZ-CD24-16	P	40.000	0.010	0.010	0.025	8.940	0.116	0.355	48.250	0.070	0.030	97.806
SZ-CD24-17	P	39.760	0.014	0.000	0.075	8.760	0.098	0.365	48.120	0.074	0.025	97.291
SZ-CD24-18	P	41.180	0.013	0.037	0.115	8.800	0.109	0.396	48.980	0.061	0.008	99.699
SZ-CD24-19	P	41.250	0.021	0.026	0.054	8.600	0.125	0.378	48.790	0.058	0.027	99.329
SZ-CD24-20	P	41.030	0.000	0.016	0.059	8.790	0.107	0.366	49.150	0.065	0.017	99.600
SZ-JBP16-1	ME	39.670	0.010	0.000	0.020	15.750	0.185	0.069	43.960	0.036	0.025	99.725
SZ-JBP16-2	ME	39.340	0.047	0.025	0.000	15.650	0.175	0.075	43.690	0.035	0.028	99.065
SZ-JBP16-3	ME	38.800	0.033	0.010	0.027	15.340	0.182	0.085	43.260	0.034	0.013	97.784
SZ-JBP16-4	ME	37.510	0.015	0.000	0.010	14.970	0.180	0.072	42.700	0.030	0.016	95.503
SZ-JBP16-5	ME	36.460	0.010	0.000	0.000	15.640	0.183	0.057	42.030	0.030	0.022	94.432
SZ-JBP16-6	ME	35.580	0.008	0.000	0.010	14.960	0.177	0.067	41.670	0.031	0.012	92.515
SZ-JBP16-7	ME	35.060	0.018	0.000	0.000	15.820	0.174	0.067	41.770	0.029	0.031	92.969
SZ-JBP16-8	ME	34.660	0.052	0.017	0.000	15.780	0.187	0.078	41.300	0.029	0.010	92.113
SZ-JBP16-9	ME	32.970	0.019	0.000	0.000	15.570	0.185	0.073	40.340	0.032	0.023	89.212
SZ-JBP16-10	ME	40.170	0.043	0.000	0.000	15.350	0.182	0.072	43.970	0.023	0.022	99.832
SZ-JBP16-11	ME	40.060	0.000	0.026	0.010	15.860	0.180	0.068	44.060	0.037	0.019	100.320
SZ-JBP16-12	ME	40.050	0.010	0.000	0.000	15.800	0.178	0.071	44.020	0.037	0.026	100.192
SZ-JBP16-13	ME	39.620	0.027	0.000	0.015	15.790	0.164	0.068	43.720	0.038	0.018	99.460
SZ-JBP16-14	ME	40.080	0.024	0.010	0.000	15.800	0.172	0.063	43.960	0.033	0.032	100.174
SZ-JBP16-15	ME	40.100	0.009	0.000	0.000	15.710	0.183	0.082	43.860	0.026	0.015	99.985
SZ-JBP16-16	ME	39.960	0.021	0.000	0.000	15.420	0.166	0.079	43.690	0.033	0.022	99.391
SZ-JBP16-17	ME	40.090	0.039	0.000	0.010	15.200	0.164	0.080	43.710	0.029	0.034	99.356

Churchill Kimberlite Olivine Analyses

Sample		SiO_2	TiO_2	Al_2O_3	Cr_2O_3	FeO	MnO	NiO	MgO	CaO	Na_2O	Oxide Total
SZ-JBP16-18	ME	39.800	0.046	0.023	0.000	15.490	0.177	0.082	44.050	0.024	0.008	99.700
SZ-JBP16-19	ME	39.750	0.037	0.000	0.000	15.850	0.188	0.070	43.940	0.016	0.029	99.880
SZ-JBP16-20	ME	38.850	0.013	0.036	0.000	15.850	0.190	0.066	43.480	0.025	0.015	98.525
SZ-CD01-1	MA	40.660	0.052	0.046	0.111	10.090	0.127	0.360	49.020	0.061	0.041	100.568
SZ-CD01-2	MA	40.350	0.023	0.068	0.047	10.060	0.124	0.367	48.900	0.065	0.025	100.029
SZ-CD01-3	MA	40.300	0.047	0.063	0.019	10.080	0.128	0.364	48.950	0.078	0.035	100.064
SZ-CD01-4	OPX	39.330	0.050	0.032	0.000	15.910	0.192	0.100	45.060	0.046	0.049	100.769
SZ-CD01-5	OPX	39.370	0.014	0.054	0.053	17.160	0.182	0.090	44.190	0.046	0.031	101.190
SZ-CD01-6	OPX	39.250	0.063	0.028	0.000	16.850	0.200	0.088	43.830	0.053	0.020	100.382
SZ-CD01-7	OPX	55.970	0.157	0.703	0.000	10.280	0.194	0.031	31.740	0.704	0.153	99.932
SZ-CD01-8	OPX	56.220	0.123	0.622	0.026	10.340	0.195	0.042	31.680	0.739	0.136	100.123
SZ-CD01-9	MA	39.620	0.033	0.000	0.035	16.940	0.188	0.113	44.480	0.052	0.045	101.506
SZ-CD01-10	MA	39.980	0.034	0.028	0.000	14.410	0.154	0.116	45.870	0.130	0.021	100.743
SZ-CD01-11	MA	40.280	0.000	0.018	0.000	13.640	0.170	0.121	46.320	0.048	0.037	100.634
SZ-CD01-12	MA	40.110	0.059	0.047	0.020	12.800	0.165	0.155	47.280	0.067	0.033	100.736
SZ-CD01-13	MA	41.790	0.037	0.026	0.000	2.470	0.215	0.057	54.040	0.269	0.020	98.924
SZ-CD01-14	MA	41.580	0.013	0.058	0.073	2.420	0.213	0.161	53.580	0.275	0.007	98.380
SZ-CD01-15	MA	41.550	0.000	0.028	0.000	2.110	0.216	0.067	53.880	0.272	0.026	98.149
SZ-CD01-16	MA	41.880	0.011	0.057	0.000	2.410	0.211	0.124	54.300	0.271	0.013	99.277
SZ-CD01-17	MA	41.720	0.009	0.061	0.039	2.500	0.228	0.082	54.200	0.277	0.030	99.146
SZ-CD01-18	MA	39.990	0.074	0.057	0.129	11.630	0.142	0.322	48.070	0.062	0.037	100.513
SZ-CD01-19	MA	40.450	0.000	0.032	0.084	11.620	0.132	0.290	47.980	0.059	0.050	100.697
SZ-CD01-20	MA	40.350	0.038	0.086	0.015	11.270	0.146	0.288	48.060	0.068	0.050	100.371
SZ-CD01-21	MA	40.740	0.010	0.066	0.091	11.270	0.142	0.301	48.050	0.066	0.055	100.791
SZ-CD01-22	MA	40.120	0.030	0.053	0.010	11.120	0.143	0.329	47.900	0.052	0.032	99.789
SZ-CD01-23	MA	40.450	0.043	0.080	0.011	11.310	0.156	0.292	48.080	0.073	0.027	100.522
SZ-CD01-24	MA	39.880	0.034	0.011	0.073	11.740	0.134	0.269	47.440	0.044	0.018	99.643
SZ-CD01-25	MA	40.270	0.000	0.089	0.174	9.670	0.160	0.382	48.450	0.101	0.038	99.334
SZ-CD01-26	MA	39.210	0.057	0.000	0.000	18.720	0.218	0.161	42.730	0.031	0.038	101.165

Churchill Kimberlite Olivine Analyses

Sample		SiO_2	TiO_2	Al_2O_3	Cr_2O_3	FeO	MnO	NiO	MgO	CaO	Na_2O	Oxide Total
SZ-CD01-27	MA	39.260	0.030	0.030	0.000	18.810	0.227	0.143	43.260	0.023	0.036	101.819
SZ-CD01-28	MA	39.250	0.015	0.047	0.139	18.650	0.226	0.125	43.020	0.045	0.040	101.557
SZ-CD01-29	MA	40.590	0.041	0.036	0.071	9.490	0.138	0.380	49.090	0.081	0.061	99.978
SZ-CD01-30	P	40.220	0.034	0.044	0.019	12.060	0.131	0.260	47.430	0.065	0.036	100.299
SZ-CD01-31	P	40.280	0.000	0.053	0.000	12.230	0.127	0.263	47.510	0.052	0.036	100.551
SZ-CD01-32	P	39.620	0.038	0.033	0.038	13.610	0.155	0.202	46.440	0.033	0.022	100.191
SZ-CD01-33	P	39.610	0.027	0.044	0.000	11.380	0.140	0.287	48.150	0.055	0.048	99.741
SZ-CD01-34	P	40.090	0.049	0.048	0.111	11.040	0.127	0.321	48.450	0.045	0.028	100.309
SZ-CD01-35	P	39.560	0.000	0.067	0.000	14.160	0.189	0.220	46.110	0.067	0.039	100.412
SZ-CD01-36	P	39.800	0.055	0.073	0.000	14.720	0.141	0.219	45.630	0.059	0.062	100.759
SZ-CD01-37	P	41.030	0.000	0.019	0.000	2.220	0.182	0.119	53.930	0.250	0.019	97.769
SZ-CD01-38	P	41.510	0.000	0.013	0.000	2.250	0.199	0.202	53.840	0.232	0.020	98.266

Churchill Kimberlite Perovskite Analyses

	Na_2O	Nb_2O_5	FeO	Pr_2O_3	MgO	ThO_2	Ce_2O_3	Al_2O_3	CaO	Ta_2O_5	SrO	TiO_2	SiO_2	Total
SZ-CD1-1	0.482	0.83	1.232	0.29	0.06	0.563	1.99	0.291	37.48	0.176	0.107	56.48	0.043	100.026
SZ-CD1-2	0.391	0.852	1.216	0.216	0.098	0.182	1.92	0.251	37.53	0.119	0.189	56.68	0.03	99.675
SZ-CD1-3	0.433	0.961	1.245	0.22	0.096	0.106	1.73	0.256	37.61	0.084	0.18	56.56	0.038	99.521
SZ-CD1-4	0.452	0.949	1.246	0.267	0.109	0.179	1.85	0.278	37.4	0.096	0.118	56.51	0.049	99.503
SZ-CD1-5	0.471	0.921	1.34	0.254	0.071	0.173	1.89	0.291	37.34	0.157	0.083	56.85	0.014	99.856
SZ-CD1-6	0.386	0.797	1.32	0.196	0.101	0	1.33	0.224	38.33	0	0.134	57.11	0.045	99.973
SZ-CD1-7	0.418	0.838	1.29	0.184	0.097	0.02	1.4	0.249	38.33	0.019	0.131	56.96	0.034	99.971
SZ-CD1-8	0.346	0.694	1.115	0.203	0.094	0	1.37	0.208	38.76	0.036	0.178	57.53	0.03	100.564
SZ-CD1-9	0.45	1.027	1.4	0.186	0.101	0.045	1.79	0.283	37.86	0.15	0.14	56.57	0.016	100.018
SZ-CD1-10	0.417	1.161	1.32	0.296	0.096	0.16	1.83	0.332	37.68	0.141	0.134	56.34	0.054	99.959
SZ-CD1-11	0.373	1.076	1.35	0.238	0.084	0	1.78	0.259	37.46	0.013	0.141	57.04	0.036	99.85
SZ-CD1-12	0.489	0.805	1.31	0.251	0.108	0.072	1.55	0.263	37.85	0.073	0.143	57.09	0.065	100.07
SZ-CD1-13	0.409	0.757	1.34	0.225	0.12	0.463	1.97	0.285	37.16	0.156	0.107	56.39	0.038	99.42
SZ-CD1-14	0.45	0.803	1.38	0.295	0.105	0.5	2.05	0.317	37.16	0.191	0.121	56.19	0.089	99.651
SZ-CD1-15	0.482	0.818	1.37	0.276	0.104	0.478	2.03	0.29	36.34	0.168	0.143	55.5	0.073	98.072
SZ-CD1-16	0.366	0.769	1.34	0.3	0.086	0.293	1.97	0.286	37.24	0.079	0.117	56.11	0.062	99.018
SZ-CD1-17	0.425	0.805	1.42	0.218	0.105	0.528	1.99	0.285	37	0.183	0.14	56.33	0.04	99.467
SZ-CD1-18	0.385	0.853	1.36	0.294	0.109	0.542	2.02	0.3	36.97	0.126	0.13	56.21	0.033	99.332
SZ-CD1-19	0.426	0.862	1.35	0.237	0.099	0.371	1.9	0.265	37.22	0.095	0.159	56.7	0.029	99.713
SZ-CD1-20	0.462	0.79	1.48	0.304	0.092	0.583	2.05	0.308	36.9	0.153	0.096	55.84	0.038	99.122
SZ-CD1-21	0.415	0.933	1.46	0.363	0.068	0.706	2.09	0.281	36.93	0.211	0.145	56.11	0.046	99.757
SZ-CD1-22	0.503	0.963	1.53	0.276	0.075	0.85	2.07	0.328	36.69	0.294	0.14	55.66	0.062	99.44
SZ-CD1-23	0.465	0.777	1.41	0.395	0.088	0.553	2.14	0.329	36.79	0.146	0.16	56.01	0.064	99.375
SZ-CD1-24	0.403	0.898	1.48	0.326	0.09	0.539	2.07	0.306	36.89	0.202	0.12	56.07	0.066	99.483
SZ-CD1-25	0.429	0.881	1.5	0.27	0.077	0.614	2.09	0.271	37.17	0.169	0.122	56.27	0.077	99.94
SZ-CD1-26	0.491	0.988	1.48	0.324	0.068	0.684	2.05	0.272	36.92	0.203	0.13	55.73	0.062	99.402
SZ-CD1-27	0.507	0.937	1.5	0.306	0.084	0.753	2.15	0.281	36.72	0.171	0.119	55.82	0.065	99.414
SZ-CD24-1	0.2	0.881	1.8	0.183	0.065	0.05	1.044	0.345	38.55	0.043	0.192	56	0.097	99.45

Churchill Kimberlite Perovskite Analyses

	Na_2O	Nb_2O_5	FeO	Pr_2O_3	MgO	ThO_2	Ce_2O_3	Al_2O_3	CaO	Ta_2O_5	SrO	TiO_2	SiO_2	Total
SZ-CD24-2	0.511	0.902	1.35	0.258	0.102	0.631	2.18	0.325	36.5	0.218	0.126	55.73	0.063	98.944
SZ-CD24-3	0.375	0.758	1.3	0.236	0.115	0.198	1.87	0.258	37.73	0.131	0.153	56.91	0.06	100.095
SZ-CD24-4	0.431	0.845	1.39	0.279	0.062	0.518	2.01	0.298	36.68	0.211	0.133	56.48	0.054	99.393
SZ-CD24-5	0.42	0.802	1.36	0.334	0.101	0.337	1.89	0.272	37.08	0.126	0.133	56.69	0.032	99.578
SZ-CD24-6	0.421	0.684	1.33	0.233	0.094	0.398	2.03	0.277	37.12	0.162	0.148	56.55	0.035	99.483
SZ-CD24-7	0.441	0.746	1.36	0.178	0.078	0.499	2.02	0.327	37.36	0.11	0.145	56.69	0.069	100.022
SZ-CD24-8	0.454	0.814	1.36	0.232	0.084	0.359	1.88	0.298	36.93	0.122	0.1	56.47	0.06	99.163
SZ-CD24-9	0.521	0.882	1.36	0.226	0.076	0.516	2.01	0.297	37.36	0.156	0.166	56.3	0.032	99.903
SZ-CD24-10	0.442	0.828	1.36	0.282	0.102	0.508	1.96	0.313	37.37	0.217	0.145	56.1	0.034	99.66
SZ-CD24-11	0.474	0.754	1.38	0.216	0.111	0.491	2.05	0.285	37.07	0.216	0.114	56.74	0.031	99.931
SZ-CD24-12	0.571	0.956	1.34	0.355	0.097	0.818	2.1	0.338	36.67	0.21	0.151	55.95	0.018	99.624
SZ-CD24-13	0.549	0.941	1.33	0.3	0.092	0.753	2.05	0.296	36.7	0.219	0.112	56.2	0.034	99.578
SZ-CD24-14	0.477	0.962	1.36	0.348	0.072	0.55	2.16	0.322	36.73	0.196	0.107	56.32	0.05	99.722
SZ-CD24-15	0.374	0.721	1.46	0.315	0.094	0.117	1.85	0.309	37.21	0.039	0.163	56.85	0.059	99.56
SZ-CD24-16	0.421	0.866	1.32	0.25	0.085	0.63	2.01	0.3	36.73	0.201	0.113	56.39	0.023	99.372
SZ-CD24-17	0.478	0.718	1.3	0.153	0.103	0.566	2.06	0.305	36.67	0.155	0.116	56.62	0.047	99.31
SZ-CD29-1	0.283	0.575	1.192	0.125	0.082	0.039	1.24	0.243	39.13	0	0.137	58.03	0.034	101.109
SZ-CD29-2	0.309	0.578	1.146	0.194	0.056	0.031	1.32	0.222	38.47	0.045	0.127	58.04	0.07	100.608
SZ-CD29-3	0.215	0.644	1.41	0.136	0.053	0.083	1.053	0.245	39.22	0.009	0.151	57.89	0.062	101.172
SZ-CD29-4	0.271	0.63	1.265	0.166	0.066	0.045	1.14	0.24	38.51	0.014	0.138	57.23	0.071	99.785
SZ-CD29-5	0.324	0.583	1.32	0.155	0.105	0.01	1.037	0.241	38.39	0.022	0.139	57.18	0.093	99.599
SZ-CD29-6	0.285	0.622	1.48	0.078	0.067	0	1.029	0.304	38.86	0	0.186	57.09	0.058	100.059
SZ-CD29-7	0.38	0.831	1.144	0.243	0.086	0	1.57	0.282	37.95	0.109	0.132	57.76	0	100.487
SZ-CD29-8	0.286	0.646	1.081	0.171	0.066	0.047	1.37	0.222	38.17	0.055	0.137	57.51	0.025	99.787
SZ-CD29-9	0.212	0.757	1.4	0.164	0.044	0	1.021	0.261	38.64	0.026	0.142	56.54	0.068	99.275
SZ-CD29-10	0.322	0.681	1.195	0.175	0.081	0.033	1.3	0.243	38.62	0.022	0.124	57.38	0.057	100.233

Churchill Kimberlite Perovskite Analyses

	Na_2O	Nb_2O_5	FeO	Pr_2O_3	MgO	ThO_2	Ce_2O_3	Al_2O_3	CaO	Ta_2O_5	SrO	TiO_2	SiO_2	Total
SZ-CD29-11	0.199	0.855	1.6	0.135	0.162	0	1.059	0.368	39.11	0	0.163	56.47	0.26	100.382
SZ-CD29-12	0.31	0.527	1.006	0.208	0.095	0.011	1.38	0.255	38.51	0.067	0.148	57.89	0.024	100.431
SZ-CD29-13	0.416	0.746	1.29	0.134	0.11	0	1.28	0.248	38.2	0.049	0.131	57.75	0.036	100.389
SZ-CD29-14	0.383	0.811	1.47	0.141	0.093	0.05	1.047	0.242	38.57	0.017	0.122	57.96	0.036	100.943
SZ-CD29-15	0.387	0.682	1.189	0.186	0.087	0.145	1.59	0.239	37.98	0.042	0.146	57.52	0.057	100.25
SZ-CD29-16	0.354	0.651	1.191	0.173	0.09	0.031	1.58	0.287	38.5	0.026	0.179	57.32	0.065	100.444
SZ-CD29-17	0.277	0.675	1.41	0.19	0.089	0	1.24	0.256	38.62	0.024	0.134	57.87	0.046	100.83
SZ-CD29-18	0.276	0.545	1.3	0.161	0.103	0	1.43	0.22	38.23	0.042	0.169	58.02	0.054	100.551
SZ-CD29-19	0.289	0.614	1.257	0.189	0.098	0.058	1.25	0.322	38.57	0	0.193	57.09	0.069	100
SZ-CD29-20	0.296	0.548	1.265	0.137	0.088	0	1.43	0.271	38.45	0.133	0.126	57.24	0.058	100.041
SZ-CD29-21	0.342	0.673	1.33	0.094	0.073	0.075	1.4	0.282	38.6	0.067	0.163	57.19	0.035	100.324
SZ-CD29-22	0.258	0.663	1.3	0.171	0.074	0.042	1.41	0.25	38.27	0	0.166	57.41	0.069	100.082
SZ-CD29-23	0.148	0.975	2.03	0.194	0.091	0.008	1.099	0.48	37.88	0.087	0.185	54.76	0.14	98.078
SZ-CD29-24	0.284	0.689	1.38	0.155	0.087	0.017	1.29	0.26	38.55	0.053	0.123	57.38	0.083	100.352
SZ-CD29-25	0.237	0.763	1.5	0.039	0.083	0.081	1.022	0.246	38.6	0	0.15	57.1	0.036	99.856
SZ-CD29-26	0.277	0.616	1.35	0.158	0.067	0.081	1.25	0.253	38.58	0	0.114	57.83	0.034	100.61
SZ-CD29-27	0.245	0.727	1.43	0.128	0.062	0	1.141	0.241	38.41	0.019	0.143	57.41	0.055	100.012
SZ-CD29-28	0.322	0.616	1.31	0.099	0.079	0.036	1.42	0.251	38.37	0.059	0.183	57.4	0.063	100.208
SZ-CD29-29	0.257	0.548	1.3	0.135	0.089	0.044	1.28	0.241	38.09	0	0.111	57.53	0.063	99.688
SZ-CD29-30	0.349	0.58	1.193	0.208	0.051	0.07	1.45	0.275	38.31	0.026	0.154	57.76	0.017	100.442
SZ-CD29-31	0.285	0.622	1.41	0.052	0.071	0.025	1.33	0.277	37.87	0.053	0.147	57.58	0.039	99.761
SZ-CD29-32	0.25	0.668	1.33	0.12	0.093	0.061	1.21	0.273	38.21	0.015	0.145	57.08	0.035	99.49
SZ-CD29-33	0.29	0.758	1.258	0.165	0.082	0.022	1.56	0.297	38	0.075	0.132	57.52	0.036	100.195
SZ-CD29-34	0.257	0.662	1.32	0.168	0.088	0.008	1.39	0.305	38.16	0	0.163	57.61	0.015	100.147
SZ-CD29-35	0.28	0.649	1.269	0.189	0.072	0.092	1.6	0.286	37.93	0.023	0.156	57.25	0.053	99.85
SZ-CD29-36	0.326	0.705	1.46	0.204	0.081	0.028	1.7	0.26	37.32	0.088	0.16	57.43	0.062	99.825

Churchill Kimberlite Perovskite Analyses

	Na_2O	Nb_2O_5	FeO	Pr_2O_3	MgO	ThO_2	Ce_2O_3	Al_2O_3	CaO	Ta_2O_5	SrO	TiO_2	SiO_2	Total
SZ-CD29-37	0.336	0.802	1.247	0.164	0.101	0.031	1.6	0.256	38.5	0.058	0.161	57.39	0.039	100.685
SZ-CD29-38	0.241	0.66	1.32	0.211	0.05	0	1.4	0.289	38.54	0.019	0.188	57.93	0.095	100.943
SZ-CD29-39	0.252	0.761	1.48	0.129	0.052	0	1.19	0.281	38.85	0.088	0.169	57.35	0.031	100.633
SZ-CD29-40	0.282	0.712	1.34	0.112	0.044	0	1.35	0.26	38.68	0.043	0.137	57.46	0.042	100.462
SZ-CD29-41	0.323	0.681	1.286	0.249	0.05	0.1	1.65	0.274	38.04	0	0.134	57.09	0.065	99.943
SZ-CD29-42	0.235	0.678	1.32	0.23	0.075	0.078	1.39	0.285	38.57	0	0.172	56.87	0.038	99.939
SZ-CD29-43	0.233	0.859	1.5	0.156	0.075	0	1.22	0.32	39.2	0	0.116	57.11	0.045	100.832
SZ-CD29-44	0.241	0.858	1.42	0.227	0.072	0.031	1.34	0.255	38.98	0.011	0.151	57.47	0.052	101.106
SZ-CD29-45	0.268	0.82	1.49	0.128	0.091	0	1.31	0.289	38.62	0.04	0.135	57.22	0.075	100.485
SZ-CD1-a1	0.314	0.791	1.39	0.097	0.052	0.078	1.4	0.275	38.8	0.068	0.143	57.1	0.063	100.571
SZ-CD1-a2	0.221	0.871	1.52	0.154	0.084	0.031	1.35	0.259	39.12	0	0.13	57.24	0.052	101.033
SZ-CD1-a3	0.263	0.666	1.252	0.178	0.074	0.058	1.46	0.244	38.19	0.069	0.161	57.36	0.03	100.005
SZ-CD1-a4	0.247	0.692	1.42	0.09	0.059	0	1.158	0.269	38.72	0.081	0.155	57.81	0.076	100.778
SZ-CD1-a5	0.247	0.768	1.51	0.146	0.052	0.1	1.072	0.279	38.82	0.026	0.171	56.94	0.067	100.198
SZ-CD1-a6	0.124	1.31	2.92	0.114	1.233	0	1.027	0.777	35.99	0.03	0.319	50.29	1.399	95.634
SZ-CD1-a7	0.947	0.935	2.33	0.108	4.25	0	0.806	1.001	34.69	0.024	0.53	47.72	4.25	97.592
SZ-CD1-a8	0.388	0.945	2.34	0.205	4.19	0	0.844	0.638	35.29	0	0.385	49.85	3.41	98.485
SZ-CD1-a9	0.3	1.389	2.53	0.151	0.702	0.02	0.887	0.702	37.13	0	0.442	52.07	0.855	97.246
SZ-CD1-a10	0.208	0.753	1.59	0.169	0.048	0.081	1.14	0.269	38.82	0.018	0.143	57.3	0.07	100.609
SZ-CD1-a11	0.304	0.654	1.33	0.13	0.073	0	1.29	0.257	38.46	0.048	0.169	57.78	0.047	100.542
SZ-CD1-a12	0.364	0.661	1.33	0.192	0.09	0	1.29	0.218	38.44	0.04	0.159	57.61	0.02	100.412
SZ-CD1-a13	0.326	0.715	1.268	0.181	0.117	0	1.27	0.244	38.64	0.028	0.123	57.73	0.058	100.698
SZ-CD1-a14	0.338	0.647	1.39	0.103	0.135	0.022	0.973	0.234	38.31	0	0.137	57.6	0.053	99.943
SZ-CD1-a15	0.312	0.661	1.244	0.154	0.082	0.07	1.33	0.22	38.54	0.023	0.166	57.98	0.088	100.869
SZ-CD1-a16	0.393	0.706	1.154	0.279	0.081	0.045	1.67	0.257	38.53	0.114	0.168	57.99	0.05	101.436
SZ-CD1-a17	0.193	0.773	1.43	0.09	0.041	0.056	1.067	0.282	39.3	0.031	0.123	57.55	0.036	100.973

Churchill Kimberlites Phlogopite Microprobe Analyses

	K_2O	MgO	Na_2O	NiO	TiO_2	Al_2O_3	CaO	SiO_2	FeO	Cr_2O_3	MnO	Total
CD20 20m-1	8.23	29.99	0.118	0.029	0.023	8.78	0.163	41.97	4.29	0	0.081	93.684
CD20 20m-2	9.81	29.02	0.143	0.023	0.045	9.79	0.234	42.97	3.53	0.041	0.038	95.659
CD20 20m-3	8.98	26.84	0.377	0.016	0.073	14.34	0.218	40.23	2.08	0.063	0.031	93.274
CD20 20m-4	5.68	31.35	0.537	0.032	0.034	8.73	0.123	40.43	3.25	0	0.089	90.255
CD20 20m-5	9.66	27.87	0.164	0.03	0.055	10.42	0.113	42.64	3.95	0.044	0.032	94.996
CD20 20m-6	5.83	29.76	0.961	0.033	0.236	13.6	0.194	37.68	3.42	0.023	0.067	91.803
CD20 20m-7	9.95	26.54	0.166	0.025	0.084	13.94	0.055	41.4	2.22	0.03	0.013	94.432
CD20 64m-1	9.67	23.16	0.102	0.015	0.581	16.91	0.09	37.34	3.17	0.009	0.031	91.108
CD20 64m-2	9.82	23.55	0.093	0.019	0.553	16.55	0.019	37.67	3.05	0	0.034	91.368
CD20 64m-3	9.78	23.43	0.09	0.021	0.574	16.63	0.024	37.6	3.1	0	0.015	91.274
CD20 64m-4	10.03	23.82	0.081	0.016	0.571	16.61	0.027	37.95	3.18	0.056	0.03	92.406
CD2 34m-1	9.74	21.59	0.285	0.107	3.3	13.52	0.01	39.85	5.16	1.5	0.024	95.13
CD2 34m-2	9.38	20.74	0.342	0.095	3.82	12.97	1.6	39.6	5.03	0.969	0.034	94.641
CD2 34m-3	10.08	23.44	0.296	0.043	1.128	12.05	0	42.03	5.8	0.038	0.032	94.969
CD2 34m-4	9.97	23.65	0.225	0.041	1.152	12	0.024	42.04	5.99	0.035	0.025	95.166
CD2 34m-5	10.22	23.27	0.257	0.045	1.109	12.1	0	42.23	6.02	0.055	0.04	95.363
CD2 34m-6	10.09	23.32	0.252	0.025	1.146	12.13	0.015	42.19	6.12	0.039	0.024	95.398
CD2 34m-7	10.07	21.91	0.287	0.045	3.16	13.16	0.021	40.46	6.23	0.148	0.035	95.556
CD2 34m-8	9.98	21.86	0.325	0.048	3.12	13.06	0.013	40.48	6.34	0.141	0.035	95.43
CD2 34m-9	10	21.96	0.306	0.05	3.13	13.03	0.01	40.59	6.31	0.138	0.03	95.596
CD24-1	8.45	27.87	0.062	nd	0.618	12.78	0	38.85	3.72	0.013	0.151	92.984
CD24-2	10.35	24.1	0.018	nd	1.018	15.67	0	37.84	4.38	0	0.093	93.906
CD24-3	10.29	25.59	0.03	nd	0.928	11.28	0.056	40.42	4.95	0.062	0.065	94.147
CD24-4	10.63	27.49	0.071	nd	0.079	8.88	0.019	41.75	4.94	0.022	0.022	94.102

Churchill Kimberlite Phlogopite Microprobe Analyses

	K_2O	MgO	Na_2O	NiO	TiO_2	Al_2O_3	CaO	SiO_2	FeO	Cr_2O_3	MnO	Total
CD24-5	10.32	24.52	0.065	nd	0.901	15	0.029	38.33	4.3	0	0.083	94.237
CD24-6	9.94	25.43	0.03	nd	0.755	14.92	0.022	38.37	4.09	0	0.104	94.138
CD24-7	10.17	26.43	0.052	nd	0.498	10.39	0	40.11	5.86	0.009	0.044	93.896
CD24-8	10.38	27.94	0.032	nd	0.018	8.21	0.05	42.12	5.59	0	0.055	94.508
CD24-9	10.2	25.92	0.086	nd	0.786	11.63	0	40.42	4.52	0.025	0.054	94.386
CD24-10	9.86	28.48	0.098	nd	0	5.26	0.01	41.41	9.6	0.009	0.051	94.778
CD24-11	8.82	26.58	0.115	nd	0.74	12.56	0.018	38.06	4.79	0	0.076	92.251
CD24-12	9.84	27.36	0.105	nd	0.424	8.44	0.027	40.06	7.89	0	0.064	94.546
CD1-1	7.26	30.34	0.078	nd	0.724	9.97	0.009	39.93	4.61	0.009	0.095	93.754
CD1-2	8.55	27.76	0.084	nd	0.354	9.12	0.008	38.52	7.57	0.01	0.072	92.15
CD1-3	10.51	27.73	0.031	nd	0.01	4.19	0.015	40.78	11.26	0.008	0.053	94.599
CD1-4	10.06	24.53	0.028	nd	0.957	14.17	0	38.04	4.99	0	0.073	93.352
CD1-5	9.1	25.97	0.06	nd	0.636	14.45	0.012	38.2	3.54	0.01	0.057	92.32
CD1-6	10.29	24.4	0.032	nd	0.687	16.04	0	37.48	3.68	0	0.069	93.202
CD1-7	7.9	31.4	0.122	nd	0.368	6.82	0.014	41.07	7.71	0.023	0.077	95.558
CD1-8	8.6	28.31	0.099	nd	0.207	5.16	0.016	39.76	9.61	0.01	0.134	92.036
CD1-9	10.18	24.56	0.049	nd	0.56	17.23	0	37.92	3.21	0.008	0.053	94.18
CD1-10	5.4	33.22	0.067	nd	0.563	6.69	0.112	41.65	4.97	0.023	0.153	93.262
CD1-11	10.4	25.27	0.045	nd	0.664	15.76	0.149	38.8	3.67	0	0.074	95.356
CD1-12	10.04	25.39	0.055	nd	0.723	15.96	0.131	39.15	3.7	0.021	0.06	95.724
CD1-13	10.25	25.2	0.084	nd	0.973	12.97	0.061	39.14	3.97	0	0.063	93.383
CD1-14	9.93	25.01	0.07	nd	0.562	14.88	0.071	37.54	3.63	0.01	0.065	92.253
CD1-15	10.28	24.69	0.067	nd	0.7	15.81	0	37.49	3.47	0.023	0.056	93.144
CD1-16	9.36	28.15	0.066	nd	0.234	4.56	0.012	39.4	11.79	0	0.101	93.696
CD1-17	10.1	27.58	0.037	nd	0.056	5.36	0.014	41.04	9.42	0	0.054	93.836
CD1-18	10.15	26.55	0.044	nd	0.495	12.42	0.041	40.11	3.8	0	0.05	94.115

Churchill Kimberlite Monticellite Microprobe Analyses

	K_2O	MgO	P_2O_5	Na_2O	NiO	TiO_2	Al_2O_3	CaO	SiO_2	FeO	Cr_2O_3	MnO	V_2O_3	Total
CD20-1	0.00	23.93	0.07	0.08	0.02	0.04	0.02	30.96	37.92	3.96	0.00	0.35	0.01	97.37
CD20-2	0.01	23.43	0.06	0.09	0.05	0.02	0.06	31.32	37.76	3.74	0.03	0.32	0.01	96.91
CD20-3	0.00	22.98	0.05	0.04	0.02	0.02	0.01	31.07	37.78	4.56	0.00	0.36	0.00	96.88
CD20-4	0.00	23.87	0.05	0.06	0.02	0.05	0.02	31.19	37.98	3.57	0.02	0.35	0.00	97.18
CD20-5	0.00	23.52	0.06	0.04	0.02	0.04	0.02	31.00	38.01	3.68	0.01	0.37	0.00	96.77
CD20-6	0.00	22.79	0.04	0.02	0.03	0.01	0.04	31.41	37.43	4.29	0.00	0.34	0.00	96.40
CD20-7	0.00	24.59	0.08	0.04	0.02	0.00	0.02	31.67	38.44	2.69	0.00	0.29	0.00	97.82
CD20-8	0.01	23.87	0.05	0.07	0.04	0.24	0.18	29.76	37.25	5.77	0.00	0.35	0.00	97.59
CD20-9	0.00	27.87	0.03	0.03	0.05	0.00	0.02	26.27	37.33	2.39	0.00	0.16	0.00	94.16
CD20-10	0.00	23.86	0.04	0.04	0.07	0.01	0.00	31.37	38.05	2.70	0.00	0.18	0.00	96.32
CD20-11	0.00	23.58	0.04	0.04	0.05	0.00	0.00	32.04	38.10	3.51	0.00	0.21	0.01	97.59
CD24-1	0.02	23.27	0.09	0.05	0.02	0.03	0.01	31.46	37.94	3.53	0.00	0.28	0.00	96.71
CD24-2	0.00	23.55	0.21	0.08	0.03	0.06	0.03	30.96	37.94	3.46	0.00	0.28	0.02	96.61
CD24-3	0.00	23.47	0.07	0.03	0.03	0.06	0.01	31.18	38.13	3.54	0.00	0.32	0.00	96.83
CD24-4	0.00	23.77	0.09	0.02	0.02	0.00	0.00	30.83	38.18	3.00	0.00	0.30	0.00	96.21
CD24-5	0.00	22.99	0.05	0.04	0.03	0.01	0.01	30.56	37.98	4.19	0.01	0.32	0.00	96.19
CD24-6	0.00	23.32	0.06	0.04	0.04	0.00	0.00	30.94	38.03	3.48	0.00	0.21	0.00	96.11
CD24-7	0.00	25.07	0.05	0.02	0.04	0.03	0.00	29.92	38.11	2.78	0.00	0.17	0.00	96.19
CD24-10	0.01	24.36	0.12	0.03	0.00	0.09	0.05	31.47	37.50	3.62	0.00	0.55	0.00	97.80
CD24-11	0.00	23.55	0.04	0.03	0.00	0.00	0.00	32.50	38.64	2.57	0.00	0.36	0.01	97.69
CD24-12	0.00	23.64	0.06	0.01	0.01	0.04	0.04	32.49	38.45	2.40	0.00	0.39	0.01	97.54
CD24-13	0.01	24.09	0.04	0.01	0.02	0.00	0.04	32.74	38.44	2.35	0.00	0.36	0.00	98.11
CD24-14	0.00	24.54	0.06	0.01	0.01	0.00	0.01	32.97	38.42	2.45	0.00	0.38	0.00	98.84

Churchill Kimberlite Monticellite Microprobe Analyses

	K_2O	MgO	P_2O_5	Na_2O	NiO	TiO_2	Al_2O_3	CaO	SiO_2	FeO	Cr_2O_3	MnO	V_2O_3	Total
CD24-15	0.00	24.48	0.06	0.03	0.01	0.03	0.00	33.07	38.30	2.52	0.00	0.39	0.00	98.89
CD24-16	0.00	23.64	0.03	0.02	0.01	0.00	0.02	33.70	38.31	2.56	0.00	0.38	0.00	98.66
CD24-17	0.00	23.77	0.06	0.04	0.00	0.02	0.00	33.56	38.46	2.48	0.00	0.35	0.01	98.74
CD24-18	0.00	23.70	0.05	0.02	0.01	0.05	0.00	33.93	38.31	2.41	0.00	0.35	0.00	98.83
JBP16-1	0.00	23.48	0.07	0.02	0.02	0.00	0.00	33.71	38.39	2.30	0.00	0.40	0.00	98.38
JBP16-2	0.00	23.27	0.05	0.01	0.01	0.03	0.01	33.62	38.41	2.44	0.00	0.41	0.00	98.26
JBP16-3	0.00	23.39	0.05	0.02	0.02	0.03	0.01	33.16	38.48	2.51	0.01	0.35	0.00	98.03
JBP16-4	0.00	23.39	0.05	0.03	0.01	0.02	0.02	33.01	38.50	2.47	0.01	0.39	0.00	97.89
JBP16-5	0.00	25.39	0.04	0.00	0.01	0.00	0.10	28.66	36.11	3.99	0.00	0.38	0.00	94.68
JBP16-6	0.02	23.25	0.04	0.04	0.01	0.03	0.20	32.64	38.20	2.67	0.00	0.38	0.00	97.48
JBP16-7	0.00	23.33	0.06	0.01	0.00	0.03	0.04	32.92	38.43	2.59	0.00	0.40	0.00	97.81
JBP16-8	0.01	23.55	0.04	0.04	0.01	0.00	0.00	33.56	38.49	2.42	0.00	0.39	0.00	98.51
JBP16-9	0.00	23.60	0.07	0.02	0.01	0.02	0.00	32.92	38.49	2.44	0.03	0.40	0.00	98.00
JBP16-10	0.01	23.35	0.04	0.03	0.01	0.03	0.00	34.25	38.15	2.29	0.00	0.39	0.00	98.55
JBP16-11	0.00	22.95	0.14	0.04	0.00	0.02	0.08	33.97	38.00	2.31	0.04	0.45	0.00	98.01
JBP16-12	0.00	22.70	0.26	0.10	0.03	0.06	0.00	34.40	37.76	3.19	0.00	0.39	0.00	98.89
JBP16-13	0.01	23.25	0.05	0.02	0.02	0.02	0.04	34.04	37.91	2.42	0.00	0.38	0.00	98.16
JBP16-14	0.00	23.36	0.04	0.00	0.00	0.03	0.00	33.60	38.14	2.49	0.00	0.41	0.00	98.07
JBP16-15	0.01	23.37	0.08	0.03	0.00	0.01	0.01	33.87	37.99	2.40	0.00	0.38	0.00	98.15
JBP16-18	0.02	21.96	0.51	0.17	0.00	0.12	0.09	33.89	37.28	3.30	0.02	0.45	0.00	97.80
JBP16-19	0.00	24.62	0.06	0.03	0.01	0.02	0.02	32.03	38.68	2.57	0.00	0.37	0.01	98.43
JBP16-21	0.01	24.35	0.04	0.00	0.00	0.00	0.00	34.18	38.62	1.94	0.00	0.28	0.00	99.41

Churchill Kimberlite Monticellite Microprobe Analyses

	K_2O	MgO	P_2O_5	Na_2O	NiO	TiO_2	Al_2O_3	CaO	SiO_2	FeO	Cr_2O_3	MnO	V_2O_3	Total
JBP16-22	0.01	23.70	0.04	0.02	0.00	0.03	0.01	33.84	38.29	2.48	0.00	0.41	0.01	98.85
JBP16-23	0.00	23.76	0.05	0.01	0.01	0.02	0.00	33.64	38.14	2.56	0.02	0.33	0.01	98.54
JBP16-24	0.00	26.48	0.05	0.02	0.00	0.25	0.23	29.38	37.63	2.87	0.00	0.38	0.00	97.29
JBP16-25	0.01	25.88	0.03	0.02	0.00	0.01	0.15	32.78	38.56	2.46	0.00	0.37	0.00	100.28
JBP16-26	0.00	24.84	0.05	0.01	0.00	0.01	0.32	32.07	37.10	2.41	0.00	0.35	0.00	97.16
JBP16-27	0.00	23.53	0.04	0.01	0.00	0.02	0.02	33.69	38.21	2.36	0.00	0.35	0.01	98.24
JBP16-28	0.00	24.00	0.06	0.02	0.00	0.04	0.00	32.62	38.16	2.28	0.00	0.35	0.00	97.53
JBP16-29	0.00	23.63	0.05	0.03	0.02	0.01	0.05	32.98	38.14	2.33	0.00	0.39	0.00	97.62
JBP16-30	0.00	23.43	0.05	0.02	0.00	0.01	0.01	32.89	38.16	2.39	0.00	0.38	0.00	97.33
JBP16-31	0.00	23.27	0.07	0.03	0.00	0.01	0.01	32.58	38.25	2.39	0.00	0.38	0.00	96.98
JBP16-32	0.00	23.79	0.05	0.03	0.01	0.02	0.06	32.43	38.07	2.49	0.00	0.38	0.01	97.33
JBP16-33	0.00	23.66	0.07	0.01	0.01	0.02	0.05	32.39	38.07	2.43	0.06	0.39	0.01	97.16
JBP16-34	0.00	23.44	0.04	0.02	0.01	0.03	0.01	32.74	38.22	2.42	0.00	0.38	0.00	97.32
JBP16-35	0.02	23.79	0.04	0.01	0.01	0.04	0.03	33.01	38.38	2.60	0.00	0.35	0.01	98.30
JBP16-36	0.00	23.20	0.04	0.00	0.01	0.01	0.03	33.88	37.94	2.38	0.00	0.43	0.00	97.92
JBP16-37	0.00	23.48	0.05	0.04	0.01	0.03	0.06	33.76	37.97	2.47	0.00	0.39	0.00	98.25
JBP16-38	0.00	23.48	0.06	0.01	0.01	0.02	0.05	33.22	37.94	2.67	0.00	0.38	0.01	97.85
JBP16-39	0.00	23.54	0.04	0.00	0.01	0.00	0.01	33.00	38.18	2.46	0.00	0.37	0.00	97.62
JBP16-40	0.00	23.62	0.03	0.01	0.00	0.05	0.01	32.86	38.03	2.37	0.00	0.38	0.00	97.36
JBP16-41	0.00	23.29	0.04	0.03	0.00	0.00	0.04	32.24	38.17	2.42	0.00	0.38	0.01	96.62
JBP16-42	0.00	23.64	0.04	0.01	0.01	0.03	0.03	33.43	38.15	2.39	0.00	0.39	0.00	98.13
JBP16-43	0.00	23.55	0.04	0.03	0.00	0.03	0.05	33.29	37.84	2.36	0.04	0.44	0.00	97.66
JBP16-44	0.00	23.67	0.03	0.03	0.00	0.02	0.00	32.50	38.43	2.41	0.02	0.34	0.00	97.45

Churchill Kimberlite Spinel Microprobe Analyses

	K_2O	MgO	NiO	TiO_2	Al_2O_3	CaO	SiO_2	FeO	Cr_2O_3	MnO	V_2O_3	Total
CD24-1	0	12.63	0.146	3.68	13.52	0.009	0.156	25.11	43.72	0.114	0.246	99.381
CD24-2	0	12.43	0.155	3.64	13.61	0.011	0.136	25.68	43.51	0.132	0.255	99.614
CD24-3	0	12.27	0.158	3.76	13.41	0.008	0.131	25.88	43.42	0.13	0.261	99.469
CD24-4	0.014	11.68	0.161	3.54	13.18	0.033	0.153	25.05	41.8	0.117	0.24	96.051
CD24-5	0	12.51	0.17	3.69	13.57	0.009	0.158	25.25	44.18	0.125	0.247	99.936
CD24-6	0.017	12.4	0.181	3.7	13.53	0.034	0.168	24.37	43.92	0.124	0.233	98.871
CD24-7	0	12.45	0.175	3.71	13.48	0	0.152	25.61	43.99	0.114	0.213	99.932
CD24-8	0.007	12.51	0.16	3.75	13.42	0.014	0.159	24.97	44.21	0.126	0.246	99.625
CD24-9	0.01	12.51	0.148	3.77	13.33	0.009	0.148	25.72	43.98	0.117	0.262	100.012
CD24-10	0	12.42	0.181	3.79	13.19	0.008	0.155	25.92	43.93	0.119	0.257	100.004
CD24-11	0	12.37	0.156	3.86	13.08	0.01	0.166	25.99	43.88	0.116	0.24	99.929
CD24-12	0.03	12.28	0.168	3.97	12.87	0.019	0.153	25.22	43.92	0.13	0.248	99.176
CD24-13	0	12.21	0.163	4.09	12.66	0.014	0.113	26.18	43.77	0.127	0.271	99.642
CD24-14	0.015	11.98	0.172	4.18	12.17	0.013	0.164	26.35	43.69	0.125	0.27	99.15
CD24-15	0	12.06	0.167	4.2	11.96	0.012	0.131	26.52	43.85	0.132	0.234	99.324
CD24-16	0	11.94	0.177	4.27	11.7	0.012	0.142	26.65	44.01	0.131	0.262	99.364
CD24-17	0	11.9	0.184	4.35	11.29	0.01	0.138	26.73	44.24	0.132	0.253	99.291
CD24-18	0.025	11.97	0.17	4.54	10.87	0.009	0.18	26.61	43.04	0.157	0.272	97.907
CD24-19	0.016	13.98	0.041	13.81	7.15	0.21	0.095	47.64	12.88	1.267	0.176	97.338
CD24-20	0.009	13.31	0.047	9.93	7.47	0.168	0.164	41.1	25.01	1.025	0.225	98.517
CD24-21	0	12.82	0.137	6.06	10.32	0.111	0.136	28.14	41.38	0.429	0.33	99.912
CD24-22	0	12.36	0.162	4.4	13.66	0.085	0.147	26.26	41.89	0.206	0.282	99.492
CD24-23	0.007	12.16	0.143	4.55	13.27	0.064	0.109	26.62	42.46	0.178	0.299	99.905
CD24-24	0.006	12.19	0.148	4.84	12.4	0.061	0.105	27.78	42.26	0.192	0.265	100.308
CD24-25	0	12.03	0.144	5.16	11.52	0.066	0.167	28.27	41.89	0.212	0.309	99.798
CD24-26	0	12.63	0.104	6.62	8.77	0.112	0.107	32.11	38.55	0.393	0.317	99.764
CD24-27	0.02	14.05	0.073	16.73	5.43	0.106	0.116	50.93	11.01	0.858	0.272	99.653
CD1-1	0	15.41	0.05	20.62	6.66	0.04	0.086	55.57	0.048	0.76	0.175	99.453
CD1-2	0.018	15.55	0.053	17.28	10.79	0.103	0.098	54.15	0.185	0.795	0.131	99.155

Churchill Kimberlite Spinel Microprobe Analyses

	K_2O	MgO	NiO	TiO_2	Al_2O_3	CaO	SiO_2	FeO	Cr_2O_3	MnO	V_2O_3	Total
CD1-3	0.014	14.79	0.067	16.5	9.86	0.076	0.074	56.96	0	0.726	0.113	99.197
CD1-4	0.021	13.47	0.167	5.49	11.3	0.022	0.13	26.02	41.88	0.427	0.3	99.26
CD1-5	0.009	12.44	0.148	4.19	11.49	0.009	0.171	25.71	45.14	0.147	0.28	99.762
CD1-6	0	12.26	0.17	3.81	12.35	0.016	0.158	25.15	45.78	0.13	0.238	100.143
CD1-7	0	12.32	0.158	3.91	12.51	0.013	0.17	24.28	45.43	0.145	0.25	99.232
CD1-8	0	12.42	0.14	4.02	12.84	0	0.176	24.57	44.72	0.119	0.283	99.366
CD1-9	0.007	12.53	0.183	4.29	13.43	0	0.159	25.04	43.67	0.109	0.245	99.707
CD1-10	0	12.85	0.177	4.52	14.03	0.012	0.16	25.71	42.29	0.138	0.28	100.199
CD1-11	0	12.89	0.189	4.6	14.29	0.01	0.172	25.82	41.73	0.127	0.291	100.173
CD1-12	0	12.89	0.202	4.73	14.64	0.008	0.162	25.98	40.93	0.136	0.276	99.98
CD1-13	0	13.06	0.197	4.83	14.86	0.009	0.156	26.12	40.72	0.128	0.301	100.419
CD1-14	0	13.06	0.205	4.86	14.91	0.008	0.155	26.04	40.22	0.126	0.296	99.909
CD1-15	0	13.02	0.204	4.91	14.87	0.007	0.219	25.44	40.31	0.134	0.277	99.427
CD1-16	0	13.04	0.185	4.97	15.01	0.06	0.149	25.47	39.98	0.137	0.268	99.696
CD1-17	0.011	13.01	0.188	4.94	14.96	0.01	0.148	25.88	40.2	0.111	0.281	99.78
CD1-18	0	12.95	0.19	4.91	14.95	0.009	0.159	25.82	40.01	0.145	0.315	99.468
CD1-19	0	13.03	0.179	4.98	14.86	0.008	0.197	26.13	40.12	0.124	0.293	99.961
CD1-20	0	13.03	0.2	4.94	14.86	0.018	0.162	26.21	40.34	0.133	0.276	100.246
CD1-21	0	12.89	0.199	4.89	14.75	0.011	0.153	25.53	40.37	0.156	0.289	99.245
CD1-22	0	12.79	0.196	4.81	14.58	0.033	0.158	25.11	40.7	0.12	0.279	98.808
CD1-23	0	12.74	0.177	4.83	14.43	0.01	0.179	25.26	41.04	0.143	0.288	99.157
CD1-24	0	12.62	0.161	4.47	13.84	0.011	0.186	26.15	42.16	0.141	0.306	100.123
CD1-25	0	13.27	0.182	5.29	11.45	0.009	0.12	26.3	42.01	0.339	0.296	99.299
CD1-26	0	11.89	0.162	3.91	12.43	0.017	0.11	26.18	45.01	0.143	0.236	100.147
CD1-27	0	12.16	0.167	4.12	13.06	0.016	0.153	25.62	44.04	0.136	0.272	99.807
CD1-28	0.013	11.31	0.143	3.56	11.31	0.089	0.148	24.72	47.27	0.148	0.253	99.392

Churchill Kimberlite Spinel Microprobe Analyses

	K_2O	MgO	NiO	TiO_2	Al_2O_3	CaO	SiO_2	FeO	Cr_2O_3	MnO	V_2O_3	Total
CD1-29	0	11.58	0.136	4.12	11.04	0.009	0.139	26.31	45.77	0.136	0.28	99.623
CD1-30	0	12.12	0.148	4.23	11.77	0	0.146	27.08	43.63	0.187	0.281	99.641
CD1-31	0	12.33	0.155	4	12.34	0.007	0.17	26.17	44.86	0.135	0.262	100.466
CD1-32	0.007	12.77	0.152	4.86	11.63	0.011	0.148	27.15	42.5	0.332	0.287	99.906
CD1-33	0	12.75	0.165	4.75	11.74	0	0.146	27.19	42.64	0.303	0.262	100.01
CD20-1	0	12.72	0.172	3.91	14.68	0.023	0.155	22.99	44.32	0.161	0.256	99.423
CD20-2	0	12.81	0.154	3.93	14.65	0.018	0.184	23.8	44.39	0.146	0.264	100.418
CD20-3	0.007	12.88	0.167	3.94	14.82	0.023	0.189	24.55	43.93	0.188	0.249	101.021
CD20-4	0	12.82	0.178	3.89	14.86	0.013	0.151	24.37	43.98	0.209	0.287	100.793
CD20-5	0.015	13.26	0.131	4.27	13.4	0.02	0.145	24.29	43.16	0.282	0.249	99.259
CD20-6	0	16.98	0.081	19.46	6.9	0.105	0.145	52.74	0.434	0.868	0.187	97.961
CD20-7	0	17.21	0.078	19.33	7.21	0.07	0.083	52.71	0.28	0.859	0.195	98.071
CD20-8	0	17	0.069	18.95	7.82	0.159	0.095	54.54	0.148	0.814	0.159	99.843
CD20-9	0	17.08	0.07	18.81	8.18	0.141	0.125	53.99	0.142	0.813	0.18	99.586
CD20-10	0	16.45	0.085	18.34	7.03	0.125	0.102	52.19	3.27	0.803	0.206	98.685
CD20-11	0	15.7	0.071	18.07	6.3	0.107	0.202	54.63	2.76	0.792	0.205	98.914
CD20-12	0	17.02	0.064	19.22	6.85	0.082	0.119	54.64	0.405	0.833	0.183	99.488
CD20-13	0	17.64	0.087	19.68	6.85	0.081	0.121	52.64	0.6	0.873	0.205	98.853
CD20-14	0.018	16.49	0.093	11.44	11.32	0.108	0.098	57.85	0.208	0.516	0.089	98.256
CD20-15	0.007	15.57	0.108	11.34	11.24	0.11	0.11	58.93	0.107	0.495	0.102	98.199
CD20-16	0.013	15.44	0.108	11.89	10.07	0.089	0.091	59.75	0.059	0.517	0.088	98.19
CD20-17	0.007	13.74	0.052	11.29	8.57	0.266	0.18	63	0.016	0.59	0.067	97.844
CD20-18	0.015	13.29	0.126	5.21	11.3	0.054	0.14	29.21	39.48	0.233	0.298	99.394
CD20-19	0	12.94	0.083	11.39	7.14	0.018	0.089	43.77	23.15	0.453	0.196	99.278
CD20-20	0	12.88	0.056	16.47	6.25	0.077	0.1	61.96	0.105	0.598	0.127	98.776

Churchill Kimberlite Spinel Microprobe Analyses

	K_2O	MgO	NiO	TiO_2	Al_2O_3	CaO	SiO_2	FeO	Cr_2O_3	MnO	V_2O_3	Total
CD20-21	0.009	13.52	0.062	20.35	4.95	0.068	0.121	58.37	0.138	0.577	0.152	98.391
CD20-22	0	13.01	0.053	18.57	5.54	0.063	0.123	60.92	0.135	0.61	0.157	99.22
CD20-23	0.023	13.7	0.043	16.92	6.29	0.095	0.126	61.04	0.072	0.675	0.132	99.202
CD29-1	0.018	14.99	0.05	11.62	9.55	0.331	0.076	42.1	16.67	0.582	0.147	96.185
CD29-2	0.01	14.71	0.113	8.34	11.81	0.246	0.12	35.73	28.17	0.411	0.22	99.934
CD29-3	0.02	14.03	0.067	6.44	11.3	0.269	0.134	31.12	34.85	0.424	0.254	98.92
CD29-4	0	14.42	0.078	9.2	10.49	0.292	0.117	38.15	24.31	0.48	0.19	97.764
CD29-5	0	15.53	0.051	18.37	5.38	0.35	0.11	57.42	0	0.832	0.13	98.236
CD29-6	0	15.06	0.031	18.1	5.96	0.28	0.098	57.89	0.036	0.796	0.138	98.499
CD29-7	0	13.09	0.106	6.14	11.54	0.235	0.122	29.78	37.22	0.317	0.24	98.836
CD29-8	0	13.69	0.116	6.67	11.66	0.237	0.097	31.23	34.82	0.347	0.283	99.162
CD29-9	0	13.64	0.105	7.12	11.58	0.243	0.086	33.02	32.41	0.366	0.247	98.817
CD29-10	0	15.65	0.051	11.98	9.37	0.177	0.09	44.17	16.59	0.608	0.183	98.869
CD29-11	0.007	14.56	0.069	10	10.11	0.125	0.083	41.11	21.72	0.545	0.187	98.517
CD29-12	0.01	13.77	0.116	7.27	11.7	0.112	0.125	32.23	32.11	0.388	0.256	98.111
CD29-13	0.013	12.29	0.18	4.67	12.36	0.066	0.116	28.17	41.09	0.156	0.292	99.429
CD29-14	0.012	12.35	0.191	4.92	11.83	0.067	0.16	28.55	40.9	0.153	0.297	99.43
CD29-15	0.016	12.48	0.17	5.11	11.9	0.104	0.145	28.69	39.97	0.176	0.285	99.098
CD29-16	0.049	13.29	0.125	7.16	12.47	0.171	0.119	34.15	29.94	0.329	0.239	98.056
JBP16-1	0.019	28.98	0.046	1.95	9.84	0.174	5.88	51.44	0.048	0.769	0.028	99.19
JBP16-2	0.007	19.58	0.058	21.37	6.57	0.068	0.105	49.41	0.997	0.997	0.29	99.477
JBP16-3	0	18.21	0.036	17.93	8.38	0.125	0.108	52.53	0.613	0.882	0.278	99.132
JBP16-4	0.012	18.42	0.047	18.99	7.78	0.082	0.113	51.54	1.038	0.945	0.282	99.307
JBP16-5	0	16.98	0.034	51.73	0.969	0.04	0.036	23.88	5.39	0.61	0.348	100.07
JBP16-6	0	15.3	0.045	52.02	0.295	0.029	0.062	27.16	4.7	0.496	0.394	100.51
JBP16-7	0.017	15.35	0.05	51.77	0.34	0.028	0.064	27.65	4.69	0.496	0.405	100.912
JBP16-8	0	15.26	0.034	51.7	0.296	0.032	0.046	27.82	4.49	0.494	0.429	100.632

Churchill Kimberlite Spinel Microprobe Analyses

	K_2O	MgO	NiO	TiO_2	Al_2O_3	CaO	SiO_2	FeO	Cr_2O_3	MnO	V_2O_3	Total
JBP16-9	0	14.56	0.096	20.68	4.93	0.472	0.048	54.86	2.41	0.8	0.3	99.261
JBP16-10	0	11.16	0.164	4.67	11.55	0.008	0.099	27.83	43.48	0.14	0.316	99.444
JBP16-11	0.015	11.42	0.162	4.84	11.57	0.055	0.168	28.93	42.52	0.154	0.301	100.199
JBP16-12	0.01	11.44	0.175	4.97	11.36	0.012	0.119	28.6	43.06	0.169	0.323	100.268
JBP16-13	0	11.4	0.179	4.52	11.5	0.01	0.107	28.31	43.66	0.156	0.329	100.203
JBP16-14	0	12.27	0.095	13.71	8.38	0.026	0.102	50.01	12.02	0.428	0.319	97.37
JBP16-15	0	12.73	0.101	18.2	7.41	0.046	0.154	56.74	1.19	0.506	0.31	97.428
JBP16-16	0	13.44	0.077	18.44	7.44	0.059	0.094	56.11	0.867	0.56	0.303	97.398
JBP16-17	0	14.72	0.063	18.2	7.79	0.112	0.105	56.57	0.849	0.574	0.273	99.273
JBP16-18	0.011	13.87	0.07	17.87	7.91	0.105	0.12	57.44	1.025	0.551	0.306	99.352
JBP16-19	0	13.03	0.082	18.19	7.51	0.051	0.123	58.22	1.029	0.526	0.317	99.095
JBP16-20	0	12.85	0.065	18.21	7.48	0.046	0.113	58.59	0.974	0.535	0.276	99.173
JBP16-21	0	12.61	0.074	18.36	7.22	0.036	0.131	58.58	1.286	0.512	0.329	99.17
JBP16-22	0.008	16.08	0.038	17.82	7.31	0.056	0.127	55.78	0.437	0.756	0.297	98.731
JBP16-23	0	16.53	0.049	18.12	6.96	0.077	0.112	55.4	0.563	0.787	0.293	98.901
JBP16-24	0	16.92	0.062	18.26	7.21	0.073	0.102	54.79	0.584	0.84	0.273	99.148
JBP16-25	0	16.31	0.037	17.96	7.23	0.063	0.1	55.64	0.592	0.79	0.309	99.077
CD2-1	0.021	12	0.134	6.11	11.42	0.095	0.126	28.67	40.97	0.229	0.329	100.113
CD2-2	0	12.26	0.14	5.76	12.62	0.111	0.162	27.79	40.3	0.182	0.345	99.703
CD2-3	0.01	11.94	0.132	5.87	12.49	0.084	0.198	28.08	40.2	0.236	0.337	99.606
CD2-4	0.01	12.03	0.135	6.03	12.16	0.08	0.178	28.62	40.08	0.255	0.331	99.918
CD2-5	0.013	12.42	0.126	5.89	12.28	0.075	0.167	28.25	40.51	0.261	0.344	100.361
CD2-6	0.019	12.14	0.11	5.77	11.32	0.082	0.188	28.6	40.92	0.303	0.292	99.798